Aalborg Universitet

Power Management and Voltage Control using Distributed Resources

Pedersen, Rasmus

Publication date:
2016

Document Version
Publisher's PDF, also known as Version of record

Link to publication from Aalborg University

POWER MANAGEMENT AND VOLTAGE CONTROL USING DISTRIBUTED RESOURCES

BY
RASMUS PEDERSEN

DISSERTATION SUBMITTED 2016

AALBORG UNIVERSITY
DENMARK

Power Management and Voltage Control using Distributed Resources

Ph.D. Thesis
Rasmus Pedersen

AALBORG UNIVERSITY
DENMARK

Abstract

Today's power systems are experiencing rapid and fundamental changes. A decade ago the power system had unidirectional power flow from large production units to end-users. This situation is being changed towards a more distributed system, where production units are entering on all levels of the grid and the large, typically fossil fueled production units, are being decommissioned. This ongoing transition is challenging the system operators, as they can no longer rely on traditional methods to ensure a reliable operation of the electrical grid.

If power is produced close to where it is consumed the cost of transportation is lowered. However, the production units entering the distribution grids are typically renewables in form of solar and wind power. These volatile resources raise challenges when solving the two main challenges of any power system, namely ensuring that power is balanced and that voltages are maintained within constraints. Therefore, including the distributed resources in the power balancing and voltage control solution is imperative for this transition to become a success.

The main focus of this thesis is to derive control solutions, allowing the distributed resources to become part of the power balancing and voltage control effort. We start by elaborating on the expected challenges from introducing distributed production and additional consumption in the power distribution grids. One of the main challenges stems from units entering on the low voltage residential level, where there are no means of monitoring system behavior or applying control. Subsequently, we discuss the role of a distribution system operator (DSO) and motivate the need for new tools to help them cope with power balancing and voltage control issues originating from new units entering the distribution grids.

The proposed strategies strive to not only alleviate the distribution grids of potential problems, but also to be simple in nature, making them easy to deploy in a highly complex and distributed system. We rely on combining well-established control and estimation methods in new constellations and tailoring them for coordinating the flexibility of distributed resources, enabling them to become part of the power balancing and voltage control

solution instead being the root cause of them. To coordinate the systems on lower voltage levels of the electrical grid we take into account the time-varying properties of the communication network connecting the control unit with the flexible distributed resources. Furthermore, we provide a verification framework for stating if a power systems voltages are always within bounds, leaving out the need for exhaustive and time consuming simulation studies.

The work presented in this thesis adds to the insight of power management and voltage control in power distribution grids with a high penetration of distributed resources, by demonstrating how the potential challenges and concerns may be alleviated, by identifying, coordinating, and utilizing the available flexibility of the distributed resources, through various control and estimation related techniques.

Resumé

De nuværende el-systemer verden over oplever store og fundamentale foran-
dringer. For bare 10 år siden var størstedelen af vores el-net baseret på at
transportere elektrisk energi fra store kraftværker til slutbrugerne. Denne sit-
uation er ved at blive ændret drastisk i retning af et mere distribueret system,
hvor produktions enheder bliver installeret på alle niveauer i el-nettet og de
store konventionelle olie og kul fyret kraftværker bliver udfaset. Denne ud-
vikling udfordre de virksomheder, som er ansvarlige for driften af el-nettet,
da de ikke længere kan anvende de traditionelle løsninger til at sikre en
pålideligt drift.

Det giver god mening at distribuere produktionen ud til hvor forbrugerne
er, da dette vil mindske tabet fra at transportere energien over lange afstande.
Men en af udfordringerne er at produktionsenhederne som bliver installeret
er baseret på vedvarende kilder så som sol og vind. Disse resurser er meget
fluktuerende, hvilket øger udfordringen med at løse de to primære udfor-
dringerne i ethvert el-system, hvilket er balance imellem produktion og for-
brug, samt at sikre at spændinger holdes indenfor grænserne. Derfor er det
nødvendigt at de distribuerede enheder, så som vindmøller og solceller, in-
dgår i den samlede effektbalance- og spængingsregulerings løsning, for at
den fortsatte udvikling mod en mere vedvarende energisektor, kan blive en
succes.

Et af temaerne i denne afhandling er at udvikle reguleringsløsninger, så
de distribuerede enheder kan blive en del af effektbalance og spængingsreg-
ulerings løsningen. Vi starter med at beskrive de forventede udfordringer
som følger med at udrulle mere distribueret produktion og øge effektfor-
bruget i distributionsnettet. En af de største udfordringer stammer fra at flere
og flere produktionsenheder bliver installeret helt ned på husstandsniveau,
hvor der ikke på nuværende tidspunkt findes udstyr til at overvåge nettets
tilstand eller afhjælpe potentielle problemer. Dette leder os hen på hvilken
rolle en distributions system operator (DSO) spiller og motivere behovet for
nye værktøjer til at afhjælpe dem med at fortsat sikre et stabilt distribution-
snet.

De strategier og metoder vi forslår stræber ikke alene imod at løse de po-

tentielle problemer, men også imod at være simple, hvilket gør dem nemme at implementere i et meget komplekst system som el-nettet. Vi kombinere veletablerede regulerings- og estimerings metoder i nye konstellationer og skræddersyer dem til at løse problemet med at koordinere fleksibiliteten af distribuerede enheder, så de kan blive en del af løsningen, i stedet for at være en del af problemet. I forbindelse med at koordinere enheder på de lavere niveauer at distributionsnettet tager vi højde for kommunikationsnetværket, som forbinder reguleringssystemet med de fleksible enheder, kan have tidvarierende egenskaber. Ydermere har vi udviklet en metode, som kan angive om et givet el-system altid vil overholde begrænsningerne på spændingsværdier, hvilket fjerner behovet for tidskrævende simuleringsstudier.

Arbejdet præsenteret i denne afhandling øger indsigten i effektbalance og spændingsregulering i distributionsnetværk, med en stor mængde produktion fra distribueret vedvarende kilder. Dette gøres ved at demonstrerer hvordan de potentielle udfordringer kan løses, samt at identificere, koordinere og udnytte den fleksibilitet de distribuerede enheder stiller til rådighed, gennem en række froskellige regulerings og estimerings teknikker.

Contents

Contents

Contents

Thesis Details

Thesis Title: Power Management and Voltage Control using Distributed
                     Resources
Ph.D. Student: Rasmus Pedersen
Supervisors: Prof. Rafael Wisniewski, Aalborg University
                     Assoc. Prof. Christoffer Sloth, Aalborg University

The main body of this thesis consist of the following papers.

[A] Rasmus Pedersen, Christoffer Sloth, and Rafael Wisniewski, "Active Power Management in Power Distribution Grids: Disturbance Modeling and Rejection," *Proceedings of the European Control Conference*, Aalborg, Denmark, June 2016.

[B] Rasmus Pedersen, Mislav Findrik, Christoffer Sloth, and Hans-Peter Schwefel, "Adaptive Power Balancing over Congested Communication Links," *submitted to Elsevier Sustainable Energy, Grids and Networks*, August 2016.

[C] Rasmus Pedersen, Christoffer Sloth, and Rafael Wisniewski, "Coordination of Electrical Distribution Grid Voltage Control - A Fairness Approach," *Proceedings of the IEEE Multi-Conference on Systems and Control*, Buenos Aires, Argentina, September 2016 .

[D] Rasmus Pedersen, Christoffer Sloth, and Rafael Wisniewski, "Verification of Power Grid Voltage Constraint Satisfaction - A Barrier Certificate Approach," *Proceedings of the European Control Conference*, Aalborg, Denmark, June 2016.

[E] Rasmus Pedersen, Christoffer Sloth, and Rafael Wisniewski, "Verification of Power System Voltage Constraint Satisfaction," *Submitted to IEEE Transaction on Control Systems Technology*, August 2016.

[F] Rasmus Pedersen, Christoffer Sloth, Gorm Bruun Andresen, and Rafael Wisniewski, "DiSC: A Simulation Framework for Distribution System

Voltage Control," *Proceedings of the European Control Conference*, Linz, Austria, July 2015.

In addition to the main papers, the following publications have also been made.

[1] Rasmus Pedersen, John Schwensen, Benjamin Biegel, Jakob Stoustrup, and Torben Green, "Aggregation and Control of Supermarket Refrigeration Systems in a Smart Grid," *Proceedings of the 19th World Congress of the International Federation of Automatic Control*, Cape Town, South Africa, August, 2014.

[2] Rasmus Pedersen, Christoffer Sloth, Rafael Wisniewski, and Torben Green, "Supermarket Defrost Cycles as Flexible Reserve," *Proceedings of the IEEE Multi-Conference on Systems and Control*, Sidney, Australia, September 2015.

[3] Rasmus Pedersen, John Schwensen, Benjamin Biegel, Torben Green, and Jakob Stoustrup, "Improving Demand Response Potential of a Supermarket Refrigeration System: A Food Temperature Estimation Approach," *IEEE Transactions on Control Systems Technology (Issue: 99)*, July 2016.

[4] Mislav Findrik, Rasmus Pedersen, Eduard Hasenleithner, Christoffer Sloth, and Hans-Peter Schwefel, "Test-bed Assessment of Communication Technologies for a Power-Balancing Controller," *Proceedings of the IEEE International Energy Conference*, Leuven, Belgium, August 2016.

[5] Mislav Findrik, Rasmus Pedersen, Christoffer Sloth, and Hans-Peter Schwefel, "Evaluation of Communication Network State Estimators for Adaptive Power-Balancing," *Computer Science - Research and Development Special Issue*, July 2016.

[6] Catalin-Iosif Ciontea, Rasmus Pedersen, Thomas Le Fevre Kristensen, Christoffer Eg Sloth, Rasmus Løvenstein Olsen, and Florin Iov, "Smart Grid Control and Communication: the SmartC2net Real-Time HIL Approach," *Proceedings of The PowerTech Conference*, Eindhoven, Netherlands, June 2015.

[7] Patent: Rasmus Pedersen, John Schwensen, Benjamin Biegel, Jakob Stoustrup, and Torben Green (Danfoss A/S and Aalborg Univeristy), "A Method for Estimating and/or Controlling a Temperature of Foodstuff Stored in a Refrigerated Cavity," *Patent number:* WO2015165937 A1, *Publication date:* November 2015.

This thesis has been submitted for assessment in partial fulfillment of the PhD degree. The thesis is based on the submitted or published scientific papers

which are listed above. Parts of the papers are used directly or indirectly in the extended summary of the thesis. As part of the assessment, co-author statements have been made available to the assessment committee and are also available at the Faculty. The thesis is not in its present form acceptable for open publication but only in limited and closed circulation as copyright may not be ensured.

Thesis Details

Preface

This thesis is submitted as a collection of papers in partial fulfillment of a Ph.D. study at the Section of Automation and Control, Department of Electronic Systems, Aalborg University, Denmark. The work was conducted from July 2013 to August 2016 under the supervision of Associate Professor Christoffer Sloth and Professor Rafael Wisniewski, and was supported by the European Community's Seventh Framework Programme (FP7/2007-2013) under grant agreement nº 318023 for the SmartC2Net project.

The thesis consists of two main parts. The first part encompasses Chapters 1–4, containing the introduction, motivation, and summary of the contributions, complemented by Chapter 5 that gives the concluding remarks and perspectives. The second part details the contributions inform of the publications enclosed as [Paper A- Paper F]. The order of the enclosed papers follows points of focus, namely *power management*, *voltage control*, and *modeling and simulation of power systems*.

Besides the layout, modification and reformatting, all enclosed publications are presented in the same form as they were published. As no other changes have been made, the notation varies from one paper to another, reflecting the progress and refinement of the work.

Rasmus Pedersen
Aalborg University, September 5, 2016

Preface

Acknowledgments

The work presented here has been completed under the careful supervision of Associated Professor Christoffer Sloth and Professor Rafael Wisniewski. I owe immeasurable gratitude to both, for their support, guidance, and always positive attitude towards my ideas. Especially, I would like to thank Christoffer for countless hours of supervision and brainstorming; You are a true researcher and inspiration.

Besides my supervisors I extend my gratitude to the people in the Automation & Control Section, for helping create the most enjoyable work place imaginable. In particular I wish to thank John Leth for numerous technical discussions and Tobias Leth for being a great workout buddy.

As part of my Ph.D. study I had the opportunity to visit the Pacific Northwest National Laboratory, in Richland, WA, USA. I would like to thank Professor Jakob Stoustrup for being a perfect host and sparing partner, for introducing me to many of his colleagues, showing me the hiking routes around Richland, and introducing me to the great wine of the Columbia Basin. Furthermore, I wish to thank Jacob Hansen for being a great friend during my stay. Also, I received invaluable input from Jason Fuller, for which i am equally grateful.

Last, but absolutely not least, I express my gratitude to my girlfriend Gitte, for her constant and loving support, having patience with me, and for being the mother to our son Nor. And to you Nor; thank you for showing me the true meaning of life and tiredness.

<div align="right">

Rasmus Pedersen
Aalborg University, September 5, 2016

</div>

Acknowledgments

1 Introduction

This chapter provides the motivation for studying power management and voltage control problems in electrical distribution grids with a high penetration of distributed resources. An overview of relevant literature is given, followed by a statement of the considered research objectives. Finally, the remainder of the thesis is outlined.

1.1 Motivation

For any power system to function there are two main challenges; first, the frequency must be kept close to the reference value, which in practice entails that power production needs to match consumption. Secondly, voltage magnitudes need to be within predefined bounds in order for grid connected equipment to function properly. These issues are fundamental and have been well known ever since the birth of the power grid some 120 years ago. When first constructed the electrical distribution grid was the transport layer between large centralized, typically fossil fueled, power plants and the end-users in form of industry and residential households. Throughout the decades we have modified and optimized the power grid for this type of operation, and it is widely accepted as one of the greatest human achievements of the 20$^{\text{th}}$ century [72]. It was truly an impressive system, but also a "well" behaved system, where the need for real-time monitoring and control on lower distribution levels where both impractical and irrelevant (the behavior was "known"). The system relied on cables having the capacity to get the power from point A to point B, resulting in deterministic voltages drops along the distribution lines and no congestion problems, as power plants where placed strategically. Further, the large power plants where the main providers of stabilizing services such as the aforementioned voltage control and power management. But a question arises, with the ongoing transition towards a more renewable power sector: Can we rely on control solutions based on these historical assumptions, to guarantee satisfactory operation of the grid?

Large fossil fueled power plants are being replaced by distributed volatile

resources, such as wind and solar. Consequently, the system is becoming more and more distributed and stochastic in nature. Not only are the centralized power plants replaced, but new renewable production and additional consumption units are entering on lower levels in the distribution grid, where no monitoring or means to alleviate potential problems are present. In fact the power system, and especially the distribution grids, are undergoing a paradigm shift, where the system designed for unidirectional power flow is suddenly becoming bidirectional. This rises challenges to the existing infrastructure and may require new equipment and widespread grid reinforcements, which is both economically costly and time consuming. Fig. 1.1 conceptually illustrates the power systems transition towards are more distributed and renewable future.
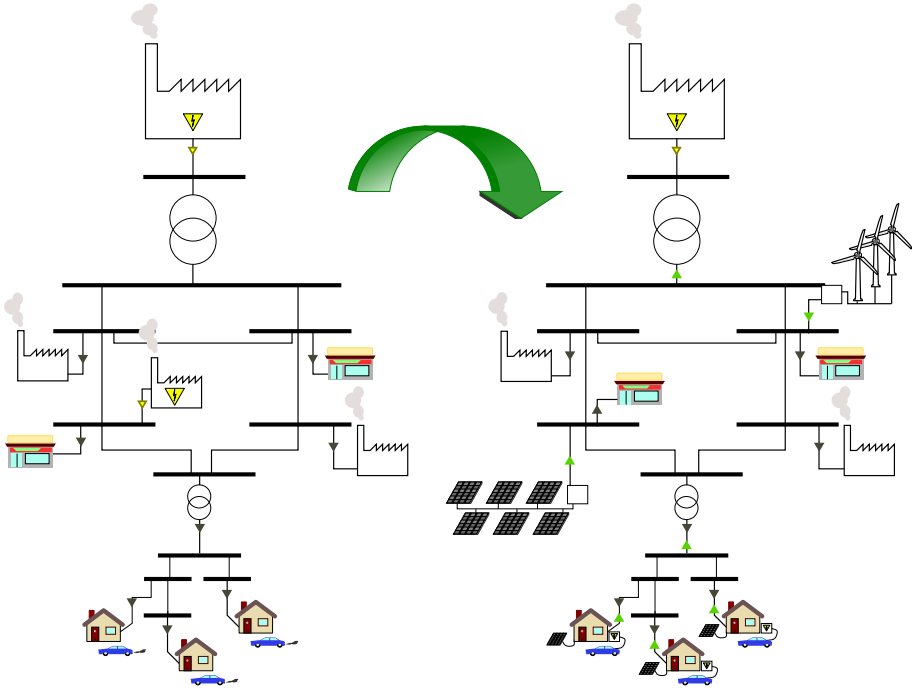
Fig. 1.1: Conceptual illustration of the electrical grids transition towards are more renewable and distributed future, where the traditional unidirectional power flow is becoming bidirectional. The black arrows indicate power flow from consumption, the yellow arrows represent production from traditional power plants, and the green arrows represent production from renewables.

To tackle these new challenges the distribution system operators (DSOs) call for new and innovative power management and voltage control features, enabling the use of distributed resources to ensure satisfactory operation on all levels of the electrical grid [31]. Hence, leaving out the need for costly

equipment upgrades and reinforcements of the grid [4]. This thesis addresses exactly these future challenges and provide control related ideas and solutions, utilizing the flexibility of distributed resources. In the following sections the presented work is related to the SmartC2Net project, the role of a distribution system operator is shortly described, and more technical details on power management and voltage control are given.

1.1.1 The SmartC2Net Project

The studies detailed in this thesis take their beginning in the *Smart Control of Energy Distribution Grids over Heterogeneous Communication Networks* project (SmartC2Net) [36]. The goal of SmartC2Net was: "The SmartC2Net project will develop, implement and validate robust solutions that enable Smart Grid operation on top of heterogeneous off-the-shelf communication infrastructures with varying properties."

In essence the project combined the fields of control and communication to address the issues stated above. Therefore, many of my contributions are directly connected to the objectives of SmartC2Net and e.g., the hierarchical control architecture shown in Fig. 1.2, has been adopted. Hierarchical control theory is well studied [92] and has been applied for the control of power systems in [43, 53, 95].

In the SmartC2Net control architecture there are three layers. The top layer *Central Management System* takes the role of the distribution system operator (DSO) and is in charge of the overall distribution system operation. It is envisioned that the *Central Management System* can offer services to upper layers in the electrical infrastructure, such as transmission system operators, by utilizing the flexibility of distributed resources in the distribution grid. The middle layer consist of the medium voltage (MV) distribution grid and has an associated *Medium Voltage Grid Controller*, which manages active and reactive power of distributed resources connected to the MV grid, to offer services to the *Central Management System*, and to ensure satisfactory operation of the MV grid. The bottom layer consist of a low voltage (LV) distribution grid, with an associated *Low Voltage Grid Controller* for managing the active and reactive power of distributed resources in the LV grid. From the *Central Management System* the entire distribution grid is seen as one flexible unit. Similarly, the LV distribution grid is seen as one flexible unit by the *Medium Voltage Grid Controller*. Notice that different communication technologies are present on each layer, where on the MV level dedicated wide area networks (WAN) are installed, whereas on a low voltage level the communication network technology is based on access networks (AN), which are shared with other systems such as mobile phones and computers. Therefore, potential communication issues such as delay and loss of information is only assumed to be present on the LV level.
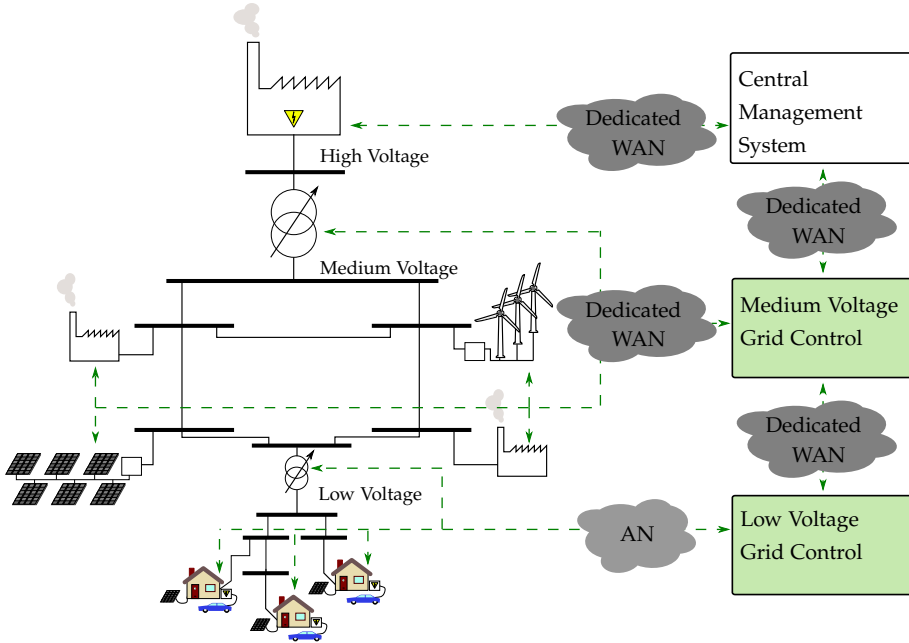
Fig. 1.2: The SmartC2Net hierarchical control architecture. It contains three levels based on the electrical grid structure, from central management down to low voltage grid [10]. The communication technology on the medium voltage level is based on dedicated Wide Area Networks (WAN), whereas on the low voltage level it is based on Access Networks (AN).

My role in the SmartC2Net project was to provide models of the different distributed resources and electrical grid components, and to design power management and voltage control algorithms for the *Medium Voltage Grid Controller* and the *Low Voltage Grid Controller*, highlighted in Fig. 1.2 by the green boxes. Therefore, no market based strategies are considered, instead the work focuses on the challenges seen from a DSO's point of view, which are to maintain a reliable electrical grid with a high quality of power delivery.

In the following we briefly describe the role of a DSO.

1.1.2 Distribution System Operator

The distribution system operator (DSO) is in charge of delivering a high quality supply of electricity, maintaining a secure and stable distribution grid, reduce losses, and make future long term investment plans to ensure the above. In Denmark a DSO is a non-profit organization regulated by the government, and all potential problems must be solved in the cheapest possible way, as expenses are socially distributed. Further, the DSO must comply to strict

requirements such as EN-50160 [5]:

- *The voltage magnitudes at all busses must be within ±10 % of the nominal voltage magnitude as a 10 minute mean, for 95/99 % of the time for a low voltage/medium voltage grid, evaluated over a week.*

To fulfill the above requirements a DSO will typically install new equipment, reinforce the electrical grid, and upgrade existing components. This strategy has proven reliable in the past, when maintaining a fairly deterministic grid, with only small and slow changes. However, as already mentioned, new equipment is costly, reinforcements can be difficult and time consuming (in Denmark the distribution grid is buried under the ground). To illustrate the current challenges faced by the DSO, the evolution of solar photovoltaic (PV) capacity in Denmark from 2011 to 2016 is plotted in Fig. 1.3.
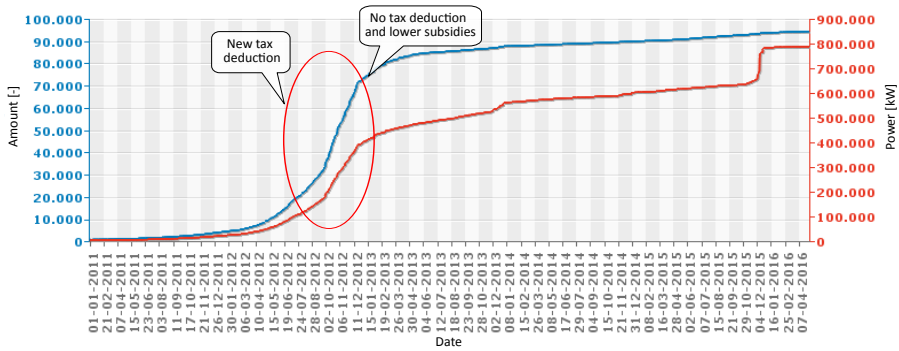
Fig. 1.3: Solar PV capacity growth in Denmark from 2011 to 2016 [33].

It is clear that with the exponential growth seen throughout 2012, installing new equipment or reinforcing lines to cope with the extra production capacity is simply not feasible at this rate. This leaves the DSO helpless when trying to maintain a relayble grid, as they are not allowed to prevent further installation of PVs or even to curtail the production of these systems [31]. They must rely on what is known as grid codes, describing the requirements a system needs to fulfill in order to be connected to the grid [26]. One requirement is, that in case of voltage being above a certain limit, production units must shut-down []. However, writing new grid codes to handle these new challenges are time consuming, and the problems might not even be known before they occur, i.e., writing new grid codes might be too late. This results in a conflict as the political goals of Denmark are for the entire energy and transportation sector to be fossil free in 2050 [8]. But is this achievable without jeopardizing the reliability of the grid? The DSOs of Europe have tried to answer this question by allowing them to use flexibility of the installed systems for power balancing services, congestion mitigation, loss minimization,

and voltage control, making individual systems part of the solution, instead of the problem [31]. In this thesis we follow the solution approach proposed by the DSOs, and actively control the distributed resources entering the distribution grid.

The next two sections take a more technical point of view and motivate the need for new power management and voltage control features utilizing the flexibility of systems connected to the distribution grids.

1.1.3 Power Management

If the active and reactive power of a distribution grid can be managed to e.g., follow a referenced value or always be below a certain limit, then a distribution grid could offer services such as power balancing and congestion mitigation to the DSO. In the following we detail the importance of these issues in distribution grids.

Imbalances between production and consumption leads to frequency deviations. Frequency variations may cause damage to grid connected induction motors and transformer stations, caused by high magnitizing currents. Further, in the most extreme cases frequency deviations may cause grid wide collapse [61, 65]. Also, more and more systems are introducing micro-grid concepts [6, 108], where a part of the grid can be switched to islanded mode, meaning that it is not connected by a tie line to any neighboring systems and is thus self sustained. Thereby, if the main system experiances large imbalances it can sheed part of the grid, to again attaine balance. In such a situation, it is mandatory to have some governing control unit ensuring power balance in the islanded grid [61].

In all liberalized electricity systems, the majority of the power balancing effort is handled by the transmissions system operators (TSOs), through contracts with power producers, and through day-ahead and intraday market mechanisms [2]. Frequency balance is in large a centralized problem. However, when plans are not met, the system experiences unforeseen faults, weather conditions change rapidly, etc. the TSOs rely on what is know as ancillary services from generators or other flexible units to restore balance. To provided fast restoration of power balance, some generators in the system applies automatic generator control (AGC), which in many cases is a linear relation between measured frequency and active power output, known as a droop curve [65], see Fig. 1.4.

Traditionally, the fast frequency control has been carried out by the large centralized generation units, but with the transition towards a more distributed renewable production, other systems must take over the balancing effort. As many of the new production and consumption units are connected to the distribution grids, the coordination of these systems to offer services such as power balancing is important. This will allow the increase of re-
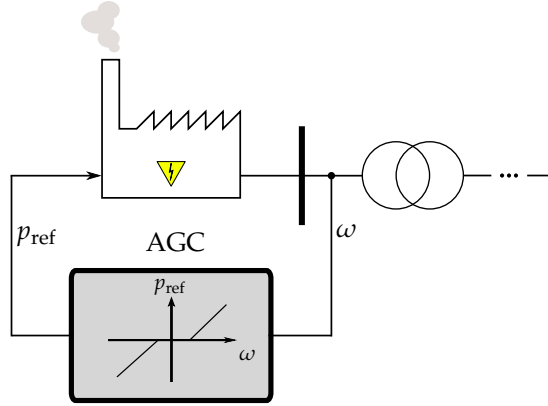
Fig. 1.4: Illustration of the automatic generator control, which measures the grid frequency at its coupling point, and increase or decrease power plant injection based on a droop curve.

newables without jeopardizing system reliability. Also, if a distribution grid could act as a flexible unit capable of e.g., following a power reference or deviate from the original plan, then the DSO can offer balancing services directly to the TSO.

Another problem arising when installing new consumption and production units on the distribution level is congestion [9]. On the transmission level congestion is avoided through market mechanishm, accounting for cable limitations, etc. However, there are no market structures for incorporating similar actions on the distribution level, and in fact the current market structures might lead to congestion problems in distribution grids, as high levels of concurrency might occur if numerous units are optimized towards an energy price [69]. Furthermore, in [82] it is argued that the future increase of consumption in low voltage distribution grids, from electrical vehicle charging, will result in capacity constraints being violated, which is also the topic of [42]. Similarly, if production increases the upper capacity constraint on cables and transformers might be violated. To alleviate potential distribution grid congestion issues, a solution is to use wide-spread monitoring and communication technologies, along with the flexibility of distributed resources to manage the power flow. Thereby, a DSO can postpone the conventional approach of installing new equipment or reinforcing the grid.

The problem of managing the power flexibility of resources in a distribution grid, for offering services to the DSO constitutes one of the main focus areas of this thesis.

1.1.4 Voltage Control

In contrast to power balancing, which is a global issue, voltage control problems are local, meaning that they must be handled at the bus where they occur or close to it [65]. This indicates that relying on large centralized units to solve potential problems was in fact never the solution. But as already mentioned, power traditionally flowed from production sources in upper layers of the grid to consumers on the lower levels, resulting in a predictable voltage drop along the distribution lines. So as long as the installed cabling had the needed capacity to ensure that voltage magnitudes was always within bounds, the system performance would be satisfactory. If loading in some parts of the grid would be to high, remedies such as capacitor banks, static condensers, or on-load tap-changers (OLTC), would be installed [61]. Typically, the setting of these systems would change with e.g., seasonal variations. However, with the increase of additional consumption and production in all levels of the distribution grid, relying on such technologies to maintain voltages within bounds might not be possible in the future. The reason for this, is that every time e.g., a tap-change is carried out it stresses the equipment, which consequently degrades its life-time. Therefore, if the frequency of tap-changes increases, so does the economical cost of maintaining the grid, a cost carried by the DSO. As already argued, this is not seen as a viable solution by the DSOs and they are therefore looking for solutions that utilize the flexibility of systems entering the grid to apply voltage control.

Production units entering the distribution grids are mostly renewables in form of PV and wind. On the consumption side heat pumps are becoming a popular alternative to oil fired burners, and electrical vehicles (EVs) are a competitive and attractive alternative to combustion engine vehicles. What characterizes many of these systems is that they are connected to the grid through power electronics, which offers an interface to control not only the active power output, but also the reactive power output, both crucial when considering voltage control problems.

The voltage control problem is illustrated through an example. Consider the simple distribution grid in Fig. 1.5, where a generator provides power for a load through a distribution line, modeled as an impedance, $z \in \mathbb{C}$. The generator is capable of maintaining a constant voltage $v_1 = V_1 e^{j\delta} \in \mathbb{C}$, with magnitude $V_1 = 1$ p.u. (per unit) and angle $\delta_1 = 0$ rad. The load consumes active power, $p_2 \in \mathbb{R}$, and reactive power, $q_2 \in \mathbb{R}$. Furthermore, a local voltage controller is present at bus B_2 and is capable of injecting active power, $p_c \in \mathbb{R}$, and reactive power, $q_c \in \mathbb{R}$. The voltage at bus B_2 is given by

$$v_2 = v_1 - zi = v_1 - (r + jx)\frac{(p_2 + p_c) - j(q_2 + q_c)}{v_2^*}, \tag{1.1}$$

where $j^2 = -1$ is the imaginary unit and * denotes the complex conjugate. It

is apparent from (1.1), that even for the simplest system, the voltage control problem has a high complexity. To graphically show this, traces of the voltage magnitude at bus B_2 are plotted in Fig. 1.6, for a constant load and varying p_c and q_c. It can be observed that reactive power injection has more effect on the voltage magnitude than active power injection. This is caused by the line impedance being mostly conductive, i.e., voltage control is dependent not only on grid loading but also on line parameters. This is further elaborated in Section 1.2.3.
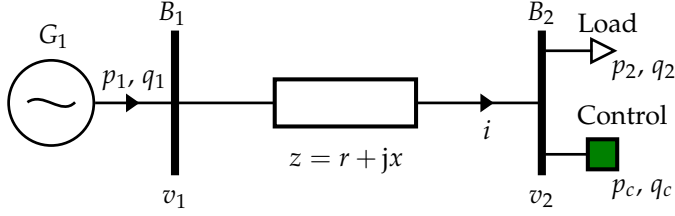
Fig. 1.5: Example of simple distribution grid, where a generator supply power for a load through an impedance. An additional voltage controller is present for maintaining the voltage magnitude at bus 2.

Development of distribution system voltage control solutions and verification of these, constitute the second focus of this thesis.

1.2 State of the Art and Background

The purpose of this section is to introduce related work and material, which form the background of this thesis. The thesis contains contributions within power management, load modeling and estimation, coordination of flexible assets over unreliable communication links, voltage control strategies, safety
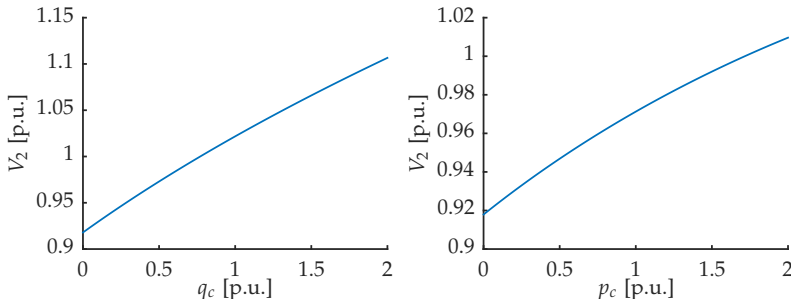
Fig. 1.6: Left: Impact of varying q_c on voltage magnitude V_2, with $p_c = 0$. Right: Impact of varying p_c on voltage magnitude, with $q_c = 0$. The impedance is given by $r = 0.05$ [p.u.], $x = 0.1$ [p.u.] and the load draws constant power $p_2 = q_2 = 0.5$ [p.u.].

verification of power systems, and the development of a MATLAB simulation framework, with focus on the distribution part of the grid. The section is divided into categories addressing each topic. This should not be seen as a full survey, but as a selection of related work and methods.

1.2.1 Power Management

In order for a power system to ensure balance, congestion mitigation etc. the power injection of distributed generation and flexible consumption units must to be managed.

Coordination Strategies

There are two concepts for mobilizing the flexibility of distributed resources; indirect control based on economic incentives, where each individual system plans it operation according to a price signal [47]. The second approach is known as direct control, where the flexibility of smaller units are aggregated through an aggregator, so they together act as one unit. In this setup the utilization of flexibility is based on e.g., flexibility contracts [45]. The two concepts was also mentioned by the Danish TSO Energinet.dk in [4].

The concept of indirect control was investigated in [81] for managing the consumption behavior of heat pumps so they collectively followed a power reference. Similarly, [51, 52, 97] showed how a refrigeration system could be controlled based on economic incentives. The applicability of indirect control for general heating systems and demand response devices was further investigated in [27, 102]. Although indirect control provides a simple interface for utilizing the flexibility of distributed resources, the authors in [54] express their concerns regarding stability of this approach. They explain how greedy behavior amongst flexible units might cause instability, and provide a solution to this behavior.

Converse to the indirect control approach is direct control, where the distributed resources allow an external party to control the flexibility. The benefits of the individual systems for participating is then based on contracts [46]. The direct control scheme has been the topic of [59, 79, 104], to mention a few. To coordinate number of distributed resources by direct control a popular concept, know as a virtual power plant (VPP), has been adopted in many works [18, 84, 90, 91]. The VPP is a technical unit in charge of coordinating the behavior of several systems, so they collectively can fulfill some objective [86]. Many control algorithms have been proposed for the VPP taking into account different flexible units. In [19], the control of a portfolio of heat-pumps towards a power reference was experimentally investigated. Further, the work in [51] considers coordination of refrigeration systems in a similar fashion based on economic incentives, and [85] investigated the aggregation

and control of a combination of different large scale thermal units towards a power reference. What is common throughout the cited work is no regards for the underlying electrical grid and what impact these control algorithms can have on e.g., voltage profiles, power loss or even grid stability. Furthermore, the derived solutions pay little attention to the communication network connecting the distributed units with the VPP. Therefore, further investigation is needed before these algorithms are readily deployable.

Power Balancing

The coordination of flexible resources can be used for power balancing services. In power systems implementing a market structure (such as the Nordic countries), the main power balancing effort is handled by the TSO through a scheduling approach, where market players[1] bid production and/or consumption plans into the markets. Thereby, the economical optimal solution can be found based on the aforementioned bids. When the market closes, the market players, whos plans are accepted, are responsible for ensuring that the submitted plans are actually followed during run-time. If the market players for some reason fail to follow the plans, the TSO will procure additional power on the intra-day markets or activate ancillary services. This comes with an extra cost, which is covered by the market players not capable of delivering as planed. This will result in a decrease of revenue for the market players [32], hence following the plans are important seen from all parties.

While most of the scheduling is markets based, other factors must be taken into consideration, such as congestion, power loss, and constraints on individual systems. This scheduling problem was first stated in 1962 and is formally known as the optimal power flow problem (OPF) [24], and is in fact one of the most well studied optimization problems [38]. The reason for the huge interest in this particular problem is of cause its practical relevance, but also that it is a difficult non-convex problem, which is ever evolving along with the power grid, see [38, 39] for a thorough survey on OPF. With the inherent complexity of the OPF, solving it during run time might not be feasible in its original form. This has led to relaxation approaches such as in [62, 63], where they solve the Lagrangian dual problem and recover the primal solution from the dual solution. To solve the problem a coordinate change is applied, which results in additional variables, and the system is only allowed to have a specific structure (mesh grids are not allowed). The authors have in recent publications provided methods for applying their approach to systems having specific mesh structures and additional constraints [67, 68]. In [55, 56] the authors propose a similar scheduling method applied to LV residential

---

[1]In this connection a market player could be a power plant, an electrical energy retailer, or a combination of both [3].

grids. The idea is to utilize flexibility of distributed resources such as charging of electrical vehicles (EV) and derating of PV systems to minimize power losses and ensure voltage constraint satisfaction. However, the approach is based on knowledge of EV behavior and environmental properties such as solar irradiation, along with an assumption of ideal communication links. Also, the approach is still to schedule, meaning that there is no guarantee of system behavior during run-time. The authors have extended their method to also run in a distributed manner [57]. The above illustrates that there are many approaches to manage the power of distributed resources. However, they are mostly based on scheduling without considering the dynamic behavior of individual units.

1.2.2 Load Modeling and Estimation

Load modeling is a well established area spanning from the very general ZIP[2] model [61, p. 273] to dynamic voltage dependent load models [28, p. 127]. What characterizes these models is that they aggregate the behavior of all load components and represent them with a simplistic model. These models do not capture the seasonally or daily variations, and have mainly been used to conduct load flow analysis and study voltage instability on the transmission system level. The work in [49, 50] address the importance of dynamic load modeling and estimation to eliminate reactionary and unanticipated protection operation, which has historically led to cascading failures. On the distribution side [23] takes a bottom up approach to model individual household loads. This results in a complex model with several components, also examplified by the residential module implemented in the simulation tool GridLab-D [76], which is one of the most complex modules developed. This indicates that there is room for models, which capture the dynamic behavior of loads, without incorporating all details.

Consumption Profiles

To illustrate the challenges of modeling loads in distribution systems, consumption profiles of five houses are plotted in Fig. 1.7, along with the aggregated consumption profile of 120 houses. Developing a generic model for capturing the behavior of individual houses might be challenging. However, the aggregated consumption exhibits periodic behavior which could be used for creating a model of it.

To estimate power system states, [14] uses periodic models to forecast seasonal and daily consumption patterns of loads. These types of models and estimation techniques have been used to create strong statistical tools used for for long term planning, component upgrades and line reinforcements [30, 35].

---

[2]Constant impedance (Z), constant current (I), and constant power (P).
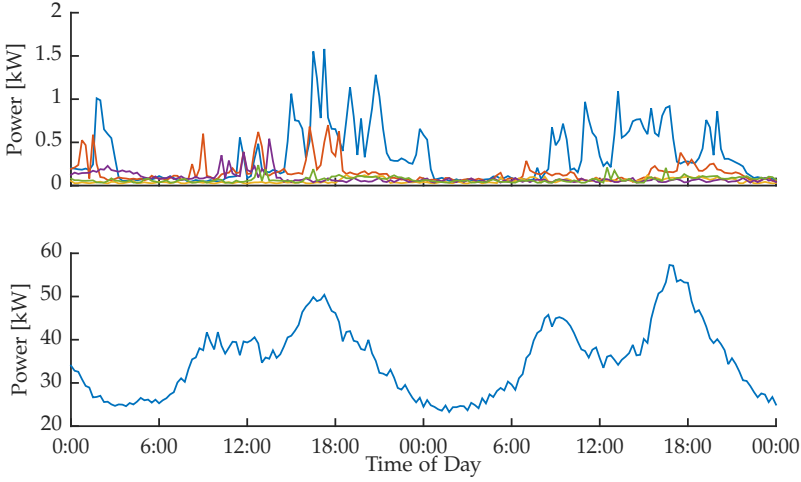
Fig. 1.7: Top: Consumption profiles of five individual houses for two days. Notice the difference in both magnitude and time. Bottom: Aggregated consumption of 120 houses for the same two days. Notice the periodicity in consumption profile.

However, the presented models and techniques, are not intended for implementation in a dynamic control system setting. In [17, 41, 110] different forms of Kalman filtering methods are used to estimate higher order harmonics, slowly varying load behavior, and synchronous machine states. Further, [98] extends these methods by adding robustness to the estimators. The methods where intended to be used by e.g., a power plant to attenuate disturbances, but they could also be used by a control unit coordinating multiple distributed resources. In [71] a survey on power systems state estimation is given.

In all the cited work, little attention has been payed to combining the load models and estimation approaches with a control system. Essentially, inflexible load behavior can be seen as a disturbance by the control system and obtaining a model of such a disturbance is extremely valuable for the control system.

1.2.3 Voltage Control

Traditionally, the control of voltage is accomplished by controlling injection and flow of reactive power in the system, known as volt/var control, where generation units are the main provider of these services. The generators typically control the voltage at its connection point, through a droop curve similar to the frequency control depicted in Fig. 1.4. To maintain satisfactory voltage levels throughout the system, where generators are not present,

other devices such as tap-changing transformers, static reactive power compensators, shunt capacitors and reactors are installed [61, p. 627]. In [93] the development of a 100 Mvar static condenser (STATCON) is described. The system is designed using power electronics to mimic the operation of a rotating synchronous condenser. Further, the system was installed in Tennessee under the FACTS program, and illustrates the volt/var control approach, see also [87] for more information on classical volt/var control. Not much attention has been payed to voltage control in the lower voltage levels of the distribution grid, as there historically has not been a need for it. However, with the introduction of additional consumption from e.g., electrical vehicle charging and heat pumps, along with the increasing installation of household production units in form of PV and wind, the need for voltage control on the lower levels of the distribution grid is expected to increase [106]. This raises many challenges, as the LV distribution grids in many ways are different from the transmission grid; lines are predominantly resistive, whereas transmission lines are often seen as purely conductive [61], distribution grids have a tree-like structure, whereas the transmission grid is more mesh-like, there is a low reactive power loading in LV distribution grids, wheras the inductive loading on the transmission level is higher [61]. Furthermore, an abundance of sensory equipment and controllers are present in the transmission grid, whereas, already stated, little to non is present in the distribution grids [31]. However, many of the systems entering into the distribution grids are inverter based, where e.g., [20, 22] shows how inverter based systems can be used to offer the aforementioned volt/var control. But with distribution lines being mostly resisitive, relaying solely on reactive power for voltage control might not be sufficient. Consequently, the voltage control approach in distribution grids requires further investigation, as the standing assumption of voltages decreasing along the line no longer applies. This will undoubtedly increase the complexity of new distribution system voltage approaches.

Flexibility of Invert Based Systems

Using inverter based technologies for voltage control purposes has gained much attention in recent years. The inverters provide an opportunity to control active and reactive power output [44], which could be used for offering voltage control services [34, 109]. One of the main inverter-based technologies entering the distribution grids are solar PV, where e.g., in Germany close to 95 % of all PV installations are connected to the MV and LV distribution grids [34]. As already argued this could result in increased voltage variations, however it also provides means of alleviating these issues through the flexibility offered by the inverter. The flexibility of inverter based systems are illustrated in Fig. 1.8, where active power output is dependent on external

conditions such as solar irradiance[3]. However, the reactive power output can freely be controlled, only limited by a constraint on rated apparent power.

$$s^2 = p^2 + q^2$$

$$|q| \leq \sqrt{s_{max}^2 - p^2}$$
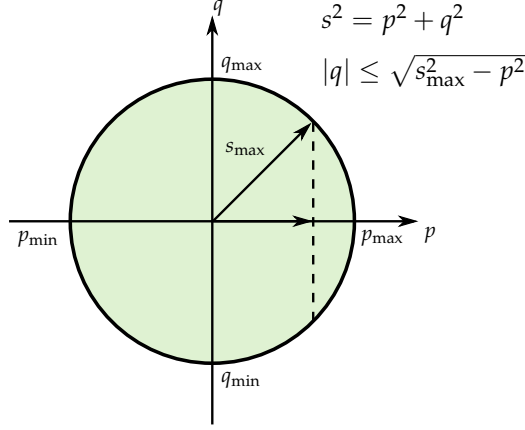
Fig. 1.8: Constraints on active power, p, and reactive power, q, according to rated apparent power, s_{max}, of inverter based systems. The figure can be specialized to e.g., PV systems only capable of operating with non-negative real power, p.

In [15] and [101] PV inverters implement a droop curve to apply local volt/var control, whereas the approach taken in [99] is to coordinate inverter based systems to reach a stable voltage equilibrium by a quadratic volt/var control law. The authors however rely on the assumption of lines being purely conductive, which excludes the method for being implemented in distribution grids. Both centralized and distributed voltage control solutions, using inverter based PV systems, are presented in [21, 60, 64], where also loss minimization is considered. Similarly, the works in [25, 96, 112] considers coordination of distributed generation units to limit voltage rises, and thereby allow for further penetration of renewable production in distribution grids. In [107] they demonstrate various approaches for controlling reactive power to lower voltage variations and reduce loss. In [101] they investigate the effect of PV systems offering local vol/var control according to the traditional droop curve, where in [73], they extend this approach by adding a coordination strategy for maximizing PV penetration. Also, [111] address the potential voltage problems from introducing solar PV into residential networks by combining the PV systems with a local energy storage. Energy is stored whenever there is a surplus in PV production. The stored energy can then be used in various ways, for example locale voltage control.

---

[3]The active power output of a PV systems is dependent on the intensity of solar irradiation, whereas the active power output of an energy storage is dependent on its state of charge, i.e., it cannot inject active power if it is empty.

Voltage Control in Distribution Grids

The common focus in the cited work is reactive power support which needs to be combined with active power control if the solutions are to be implemented on the low voltage levels of the distribution grid. To further strengthen this assertion, the voltage dependence of the two bus system in Fig 1.5, is plotted in Fig. 1.9 for different values of line impedance and active/reactive power output of the control unit. In this example the load draws constant active and reactive power.
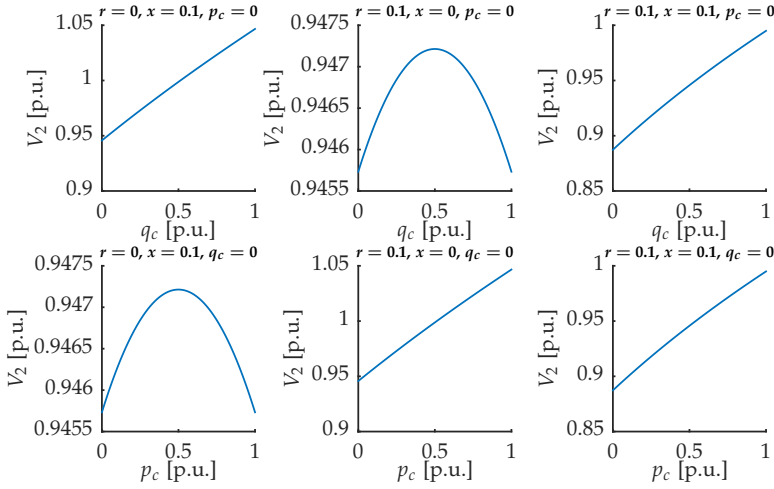
Fig. 1.9: Voltage versus active and reactive power for the two bus system in Fig 1.5, for different values of line reactance r and conductance x. The load has a constant consumption: $p_2 = 0.5$ [p.u.], $q_2 = 0.5$ [p.u.].

Fig. 1.9 clearly indicates that caution should be taken when deploying voltage control approaches. It is observed that if the line is purely resesitive, reactive compensation has little effect, and the voltage actually begins to decrease when the reactive compensation exceeds the reactive power consumption of the load.

Another approach, taken in [105, 106], is to curtail the active power injection of PV systems to limit voltage variations. The strategy is based on the traditional droop curves and shows how droop coefficients can be determined offline based on electrical grid parameters. Furthermore, according to German grid codes, PV systems above a certain capacity are limited to 70 % of their rated power, and must be capable of offering volt/var support [7, 109]. Similar changes has been proposed for the California rule 21, regulating grid connected generation [11]. As already explained, using active power curtailment for alleviating over-voltage issues might be necessary in

distribution systems. However, conservative tuning might lead to excessive loss of renewable power, which is costly for the system owner.

Fairness in Participation

Another issue occurring when distributed systems apply local voltage control is the effect of physical placement. In a power system some busses might be more sensitive to loading e.g., the bus farthest away from the substation. Thereby, distributed systems connected to that bus will inject more power than systems connected to busses closer to the substation. Consequently, the wear and tear of the systems connected to the most sensitive busses are higher. This issue was adressed in [105, 106] where droop coefficients where chosen to achieve equal curtailment of all systems. However, this method shows an increase in overall active power loss due to curtailment, compared to a method of all systems having equal droop coefficients. Moreover, the droop coefficients are only set ones, utilizing no feedback of the actual system state. Further, in [58] they propose a fairness scheme where systems should participate in the volt/var control according to size. In this setting all systems must always inject reactive power according to a certain percentage of their active power output. However, the method does not consider physical placement of the systems or locally measured voltages, and the authors give little information on the complexity of their approach. The above indicates the need for additional voltage control features based on both active and reactive power support, where notions such as fairness in system participation must be considered.

What is common practice throughout all the cited work on voltage control, is that the approaches are verified based on time consuming and exhaustive simulation studies [109]. The studies provides statistically useful insight, but they do not guarantee that the developed methods will ensure satisfactory voltage profiles throughout a distribution grid.

1.2.4 Accommodation of Communication Issues in Control

When coordinating distributed resources in a power grid this is achieved over a communication network. On the higher levels of the distribution grid the distributions system operators have installed dedicated networks for collecting sensory data and dispatching commands to controllable units [4]. Thereby, effects such as delay and loss of information is negligible. However, on the low voltage level there are currently no coordination of distributed resources, hence no dedicated communication network has been installed. However, this is expected to change with the increase of distributed resources entering on a household level. Instead of installing a dedicated communication network on this level it would be desirable to investigate if networks

already in place could be used. This would reduce the cost of deploying coordination strategies on the low voltage level significantly. One problem with relying on these communication networks is that they are shared with other traffic generating sources, such as mobile phones and computers. Consequently, data packets are subject to increased delay and loss. Such effects need to be taken into account when deploying the coordination approaches, when basing the communication on already in place networks and technologies.

There are several methods for analyzing and designing networked control systems, with focus on delay and packet loss, where an overview is given in [114]. For handling delays several general methods have been presented. The methods range from classical delay compensation [94, 114], through methods based on robust control techniques [70], to hybrid control methods [16], where e.g., delay modes are modeled with a Markov chain [74, 113]. In the consensus framework communication issues are well studied. Stability bounds for allowable delays are available, along with convergence rate for systems with switching communication network topology [75]. Further, these methods have been extended for linear systems with a higher order [29]. Also, results have been given for consensus based systems with multiple time-varying delays [77, 103, 115]. It is expected that these methods can be applied, when coordinating distributed resources on the low voltage level over unreliable communication links.

1.2.5 Modeling and Simulation of Electrical Power Systems

This section briefly mentions two of the power systems simulation tools with relevance for the work presented in this thesis. It should be noted that there are several tools available, both free and commercial. The tools mentioned here are all free and follows the mission of IEEE task force on open source software for power systems [1]. An example of such a tool is the MATLAB toolbox MATPOWER [116]. MATPOWER was originally developed for studying power flow and optimal power flow problems. Hence, it does not consider dynamic behavior of connected components or interfaces for accessing flexibility of distributed resources. Another popular software tool is GridLAB-D [76], which is a detailed simulation framework tailored for the American distribution system, which has a significantly different structure than European distribution grids. Further, GridLab-D is implemented in C++, which results in fast execution of simulations, but makes it difficult to change existing modules and setup simulation scenarios. For a full list of freely available power systems software tools see [1].

What is common for most of the existing free tools is that they have not been developed with a main focus on electrical grid control validation and design. They do e.g., not include modern assets such as electrical vehicles and

solar photovoltaics, realistic consumption and production patterns, a model of the underlying communication network, the importance of empirical data, or the implementation in a control design environment, such as MATLAB. Therefore, there are a need for new tools which incorporates all of the above.

1.3 Research Objectives

The overall objective of the work presented in this thesis is to provide control solutions, which makes it possible to manage the installed distributed resources for offering services to grid operators and for applying voltage control. A second objective is to devise solutions with low complexity, tailored for easy implementation and fast deployment. These objectives has led to the following research hypothesis, tested in this work.

1.3.1 Power Management

From a control point of view power management is a *reference tracking problem*, which must be solved on different layers of the electrical grid, according to the adopted hierarchical control structure. On the medium voltage distribution layer more computing power will be present, and the communication is based on dedicated links, meaning that they can be seen as ideal. On the low voltage layer, where communication is non-ideal, effects such as loss and delay of information needs to be taken into consideration. Consequently, two research hypothesis are stated.

Hypothesis 1. *By coordinating the active power output of distributed resources connected to a medium voltage distribution grid it is possible to make the entire medium voltage grid follow a power reference.*

Hypothesis 2. *By coordinating the active power output of distributed resources connected to a low voltage distribution grid, it is possible to make the entire low voltage grid follow a power reference, under communication with information loss and delay.*

Hypothesis 1 is validated by the development of a combined control and disturbance estimation system, utilizing distributed resources such as wind turbines and solar PV system to make an entire medium voltage distribution grid follow a power reference.

Hypothesis 2 is validated through a leader-follower consensus based control system, coordinating distributed resources in a low voltage residential distribution grid. Furthermore, the developed controller is capable of adapting gains according to estimates on communication network state.

1.3.2 Voltage Control

In contrast to power balancing, voltage control is a *feasibility problem*, where voltage magnitudes need to be within predetermined bounds. Therefore, the research objective have been divided into two parts; one is concerned with fairness in contribution of distributed voltage control approaches and the other with verifying voltage constraint satisfaction. This has resulted in two research hypothesis.

Hypothesis 3. *Given a set of distributed systems implementing a local voltage controller, it is possible to reach fairness in participation, i.e., the difference in system output is minimized, while respecting constraints.*

Hypothesis 4. *Given an electrical distribution grid and models of connected units, it is possible to verify whether the system will always satisfy constraints, without the need for simulation studies.*

Hypothesis 3 is validated through a centralized coordination approach based on distributing gain values for local volt/var droop controllers. To obtain new gain values an optimization problem is formulated, which minimizes difference between the reactive power output of the distributed systems, taking into account the underlaying electrical grid structure and parameters.

Hypothesis 4 is validated by formally stating *the voltage constraint satisfaction problem*, which is a safety verification problem, and reformulating it into a polynomial programming problem, solvable by existing tools.

1.4 Overview of Contributions

In the following section the main contributions of this thesis are outlined. The contributions are divided into two main categories. The first category considers *Power Management* and consists of two papers, which address Hypothesis 1 and Hypothesis 2. The second category is devoted to *Voltage Control* and consists of three papers addressing Hypothesis 3 and Hypothesis 4. A third category, *Modeling of Power Systems for Control Verification*, is added to bind the two main parts together through a developed MATLAB power systems simulation toolbox.

With each listed paper a small overview is given which summaries the contribution. In the following Chapter, a more detailed description of the work is provided. Finally, all papers are presented in the second part of the thesis.

Power Management using Distributed Resources

The following two papers address power management in distribution grids with distributed flexible production and consumption.

Paper A

Title: Active Power Management in Power Distribution Grids: Disturbance Modeling and Rejection
Authors: Rasmus Pedersen, Christoffer Sloth, and Rafael Wisniewski
Published in: Proceedings of the European Control Conference, Aalborg, Denmark, June 2016

Paper A describes a combined disturbance estimation and control system for managing a distribution grid towards a power reference. The disturbance in the system originates from the uncontrollable consumption of loads, where a linear model based on harmonic oscillators is constructed to capture the periodic behavior. This model is combined with a Kalman filter, and the resulting estimate is used as feedforward in the control system. Finally, a dispatch algorithm is proposed, which minimizes active power loss. All elements of the estimation and control system has been tailored for simple implementation.

Paper B

Title: Adaptive Power Balancing over Congested Communication Links
Authors: Rasmus Pedersen, Mislav Findrik, Christoffer Sloth, and Hans-Peter Schwefel
Submitted to: Elsevier Sustainable Energy, Grids and Networks, August 2016

Paper B focuses on an adaptive multi-agent leader-follower consensus based coordination strategy for allowing flexible assets in a low voltage residential grid to follow a power reference, over an unreliable communication network. The control approach is developed for simple implementation, where each asset implements a control protocol only dependent on neighboring agent states. To attenuate disturbances and add robustness to the reference tracking the leader agent updates its state value based on a PI control law. Further, the leader agent's controller gains are adapted based on estimates of the communication network state. The adaptive gain scheduling approach ensures stability during periods with highly congested communication links, and allows for performance increase during periods with no congestion problems in the communication network.

Voltage Control using Distributed Resources

The following three papers are concerned with coordination of local voltage control approaches, development of a local voltage control strategy, and

verification of voltage constraint satisfaction.

Paper C

Title: Coordination of Electrical Distribution Grid Voltage Control - A Fairness Approach
Authors: Rasmus Pedersen, Christoffer Sloth, and Rafael Wisniewski
Accepted for publication in: Proceedings of the IEEE Multi-Conference on Systems and Control, Buenos Aires, Argentina, September 2016

Paper C addresses fairness in local volt/var control. Fairness is defined as all control units contributing equally to the voltage control, i.e., the difference in reactive power output should be minimal. The method is based on updating the droop gains of local volt/var controllers, by solving a convex optimization problem. The approach is simple to implement allowing for rapid deployment.

Paper D

Title: Verification of Power Grid Voltage Constraint Satisfaction - A Barrier Certificate Approach
Authors: Rasmus Pedersen, Christoffer Sloth, and Rafael Wisniewski
Published in: Proceedings of the European Control Conference, Aalborg, Denmark, June 2016

Paper D formally states *the voltage constraint satisfaction problem*, which is concerned with verifying under given conditions, will voltage constraints always be satisfied? To answer this question, the problem is put on polynomial form and it is show that computing a barrier certificate for the reformulated problem is equivalent to solving the original problem.

Paper E

Title: Verification of Power System Voltage Constraint Satisfaction
Authors: Rasmus Pedersen, Christoffer Sloth, and Rafael Wisniewski
Submitted to: IEEE Transaction on Control Systems Technology, August 2016

Paper E extends the approach in Paper D and gives explicit models for loads and voltage controllers, and shows how a barrier certificate can be found for this system. Further, a novel four quadrant voltage controller (4Q-VC) is introduced, and its effectiveness is illustrated through extensive simulation studies using GridLab-D.

Modeling of Power System for Control Verification

To verify the developed power management and voltage control approaches a MATLAB simulation framework was developed.

<div align="center">

Paper F
</div>

Title: DiSC: A Simulation Framework for Distribution System Voltage Control

Authors: Rasmus Pedersen, Christoffer Sloth, Gorm Bruun Andresen, and Rafael Wisniewski

Published in: Proceedings of the European Control Conference, Linz, Austria, July 2015

Paper F details the simulation framework DiSC, which was developed in order to verify the control approaches detailed in the above. DiSC implements a Newton-Raphson solver to solve the nonlinear power flow equations, along with a wide variety of renewable resources, flexible consumption units, grid components, communication links, and real consumption data.

Chapter 1. Introduction

2   Simulation Framework

The purpose of this chapter is to briefly describe the developed MATLAB simulation framework DiSC, detailed in Paper F. Many of the simulations conducted throughout my work is based on DiSC and it is therefore an important part of the thesis. The chapter is organized as follows. Section 2.1 summarizes the main contributions of DiSC. Next, in Section 2.2 the household data included with DiSC is presented. Then Section 2.3 provide details on some of the models included in DiSC, and Section 2.4 shortly introduces the Smart Energy Systems Laboratory at Aalborg University, which relies on the models implemented in DiSC. Finally, the results are summarized in Section 2.5.

2.1   Contributions

This section summarizes the main contributions of DiSC.

Real Consumption Data: Data for a one year period of approximately 1200 houses in Denmark is included, along with data from a supermarket refrigeration system, industrial load, commercial load, and agricultural load. This allows for realistic simulations studies. Details on the household consumption data is given in Section 2.2.

Realistic Stochastic Models: All the implemented models are based on standard models found in the litterateur, along with empirical data. Furthermore, all models include a control interface, making it possible for an external coordinator to access their flexibility. This allows for a wide variety of simulation studies spanning from fully centralized coordination to fully distributed coordination. Models such as wind turbine, solar PV, and EV mobility are all stochastic. Some of the implemented models are detailed in Section 2.3.

Modular MATLAB Model: The simulation framework is implemented using object orientated programming in MATLAB. This results in a modular
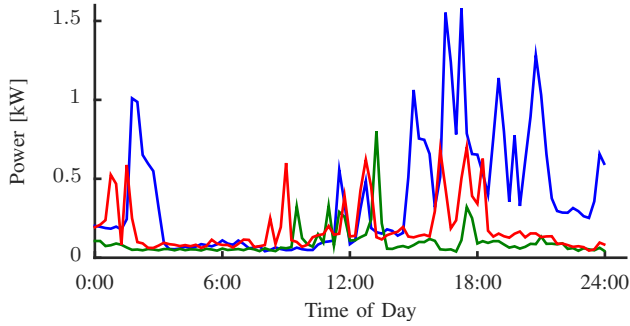
Fig. 2.1: Consumption profiles of three different households during a day in November 2011.

model, where it is easy to setup new simulation scenarios, implement new models, alter existing models, and add/remove assets on each bus. The simulation framework and data is freely available at [80].

2.2 Consumption Data

Many distribution system operators are logging consumption data with a high temporal resolution through smart meters, all the way down to a household level. This data is usually used for billing purposes and is not readily available to researchers, because of privacy issues. However, the data included in the DiSC simulation framework were obtained as anonymized data from the Danish DSO NRGi, and it represents about 1200 individual household consumption profiles from the area around the Danish city Horsens. Each profile has a temporal resolution of 15 minutes, spans more than a year, and have been validated by the DSO for billing purposes.

Significant variations between individual profiles reveals that basing household consumption patterns on an average profile is not possible. This is illustrated in Fig. 2.1, where consumption profiles from three different households are depicted. Not only do the individual profiles differ in magnitude but also in time. The data provided in the simulation framework will allow for realistic simulation scenarios, and is a key feature of DiSC.

Besides the household consumption data the framework also includes consumption data from an industrial load, a commercial load, an agricultural load and a supermarket refrigeration system.

2.3 Models

The purpose of this section is to demonstrate a subset of the models used in the following two chapters. A full list of implemented models can be found

in Paper F.

2.3.1 Electrical Grid

The implemented Newton-Raphson power flow solver [61] assumes a balanced three phase system, similar to other popular MATLAB power flow analysis tools, such as MATPOWER [116]. It is assumed that the high voltage grid is capable of delivering the active and reactive power needed; thus the frequency is kept constant.

2.3.2 Wind Turbine Model

The wind turbine model consist of a wind speed model based on the Van der Hoven Spectrum for the mean component and a von Karman spectrum for the turbulent component, a variable-speed, variable-pitch turbine, along with a control interface for active and reactive power.

The control interface consists of the following control modes for active power:

- Curtail active power (the maximum output of the wind turbine is limited below rated power),

And the following modes for reactive power:

- Constant power factor (the wind turbine ensures a reactive power output proportional to the active power output),

- Reference following on reactive power (the wind turbine will try to follow a reference on reactive power),

- Local voltage control (the reactive power output depends on local voltage measurements).

Different operating modes of the wind turbine model is illustrated in Fig. 2.2.

2.3.3 Solar Photovoltaic System

The solar power plant model consists of a solar irradiance model based on a stochastic Markov model dependent on cloud coverage [], a photovoltaic system model, along with a control interface identical to the wind turbines.

To illustrate the performance of the model, power production during one day in September is compared with the power production of a real household PV system located in Denmark. This comparison can be seen in Fig. 2.3.
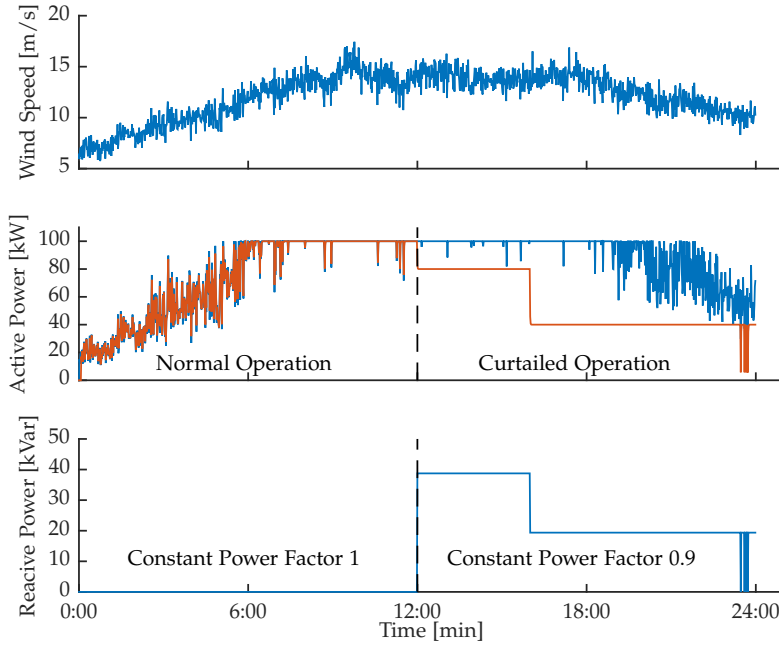
Fig. 2.2: 100 kW Wind turbine operating in normal mode and curtailed mode on active power, and with different power factors on reactive power.
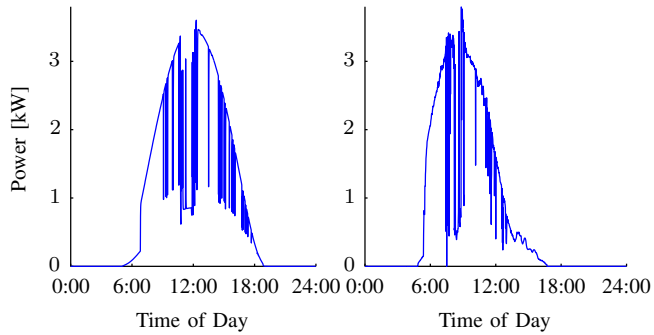
Fig. 2.3: Left; power production of the implemented solar PV model during a day in September. Right; power production of a real PV system during the same day.
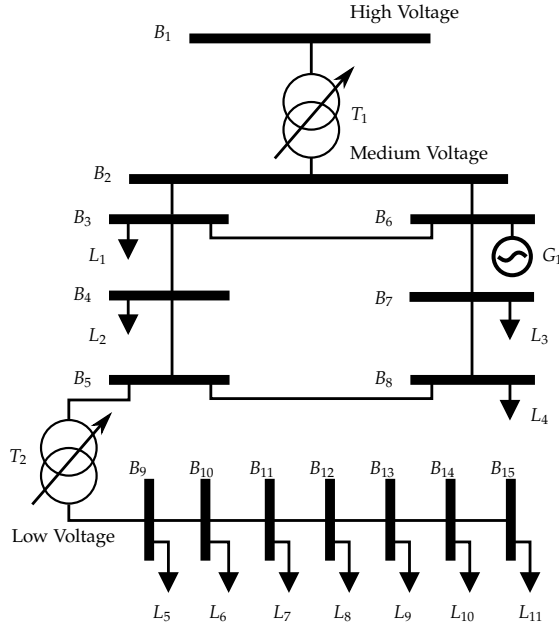
Fig. 2.4: Grid used in the simulation example. The generator on bus 6 (G_1), is a wind power plant. L_1 is an aggregated residential grid, L_2 is a commercial load, L_3 is an industrial load, L_4 is an agricultural load and L_5-L_{11} are aggregated residential loads of approx. 20 households each.

2.3.4 On-Load Tap Changing Transformer

The on-load tap changing transformer (OLTC) consist of a transformer model [61, p. 232] along with a control interface for changing tap position.

The transformers tap position can be controlled in two different modes

- Follow tap position reference (the OLTC will change tap-position according to a received reference position.),

- Local voltage control (the OLTC will automatically change tap-position according to locally measured voltage).

The operation of the OLTC model is demonstrated by an example considering the electrical distribution grid in Fig. 2.4, with a high penetration of wind power G_1. The resulting OLTC behavior on the MV and LV level is shown in Fig. 2.5. The tap-positions need to change often in order to keep the voltages within bounds.
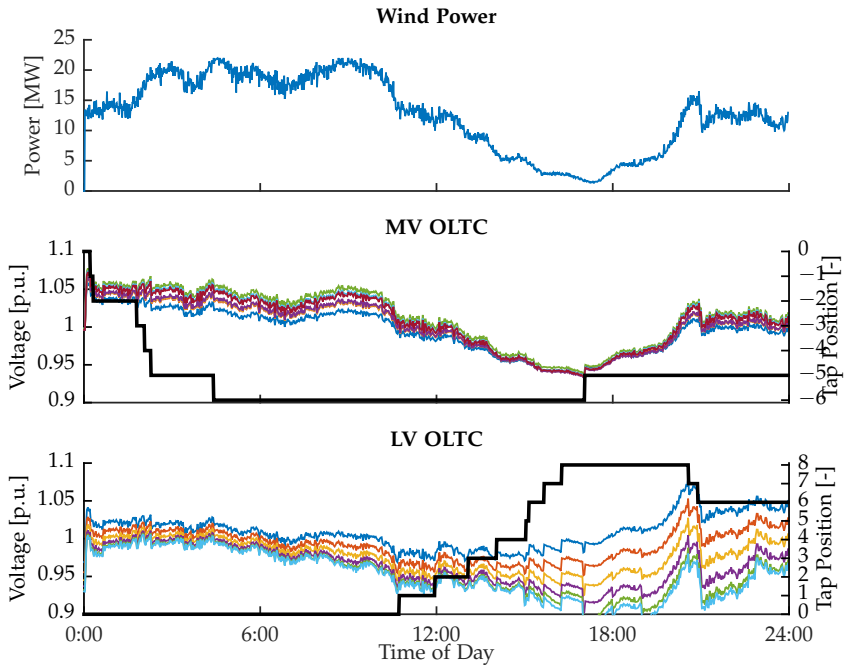
Fig. 2.5: Power production of a wind power plant consisting of ten 2.2 MW wind turbines along with the tap position of the HV/MV and MV/LV transformers. To ensure satisfactory voltage levels throughout the distribution grid, a total of 17 tap changes are needed, 7 on the HV/MV transformer and 10 on the MV/LV transformer.

Fig. 2.6: Picture of the Smart Energy Systems Laboratory at Aalborg University [12].

2.4 Test-Bed Implementation

The models contained in DiSC has been implemented in the *Smart Energy Systems Laboratory* at the Energy Department, Aalborg University [12]. The test-bed consist of a real-time energy systems emulator based on Opal-RT technology, a fully regenerative four quadrant power converter for emulating a distributed generation unit, A Controllable AC/DC Load is used to mimic the behavior of loads in a typical household, a communication network emulator for emulating different network technologies and topologies, three separate control layers as illustrated in Fig. 1.2, and real smart meters for logging data. Fig. 2.6 shows a picture of the test-bed.

The DiSC models have been converted to MATLAB Simulink and can directly be used within the Opal-RT framework.

2.5 Summary

This chapter introduced the power systems simulation framework DiSC. DiSC consist of a power flow solver, numerous flexible assets and grid components, along with real consumption data. In the following sections many of the conducted simulation studies are carried out using DiSC. DiSC should not be seen as a replacement of more detailed tools such as GridLab-D, but more as a compliment that allows for faster simulation scenario setup for testing grid-wide control solutions. However, it is the authors experience, that if it does not work in DiSC, it will not work in GridLab-D. DiSC and consumption data is freely available at [80].

3 Power Management

This chapter provides a summary of the main contributions within power management, detailed in the enclosed Paper A and Paper B. The chapter is organized as follows. Section 3.1 briefly states the main contributions within power management, followed by Section 3.2, which provides an example illustrating the hierarchical control structure. Then in Section 3.3 the control system on the medium voltage layer is detailed. Next, Section 3.4 describes the control system on the low voltage layer, and finally Section 3.5 summarizes the chapter.

3.1 Contributions

The contributions within power management are summarized in this section.

Load Modeling and Estimation: A simple linear model of uncontrollable loads is provided, which is intended to be used for model-based control. Specifically, it is shown how the power consumption of an aggregated residential grid can be modeled and used for online estimation. Furthermore, the work is validated based on smart meter measurements. Details on this contribution are provided in Section 3.3.1.

Control Structure Utilizing Load Estimations: A control scheme is developed, which utilizes the estimates of uncontrollable loads, to attenuate their impact on reference tracking. Further, the control scheme consist of a dynamic feedback loop for controlling flexible assets along with a dispatch algorithm for minimizing active power loss. Specifically, the control scheme uses the estimates of uncontrollable load as feedforward and incorporates asset dynamics in the dynamic feedback law. Under assumptions, such as bus voltages being known, the optimal dispatch problem can be shown to be convex, making it solvable even for a large distribution grid, with several busses. The control scheme is detailed in Section 3.3.2.

Adaptive Power Balancing over Unreliable Communication Networks: An adaptive control system is developed, for managing flexible assets in a low voltage residential grid towards a power reference. To coordinate the flexible assets the approach relies on a leader-follower consensus based formulation, where the leader agent updates its state according to a proportional and integral (PI) control law. To handle time-varying communication delays the PI control gains are adapted based on estimates of communication network state. The consensus framework was chosen for its applicability in large scale distributed systems, and for ensuring fairness in asset contribution. However, when closing the loop with a PI controller, the classical results within leader-follower consensus can no longer be applied. Section 3.4 details the adaptive leader-follower based control design and explain what is meant by fairness.

3.2 Example

This example considers the electrical distribution grid in Fig. 3.1. The grid consists of a medium voltage distribution grid and a low voltage residential distribution grid. There are flexible assets present on both layers of the distribution grid. The medium voltage grid controller (MVGC) receives a power reference and manages the flexible assets in the grid towards this reference. A second control unit (LVGC) placed at the secondary low voltage substation, ensures that the flexible assets in the low voltage grid act as one aggregated flexible asset seen from the MVGC. The MVGC implements the load estimation procedure detailed in Section 3.3.1, along wit the control scheme detailed in Section 3.3.2. The LVGC implements the adaptive control algorithm detailed in Section 3.4, which takes into account an unreliable communication.

In Fig. 3.2 the tracking performance of both controllers are seen. Fig. 3.3 shows the behavior of the flexible assets. To illustrate the adaptability of the LVGC to changes in communication network state, the communication delay along with control switching is depicted in Fig. 3.4, for a small window of the simulation in Fig. 3.2.

The overall system exhibits good tracking performance indicating that the developed control architecture enables a distribution grid to follow a power reference. Further, Fig. 3.4 shows how the LVGC adapts the controller according to communication network delays, and it can be observed that the system is stable.

In the following sections the different components of the hierarchical control structure are detailed.
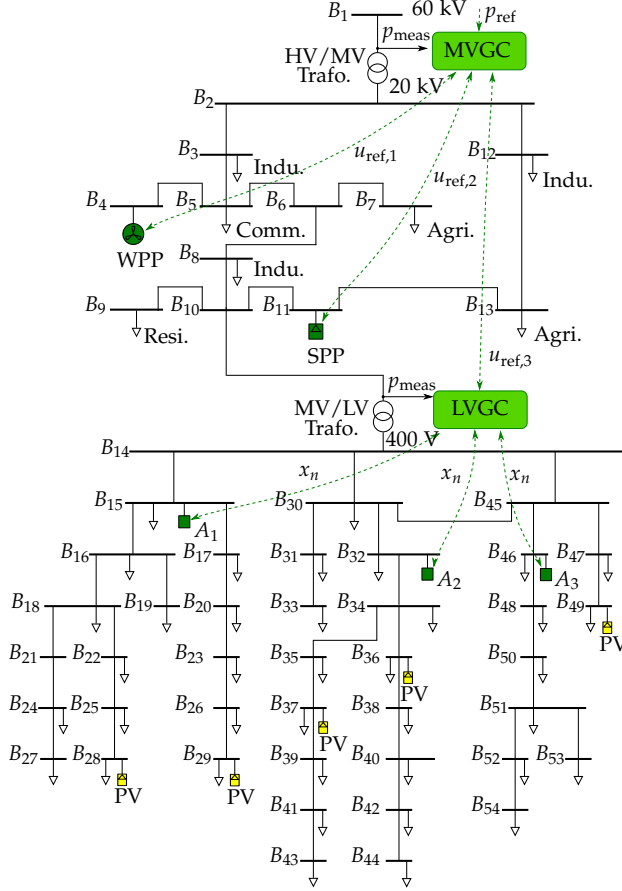
Fig. 3.1: Electrical distribution grid used in the introductory example. There are flexible assets present on both the medium and low voltage level, along with a controllers for managing the flexibility on both the MV and LV layer.
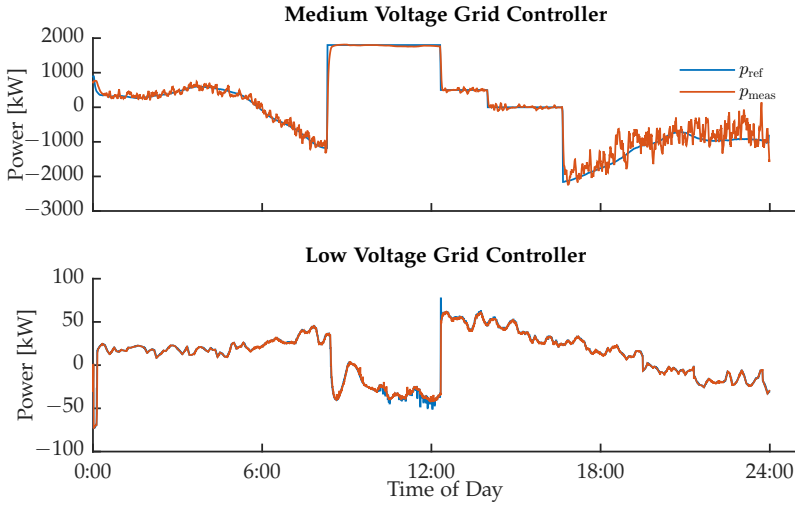
Fig. 3.2: Top: Tracking performance of the medium voltage controller, where oscillations are caused by fluctuations in wind power production. Bottom: Tracking performance of the low voltage grid controller, where it is observed that the LV grid cant follow the reference from approximately 8:00 - 13:00.
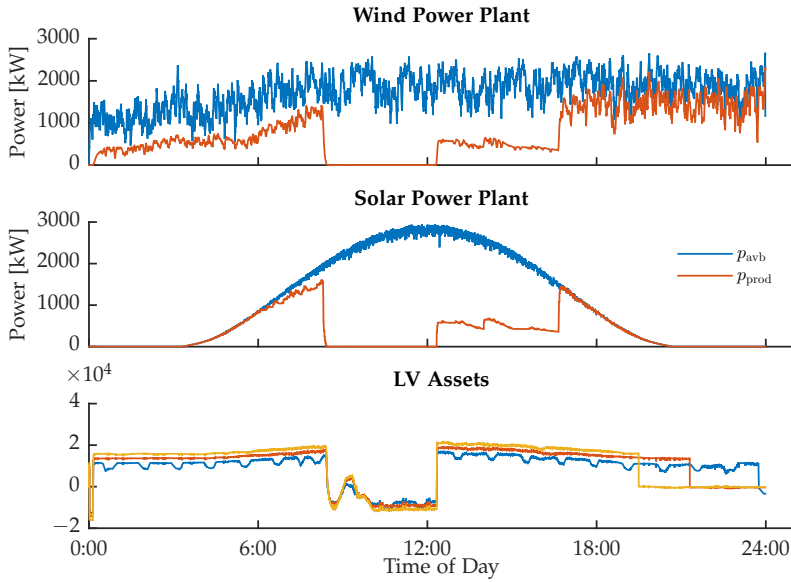
Fig. 3.3: Top: Available and produced power of the wind power plant. Middle: Available and produced power of the solar power plant. Bottom: power output of the three assets in the LV grid.
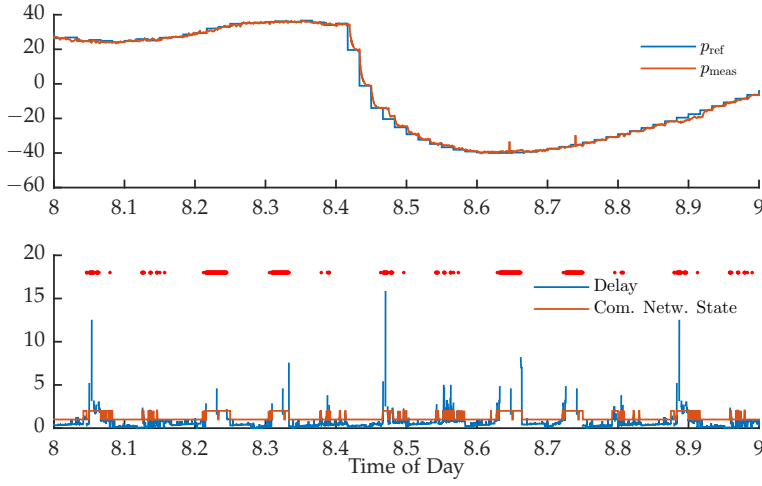
Fig. 3.4: Top: Reference tracking of the LVGC. Bottom: delay trace and controller switching pattern. The red dots represent packet loss.

3.3 Medium Voltage Layer

This section summarizes the contributions which are part of the *medium voltage grid controller*. First, details on the load estimation approach are given, followed by an example of how it can be incorporated into a control system. Next, a simple dispatch algorithm for minimizing active power loss is presented, and finally additional numerical examples are provided. The control system structure is shown in Fig. 3.5.

3.3.1 Load Modeling and Estimation

The uncontrollable load profiles from consumers can be seen as a disturbance affecting the performance of the control system. Knowledge of the uncontrollable load can be incorporated into the control strategy in different ways, e.g., using model predictive control (MPC) or the internal model principle. Obtaining a model of the uncontrollable part of a dynamic system is extremely valuable for the following reason: *A disturbance can be completely rejected, only if the controller contains a model of it* [37]. This is the motivation for developing the following model of the aggregated power consumption of a residential grid. The model is validated upon empirical data.

It can be observed from Fig. 3.6, that an aggregated residential load exhibits periodic behavior. It is well-known that this type of behavior can be captured by a linear model [48]. However, this has not been validated on smart meter measurements before.
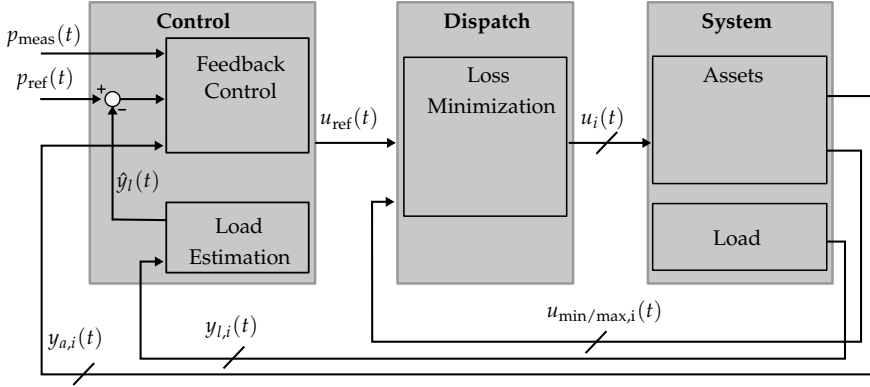
Fig. 3.5: Control system structure, with the system consisting of flexible assets, both production and consumption, inflexible load, and electrical grid. Based on estimation of inflexible load and reference signal the feedback controller calculates an output which is then dispatched to the flexible assets.

The load models can be combined with a Kalman filter to estimate the load, which can be used for feedforward in the control algorithm. The effectiveness of estimating the aggregated load of 200 households using the described model and a Kalman filter is demonstrated in Fig. 3.6. The model consist of two periodic models with frequencies; $\beta_{1,1} = \frac{2\pi}{24 \text{ hours}}$ and $\beta_{2,1} = \frac{2\pi}{12 \text{ hours}}$, to capture the bi-daily peaks. The convergence of the filter dependt on its tuning, a procedure which can be automated [13], and in this case it takes a couple of days to converge. See also Fig. 3.7 where the evolution of Kalman gains is illustrated.

The presented estimation method is seen as a main contribution for the following reasons; first, it has a low complexity, enabling easy implementation and fast deployment. Secondly, it has been verified on real data and shows good performance on both a step-ahead and day-ahead basis. Lastly, these types of estimates can be used in a wide variety of electrical grid control problems.

3.3.2 Medium Voltage Control System

The control system consist of a feedforward control from the load estimation, a feedback control based on the flexible assets, and a dispatch algorithm for minimizing active power loss.

Feedback Control

Even though the estimation method described in Sec. 3.3.1 shows good performance there are still discrepancies between the measured and estimated
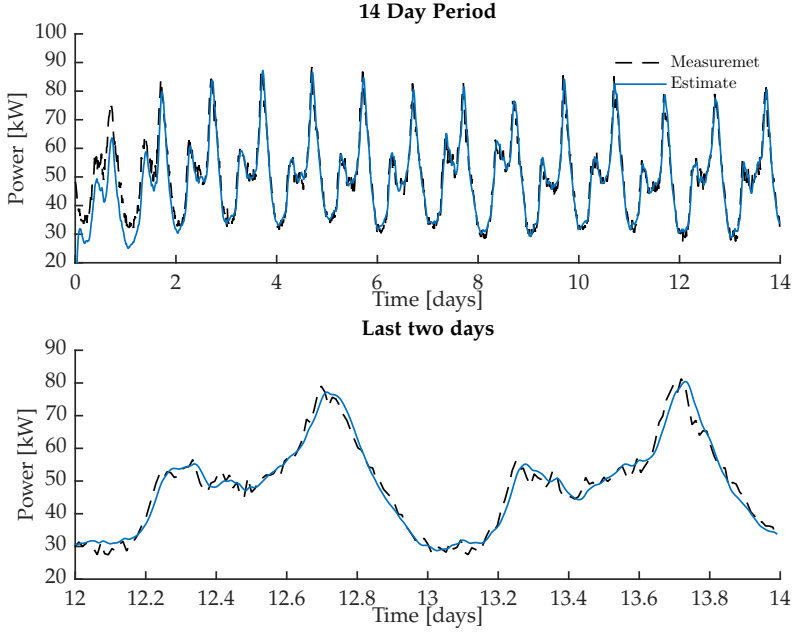
Fig. 3.6: Performance of proposed estimation method throughout a 14 day period. The measurement is a residential load, based on data from 200 houses in Denmark, sampled every 15 minutes. The two last days of the estimation is highlighted and it can be seen that even with a simplistic estimation model, good tracking capabilities are achieved.
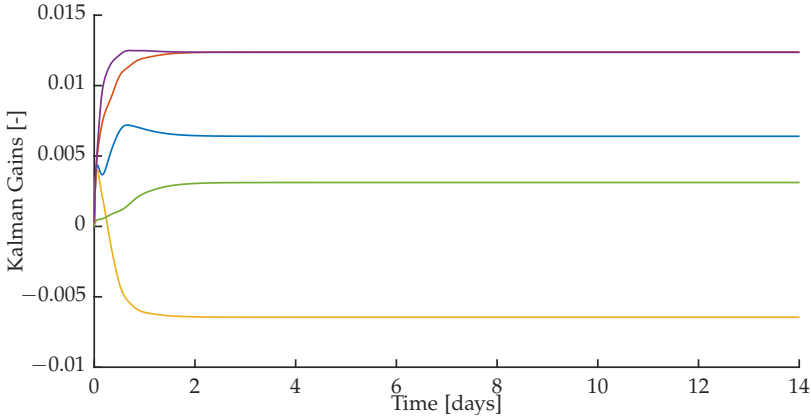
Fig. 3.7: Convergence of the Kalman Gains throughout the 14 day period.

output. Therefore, a dynamic feedback control law is formulated to handle

these discrepancies. All the controllable asset models are combined into one model as follows

$$\dot{x}(t) = A_a x(t) + B_a u_{\text{ref}}(t), \tag{3.1}$$

$$y_a(t) = C_a x(t), \tag{3.2}$$

where $x(t) \in \mathbb{R}^m$ represent the controllable system state vector, $A_a \in \mathbb{R}^{m \times m}$, $B_a \in \mathbb{R}^m$, and $C_a \in \mathbb{R}^m$ are parameters, $y_a(t) \in \mathbb{R}$ is the total active power output of all controllable assets and, $u_{\text{ref}}(t) \in \mathbb{R}$ is the input to the system.

Let $z(t) = \begin{bmatrix} r(t)^T & y_a(t)^T \end{bmatrix}^T$, with $r(t) \in \mathbb{R}$ being the reference signal in combination with the load estimate, i.e., $r(t) = p_{\text{ref}}(t) - \hat{y}_l(t)$, where $p_{\text{ref}}(t) \in \mathbb{R}$ is the reference signal received from an upper layer, $\hat{y}_l(t) = \sum_{i=1}^{S} y_{l,i}(t)$ is the feedforward signal from the load estimate, and $S \in \mathbb{N}$ is the number of estimated loads. The dynamic control law is given as

$$\dot{x}_c(t) = A_c x_c(t) + B_c z(t), \tag{3.3}$$

$$u_{\text{ref}}(t) = C_c x_c(t) + D_c z(t), \tag{3.4}$$

where $x_c(t) \in \mathbb{R}^m$ is the controller state and $u_{\text{ref}}(t) \in \mathbb{R}$ is the control output. The feedback control system parameters A_c, B_c, C_c, and D_c are determined using the controllable asset model along with state feedback gain, observer gain, and feedforward gain as follows

$$\dot{x}_c(t) = \underbrace{(A_a + B_a K + L C_a)}_{A_c} x_c(t) + \underbrace{\begin{bmatrix} M & -L \end{bmatrix}}_{B_c} z(t), \tag{3.5}$$

$$u_{\text{ref}}(t) = \underbrace{K}_{C_c} x_c(t) + \underbrace{\begin{bmatrix} N & 0 \end{bmatrix}}_{D_c} z(t), \tag{3.6}$$

where $K \in \mathbb{R}^m$ is the feedback gain, $L \in \mathbb{R}^m$ is the observer gain, $M \in \mathbb{R}^m$ is the observer feedforward gain, and $N \in \mathbb{R}^m$ is the control feedforward gain. Both M and N are determined using the zero assignment method [40, p. 510], ensuring unity gain from reference to output. The feedback gain, K and observer gain, L are designed such that $A_a + B_a K$ and $A_a + L C_a$ are both Hurwitz.

Dispatch Algorithm

The control signal, $u_{\text{ref}}(t)$, produced by the controller detailed above, can be passed through a dispatch algorithm with various objectives. This work considers active power loss minimization, where a simple approach is taken. Assumptions on knowledge of bus voltages and grid frequency are applied,

Method	Tracking Error (RMS)		Power Loss	
	[kW]	%	[MWh]	%
Uni. Disp.	94.0	100.0	0.33	100.0
Prop. Disp.	94.8	100.8	0.32	97.0

Table 3.1: Comparison between the proposed dispatch algorithm and uniformly distributing the power among the flexible assets. Total grid loading is 14 MWh, and the results have been normalized to the uniform dispatch case.

which results in a convex optimization problem.

$$
\begin{aligned}
\min_{u_1(t),\ldots,u_m(t)} \quad & s^*(t)B(t)s(t) \\
\text{s.t.} \quad & \textstyle\sum_{i=1}^{m} u_i(t) = u_{\text{ref}}(t) \\
& u_{\min,i}(t) \le u_i(t) \le u_{\max,i}(t),
\end{aligned}
\tag{3.7}
$$

with variables $u_1, \ldots, u_m$ and data $u_{\min,1}(t)$, $\ldots$, $u_{\min,m}(t)$, $u_{\max,1}(t)$, $\ldots$, $u_{\max,m}(t)$, $q_1, \ldots, q_n$, $v_1(t), \ldots, v_n(t)$, $\hat{p}_l(t)$, $u_{\text{ref}}(t)$, and $B(t)$. It should be noted that the decision variables u_i represent active power injection/ consumption at flexible asset busses. The construction of $B(t)$ is provided in Paper A and results in a convex problem. What should be noted from the formulation of the problem in (3.7), is that it scales well with the number of variables, making it applicable even for large distribution grids with numerous flexible assets. The proposed dispatch algorithm has been compared to a strategy of uniformly dispatching set-points for the flexible assets. The results are summarized in Table 3.1.

3.4 Low Voltage Layer

This section summarizes the contributions which are part of the *low voltage grid controller*. First, the communication network state estimator is briefly mentioned. Next, the adaptive control algorithm is detailed. Finally, additional numerical examples are given.

3.4.1 Communication Network State Estimation

The communication network is modeled as having a finite number of states $S = \{S_1, \ldots, S_N\}$, where each state represent a level of congestion. For each state a maximum delay, τ_i, is associated and based on this delay a controller for each state, S_i is designed. For more information on the communication network state estimation approach the reader is referred to Paper B.

The following section elaborate on the adaptive control design procedure.

3.4.2 Adaptive Controller Design

The purpose of this section is to describe the adaptive power balancing control algorithm, which manages the flexible assets over a communication network with time-varying characteristics. First, a controller is designed under the assumption of ideal communication, followed by the design of an adaptive algorithm, that takes into account the change in communication network state. The control system architecture is illustrated in Fig. 3.8.
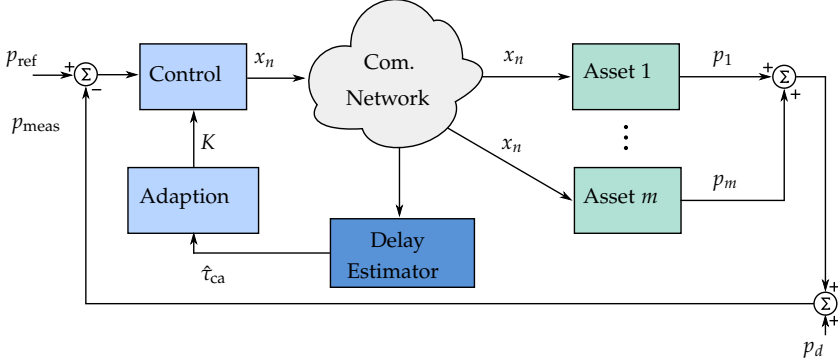
Fig. 3.8: Control system architecture. Controller gains, $(K_{P,i}, T_{I,1})$, are adapted based on estimates of the communication network state, $\widehat{S}_i$.

3.4.3 Control under Ideal Communication

The power balancing controller is based on a consensus approach, which is a natural way of formulating networked control systems that may experience time-varying delays and changing network topologies [75, 88]. Power balancing is a tracking problem, which in a consensus setting is solved by a leader-follower approach, where the leader agent (in our case the LVGC) determines the reference which all follower agents (the flexible assets) need to follow.

From leader-follower consensus the following result is used. Consider a dynamic network of agents connected through a communication graph $G = (V, E)$. Let each follower agents dynamics be given by a first-order system, and let the number of agents, including the leader be denoted by $n = |V|$. Without the loss of generality let agent n be the leader and let the remaining $n - 1$ agents apply the protocol

$$u_i = \gamma_i x_i - \sum_{j \in N_i} a_{ij}(x_i - x_j), \tag{3.8}$$

where $\gamma_i \in \mathbb{R}$ is a local control gain and $A = [a_{ij}] \in \mathbb{R}^{n \times n}$ is the graph adjacency matrix. Let $u_n = 0$ and $\gamma_i = \frac{a_i}{b_i}$, then the closed loop system can be

written as

$$\dot{x} = -Lx, \tag{3.9}$$

where $L \in \mathbb{R}^{n \times n}$ is the graph Laplacian, with all entries of the last row equal to zero. The system in (3.9) reaches leader-follower consensus, i.e.,

$$x_i(t) \to x_n(t), \ \forall i \in V \setminus \{n\}, \text{ for } t \to \infty, \tag{3.10}$$

if and only if the graph G has a directed spanning tree, with agent n as root, see Theorem 3.2 in [89, p. 57]. However, this result cannot directly be used when the leader updates it state dynamically e.g., by a control law. This is illustrated in the following sections.

Leader Agent Dynamics

Let the leader agent (agent n) update its state value according to a proportional integral (PI) control law. As already stated the above result from leader-follower consensus no longer applies.

The leader dynamics is given as

$$\dot{x}_n(t) = u_n = K_P e(t) + \frac{K_P}{T_I} x_I(t), \tag{3.11}$$

$$\dot{x}_I(t) = e(t),$$

where $e(t) = p_{\text{meas}}(t) - p_{\text{ref}}(t)$ is the tracking error, $x_I \in \mathbb{R}$ is the integral state, $K_P \in \mathbb{R}$ is the proportional gain, and $T_I \in \mathbb{R}$ is the integral time. The closed loop systems is then given by

$$\begin{bmatrix} \dot{x} \\ \dot{x}_I \end{bmatrix} = A_{cl} \begin{bmatrix} x \\ x_I \end{bmatrix} + B_r p_{\text{ref}} + B_w p_d \tag{3.12}$$

$$p_{\text{meas}} = \begin{bmatrix} C & 0 \end{bmatrix} \begin{bmatrix} x \\ x_I \end{bmatrix} + p_d,$$

with

$$A_{cl} = \begin{bmatrix} -L + K_P BC & \frac{K_P}{T_I} B \\ C & 0 \end{bmatrix}, \tag{3.13}$$

$$B_r = \begin{bmatrix} -K_P B^T & -1 \end{bmatrix}^T, \tag{3.14}$$

$$B_w = \begin{bmatrix} K_P B^T & 1 \end{bmatrix}^T. \tag{3.15}$$

Notice that the system can be viewed as a single input single output (SISO) system, allowing the use of classical frequency based control design methods, such as root locus. In the following the proposed design procedure is extended to a system with communication delays, and a gain scheduling procedure, that ensures stability for different magnitudes of delays, is described.

3.4.4 Control under Non-Ideal Communication

To handle the problem of introducing delays between the leader and the followers, the system is augmented with a delay system, and it is assumed that all communication links experience the same delay. The delay is modeled by a second order Padé approximation, resulting in the following closed-loop system

$$\begin{bmatrix} \dot{x} \\ \dot{x}_d \\ \dot{x}_I \end{bmatrix} = A_{cl} \begin{bmatrix} x \\ x_d \\ x_I \end{bmatrix} + B_r p_{\text{ref}} + B_w p_d, \tag{3.16}$$

$$p_{\text{meas}} = \begin{bmatrix} C & 0 & 0 \end{bmatrix} \begin{bmatrix} x \\ x_d \\ x_I \end{bmatrix} + p_d,$$

with

$$A_{cl} = \begin{bmatrix} -L + K_{\text{P}} BC & BC_d & \frac{K_{\text{P}}}{T_{\text{I}}} B \\ K_{\text{P}} B_d C & A_d & \frac{K_{\text{P}}}{T_{\text{I}}} B \\ C & 0 & 0 \end{bmatrix}, \tag{3.17}$$

$$B_r = \begin{bmatrix} -K_{\text{P}} B^T & -K_{\text{P}} B_d^T & -1 \end{bmatrix}^T, \tag{3.18}$$

$$B_w = \begin{bmatrix} K_{\text{P}} B^T & K_{\text{P}} B_d^T & 1 \end{bmatrix}^T. \tag{3.19}$$

Next, a gain scheduling method for adapting the control according to communication network state is presented.

3.4.5 Adaptive Gain Scheduling

It is possible to design a collection of controllers, which are resilient to different delays and then switch between the controllers according to estimates on communication network state. This setup is conceptually illustrated in Fig. 3.9.

The strategy of adapting to communication network state is compared to strategies of only applying a controller tuned for a non congested network state, and only applying a controller tuned for the congested network state. The results are summarized in Table 3.2, and shows that the adaptive control approach outperforms the strategy of applying a single controller.

3.5 Summary

This chapter summarized the contributions within power management. An example illustrating the hierarchical control architecture was presented. Details was given on all the components of this structure. A disturbance model
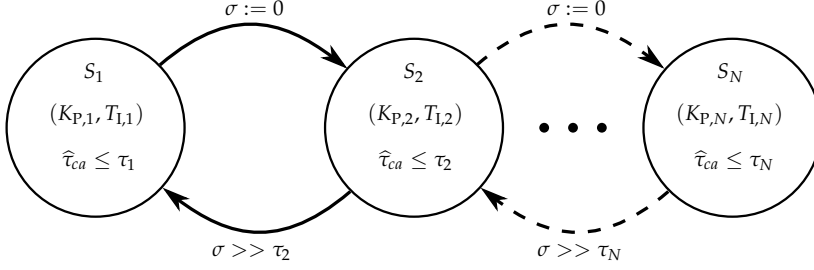
Fig. 3.9: Conceptual diagram of how the switching between communication network states affects the control parameters. The clock σ has been added to implement a minimum dwell time before switching to a controller designed for smaller delays, i.e., a more aggressive controller.

Scenario	Mean RMSE [kW]	95% Confidence Interval [kW]
Constant Control, S_1	2.422	[2.185 2.659]
Constant Control, S_2	2.197	[2.117 2.277]
Adaptive Control	1.303	[1.257 1.349]

Table 3.2: Comparison between the adaptive controller and applying either a constant controller tuned for the non-congested state S_1 or one tuned for the congested state S_2.

for capturing the uncontrollable behavior of loads was provided, and it was shown how this model could be included in a feedforward control approach. Further, a combined control and dispatch solution for allowing the distribution grid to follow a power reference, was detailed. On the low voltage level a control scheme for managing flexible assets over an unreliable communication network was introduced.

Chapter 3. Power Management

4 Voltage Control

This chapter summarizes the main contributions within voltage control, detailed in the enclosed Paper C, Paper D, and Paper E. The chapter is organized as follows. Section 4.1 briefly states the main contributions within voltage control. Next, in Section 4.2 an approach for reaching fairness in reactive power voltage control is detailed. Following in Section 4.3, the *voltage constraint satisfaction problem* is presented, and finally Section 4.4 describes the four quadrant voltage control strategy, which is based on both active and reactive power support.

4.1 Contributions

The contributions within voltage control are summarized in this section.

Fairness in Local Distributed Reactive Power Voltage Control: A method for fairly distributing the reactive power output of systems providing local volt/var control. Fairness means that all systems have the same reactive power injection over time. The strategy is based on dispatching droop gains for the local controllers, where new droop gain values are computed based on minimizing the difference between the local volt/var controllers output. The optimization problem is based on historical data, along with knowledge of electrical grid structure. The problem is convex, making it solvable even for a large distribution grid with numerous systems offering volt/var control.The procedure is detailed in Section 4.2.

The Voltage Constraint Satisfaction Problem: A safety verification procedure for determining if the bus voltages in a power system will always be within bounds. The procedure relies on dynamic models of system components and a polynomial reformulation of the power flow equations to arrive at a polynomial program, solvable by existing tools. This verification procedure leaves out the need for simulation studies. The contribution is detailed in Section 4.3.

The Four Quadrant Voltage Controller: A simple local voltage control law, which utilizes the full four quadrants of the active and reactive power plane. The control strategy is based on first using reactive power for voltage control and only if voltages exceed a predefined limit begin to use active power for voltage control. This strategy fully utilizes a systems ability to offer voltage control. The contribution is detailed in Section 4.4.

4.2 Fairness in Volt/Var Control

This section summarizes the results on fairness in local volt/ var control. First, the considered system structure and models are presented. Then the coordination approach is derived. Finally, simulation example are provided to illustrate the approach.

4.2.1 System Structure and Models

Throughout the work it is assumed that a distribution system operator (DSO) is capable of communicating with assets (systems offering volt/var support) and busses through smart meters. Based on the received data and knowledge of electrical grid structure, the DSO calculates and dispatches droop gains for the local volt/var controllers implemented by the aforementioned assets. To maintain the simple and reliable nature of the local droop controllers, gains are not updated continuously, but only at certain sample times e.g., once or twice a day. The architecture of the control system is depicted in Fig. 4.1.

To model the electrical grid the standard model is adopted [61, p. 255]. The local voltage controllers are based on the classical droop curve [61, p. 642]. Throughout it is assumed that the voltages evolve closely around a specified operating point. This enables the use of the linearized power flow equations [61, p. 264].

4.2.2 Coordination Approach

To reach fairness between assets offering local volt/var control, the problem is formulated as an optimization problem, where the objective is to minimize difference between reactive power output of assets. What should be noted from the presented algorithm is its robustness against communication failures and limited need for communication; if e.g., the DSO looses connection to an asset, the asset can just continue with the previous dispatched controller gain. The frequency of updating controller gains can freely be chosen by the DSO, i.e., it could be daily, weekly, or even seasonally. This results in a functionality which is easy to implement and serves the needs of both the DSO and the asset owner.
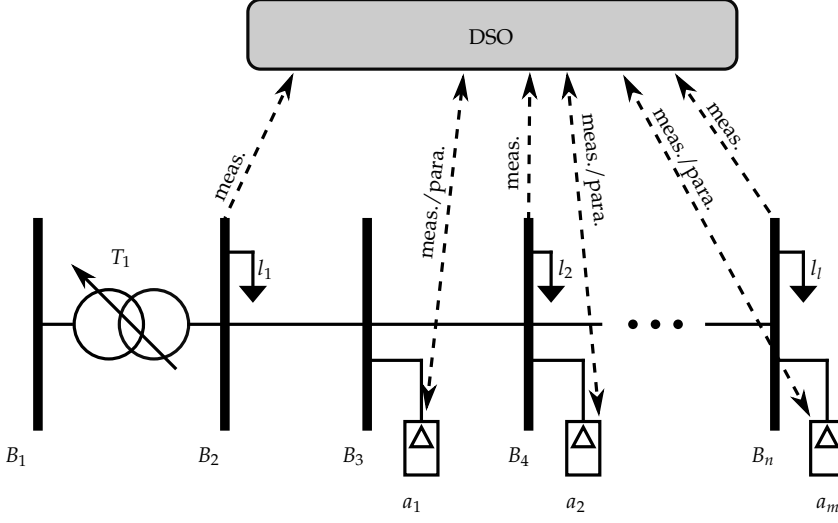
Fig. 4.1: Overview of the system architecture, consisting of a radial distribution grid with n busses, l inflexible loads, m flexible assets, and a DSO as the central coordinator. The dashed arrows represent communication channels. The parameters sent from the DSO to the assets, are droop gains.

Objective Function

Fairness is defined as all assets having the same reactive power output in the window $\mathcal{K} = \{\kappa - H, \dots, \kappa - 1\}$, where $H \in \mathbb{N}$ is the horizon to look back in time. Let $k \in \mathcal{K}$ be the sample index. Thereby, the objective function can be written as

$$F = \sum_{k \in \mathcal{K}} ||D\Delta q_k||_1, \tag{4.1}$$

where $F \in \mathbb{R}$ is the objective function, $|| \cdot ||_1$ denotes the 1-norm, $\Delta q_k \in \mathbb{R}^m$ is a column vector representing reactive output of assets at sample k, and $D \in \mathbb{R}^{m-1 \times m}$ is an upper triangular difference matrix. The structure of D ensures that each entry in Δq_k is only subtracted once from any other entry.

Constraints

Knowledge of the electrical grid structure is applied to ensure that voltage magnitudes are kept within constraints. The constraints on voltage magnitudes are as follows

$$\begin{bmatrix} \Delta\delta_k \\ \Delta V_k \end{bmatrix} = J^{-1} \begin{bmatrix} p_k^{\text{meas}} \\ q_k^{\text{meas}} - B\Delta q_k^{\text{meas}} + B\Delta q_k \end{bmatrix}, \tag{4.2}$$

$$\underline{\Delta V} \le \Delta V_k \le \overline{\Delta V}, \tag{4.3}$$

where J is the Jacobian of the power flow equations, $\underline{\Delta V}, \overline{\Delta V} \in \mathbb{R}^{n-1}$ are lower and upper bounds on voltage magnitudes, respectively, and $B \in \mathbb{R}^{(n-1) \times m}$ maps assets to busses. Each entry in the vector Δq_k is given by the local volt/var droop control strategy

$$\Delta q_i = K_i (V_i^{\text{ref}} - V_i^{\text{meas}}), \tag{4.4}$$

$$\tag{4.5}$$

Optimization Problem

The optimization problem which must be solved at sample κ, is given by

$$
\min_{K_1, \ldots, K_m \in \mathbb{R}} \quad \sum_{k=\kappa-H}^{\kappa-1} ||D \Delta q_k|| \tag{4.6}
$$
$$
\text{s.t.} \quad (4.2), (4.3), (4.4)
$$

with decision variables $K_1, \ldots, K_m$. Notice that the problem is convex and scales well with both number of variables and horizon.

4.2.3   Numerical Example

This section illustrates the proposed solution through simulation studies. The method is applied to a radial distribution feeder equipped with an on-load tap-changer (OLTC) at the transformer station. All asset are identical PV systems with a rated apparent power of 6.5 kVA, and equal initial gains $K_i = -200$. The OLTC is present to illustrate how traditional voltage control would be carried out if no asset volt/var control is active and to demonstrates that when implementing new voltage control features, those already in place, can not be ignored. Three simulations are carried out; one with only the OLTC responsible for voltage control, one where all assets are applying local voltage control with equal gains $K_i = -200$, and one demonstrating the presented method

The three simulation scenarios are compared in Table 4.1 and 4.2, and the evolution of volt/var control gains from the third simulation are shown in Fig. 4.2.

It is observed that a significant reduction in tap changes is achieved with distributed volt/var control, along with a reduction in voltage variation. From Table 4.2 it is seen that the maximum difference between the assets reactive power output, has been decreased significantly, when gains are regularly updated. Another interesting observation is that when controller gains are updated, the system adapts to seasonal changes, which further motivates the developed approach.

Method	Taps		Voltage (STD)		Total Δq	
	[-]	%	[p.u.]	%	[MVArh]	%
Only OLTC	425	100	0.0131	100	-	-
Identical K_i	91	21	0.0124	94	29.2	100
Updated K_i	67	16	0.0125	95	30.1	103

Table 4.1: Comparison between different methods of applying voltage control for a one year period. The voltage standard deviations are the maximum throughout the entire grid.

Asset	Ident. K_i	Updated K_i	Diff.
	$\sum \lvert\Delta q_i\rvert$ [MVArh]	$\sum \lvert\Delta q_i\rvert$ [MVArh]	%
a_1	3.1	4.6	33
a_2	4.4	5.0	11
a_3	3.7	4.9	24
a_4	6.1	5.2	-18
a_5	6.6	5.6	-19
a_6	5.3	4.9	-9
Max Diff.	3.5	1.0	60

Table 4.2: Difference in total reactive power delivered by the assets for a one year period. Maximum difference can be seen as an evaluation of (4.1).
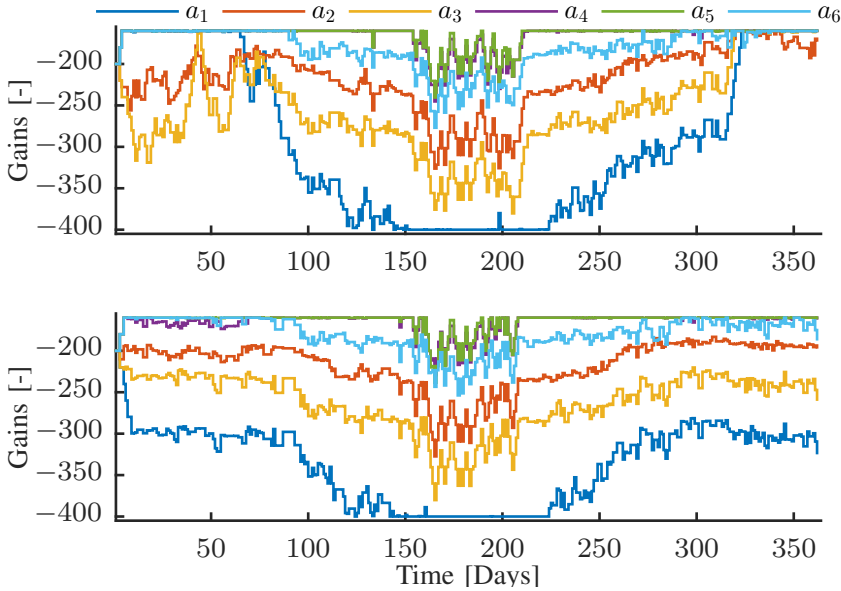

Fig. 4.2: Evolution of volt/var control gains over time. Top: with the OLTC active, 67 tap-changes performed. Bottom: With the OLTC inactive.

4.3 The Voltage Constraint Satisfaction Problem

This section details the proposed method for verifying that voltages throughout a power system will be within bounds. First, the problem is formally stated, followed by an introduction to safety verification through the barrier certificate method. Then the original problem is reformulated to a polynomial program, and it is illustrated that solving the polynomial program is equivalent to solving the original voltage constraint satisfaction problem.

4.3.1 Problem Formulation

First the model is detailed, followed by a formal statement of *the voltage constraint satisfaction problem*. Notice, it is assumed that the electrical grid is connected to an entity capable of ensuring power balance, i.e., the grid is connected to a slack bus [61, pp. 255].

System Model

The electrical grid is modeled by an admittance matrix $Y \in \mathbb{C}^{m \times m}$ [61, pp. 199]. To each bus a complex power injection $s_i = p_i + \mathrm{j}q_i$ and a phasor voltage $v_i = V_i e^{\mathrm{j}\delta_i}$ is associated, where $p_i \in \mathbb{R}$ is the active power injection and $q_i \in \mathbb{R}$ is the reactive power injection, $V_i \in \mathbb{R}$ denotes voltage magnitude, and $\delta_i \in [-\pi/2, \pi/2]$ the voltage phase angle. The vector of bus voltages is given by $v \in \mathbb{C}^m$ and the vector of complex power injections can be expressed as

$$s = \mathrm{diag}(v)(Yv)^* \in \mathbb{C}^m. \tag{4.7}$$

By defining the index sets $I_i = N_i \cup \{i\}$, Eq. (4.7) can be divided into the active and reactive power component resulting in the well-known power flow equations

$$p_i = \sum_{j \in I_i} V_i V_j \left[\mathrm{Im}(Y_{ij}) \sin(\delta_i - \delta_j) + \mathrm{Re}(Y_{ij}) \cos(\delta_i - \delta_j) \right], \tag{4.8a}$$

$$q_i = \sum_{j \in I_i} V_i V_j \left[\mathrm{Re}(Y_{ij}) \sin(\delta_i - \delta_j) - \mathrm{Im}(Y_{ij}) \cos(\delta_i - \delta_j) \right]. \tag{4.8b}$$

The active and reactive power injections in (4.8) are governed by dynamic systems describing generation and demand behavior at each bus

$$\dot{x}_i = f_i(x_i, V_i, \delta_i, d_i), \tag{4.9a}$$

$$\begin{bmatrix} p_i \\ q_i \end{bmatrix} = \varphi_i(x_i, V_i, \delta_i), \tag{4.9b}$$

where $x_i \in X_i \subseteq \mathbb{R}^n$ is the state, $d_i \in D_i \subseteq \mathbb{R}^l$ is the unknown but bounded disturbance input, $f_i : X_i \times D_i \to X_i$ is the vector field, and $\varphi_i : X_i \to \mathbb{R}^2$ the output.

The Voltage Constraint Satisfaction Problem

The aim is to solve the voltage constraint satisfaction problem described in Problem 1.

Problem 1 (Voltage Constraint Satisfaction). *Given an electrical grid admittance matrix $Y \in \mathbb{C}^{m \times m}$, vector fields $f_i : X_i \times \mathbb{R}_+ \times \mathbb{R} \times D_i \to X_i$, output maps $\varphi_i : X_i \times \mathbb{R}_+ \times \mathbb{R} \to \mathbb{R}^2$, disturbance sets D_i, upper and lower bounds on voltage magnitude $\overline{V}, \underline{V} \in \mathbb{R}_+$, and bound on difference in bus voltage phase angle $\overline{\Delta}_{ij} \in \mathbb{R}_+$, for $i = 1, \ldots, m$, show that voltage constraints*

$$\underline{V} \leq V_i \leq \overline{V}, \qquad\qquad i \in \mathcal{V},$$
$$\overline{\Delta}_{ij} \geq |\delta_i - \delta_j|, \qquad\qquad (i, j) \in \mathcal{E},$$

are always satisfied, for the system given by (4.8) and (4.9).

4.3.2 Safety Verification

To solve Problem 3, a safety verification technique known as the barrier certificate method is applied. The original problem is reformulated to polynomial form and safety for this system is defined.

Problem Reformulation

For convenience we write $\tilde{z}_i = (z_i, z_{m+i}, z_{2m+i})$ and let $z_i = V_i$, $z_{m+i} = \sin(\delta_i)$, and $z_{2m+i} = \cos(\delta_i)$. Next, it is shown that $(V_i, \delta_i, x_i, d_i)$ is a solution to Problem 3, if $(\tilde{z}_i, x_i, d_i)$ is a solution to the polynomial reformulation given by

$$\dot{x}_i = f_i(x_i, \tilde{z}_i, d_i), \tag{4.10a}$$
$$0 = \varphi_i(x_i, \tilde{z}_i) - \psi_i(\tilde{z}_{I_i}), \tag{4.10b}$$
$$0 = z_{m+i}^2 + z_{2m+i}^2 - 1, \tag{4.10c}$$
$$0 \leq \begin{bmatrix} \overline{V} - z_i \\ z_i - \underline{V} \\ \widehat{\Delta}_{ij} - z_{m+i}z_{2m+j} + z_{2m+i}z_{m+j} \\ \widehat{\Delta}_{ij} + z_{m+i}z_{2m+j} - z_{2m+i}z_{m+j} \end{bmatrix}, \tag{4.10d}$$

for all $i = 1, \ldots, m$.

The power flow equations (4.8) have been put on polynomial form by using the trigonometric identities

$$\sin(\delta_i - \delta_j) = \sin(\delta_i)\cos(\delta_j) - \cos(\delta_i)\sin(\delta_j), \qquad (4.11)$$

$$\cos(\delta_i - \delta_j) = \cos(\delta_i)\cos(\delta_j) + \sin(\delta_i)\sin(\delta_j), \qquad (4.12)$$

resulting in

$$\psi_i(z_{I_i}) = \begin{bmatrix} \sum_{j \in I_i} z_i z_j \left(\alpha_{ij}[z_{m+i}z_{2m+j} - z_{2m+i}z_{m+j}] + \beta_{ij}[z_{2m+i}z_{2m+j} + z_{m+i}z_{m+j}] \right) \\ \sum_{j \in I_i} z_i z_j \left(\beta_{ij}[z_{m+i}z_{2m+j} - z_{2m+i}z_{m+j}] - \alpha_{ij}[z_{2m+i}z_{2m+j} + z_{m+i}z_{m+j}] \right) \end{bmatrix},$$

where $\widehat{\Delta}_{ij} = \sin(\overline{\Delta}_{ij})$, $\alpha_{ij} = \mathrm{Im}(Y_{ij})$, $\beta_{ij} = \mathrm{Re}(Y_{ij})$, and equality constraint (4.10c) is added to ensure equivalence between the new variables and the sine and cosine functions. Further, it has been used, that for $(\delta_i, \delta_j) \in [-\pi/2, \pi/2]$ it holds that $\sin(|\delta_i - \delta_j|) = |\sin(\delta_i - \delta_j)|$, to rewrite constraints on the voltage phase angle.

Safety

To apply the barrier certificate method safety must formally be defined for the new system, which is a dynamic algebraic system. This is done following the lines of [83].

Definition 1 (Safety of Differential Algebraic System). *Given the differential algebraic system*

$$\dot{x} = f(x, z, d), \qquad (4.13)$$

$$0 = h(x, z), \qquad (4.14)$$

the differential state set $X \subseteq \mathbb{R}^n$, the algebraic state set $Z \subseteq \mathbb{R}^k$, the initial set $(X_0, Z_0) \subseteq X \times Z$, the unsafe set $(X_u, Z_u) \subseteq X \times Z$, and the disturbance set $D \subseteq \mathbb{R}^l$. The system is safe, if there exist no time instant $T \geq 0$ and an unknown but bounded disturbance $d : [0, T] \to D$ that results in an unsafe system trajectory, i.e., a trajectory $x : [0, T] \to X$ satisfying $x(0) \in X_0 \cap \{x \in X \mid 0 = h(x, z), z \in Z_0\}$, $x(T) \in X \cap (\{x \in X \mid 0 = h(x, z), z \in Z_u\} \cup \{x \in X_u \mid 0 = h(x, z), z \in Z\})$, and $x(t) \in \{x \in X \mid 0 = h(x, z), z \in Z\}$ for all $t \in [0, T]$.

Next it is shown how the barrier certificate for dynamic systems in [83], can be extended to dynamic algebraic systems by defining the state, initial, and unsafe sets according to the additional algebraic constraints and variables.

Barrier Certificate for Differential Algebraic System

The barrier certificate method is applied to verify safety of the differential algebraic system in (4.13) and (4.14). Consider a system described by ordinary

differential equations

$$\dot{x} = f(x, z, d), \tag{4.15}$$

with the sets X', X_0', and X_u' defined as follows

$$X' = \{(x, z) \mid 0 = h(x, z), x \in X, z \in Z\}, \tag{4.16}$$

$$X_0' = \{(x, z) \mid 0 = h(x, z), x \in X_0, z \in Z_0\}, \tag{4.17}$$

$$X_u' = \{(x, z) \mid 0 = h(x, z), x \in X, z \in Z_u\} \cup \tag{4.18}$$

$$\{(x, z) \mid 0 = h(x, z), x \in X_u, z \in Z\},$$

where X, $X_0 \subseteq X$, and $X_u \subseteq X$ are as stated in Definition 1.

Let the system trajectories be initialized at $x(0) \in X_0'$ and let the unsafe region be given by X_u'. Suppose there exists a barrier certificate, $B : X \to \mathbb{R}$, that satisfies the following conditions:

$$B(x) \le 0 \quad \forall x, \in X_0', \tag{4.19}$$

$$B(x) > 0 \quad \forall x, \in X_u', \tag{4.20}$$

$$\frac{\partial B}{\partial x}(x) f(x, z, d) \le 0 \quad \forall (x, z, d) \in X' \times D, \tag{4.21}$$

then safety of the system (4.15) is guaranteed. Next, we use the above definition to state the polynomial programming problem of finding a barrier certificate.

Barrier Certificate for Power System

Instead of solving Problem 1 directly, the established relation is used to solve the problem of computing a barrier certificate for the differential algebraic system. This problem is stated in Problem 2.

Problem 2 (Find Barrier Function for Power System). *Given an electrical grid admittance matrix $Y \in \mathbb{C}^{m \times m}$, state sets X_i', initial state sets $X_{i,0}'$, unsafe state sets $X_{i,u}'$, disturbance sets D_i, vector fields $f_i : X_i \times \mathbb{R}^3 \times D \to X_i$, and outputs $\varphi_i : X_i \times \mathbb{R}^3 \to \mathbb{R}^2$, for $i = 1, \ldots, m$, find a barrier certificate, B, for the system given by (4.10).*

4.3.3 Polynomial Programming Problem

The following sum of squares (SOS) program solves Problem 2

$$-B - \lambda_{X_0}^T g_{X_0} \text{ is SOS,} \tag{4.22}$$

$$B - \epsilon - \lambda_{X_u}^T g_{X_u} \text{ is SOS,} \tag{4.23}$$

$$-\frac{\partial B}{\partial x} f - \lambda_X^T g_X - \lambda_D^T g_D \text{ is SOS,} \tag{4.24}$$

where $\epsilon > 0$, $\lambda_{X_0}^T$ is SOS, $\lambda_{X_u}^T$ is SOS, λ_X^T is SOS, and λ_D^T is SOS. Details on the functions g_{X_0}, g_{X_u}, g_D, and g_X are provided in the two papers, Paper D and Paper E. Notice that the problem is linear in unknown polynomials B, $\lambda_{X_0}^T$, $\lambda_{X_u}^T$, λ_X^T, λ_D^T, and can therefore be solved directly using sum of squares programming.

4.3.4 Illustrative Example

This illustrative example considers the power grid depicted in Fig. 4.3, which consists of three busses, two loads and one local voltage controller detailed in Section 4.4. Bus B_1 is seen as the slack bus, meaning that V_1 and δ_1 are known constants.
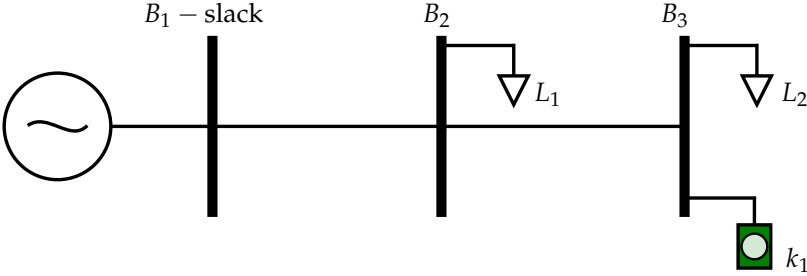
Fig. 4.3: Three bus power grid system used for the illustrative example. Arrows indicate loads, and the green box is a four quadrant voltage controller, detailed in Section 4.4.

The system parameters have been chosen such that voltage constraints will be violated when the controller k_1 is inactive. As expected, when the controller k_1 is inactive the problem of finding a barrier certificate is infeasible, whereas when the controller is active it is possible to compute a barrier certificate. Consequently, the system will not violate constraints as long as k_1 is active.

4.4 Four Quadrant Voltage Control (4Q-VC)

This section introduces the four quadrant voltage control (4Q-VC) strategy for ensuring voltage constraint satisfaction. The control strategy is described

for all four quadrants of the active and reactive power plane. The 4Q-VC is illustrated in Fig. 4.4, and the active and reactive power output of the controller is given by

$$\begin{bmatrix} p_c \\ q_c \end{bmatrix} = k(V), \tag{4.25}$$

with $p_c, q_c \in \mathbb{R}$ being the active and reactive power output of the control and $k : \mathbb{R} \to \mathbb{R}^2$ is the control law detailed in the following.

The relation between locally measured voltage magnitude, V, and active power output is

$$p_c = \begin{cases} \overline{p}_c, & \text{if } V < \underline{V} \\ K_p(V - \underline{V}_c), & \text{if } \underline{V} \leq V \leq \underline{V}_c \\ K_p(V - \overline{V}_c), & \text{if } \overline{V}_c \leq V \leq \overline{V} \\ \underline{p}_c, & \text{if } V > \overline{V} \\ 0, & \text{otherwise} \end{cases} \tag{4.26}$$

and the relation between measured voltage magnitude and reactive power is

$$q_c = \begin{cases} \sqrt{s_{\max}^2 - (\underline{p}_c + p_c)^2} & \text{if } V < \underline{V}_c \\ -\sqrt{s_{\max}^2 - (\overline{p}_c + p_c)^2} & \text{if } V > \overline{V}_c \\ K_q(V - V_0), & \text{otherwise} \end{cases} \tag{4.27}$$

where $\overline{p}_c, \underline{p}_c, \overline{q}_c, \underline{q}_c \in \mathbb{R}$ are the upper and lower bounds on active and reactive power, $\overline{V}_c, \underline{V}_c \in \mathbb{R}$ are the upper and lower bounds on when active power voltage control should be started, $V_0 \in \mathbb{R}$ is the nominal voltage, $K_p \in \mathbb{R}_-$ are the droop gain on active power, $K_q \in \mathbb{R}_-$ is the droop gain on reactive power, and $s_{\max} \in \mathbb{R}_+$ is the maximum apparent power of the control. The gains K_p and K_q are calculated as follows

$$K_p = \frac{\overline{p}_c}{\underline{V} - \underline{V}_c} = \frac{-\underline{p}_c}{\overline{V}_c - \overline{V}}, \tag{4.28}$$

$$K_q = \frac{\overline{q}_c}{\underline{V}_c} = \frac{-\underline{q}_c}{-\overline{V}_c}. \tag{4.29}$$

The design parameters are $\overline{V}_c$, and $\underline{V}_c$ defining at what voltage magnitude active power curtailment should initiate. The 4Q-VC strategy is illustrated in Fig. 4.4.

4.4.1 Numerical Example

The 4Q-VC is illustrated through simulation studies on a large scale low voltage distribution grid, implemented in GridLab-D [76]. Four simulations are conducted, where all PV systems implements the following voltage control strategy:
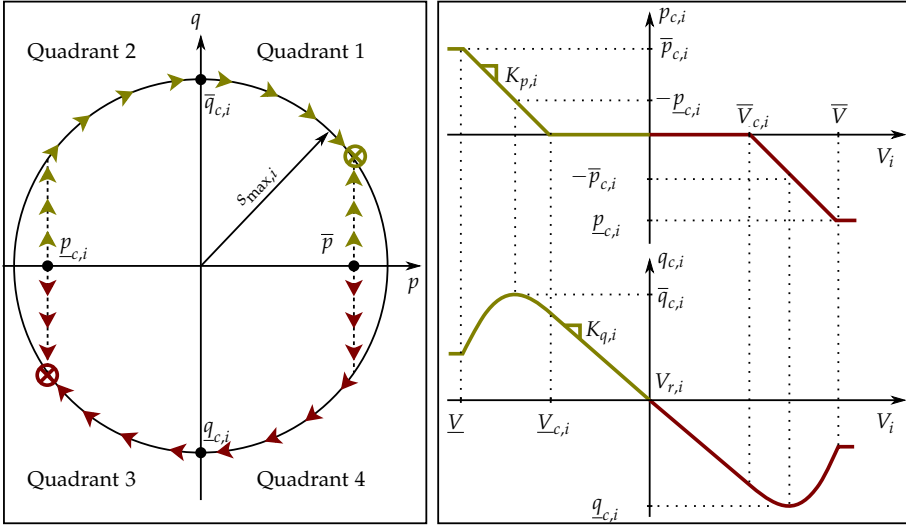
Fig. 4.4: Four quadrant voltage control strategy. Left: illustrates trajectories in the pq-plane. Right: is the associated active and reactive power control strategies.

Scenario	Active Power [MWh]	%	Reactive Power [MVArh]	%
1	29.4	100.0	0	-
2	29.3	99.4	29.4	100.0
3	27.2	92.4	29.0	98.8
4	28.9	98.1	29.6	100.9

Table 4.3: Total amount of active and reactive power produced by PV systems.

1. No curtailment of active power and no reactive power is injected.

2. No curtailment of active power and reactive power is used for voltage control.

3. 30 % curtailment of active power and reactive power is used for voltage control.

4. Curtailment of active power and injection of reactive power according to the 4Q-VC.

The four simulation scenarios all have a duration of 20 days. The simulation results are summarized in Table 4.3 and 4.4.

In Scenario 1 it can be seen that when the PV systems are allowed to produce the available power, voltage constraints are violated. Further, in

Scenario	Voltage Mean [p.u.]	Voltage STD [p.u.]	%	Voltage Max [p.u.]	%
1	0.989	0.034	100.0	1.100	100.0
2	0.994	0.018	51.4	1.073	73.3
3	0.993	0.013	39.1	1.028	28.7
4	0.994	0.013	39.1	1.043	43.4

Table 4.4: Voltage variations over all busses.

Scenario 2, when relying only on reactive power for voltage control, voltage constraints are still violated during peak production hours. When the PVs active power injections are curtailed by 30 % in Scenario 3, no voltage constraints are violated. This is because of the decrease in active power injection, but also because of the extra reactive power available during peak production hours. Finally in Scenario 4, it is observe that by deploying the 4Q-VC the voltages increase a little, which in turn allows for an approximately 6 % increase in active power production compared to the 30 % curtailment case in Scenario 3.

4.5 Summary

This chapter presented a method for coordinating the reactive output of systems offering local volt/var support. The objective was to achieve fairness in participation, defined as all systems having equal reactive power injection over time. Further, the voltage constraint satisfaction problem was introduced, and it was shown how solving a sum of squares program was equivalent to verifying that bus voltages in a power grid would always be within bounds. Finally, a local voltage controller named the four quadrant voltage controller (4Q-VC) was proposed, and its effectiveness was demonstrated through simulations on a large scale low voltage distribution grid, implemented in GridLab-D.

5 Concluding Remarks

This chapter summarizes the work presented in this thesis and provide conclusions on the research hypothesis. Subsequently, perspectives and suggestions for future work are provided.

5.1 Conclusion on Hypothesis

This thesis examined how distributed resources in power distribution grids could be managed for delivering power and voltage control services.

Paper A addressed Hypothesis 1 and illustrated how the flexibility of distributed renewable resources could be managed, enabling a medium voltage distribution grid to follow a power reference. This was achieved by using an estimation of the uncontrollable load for feedforward control and a dispatch algorithm for minimizing active power loss. This approach enables a distribution system operator (DSO) to offer services to upper layers of the grid.

Paper B addressed Hypothesis 2 and it was shown how a leader-follower based control scheme could be used for managing the power flexibility of distributed resources in a low voltage distribution grid, enabling the grid to follow a power reference. The designed controller took into account a time-varying communication network state, representing different levels of congestion. By letting the leader agent update its state according to a PI control law, the classical results from leader-follower consensus no longer applied. Therefore, designing the PI control depends on number of systems connected and communication network topology, adding an extra layer of complexity to the control design. However, the results obtained in Paper B, clearly indicates that it is possible to control distributed resources over off-the-shelf communication technologies, which was the main goal of SmartC2Net.

Paper C addressed Hypothesis 3 and it was demonstrated how fairness between systems providing local volt/var control could be achieved by changing the local droop gains. This eliminated the challenge associated with dependence on physical placement of local controllers in the grid. The presented approach was simple, reliable, and with a limited need for communi-

cation, making it easily implementable in today's electrical grids. The proposed method served the needs of the DSO by letting it use the distributed resources for voltage control instead of having to reinforce the grid. This allows for more renewable penetration in distribution grids. Also, with the notation of fairness the method also addressed the concerns of individual system owners. However, the method relied on a centralized unit for coordinating the distributed systems. This introduces a single point of failure, and distributing the coordination amongst the systems them-self seems as an attractive alternative.

Paper D and Paper E addressed Hypothesis 4 and illustrated that guaranteeing voltages would always be within bounds, was equivalent to solving a polynomial sum of squares program. Further, the developed method leaved out the need for simulation studies. Although the presented method made it computational feasible to solve the voltage constraint satisfaction problem without the need for simulation studies, it was only applicable for small systems with a few busses. The problem scales badly with number of variables, and further work is needed for the method to be readily used for verification of real power systems.

5.2 Perspectives and Future Directions

The control algorithm provided in Paper A was based on a static feedback law, which makes it simple to implement. However, it is expected that tracking performance and loss minimization could be increased by combining the disturbance model with the control and dispatch in e.g., a model predictive solution. Thereby, system dynamics and estimates of future disturbance state could be incorporated when computing the control output in a receding horizon fashion [66]. However, this comes at the cost of a more complex control algorithm, which consequently would increase deployment time and implementation.

The leader-follower coordination strategy described in Paper B only considered a star-like communication topology. However, the leader-follower consensus framework allows for a wide variaty of communication graphs, as long as there is a directed spanning tree from the leader to all followers. It would be natural to extend the analysis and control design procedure to such communication graphs. Furthermore, the developed procedure relied on classical frequency based methods for ensuring stability. It would be natural to pursue a more rigid approach based on Lyapunow-Krasovskii stability analysis [78], considering different delays for each communication link.

When addressing fairness in voltage control, as done in Paper C, a natural extension would be to also consider active power in the local control formulation. It would be interesting to conduct a similar analysis where each voltage control unit implemented the proposed *four quadrant voltage controller*

(4Q-VC) and derive solutions for achieving fairness in active power output. It is clear that if the distributed resources, implementing the local voltage controller are renewables, curtailing some systems more than others could have a negative economic impact on the system owner placed on the most sensitive bus. Therefore, fairness in such a situation is extremely important for the deployment of the 4Q-VC to become a success. Also, distributing the coordination approach, with out the need for a central coordinating unit, is seen as an interesting future approach.

Even though it has been shown in Paper D and Paper E, that verifying voltage constraint satisfaction is equivalent to solving a sum of squares program, solving these problems are computationally hard. Furthermore, they scale badly with the number of variables, making the method, in its current form, applicable to only small distribution grids with a few busses. However, it is expected that the inherent structure originating from the electrical grid admittance matrix can be used to decompose the problem into smaller sub-problems, where it would be feasible to compute a barrier certificate for. Furthermore, the framework should be extended to not only verify voltage constraint satisfaction for a given system, but to also include the design, tuning, and placement of local voltage controllers for ensuring that voltages would always be within bounds. Another extension would be to consider the problem in a stochastic setting, similar to what was introduced in [100].

Chapter 5. Concluding Remarks

6   References

[1] "IEEE task force on open source software for power systems," Webpage. [Online]. Available: http://ewh.ieee.org/cmte/psace/CAMS_taskforce/

[2] "Nordpool spot - leading power market in europe," Webpage. [Online]. Available: http://www.nordpoolspot.com

[3] "Regulation a: Principles for the electricity market," Energinet.dk, Tech. Rep., 2007.

[4] "Smart grid i danmark," Danish Energy Association and Energinet.dk, Tech. Rep., 2010.

[5] "Voltage characteristics of electricity supplied by public electricity networks," EN 50160, 2010.

[6] "Cell controller pilot project," Energinet.dk, Tech. Rep. Doc. 8577/12, 2011.

[7] "Act on granting priority to renewable energy sources," Renewable Energy Sources Act – EEG, Tech. Rep., 2012.

[8] "The energy- and climate goals of the danish government and results of the energy agreement 2020 (regeringens energi- og klimapolitiske mål og resultaterne af energiaftalen i 2020)," Danish Ministry for Climate, Energy and Buildings (Klima, energi og bygningsministeriet), Tech. Rep., 2012.

[9] "Managing congestion in distribution grids - market design consideration," NEAS ENERGY and Ea Eneergy Analyses, Tech. Rep., Nov. 2012.

[10] "Deliverable 4.1 - control framework and models," SmartC2Net, Tech. Rep., 2014.

[11] "Interim decision adopting revisions to electric tariff Rule 21 for Pacific Gas and Electric Company, Southern California Edison Company, and San Diego Gas & Electric Company to require "smart" inverters," California Public Utilities Commission, Tech. Rep. R.11-09-011 COM/MP6/lil, 2014.

[12] Aalborg University, "Smart energy systems laboratory," 2016. [Online]. Available: http://www.et.aau.dk/department/laboratory-facilities/smart-energy-systems-lab/

[13] B. M. Åkeson, J. B. Jørgensen, N. K. Poulsen, and S. B. Jørgensen, "A tool for kalman filter tuning," in *17th European Symposium on Computer Aided Process Engineering*, Bucharest, Romania, 2007.

[14] L. F. Amarel, R. C. Souza, and M. Stevenson, "A smooth transition periodic autoregressive (STPAR) model for short-term load forecasting," *International Journal of Forecasting*, vol. 24, pp. 603 – 615, 2008.

[15] P. Aristidou, F. Olivier, M. E. Hervas, D. Ernst, and T. V. Cutsem, "Distributed model-free control of photovoltaic units for mitigating overvoltages in low-voltage networks," in *CIRED Workshop*, Rome, Jun. 2014.

[16] N. Bauer, S. v. Loon, N. V. d. Wouw, and W. Heemels, "Exploring the boundaries of robust stability under uncertain communication: An ncs toolbox applied to a wireless control setup," *IEEE Control Systems Magazine*, vol. 34, no. 4, pp. 65 – 86, 2014.

[17] H. M. Beides and G. T. Heydt, "Dynamic state estimation of power system harmonics using kalman filter methodology," *IEEE Transactions on Power Delivery*, vol. 6, no. 4, pp. 1663–1670, oct 1991.

[18] B. Biegel, "Distributed energy resources in the liberalized electricity markets," Ph.D. dissertation, Aalborg University, 2014.

[19] B. Biegel, P. Andersen, J. Stoustrup, M. B. Madsen, L. H. Hansen, and L. H. Rasmussen, "Aggregation and control of flexible consumers - a real life demonstration," in *Proceedings of the 19th IFAC World Congress*. Cape Town, South Africa: IFAC, Aug. 2014.

[20] F. Blaabjerg, R. Teodorescu, M. Liserre, and A. V. Timbus, "A voltage and frequency droop control method for parallel inverters," *IEEE Transactions on Industrial Electronics*, vol. 53, no. 5, pp. 1398–1409, oct 2006.

[21] S. Bolognani, R. Carli, G. Cavraro, and S. Zampieri, "Distributed reactive power feedback control for voltage regulation and loss minimization," *arXiv: 1303.7173v2*, vol. math.OC, Nov. 2014.

[22] K. D. Brabandere, B. Bolsens, J. V. den Keybus, J. D. Achim Woyte, and R. Belmans, "Overview of control and grid synchronization for distributed power generation systems," *IEEE Transactions on Industrial Electronics*, vol. 22, no. 4, pp. 1107–1115, jul 2007.

[23] A. Capasso, W. Grattieri, R. Lamedica, and A. Prudenzi, "A bottom-up approach to residential load modeling," *IEEE Transactions on Power Systems*, vol. 9, no. 2, pp. 957–964, may 1994.

[24] J. Carpentier, "Contribution to the economic dispatch problem," *Bulletin Society Francaise Electriciens*, vol. 3, no. 8, pp. 431–447, 1962.

[25] P. M. S. Carvalho, P. F. Correia, and L. A. F. M. Ferreira, "Distributed reactive power generation control for voltage rise mitigation in distribution networks," *IEEE Transactions on Power Systems*, vol. 23, no. 2, pp. 766–772, may 2008.

[26] T. E. Commission, "Commission regulation (eu) 2016/631 - establishing a network code on requirements for grid connection of generators," The European Union, Tech. Rep., 2016.

[27] O. Corradi, H. Ochsenfeld, H. Madsen, and P. Pinson, "Controlling electricity consumption by forecasting its response to varying prices," *IEEE Transactions on Power Systems*, vol. 8, no. 1, pp. 421–429, feb 2013.

[28] T. V. Cutsem and C. Vournas, *Voltage Stability of Electric Power Systems*, 6th ed. Springer, 1998.

[29] X. Dong, J. Xi, G. Lu, and Y. Zhong, "Formation control for high-order linear time-invariant multiagent systems with time delays," *IEEE Transactions on Control of Network Systems*, vol. 1, no. 3, pp. 232–240, 2014.

[30] V. Dordonnat, S. J. Koopman, A. D. M. Ooms, and J. Collet, "An hourly periodic state space model for modelling french national electricity load," *International Journal of Forecasting*, vol. 24, no. 4, pp. 566 – 587, Dec. 2008.

[31] EDSO, "Flexibility: The role of DSOs in tomorrow's electricity market," European Distribution System Operators for Smart Grids, Tech. Rep., 2014.

[32] Energinet.dk, "Regulation c2: The balancing market and balance settlement," Energinet.dk, Tech. Rep., 2011.

[33] Energinet.dk, "Statistics of renewables (statistik og udtræk for ve anlæg)," 2016. [Online]. Available: http://www.energinet.dk/DA/El/Engrosmarked/Udtraek-af-markedsdata/Sider/Statistik.aspx

[34] EPIA, "Connecting the sun - solar photovoltaics on the road to large-scale grid integration," European Photovoltaic Industry Association, Tech. Rep., 2012.

[35] M. Espinoza, C. Joye, R. Belmans, and B. D. Moor, "Short-term load forecasting, profile identification, and customer segmentation: A methodology based on periodic time series," *IEEE Transactions on Power Systems*, vol. 20, no. 3, Aug. 2005.

[36] FP7 - SmartC2Net Project, "Smart control of energy distribution grids over heterogeneous communication networks," 2015. [Online]. Available: www.smartc2net.eu

[37] B. A. Francis and W. M. Wonham, "Internal model principle of control theory," *Automatica*, vol. 12, no. 5, pp. 457 – 465, sep 1976.

[38] S. Frank, I. Steponavice, and S. Rebennack, "Optimal power flow: a bibliographic survey I," *Energy Systems*, vol. 3, pp. 221 – 258, 2012.

[39] ——, "Optimal power flow: a bibliographic survey II," *Energy Systems*, vol. 3, pp. 259 – 289, 2012.

[40] G. F. Franklin, J. D. Powell, and A. Emami-Naeini, *Feedback Control of Dynamic Systems*, 6th ed. Pearson, 2010.

[41] E. Ghahremani and I. Kamwa, "Dynamic state estimation in power system by applying the extended kalman filter with unknown inputs to phasor measurements," *IEEE Transactions on Power Systems*, vol. 26, no. 4, pp. 2556–2566, nov 2011.

[42] R. C. Green, L. Wang, and M. Alam, "The impact of plug-in hybrid electric vehicles on distribution networks: a review and outlook," in *Proceedings of IEEE Power and Energy Society General Meeting*, 2010, pp. 1 – 8.

[43] J. M. Guerrero, J. C. Vasquez, J. Matas, L. G. de Vicuñña, and M. Castilla, "Hierarchical control of droop-controlled AC and DC microgrids — a general approach toward standardization," *IEEE Transactions on Industrial Electronics*, vol. 58, no. 1, pp. 158–172, 2011.

[44] H. Haeberlin and B. Fachhochschule, "Evolution of inverters for grid connected pv-systems from 1989-2000," in *17th European Photovoltaic Solar Energy Conference*, Munich, Germany, Oct. 2001.

[45] S. Harbo and B. Biegel, "Contracting flexibility services," iPower, Tech. Rep., 2012.

[46] ——, "Contracting flexibility services," in *4th IEEE PES Innovative Smart Grid Technologies Europe*, Copenhagen, Denmark, Oct. 2013.

[47] K. Heussen, S. You, B. Biegel, L. H. Hansen, and K. B. Andersen, "Indirect control for demand side management - a conceptual introduction," in *Proceedings of the 3rd IEEE PES Innovative Smart Grid Technologies*, Berlin, Germany, Oct. 2012.

[48] M. W. Hirsch, S. Smale, and R. L. Devaney, *Differential Equations, Dynamical Systems & An Introduction to Chaos*, 2nd ed. Elsevier - Academic Press, 2004.

[49] I. A. Hiskens, "Significance of load modelling in power system dynamics," in *Symposium of Specialists in Electric Operational and Expansion Planning*, Florianópolis, Brasil, 2006.

[50] I. A. Hiskens and J. V. Milanović, "Load modelling in studies of power system damping," *IEEE Transactions on Power Systems*, vol. 10, no. 4, pp. 1781–1788, nov 1995.

[51] T. G. Hovgaard, K. Edlund, and J. B. Jørgensen, "The potential of economic MPC for power management," in *49th Conference on Decision and Control*, Atlanta, GA, USA, Dec. 2010.

[52] T. G. Hovgaard, L. F. S. Larsen, and J. B. Jørgensen, "Flexible and cost efficient power consumption using economic MPC a supermarket refrigeration benchmark," in *50th IEEE Conference on Decision and Control*, Orlando, Florida, USA, Dec. 2011.

[53] M. Ilic and S. Liu, *Hierarchical Power Systems Control: Its Value in a Changing Industry*, 1st ed. Springer, 1996.

[54] M. Juelsgaard, P. Andersen, and R. Wisniewski, "Stability concerns for indirect consumer control in smart grids," in *European Control Conference*, Zürich, Switzerland., Jul. 2013.

[55] ——, "Distribution loss reduction by household consumption coordination in smart grids," *IEEE Transactions on Smart Grid*, vol. 5, no. 4, pp. 2133 – 2144, 2014.

[56] M. Juelsgaard, C. Sloth, R. Wisniewski, and J. Pillai, "Loss minimization and voltage control in smart distribution grid," in *Proceedings of the 19th IFAC World Congress*, Cape Town, South Africa, Aug. 2014.

[57] M. Juelsgaard, A. Teixeira, M. Johansson, R. Wisniewski, and J. Bendtsen, "Distributed coordination of household electricity consumption," in *IEEE Multiconference on Systems and Control*, Antibes, France, Oct. 2014.

[58] M. Kolenc, I. Papič, and B. tjan Blaž ič, "Coordinated reactive power control to ensure fairness in active distribution grids," in *IEEE 8th International Conference on Compatibility and Power Electronics (CPE)*, jun 2013, pp. 109 – 114.

[59] M. Kraning, E. Chu, E. Chu, and S. Boyd, "Dynamic network energy management via proximal message passing," *Foundations and Trends in Optimization*, vol. 1, no. 2, pp. 73 – 126, 2014.

[60] S. Kundu, S. Backhaus, and I. A. Hiskens, "Distributed control of reactive power from photovoltaic inverters," in *IEEE International Symposium on Circuits and Systems*, Beijing, China, 2013, pp. 249–252.

[61] P. Kundur, *Power System Stability and Control*, ser. The EPRI Power System Engineering Series. McGraw-Hill, 1993.

[62] J. Lavaei and S. Low, "Zero duality gap in optimal power flow problem," *IEEE Transactions on Power Systems*, vol. 27, no. 1, pp. 92–107, 2012.

[63] J. Lavaei and S. H. Low, "Convexification of optimal power flow problem," in *48th Allerton Conference on Communication, Control and Computing (Allerton)*, Allerton House, IL, USA, Sep. 2010, pp. 223 – 232.

[64] N. Li, G. Qu, and M. Dahleh, "Real-time decentralized voltage control in distribution networks," in *52nd Annual Allerton Conference*, Allerton House, UIUC, Illinois, USA, 2014, pp. 582–588.

[65] J. Machowski, J. W. Bialek, and J. R. Bunby, *Power System Dynamics - Stability and Control*, 2nd ed. John Wiley & Sons, 2008.

[66] J. M. Maciejowski, *Predictive Control with Constraints*, 1st ed. Prentice Hall, 2002.

[67] R. Madani, S. Sojoudi, and J. Lavaei, "Convex relaxation for optimal power flow problem: Mesh networks," *IEEE Transactions on Power Systems*, vol. 30, no. 1, pp. 199–211, jan 2015.

[68] R. Madani, M. Ashraphijuo, and J. Lavaei, "Promises of conic relaxation for contingency-constrained optimal power flow problem," *IEEE Transactions on Power Systems*, vol. 31, no. 2, pp. 1297–1307, 2016.

[69] J. Medina, N. Muller, and I. Roytelman, "Demand response and distribution grid operations: Opportunities and challenges," *IET Renewable Power Generation*, no. 2, pp. 193–198, Sep. 2010.

[70] L. Mirkin, "Some remarks on the use of time-varying delay to model sample-and-hold circuits," *IEEE Transactions on Automatic Control*, vol. 52, no. 6, pp. 1109 – 1112, jun 2007.

[71] A. Monticelli, "Electric power system state estimation," *IEEE invited paper*, vol. 88, no. 2, Aug. 2002.

[72] National Academy of Engineering, "Greatest engineering achievements of the 20th century," 2016. [Online]. Available: http://www.greatachievements.org

[73] J. G. ni, M. Angel, G. Yang, and S. B. Kjær, "Voltage regulation in LV grids by coordinated volt-var control strategies," *Modern Power Systems and Clean Energy*, vol. 2, no. 4, pp. 319-–328, 2014.

[74] K. Okano and H. Ishii, "Stabilization of uncertain systems with finite data rates and markovian packet losses," *IEEE Transactions on Control of Network Systems*, vol. 1, no. 4, pp. 298–307, 2014.

[75] R. Olfati-Saber and R. M. Murray, "Consensus problems in networks of agents with switching topology and time-daleys," *IEEE Transactions on Automatic Control*, vol. 49, no. 9, pp. 1520–1533, sep 2004.

[76] Pacific Northwest National Laboratory, "GridLAB-D - Power Distribution System, Simulation and Analysis Tool," 2009. [Online]. Available: http://www.gridlabd.org

[77] A. Papachristodoulou, A. Jadbabaie, and U. Munz, "Effects of delay in multi-agent consensus and oscillator synchronization," *IEEE Transactions on Automatic Control*, vol. 55, no. 6, pp. 1471 – 1477, jun 2010.

[78] A. Papachristodoulou, M. Peet, and S. Lall, "Constructing lyapunov-krasovskii functionals for linear time delay systems," in *American Control Conference*, Portland, OR, USA, 2005, pp. 2845 – 2850.

[79] R. Pedersen, J. Schwensen, S. Sivabalan, C. Corazzol, S. E. Shafiei, K. Vinther, and J. Stoustrup, "Direct control implementation of a refrigeration system in smart grid," in *Proceedings of the 2013 American Control Conference*, Washington, DC, USA, Jun. 2013.

[80] R. Pedersen, C. Sloth, G. B. Andresen, R. Wisniewski, J. R. Pillai, and F. Iov, "DiSC - A Simulation Framework for Distribution System Voltage Control," 2014. [Online]. Available: http://kom.aau.dk/project/SmartGridControl/DiSC/

[81] T. S. Pedersen, P. Andersen, K. Nielsen, H. L. Stærmose, and P. D. Pedersen, "Using heat pump energy storages in the power grid," in *IEEE Multi-Conference on Systems and Control*, Denver, CO, Sep. 2011.

[82] J. Pillai, P. Thøgersen, J. Møller, and B. Bak, "Integration of electric vehicles in low voltage danish distribution grids," in *IEEE Power and Energy Society General Meeting*, San Diego, CA, USA, Jul. 2012.

[83] S. Prajna, A. Jadbabaie, and G. J. Pappas, "A framework for worst-case and stochastic safety verification using barrier certificates," *IEEE Transactions on Automatic Control*, vol. 52, no. 8, pp. 1415 – 1428, Aug. 2007.

[84] D. Pudjianto, C. Ramsay, and G. Strbac, "Virtual power plant and system integration of distributed energy resources," *IET Renewable Power Generation*, no. 1, pp. 10–16, Apr. 2007.

[85] S. Rahnama, "Integration of large-scale consumers in smart grid," Ph.D. dissertation, Aalborg University, 2015.

[86] S. Rahnama, J. D. Bendtsen, J. Stoustrup, Henrik, and Rasmussen, "Power balancing aggregator design for industrial consumers using direct control," in *European Control Conference (ECC)*, Linz, Austria, Jun. 2015.

[87] P. Rao, M. L. Crow, and Z. Yang, "Statcom control for power system voltage control applications," *IEEE Transactions on Power Delivery*, vol. 15, no. 4, pp. 1311–1317, oct 2000.

[88] W. Ren, "Consensus based formation control strategies for multi-vehicle systems," in *Proceedings of the American Control Conference*, Minneapolis, MN, USA, 2006, pp. 4237–4242.

[89] W. Ren and R. W. Beard, *Distributed Consensus in Multi-Vehicle Cooperative Control*, 1st ed. Springer, 2008.

[90] N. Ruiz, I. nigo Cobelo, and J. Oyarzabal, "A direct load control model for virtual power plant management," in *IEEE Transactions on Power Systems*, vol. 24, no. 2, May 2009, pp. 959–966.

[91] H. Saboori, M. Mohammadi, and R. Taghe, "Virtual power plant (vpp), definition, concept, components and types," in *Power and Energy Engineering Conference (APPEEC)*, Mar. 2010.

[92] R. Scattolini, "Architectures for distributed and hierarchical model predictive control – a review," *Journal of Process Control*, vol. 19, no. 5, pp. 723–731, 2009.

[93] C. Schauder, M. Gernhardt, E. Stacey, T. Lemak, L. Gyugyi, T. W. Cease, and A. Edris, "Development of a floo mvar static condenser for voltage control of transmission systems," *IEEE Transactions on Power Delivery*, vol. 10, no. 3, pp. 1486–1496, jul 1995.

[94] L. Schenato, B. Sinopoli, M. Franceschetti, and K. Poolla, "Foundations of control and estimation over lossy networks," *IEEE Proceedings of*, vol. 95, no. 2, pp. 163 – 187, jan 2007.

[95] F. C. Schweppe and S. K. Mitter, "Hierarchical system theory and electric power systems," in *Symposium on real-time control of electric power systems*, Baden, Switzerland, 1972.

[96] T. Senjyu, Y. Miyazato, A. Yona, N. Urasaki, and T. Funabashi, "Optimal distribution voltage control and coordination with distributed generation," *IEEE Transactions on Power Delivery*, vol. 23, no. 2, pp. 1236–1242, apr 2008.

[97] S. E. Shafiei, J. Stoustrup, and H. Rasmussen, "A supervisory control approach in economic MPC design for refrigeration systems," in *Proceedings of the European Control Conference 2013*, Zurich, Schweiz, Jul. 2013.

[98] K.-R. Shih and S.-J. Huang, "Application of a robust algorithm for dynamic state estimation of a power system," *IEEE Transactions on Power Systems*, vol. 17, no. 1, pp. 141–147, feb 2002.

[99] J. W. Simpson-Porco, F. Dörfler, and F. Bullo, "Voltage stabilization in microgrids via quadratic droop control," in *IEEE 52nd Annual Conference on Decision and Control*, Firenze, Italy, Dec. 2013.

[100] C. Sloth and R. Wisneiweski, "Safety analysis of stochastic dynamical systems," in *IFAC Conference on Analysis and Design of Hybrid Systems*, 2015, pp. 62–67.

[101] J. W. Smith, W. Sunderman, R. Dugan, and B. Seal, "Smart inverter volt/var control functions for high penetration of PV on distribution systems," in *IEEE Power Systems Conference and Exposition (PSCE)*, Pnoenix, AZ, USA, Mar. 2011, pp. 1 – 6.

[102] F. Sossan, M. Marinelli, G. T. Costanzo, and H. Bindner, "Indirect control of dsrs for regulating power provision and solving local congestions," in *4th IEEE International Youth Conference on Energy*, Jun. 2013.

[103] Y. G. Suna, L. Wanga, and G. Xiea, "Average consensus in networks of dynamic agents with switching topologies and multiple time-varying delays," *Systems & Control Letters*, vol. 57, no. 2, pp. 175—-183, feb 2008.

[104] O. Sundström and C. Binding, "Flexible charging optimization for electric vehicles considering distribution grid constraints," *IEEE Transactions on Smart Grid*, vol. 3, no. 1, pp. 26 – 37, 2012.

[105] R. Tonkoski, L. A. C. Lopes, and T. H. M. El-Fouly, "Droop-based active power curtailment for overvoltage prevention in grid connected PV inverters," in *IEEE International Symposium on Industrial Electronics (ISIE)*, Bari, Italy, Jul. 2010, pp. 2388 – 2393.

[106] R. Tonkoski and L. A. Lopes, "Impact of active power curtailment on overvoltage prevention and energy production of PV inverters connected to low voltage residential feeders," *Renewable Energy*, vol. 36, no. 12, pp. 3566 – 3574, 2011.

[107] K. Turitsyn, P. Šulc, S. Backhaus, and M. Chertkov, "Options for control of reactive power by distributed photovoltaic generators," *Proceedings of the IEEE*, vol. 99, no. 6, pp. 1063 – 1073, 2011.

[108] US Department of Energy, "How microgrids work," 2014. [Online]. Available: http://www.energy.gov/articles/how-microgrids-work

[109] J. v. Appen, M. Braun, T. Stetz, K. Diwold, and D. Geibel, "Time in the sun - the challenges of high PV penetration in the German electric grid," *IEEE - Power and Energy Magazine*, pp. 55 – 64, Mar. 2013.

[110] G. Valverde and V. Terzija, "Unscented kalman filter for power system dynamic state estimation," *IET Generation, Transmission & Distribution*, vol. 5, no. 1, pp. 29–37, jul 2010.

[111] J. von Appen, T. Stetz, M. Braun, and A. Schmiegel, "Local voltage control strategies for pv storage systems in distribution grids," *IEEE Transactions on Smart Grid*, vol. 5, no. 2, pp. 1002–1009, mar 2014.

[112] P. N. Vovos, A. E. Kiprakis, A. R. Wallace, and G. P. Harrison, "Centralized and distributed voltage control: Impact on distributed generation penetration," *IEEE Transactions on Power Systems*, vol. 22, no. 1, pp. 476–483, feb 2007.

[113] L. Zhang, Y. Shi, T. Chen, and B. Huang, "A new method for stabilization of networked control systems with random delays," in *Proceedings of American Control Conference*, Portland, OR, USA, 2005, pp. 633 – 637.

[114] W. Zhang, M. S. Branicky, and S. M. Phillips, "Stability of networked control systems," *IEEE Control Systems Magazine*, pp. 84 – 99, 2001.

[115] W. Zhua and D. Cheng, "Leader-following consensus of second-order agents with multiple time-varying delays," *Automatica*, vol. 46, no. 12, pp. 1994—-1999, 2010.

[116] R. D. Zimmerman, C. E. Murillo-Sánchez, and D. Gan, "MATPOWER - a MATLAB power system simulation package," Webpage, 1997, http://www.pserc.cornell.edu//matpower/.

Contributions

Paper A

Active Power Management in Power Distribution Grids: Disturbance Modeling and Rejection

Rasmus Pedersen, Christoffer Sloth, and Rafael Wisniewski

Abstract

This paper presents a control strategy for enabling a distribution system operator (DSO) to manage a power distribution grid towards an active power reference. This is accomplished by allowing the DSO to utilize flexibility in production and consumption. The control system consists of a feedforward based on estimates of inflexible consumption profiles, a feedback based on flexible asset dynamics, and a dispatch algorithm for minimizing active power loss. The estimation approach is validated on real consumption data and illustrates the method's applicability on both a step-ahead and day-ahead scale, which makes it suited for a variety of control scenarios. Simulations demonstrate the control system's ability to track an active power reference and show a 3% reduction in active power loss, compared to a strategy of uniformly dispatching the power between assets.

1   Introduction

The ongoing introduction of renewable resources, especially into the distribution grids, are turning a well behaved system into a highly stochastic and dynamic system, challenging the distribution system operators (DSOs) [1]. Therefore, the DSOs are demanding new control and state estimation solutions, enabling them to maintain a high quality of power delivery [2]. Further, the volatile production and consumption may increase active power loss, a cost carried by the DSO. In this work we provide the DSOs with a combined estimation and control solution, enabling them to manage the active power in a distribution system, while minimizing the active power loss.

Power system state estimation has been addressed in several publications, such as [3] where the consumption patterns of loads are forecast using periodic models to describe their seasonal to daily behavior. Typically, these methods have been used to create strong statistical tools that could be used for long term planning of grid reinforcements, upgrade of transformer stations, etc. [4, 5]. However, these approaches have not been tailored for implementation in an online dynamic control scenario, with step ahead predictions and sampling time down to a sub-minute level. A popular and well-studied approach to solving the loss minimization problem is to run an optimal power flow (OPF). The OPF is a scheduling problem, which is inherently non-convex and therefore difficult to solve, making it ill-suited for fast dynamic control. In [6] the OPF problem is solved using a heuristic method based on particle swarm optimization. Similarly in [7] a genetic algorithm is applied to the problem, where also switching of discrete components are considered. The problems with these methods are that they can not guarantee a global system optimum and they can be computationally intensive. Therefore, different approaches have been taken to relax the problem as in [8], where a low rank solution is found by semi-definite programming

or as in [9] where convex approximations are combined with stochastic optimization techniques to minimize active power loss. Another approach taken in [10], is to solve the loss minimization problem by distributing the effort among the flexible assets in the grid and then apply an appropriate communication strategy to ensure convergence, see also [11] for perspectives on the communication strategies for power loss minimization in residential micro grids. This illustrates that there are numerous approaches to solving the loss minimization problem. In this work a simple, fast to compute, and easily implementable algorithm, suited for online implementation is utilized.

This paper extends the use of periodic models to estimate consumption profiles of inflexible loads to allow a distribution grid to follow a power reference. The presented method uses linear harmonic oscillators in combination with a Kalman filter to estimate the load state. The reason for this approach is twofold; first, we will obtain a model of the inflexible load, which can be seen as a disturbance and thus used for feedforward. Secondly, the method allows for implementation in a dynamic control setup, using standard methods. The presented disturbance estimation method is general and its application is not limited to the control approach taken in this work, it could e.g., be used in a model predictive control setting or for offline scheduling purposes such as solving the OPF problem. To relax the OPF problem, we apply assumptions, such as voltages being measured at each bus. Thereby, the problem becomes convex and standard optimization techniques can be applied. The control approach detailed here should not be seen as a replacement for OPF scheduling, but more as an extra functionality capable of handling fast dynamics, ensuring that the schedule is actually followed in real time. The main contribution is the derivation of a simple to implement dynamic control and estimation system, enabling a distribution grid to follow a power reference, while minimizing active power loss.

The paper is organized as follows. First in Sec. 2 the power system control architecture is introduced. Then in Sec. 3, the control system structure is given followed by estimator and controller design. In Sec. 4, the proposed control method is illustrated with numerical simulation examples. Finally in Sec. 5, we provide conclusions on the work.

2   System Architecture

In this section an overview of the electrical distribution grid structure is given and the role of the distribution grid controller (DGC) is detailed. The setup is shown in Fig. A.1 and illustrates the physical layout along with communication topology.

The idea in this architecture is that the DGC receives flexibility information and state information from assets, and measurements from inflexible entities. Asset flexibility can be in form of a wind turbine's ability to derate

active power production or a load's ability to increase consumption. Inflexible loads are seen as disturbances into the system, where such a load could be a low voltage residential grid or an industrial facility, as illustrated in Fig. A.1.

In the following sections, we develop the combined estimation and control system for managing the distribution grid towards an active power reference.
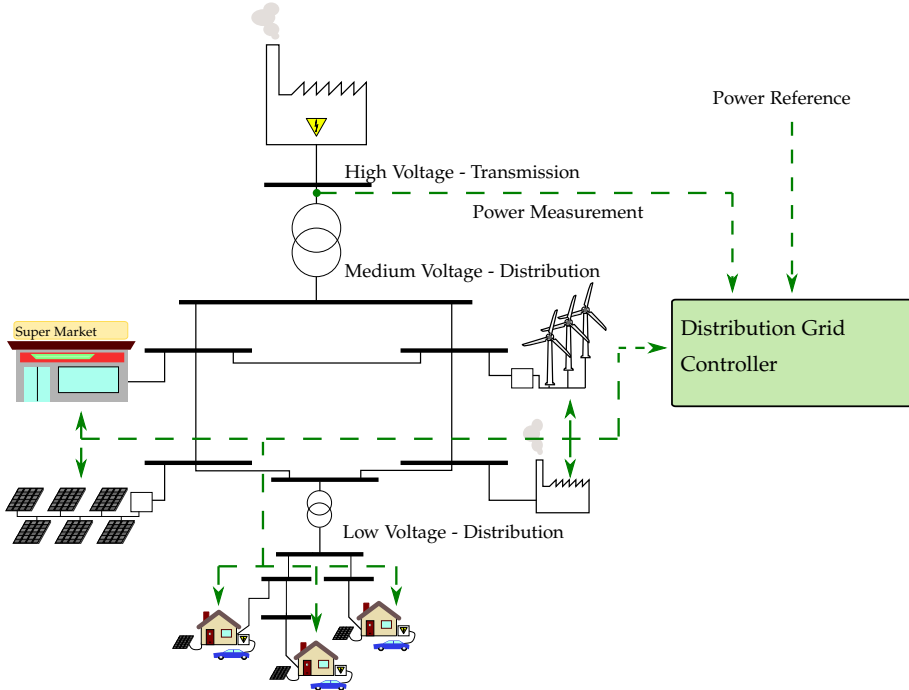

Fig. A.1: The controller communicates with assets and uses their flexibility to manage the entire distribution grid towards an active power reference.

3 Control System Design

In this section, the distribution grid control system is introduced, followed by a detailed description of the load estimation, flexible assets, feedback control law, and dispatch algorithm. The controlled system consists of the electrical grid, flexible assets, and inflexible loads illustrated in Fig. A.2.

3.1 Load Estimation

The inflexible (uncontrollable) load profiles from consumers can be seen as a disturbance affecting the control system performance. Knowledge of the
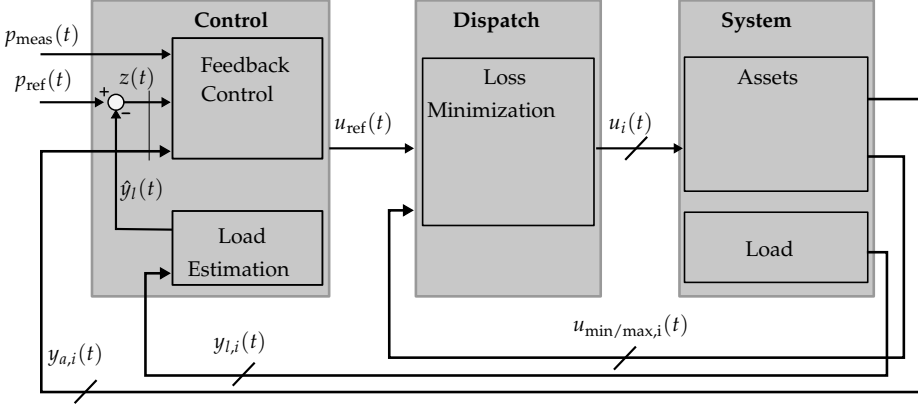
Fig. A.2: Control system structure, with the system consisting of flexible assets, both production and consumption, inflexible load, and electrical grid. Based on estimation of inflexible load and reference signal the feedback controller calculates an output which is then dispatched to the flexible assets.

disturbance behavior can be incorporated into the control strategy in different ways, e.g., using model predictive control (MPC) or the internal model principle. Obtaining a model of the uncontrollable part of a dynamic system is extremely valuable for the following reason: *A disturbance can be completely rejected, only if the controller contains a model of it* [12].

Let $\mathcal{L} = \{1, \dots, S\}$ be the set of loads. Each load is modeled by $p_i \in \mathbb{N}$ linear oscillators described by the following dynamic system

$$\dot{x}_{l,i}(t) = A_{l,i}x_{l,i}(t) + w_i(t), \qquad i \in \mathcal{L}, \qquad (A.1)$$
$$y_{l,i}(t) = C_{l,i}x_{l,i}(t) + v_i(t), \qquad (A.2)$$

where $x_{l,i}(t) \in \mathbb{R}^{2p_i+1}$ is the state vector with the last entry describing a bias term, $w_i(t) \in \mathbb{R}^{2p_i+1}$ is the process noise, $v_i(t) \in \mathbb{R}$ is the measurement noise, both assumed to be zero mean Gaussian distributed, $A_{l,i} \in \mathbb{R}^{2p_i+1 \times 2p_i+1}$ is a block diagonal matrix, where each block is on the skew symmetric form

$$A_{l,i} = \mathrm{diag}\left(\begin{bmatrix} 0 & \beta_{1,i} \\ -\beta_{1,i} & 0 \end{bmatrix}, \dots, \begin{bmatrix} 0 & \beta_{p_i,i} \\ -\beta_{p_i,i} & 0 \end{bmatrix}, 0\right), \qquad (A.3)$$

with $\beta_{j,i} \in \mathbb{R}$ describing the frequency of a single oscillator, $j = 1, \dots, p_i$, and $\mathrm{diag}(X, Y, \dots)$ is a block diagonal matrix with $X, Y, \dots$ as diagonal blocks. It should be noted that the values of $\beta_{j,i}$ represent the harmonics that the model should capture. $C_{l,i} \in \mathbb{R}^{2p_i+1}$ is the output matrix given by

$$C_{l,i} = \begin{bmatrix} \alpha_{11,i} & \alpha_{12,i} & \dots & \alpha_{p_i1,i} & \alpha_{p_i2,i} & 1 \end{bmatrix}, \qquad (A.4)$$

with $\alpha_{11,i}, \alpha_{12,i}, \dots, \alpha_{p_i1,i}, \alpha_{p_i2,i} \in \mathbb{R}$ being the amplitudes associated to the p_i oscillators.

The load models can be combined with a Kalman filter to estimate the load states, which can be used for feedforward in the control algorithm. The effectiveness of estimating one aggregated residential load ($\mathcal{L} = \{1\}$) using the described model and a Kalman filter is demonstrated in Fig. A.3. The figure shows a 14 day period of 200 households, based on data from Denmark [13]. The model used in the estimator consist of two harmonic oscillators with frequencies; $\beta_{1,1} = \frac{2\pi}{24 \text{ hours}}$ and $\beta_{2,1} = \frac{2\pi}{12 \text{ hours}}$, respectively. By choosing these harmonics the bi-daily peaks in the morning and evening are captured. The convergence of the filter is dependent on its tuning, in this case it takes a couple of days. However, Kalman filter tuning can be automated [14].
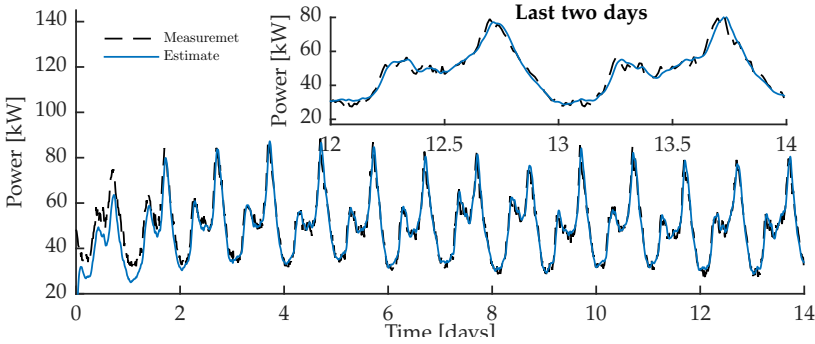

Fig. A.3: Performance of proposed estimation method throughout a 14 day period. The measurement is a residential load, based on data from 200 houses in Denmark. The two last days of the estimation is highlighted and it can be seen that even with a simplistic estimation model, good tracking capabilities are achieved.

The Kalman filter is a closed-loop method depending on measurements of the output in order to adapt. Therefore, the estimation approach should also be verified in open-loop, i.e., how well does the proposed model perform when estimating one day into the future. This is illustrated in Fig. A.4 and summarized in TABLE A.1, for different values of p_1. It is seen that a model with six oscillators captures the behavior better than a model with only two, but increasing the number of oscillators above six shows no performance increase, when measured using root mean square error (RMSE). The frequency of each oscillator, $\beta_{j,1}$, has been chosen as a harmonic of a fundamental frequency with time period of 24 hours, i.e., $\beta_{j,1} = \frac{2\pi j}{24 \text{ hours}}$, $j = 1, \ldots, p_1$. It should be noted that any frequency can be chosen for the oscillators to e.g., capture weekly or monthly tendencies.

The presented estimation method is seen as a main contribution for the following reasons; first, it has low complexity, enabling easy implementation and fast deployment. Secondly, it has been verified on real data and shows good performance on both a step-ahead and day-ahead basis. Lastly, it is a
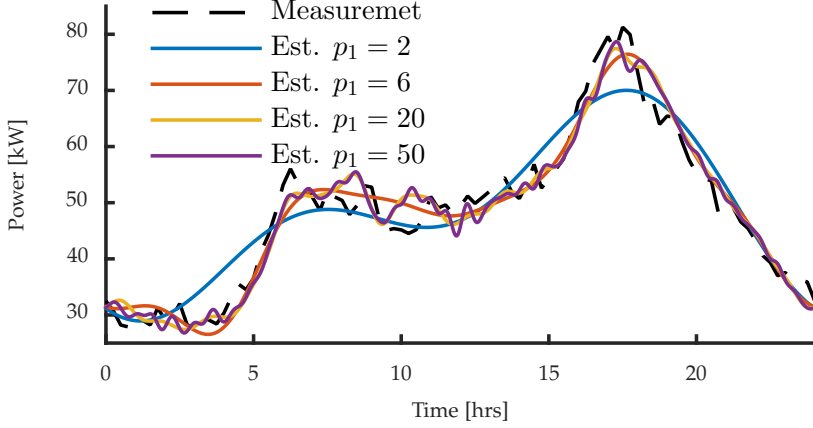
Fig. A.4: Open-loop performance of the proposed estimation method. The measurement represents an aggregated load of 200 houses, based on real data.

Table A.1: Comparison between different orders of the disturbance model. Each oscillator adds two states to the model.

Number of Oscillators	Day-ahead Tracking Error (RMS)	
	[kW]	%
$p_1 = 2$	4.16	100
$p_1 = 6$	2.83	68
$p_1 = 20$	2.91	70
$p_1 = 50$	2.96	71

general approach applicable in a wide variety of electrical grid control problems.

3.2 Flexible Assets

Let $\mathcal{A} = \{1, \ldots, m\}$ be the set of flexible assets, modeled as constrained first order systems. The choice of a first order system to model flexible assets is based on the assumption of a well behaving local control loop exhibiting no overshoot. However, the model can easily be extended to capture more complex dynamics. The control model of a flexible asset is then given by

$$\dot{x}_{a,i}(t) = a_{a,i}x_{a,i}(t) + b_{a,i}u_i(t), \qquad i \in \mathcal{A} \qquad (A.5)$$

$$y_{a,i}(t) = c_{a,i}x_{a,i}(t), \qquad (A.6)$$

$$u_{\min,i}(t) \leq u_i(t) \leq u_{\max,i}(t), \qquad (A.7)$$

where $x_{a,i}(t) \in \mathbb{R}$ is the asset state, $u_i(t) \in \mathbb{R}$ is the reference signal, $y_{a,i}(t) \in \mathbb{R}$ is the active power output, $a_{a,i}, b_{a,i}, c_{a,i} \in \mathbb{R}$ are asset parameters, $u_{\min,i}(t) \in \mathbb{R}$ is the lower bound on available flexibility, and $u_{\max,i}(t) \in \mathbb{R}$ is the upper bound on available flexibility. Further, all assets are assumed to have unity gain, i.e., $b_{a,i} = -a_{a,i}$ and $c_{a,i} = 1$. It should be noted that the bounds can change over time, e.g., the available amount of wind power depends on the wind speed.

3.3 Feedback Control

Even though the estimation method described in Sec. 3.1 shows good performance there are still discrepancies between the measured and estimated output. This indicates that we can not rely entirely on feedforward control to achieve good reference tracking. Therefore, a dynamic feedback control law is formulated to handle these discrepancies. All the controllable asset models are combined into one model as follows

$$\dot{x}(t) = A_a x(t) + B_a u_{\text{ref}}(t), \tag{A.8}$$
$$y_a(t) = C_a x(t), \tag{A.9}$$

with

$$A_a = \text{diag}(a_{a,1}, \ldots, a_{a,m}), \tag{A.10}$$
$$B_a = \begin{bmatrix} b_{a,1} & \ldots & b_{a,m} \end{bmatrix}^T, \tag{A.11}$$
$$C_a = \begin{bmatrix} c_{a,1} & \ldots & c_{a,m} \end{bmatrix}, \tag{A.12}$$

where $x(t) \in \mathbb{R}^m$ is the controllable system state vector, $A_a \in \mathbb{R}^{m \times m}$, $B_a \in \mathbb{R}^m$, and $C_a \in \mathbb{R}^m$ are parameters, $y_a(t) \in \mathbb{R}$ is the total active power output of all controllable assets and, $u_{\text{ref}}(t) \in \mathbb{R}$ is the input to the system. Note that because of the control system structure it is possible to apply model reduction techniques if a large number of flexible assets are available, i.e., the overall system dynamic might be dominated by a subset of the assets.

We define $z(t) = \begin{bmatrix} r(t)^T & y_a(t)^T \end{bmatrix}^T$, with $r(t) \in \mathbb{R}$ being the reference signal in combination with the load estimate, i.e., $r(t) = p_{\text{ref}}(t) - \hat{y}_l(t)$, where $p_{\text{ref}}(t) \in \mathbb{R}$ is the reference signal received from an upper layer, $\hat{y}_l(t) = \sum_{i=1}^S y_{l,i}(t)$ is the feedforward signal from the load estimate, and $S \in \mathbb{N}$ is the number of estimated loads. Note that production is seen as positive and load as negative power injection. The dynamic control law is given as

$$\dot{x}_c(t) = A_c x_c(t) + B_c z(t), \tag{A.13}$$
$$u_{\text{ref}}(t) = C_c x_c(t) + D_c z(t), \tag{A.14}$$

where $x_c(t) \in \mathbb{R}^m$ is the controller state and $u_{\text{ref}}(t) \in \mathbb{R}$ is the control output. The feedback control system parameters A_c, B_c, C_c, and D_c are determined

using the controllable asset model along with state feedback gain, observer gain, and feedforward gain as follows

$$\dot{x}_c(t) = \underbrace{(A_a + B_a K + L C_a)}_{A_c} x_c(t) + \underbrace{\begin{bmatrix} M & -L \end{bmatrix}}_{B_c} z(t), \qquad (A.15)$$

$$u_{\text{ref}}(t) = \underbrace{K}_{C_c} x_c(t) + \underbrace{\begin{bmatrix} N & 0 \end{bmatrix}}_{D_c} z(t), \qquad (A.16)$$

where $K \in \mathbb{R}^m$ is the feedback gain, $L \in \mathbb{R}^m$ is the observer gain, $M \in \mathbb{R}^m$ is the observer feedforward gain, and $N \in \mathbb{R}^m$ is the control feedforward gain. Both M and N are determined such that the there is unity gain from reference to output, using the zero assignment method [15, p. 510]. The feedback gain, K and observer gain, L are designed, using pole placement, such that $A_a + B_a K$ and $A_a + L C_a$ are both Hurwitz. It should be noted that robustness in reference tracking can be obtained by adding integral action to the system. This is done by augmenting the control system matrix with an additional state.

3.4 Dispatch Strategy

The control signal, $u_{\text{ref}}(t)$, produced by the controller detailed above, is passed through a dispatch algorithm. The objective of the dispatch algorithm is to minimize active power loss while respecting asset constraints. One solution could be to solve the optimal power flow problem using the method outlined in [16]. This method puts restrictions on the electrical grid topology in order to guarantee zero duality gab. The simplistic approach taken in this work relies on assumptions, such as no voltage problems (voltages are close to nominal value), resulting in a convex formulation without restrictions on grid topology.

The active power loss of an electrical grid can be written as

$$J(t) = i^*(t) \text{Re}(Z(\omega)) i(t), \qquad (A.17)$$

where $i(t) \in \mathbb{C}^n$ is the injected current at each bus, $Z(\omega) \in \mathbb{C}^{n \times n}$ is the bus impedance matrix, $\text{Re}(Z(\omega))$ denotes the real part of $Z(\omega)$, $\omega \in \mathbb{R}$ is the electrical grid frequency, $n \in \mathbb{N}$ is the number of busses in the system, and x^* denotes the conjugate transpose of x. See [17, p. 289] for a full derivation of the active power loss formula, and [17, p. 369] for an algorithm to compute $Z(\omega)$. In the following we assume a constant frequency.

The values of the currents $i(t)$ are typically not known, but can be expressed by the complex power and voltage at each bus

$$i_k(t) = \frac{s_k^*(t)}{v_k^*(t)}, \ k = 1, \dots, n, \qquad (A.18)$$

where $v_k(t) \in \mathbb{C}$ is the voltage at bus k, $s_k(t) = p_k(t) + \mathrm{j}q_k(t)$ is the complex power at bus k, with $p_k, q_k \in \mathbb{R}$ being the active and reactive power component, respectively. If the bus voltages are measured or assumed constant, they can be combined with the grid impedance matrix as follows

$$B(t) = V^*(t)\mathrm{Re}(Z)V(t), \tag{A.19}$$

with

$$V(t) = \mathrm{diag}\left(v_1^{-1}(t), \ldots, v_n^{-1}(t)\right), \tag{A.20}$$

resulting in the following expression for active power loss

$$J(t) = s^*(t)B(t)s(t), \tag{A.21}$$

where $s(t) = \begin{bmatrix} s_1(t) & \ldots & s_n(t) \end{bmatrix}^T$. Now (A.17) is formulated with respect to the complex power at each bus. With the estimate of power consumption at load busses (both active and reactive), along with assumed voltage measurements, the active power dispatch optimization problem, to be solved at time t, can be formulated as

$$
\begin{aligned}
\min_{u_1(t),\ldots,u_m(t)} \quad & J(t) \\
\text{s.t.} \quad & \sum_{i=1}^m u_i(t) = u_{\mathrm{ref}}(t) \\
& u_{\mathrm{min},i}(t) \le u_i(t) \le u_{\mathrm{max},i}(t), \\
& i \in \mathcal{A}
\end{aligned}
\tag{A.22}
$$

with variables $u_1, \ldots, u_m$ and data $u_{\mathrm{min},1}(t), \ldots, u_{\mathrm{min},m}(t)$, $u_{\mathrm{max},1}(t), \ldots, u_{\mathrm{max},m}(t)$, $q_1, \ldots, q_n$, $v_1(t), \ldots, v_n(t)$, $\hat{p}_l(t)$, $u_{\mathrm{ref}}(t)$, and $Z(\omega)$. It should be noted that the decision variables u_i represent active power injection/consumption at flexible asset busses. The cost function stated in (A.22) can be shown to be convex in the real and imaginary parts of the complex power, and with the constraints also being convex, it is a convex programming problem. The problem is similar to the one formulated in [18], but with no capacity constraints on lines, and without the voltages as variables. What should be noted from this formulation is that it is a simple problem, which can be solved fast even for a large number of decision variables, m, and thus easily implementable. However, it relies on the flexible assets having almost the same dynamics to guarantee an optimal operating point at each time instance t, i.e., in steady state the optimum will be reached. To handle differences in asset dynamics these can be included in the optimization problem in a receding horizon control strategy [19]. The caveat to adding asset dynamics in this way is an increase in problem complexity and thus computation and deployment time.

4   Simulation Example

The proposed control system is evaluated on a realistic simulation scenario with complex asset and electrical grid models, using the power systems simulation toolbox DiSC [13]. Thereby, the simplifications and assumptions made in the control design process are tested for robustness against parameter deviations, unmodeled dynamics, etc..

We consider a distribution grid with seven busses, three inflexible residential loads, and two flexible production units (wind power plant (WPP) and solar power plant (SPP)). The DGC receives a power reference signal and dispatches this to the two production units. The setup is depicted in Fig. A.5, and the parameters are summarized in TABLE A.2.
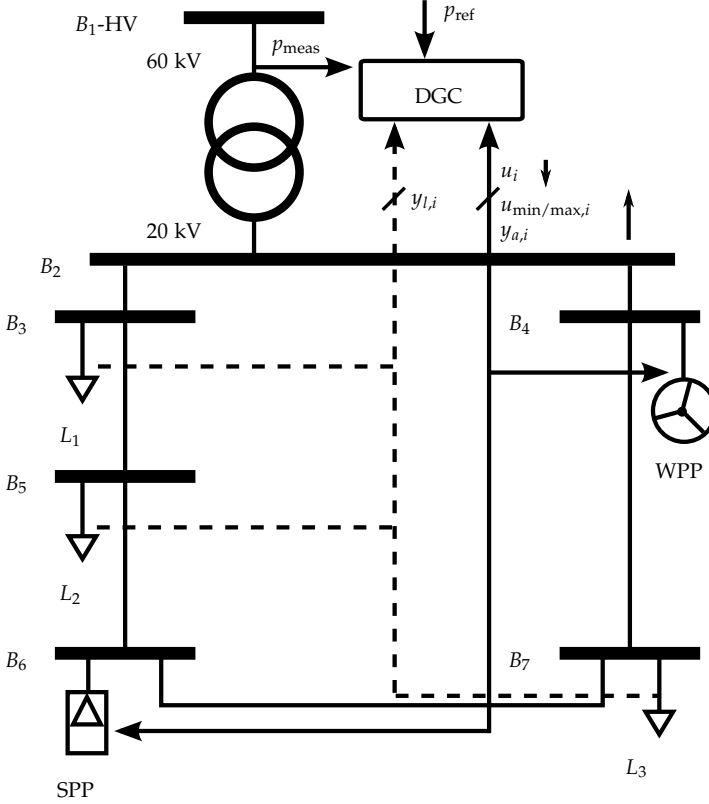

Fig. A.5: Distribution grid used in the simulation example. The distribution grid controller receives a power reference, p_{ref}, power measurements from the load busses, p_{load}, and current state along with flexibility information from the production units, p_{asset}, $u_{\mathrm{min/max}}$. The controller then dispatches reference signals to the two production units, u.

We consider a windy and cloudy day in June. The power reference re-

Table A.2: Parameters for the distribution grid shown in Fig. A.5.

Component	Parameter	Value
Wind power plant	Total rated power	2.4 MW
PV system	Total rated power	2.4 MW
Transformer	Impedance	3+j13 Ω
Line B_2-B_3	Impedance	1+j1 Ω
Line B_2-B_4	Impedance	3.25+j2.25 Ω
Line B_3-B_5	Impedance	0.65+j0.45 Ω
Line B_5-B_6	Impedance	0.13+j0.06 Ω
Line B_4-B_7	Impedance	3.25+j3 Ω
Line B_6-B_7	Impedance	0.5+j0.5 Ω
Load L_1	Number of houses	2000
Load L_2	Number of houses	2000
Load L_3	Number of houses	2000

ceived has been arbitrarily chosen to illustrate the system's tracking ability. During eight hours in the mid-day the reference is set to zero, i.e., the grid should not import or export active power. This could be caused by frequency control issues detected on the transmission level or other external factors. The DGC's reference tracking ability is illustrated in Fig. A.6 and the active power production of the WPP and SPP are shown in Fig. A.7. Further, the proposed dispatch algorithm is compared to a strategy of uniformly distributing the power reference between the two assets. This comparison is summarized in TABLE A.3.

A number of interesting results are observed. Under the developed control system the distribution grid is capable of following the reference signal with a root mean square error (RMSE) of only 94.8 kW during one day. Moreover, during the eight hours of no import/export the system evolves closely around the referenced value, indicating that the distribution grid can offer services such as frequency regulation, to upper layers. From Fig. A.7 it is seen that the proposed dispatch lowers the production from the WPP and increases the production from the SPP, during the eight hours of no import/export. This makes sense as the system should only provide power for the three loads which are placed closer to the SPP, seen from an electrical point of view. The proposed dispatch strategy decreases the power loss with 3 %. However, this number is expected to increase if the control system is applied to a larger distribution grid.
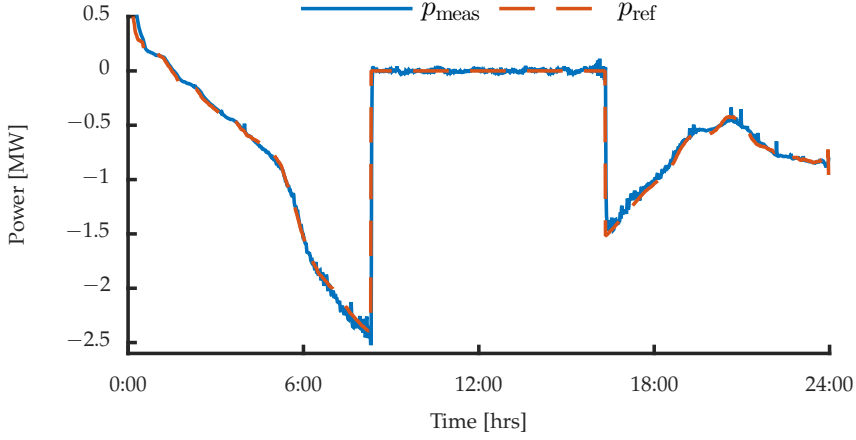
Fig. A.6: The control system's reference tracking ability. The fluctuations around the reference are caused by clouds passing over the SPP and WPP operating below rated wind speed.
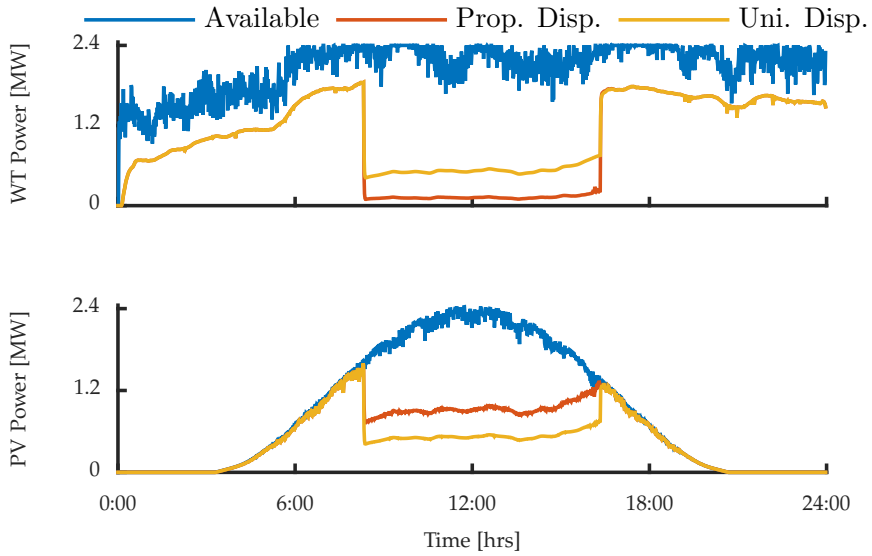

Fig. A.7: Available and actual power production of the WPP (top) and SPP (bottom).

Table A.3: Comparison between the proposed dispatch algorithm and uniformly distributing the power among the flexible assets. Total grid loading is 14 MWh, and the results have been normalized to the uniform dispatch case.

Method	Tracking Error (RMS)		Power Loss	
	[kW]	%	[MWh]	%
Uni. Disp.	94.0	100.0	0.33	100.0
Prop. Disp.	94.8	100.8	0.32	97.0

5   Conclusion

In this work, we presented a control system allowing a distribution system operator to manage a power distribution grid, towards an active power reference. The control system consisted of three main components; an inflexible load estimator based on linear harmonic oscillators, a feedback control law for managing the flexible assets, and a dispatch algorithm for minimizing active power loss. The outlined estimation procedure was validated on real consumption data and showed good estimation capability, both on a step-ahead and day-ahead scale. Through simulations on a 7 bus distribution grid with two flexible assets it was shown that the designed feedback control in combination with the dispatch algorithm provided excellent tracking ability with a root mean square error of approximately 94 kW, even with the stochastic nature of the flexible assets. Further, the proposed dispatch algorithm was compared with a strategy of evenly distributing the reference between the assets. It was possible to decrease the loss with 3 %, even for a small distribution grid. The developed control system was simple in nature, allowing for rapid implementation and deployment.

Acknowledgments

References

[1] P.-C. Chen, R. Salcedo, Q. Zhu, F. de León, D. Czarkowski, Z.-P. Jiang, V. Spitsa, Z. Zabar, and R. E. Uosef, "Analysis of voltage profile problems due to the penetration of distributed generation in low-voltage secondary distribution networks," *IEEE Transactions on Power Delivery*, no. 4, pp. 2020 – 2028, Sep. 2012.

References

[2] EDSO, "Flexibility: The role of DSOs in tomorrow's electricity market," European Distribution System Operators for Smart Grids, Tech. Rep., 2014.

[3] L. F. Amarel, R. C. Souza, and M. Stevenson, "A smooth transition periodic autoregressive (STPAR) model for short-term load forecasting," *International Journal of Forecasting*, vol. 24, pp. 603 – 615, 2008.

[4] V. Dordonnat, S. J. Koopman, A. D. M. Ooms, and J. Collet, "An hourly periodic state space model for modelling french national electricity load," *International Journal of Forecasting*, vol. 24, no. 4, pp. 566 – 587, Dec. 2008.

[5] M. Espinoza, C. Joye, R. Belmans, and B. D. Moor, "Short-term load forecasting, profile identification, and customer segmentation: A methodology based on periodic time series," *IEEE Transactions on Power Systems*, vol. 20, no. 3, Aug. 2005.

[6] A. A. A. Esmin, G. Lambert-Torres, and A. C. Z. de Souza, "A hybrid particle swarm optimization applied to loss power minimization," *IEEE Transactions on Power Systems*, vol. 20, no. 2, pp. 859 – 866, may 2005.

[7] Y. jun Zhang and Z. Ren, "Optimal reactive power dispatch considering costs of adjusting the control devices," *IEEE Transactions on Power Systems*, vol. 20, no. 3, pp. 1349 – 1356, aug 2005.

[8] R. Madani, M. Ashraphijuo, and J. Lavaei, "Promises of conic relaxation for contingency-constrained optimal power flow problem," in *52nd Allerton Conference on Communication, Control and Computing (Allerton)*, Monticello, IL, USA, Sep. 2014, pp. 1064 – 1071.

[9] V. Kekatos, G. Wang, and G. B. Giannakis, "Stochastic loss minimization for power distribution networks," in *North American Power Symposium (NAPS)*, Pullman, WA, USA, Sep. 2014, pp. 1 – 6.

[10] G. Harrison and A. R. Wallace, "Optimal power flow evaluation of distribution network capacity for the connection of distributed generation," in *6th International conference on Ubiquitous and Future Networks (ICUFN)*, Shanghai, China, Jul. 2014, pp. 205 – 210.

[11] R. Bonetto, S. Tomasin, and M. Rossi, "Distributed power loss minimization in residential micro grids: a communications perspective," *arXiv:1311.6949 [cs.OH]*, Nov. 2013.

[12] B. A. Francis and W. M. Wonham, "Internal model principle of control theory," *Automatica*, vol. 12, no. 5, pp. 457 – 465, sep 1976.

[13] R. Pedersen, C. Sloth, G. B. Andresen, and R. Wisniewski, "DiSC: A simulation framework for distribution system voltage control," in *European Control Conference*, Linz, Austria, Jul. 2015.

[14] B. M. Åkeson, J. B. Jørgensen, N. K. Poulsen, and S. B. Jørgensen, "A tool for kalman filter tuning," in *17th European Symposium on Computer Aided Process Engineering*, Bucharest, Romania, 2007.

[15] G. F. Franklin, J. D. Powell, and A. Emami-Naeini, *Feedback Control of Dynamic Systems*, 6th ed. Pearson, 2010.

[16] R. Madani, S. Sojoudi, and J. Lavaei, "Convex relaxation for optimal power flow problem: Mesh networks," *IEEE Transactions on Power Systems*, vol. 30, no. 1, pp. 199–211, jan 2015.

[17] H. Saadat, *Power System Analysis*, 2nd ed. McGraw-Hill, 2002.

[18] M. Juelsgaard, C. Sloth, R. Wisniewski, and J. Pillai, "Loss minimization and voltage control in smart distribution grid," in *Proceedings of the 19th IFAC World Congress*, Cape Town, South Africa, Aug. 2014.

[19] A. N. Venkat, I. A. Hiskens, J. B. Rawlings, and S. J. Wright, "Distributed MPC strategies with application to power system automatic generation control," *IEEE Transactions on Control Systems Technology*, vol. 16, pp. 1192–1206, 2008.

References

Paper B

Adaptive Power Balancing over Congested
Communication Links

Rasmus Pedersen, Mislav Findrik, Christoffer Sloth, and
Hans-Peter Schwefel

Abstract

To maintain a reliable and stable power grid there must be balance between consumption and production. To achieve power balance in a system with high penetration of distributed renewable resources and flexible assets, these individual system can be coordinated through a control unit to become part of the power balancing effort. Such control strategies require communication networks for exchange of control loop information. In this work, we show how a congested communication network can have a dramatic impact on the control performance of such a power balancing controller. To alleviate potential stability issues and increase control performance, an adaptive control design is proposed together with a communication network state estimation algorithm. Extensive simulation studies on a realistic model of a low voltage residential grid, using network traces obtained from a real powerline network, show significant performance improvement when the adaptive controller is used.

1   Introduction

The growing need for sustainable energy supply is resulting in increased installation of renewable energy generation resources in todays' electrical distribution grids [1]. Such power generating resources are distributed across medium voltage (MV) and low voltage (LV) grids, and are characterized by having a highly volatile power production given by environmental conditions such as wind speed and solar irradiation. This ongoing transition is challenging the system operators [2], and they are demanding new control features enabling them to maintain a reliable electrical grid with a high quality of power delivery [3].

Grouping local loads with renewable production units allows operators to construct microgrids (MGs) and maintain power balance, by coordinating these units along with flexible assets, such as energy storages. The MG is one of the key concepts that can strengthen grid resilience and mitigate large power blackouts [4]. Each MG must be able to operate autonomously in islanded mode and be capable of coordinating generating resources to meet consumption demand [5]. However, operating a MG over communication networks brings challenges for control algorithms, which require low latency and reliable network performance. In this paper, a hierarchical approach for managing flexible units in a MG is presented, where a particular focus is placed on the design of an adaptive controller that is stable despite congested and non-ideal communication links.

Successful control over imperfect networks could significantly lower infrastructural costs by enabling usage of existing communication networks. Nowadays, xDSL, fiber optics, DOCSIS, and cellular networks (e.g. GPRS, UMTS, LTE) are already widely deployed by the telecom operators in Europe with high coverage [6], hence they could be used for connecting the flexi-

ble units with the MG controllers. Alternatively, grid operators may want to deploy their own infrastructure, desirably using off-the-shelf technologies such as wireless mesh networks (e.g. 802.15.4 or 802.11) or powerline (PLC) communication, which do not require additional cabling [7]. When these networks are shared between several Smart Grid applications (e.g. advanced metering or demand response programs) or other units generating traffic, they may not deliver the network performance required by the control algorithm. In Fig. B.1, it is illustrated how congesting the communication links of the powerline communication is impacting a power balancing controller tuned for a non-congested communication network. During periods with no congestion the network delays are negligible and the controller follows the given reference tightly, however during the periods with congestion the communication links experience high delays, resulting in oscillatory closed-loop behavior.
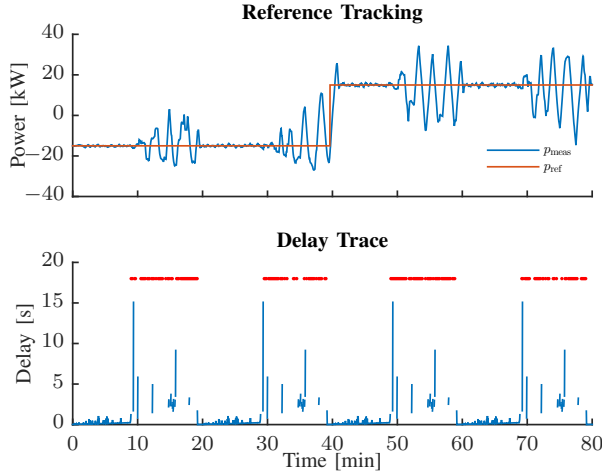

Fig. B.1: Example of closed loop reference tracking, where the controller has been tuned without regards for the time-varying congestion levels of the underlying communication network. Top: shows that when the communication network is congested the system begins to oscillate. Bottom: shows the communication network delay trace, where missing data indicates packet loss and is marked with a red dot.

The control of power systems over communication networks has been addressed in several papers. In [8] they analyse the need for new real-time control features and the need for gathering information from distributed resources through communication channels experiencing delays and loss of information. They illustrate the consequences of large delays on the operation of power systems and briefly mention possible solutions. However, the work does not cover time-varying communication network state or the coordination of distributed systems on a low voltage level, where computation

power is limited and communication networks are shared with several other systems. The approach taken in [9] is based on linear matrix inequalities to compute a controller which is stable under some given delay interval. The control law easily becomes conservative, as they do not consider adapting the system to different magnitudes of delays.

In this work, a procedure for designing a controller capable of adapting based on communication network properties is presented. To coordinate the flexibility of assets the method relies on consensus algorithms, which are suitable for large scale systems [10–12], and have been applied to achieve power sharing in micro-grids [13]. Further, for adapting controller gains, our control design approach relies on network monitoring and estimation of current communication network state, hence allowing fast convergence during good network conditions and instability avoidance when high delays are present. This approach has further been evaluated using communication network traces from a real PLC network along with real power consumption data. The main contributions of the paper are are:

- A procedure for estimating the communication network state, and a technique for parameterizing the estimator.

- An adaptive power balancing controller for coordinating the flexibility of distributed resources in a low voltage grid towards a power reference. The controller adapts based on estimates on communication network state.

- Thorough evaluation of the designed controller is carried out based on a LV distribution grid, with disturbances, models, and communication traces based on real data.

The remainder of the paper is structured as follows: in Section 2, mathematical notation and definitions are introduced; in Section 3 a problem statement is formulated and the role of the power balancing controller in the MG is explained; in Section 4 a network state estimation algorithm is given; in Section 5 a procedure for the adaptive controller design is presented; in Section 6, the communication network state estimation and controller design procedure is exemplified on the case study of a power balancing controller, exchanging information over a two state PLC communication network. Further, in Section 7 simulation data and models are detailed along with a description of conducted simulation scenarios. This is followed by Section 8 where simulation results are presented. Lastly, in Section 9 conclusions are drawn and perspectives for the adaptive control approach are outlined.

2   Preliminaries

ß This section contains the notation and definitions used throughout the paper.

We denote the set of real numbers by $\mathbb{R}$, and let $\mathbb{R}_+$ be the non-negative part of the real numbers. By $\mathbf{1}_n$ ($\mathbf{0}_n$) we denote a column vector of all ones (zeros) of dimension n, where the subscript n is omitted if dimension is clear from context. For a matrix A we denote the matrix transpose by A^T.

We rely on the following definitions from algebraic graph theory.

Definition 2 (Directed Graph). *A directed graph is a pair $G = (V, E)$, where $V = \{1, \ldots, n\}$ is a nonempty set of nodes, and $E \subseteq V \times V$ is a set of edges.*

Definition 3 (Cardinality of Set). *For a set V we denote its cardinality $|V|$.*

Definition 4 (Neighbors of Node). *Let $G = (V, E)$ be a graph. The set of neighbors of node $i \in V$ is*

$$N_i = \{j \in V \mid (v_j, v_i) \in E\}. \tag{B.1}$$

Definition 5 (Adjacency Matrix). *Given a graph $G = (V, E)$, the adjacency matrix $A \in \mathbb{R}^{|V| \times |V|}$ is*

$$A = [a_{ij}], \qquad \text{where } a_{ij} = \begin{cases} 1, & j \in N_i \\ 0, & \text{otherwise.} \end{cases} \tag{B.2}$$

Definition 6 (Graph Laplacian Matrix). *The Laplacian of a graph G, is given from its adjacency matrix A as*

$$L = [l_{ij}], \qquad \text{where } l_{ij} = \begin{cases} -a_{ij}, & j \in N_i \\ \sum_{j=1}^{|V|} a_{ij}, & i = j \\ 0, & \text{otherwise} \end{cases} \tag{B.3}$$

In the case of leader-follower consensus the leader has no ingoing edges. Let agent i be the leader agent, then the entries of the i-th row of L are all zero, i.e., $L_{ij} = 0$ for $j = 1, \ldots, |V|$.

Definition 7 (Directed Spanning Tree). *A directed spanning tree of a directed graph $G = (V, E)$ rooted at node n, is a subgraph $G' = (V, E')$, where $E' \subseteq E$ and G' is a tree and G' contains a directed path from n to any other node in V.*

3   Problem Formulation

In this section we motivate the study of power balancing, on a short time scale, in low voltage distribution grids. We provide an overview of the system structure and shortly describe the different components of the system.

We consider the micro-grid illustrated in Fig. B.2, where a local *frequency controller* is in charge of ensuring a constant grid frequency, whenever the grid is in islanded mode. In order to control the grid frequency and ensure power balance, the *frequency controller* utilizes generation units along with other flexible *assets*. To manage the *assets* on a lower voltage level, a *power controller* is implemented to obtain a hierarchical control structure, i.e., each *power controller* controls a set of assets.

This paper focuses on the greyed area in Fig. B.2, which entails the design and implementation of a *power controller*, which can adapt to changes in the communication network connecting it with the assets. The objective of the controller is to make the total power of a distribution grid follow a power reference received from the *frequency controller*. The *power controller* communicates with the assets through a communication network; hence, stability and tracking ability must be ensured, even when the communication is affected by delay and information/packet loss. Therefore, we focus on an adaptive control strategy, where gains are scheduled based on the communication system state.

In the following two sections we present a communication network state estimator and develop an adaptive control strategy.

4 Estimation of Communication Network State

The purpose of this section is to present a method for estimating the network state. In this context the network state represents different levels of congestion in the network. This is relevant for control, as congestion affects information delay and loss.

We model the communication network with a finite state model. The model has discrete states $S = \{S_1, S_2, \ldots, S_N\}$, where each network state is associated with different congestion levels of the network. An indicator of the network state is the communication delay, which can be estimated from round trip time (RTT) measurements. We denote an observation of RTT by $o_{\text{rtt}} \in \mathbb{R}_+$, and propose a threshold-based network state estimator, with threshold set $T = \{\tau_1, \tau_2, \ldots, \tau_{N-1}\}$. We then apply a moving average diagnosis procedures as follows:

$$\bar{o}_{\text{rtt}}(k) = \frac{1}{l} \sum_{i=0}^{l-1} o_{\text{rtt}}(k - i), \tag{B.4}$$

$$\widehat{S}(k) = \begin{cases} S_N & \text{if} & \bar{o}_{\text{rtt}}(k) \geq \tau_{N-1}, \\ S_j & \text{if} & \tau_j > \bar{o}_{\text{rtt}}(k) \geq \tau_{j-1}, \ j \in \{2, \ldots, N-1\}, \\ S_1 & \text{if} & \bar{o}_{\text{rtt}}(k) < \tau_1, \end{cases} \tag{B.5}$$

where $\bar{o}_{\text{rtt}}(k)$ is the moving average value at sample k, and $\widehat{S}(k)$ is the communication network state estimate at sample k. The algorithm parameters l
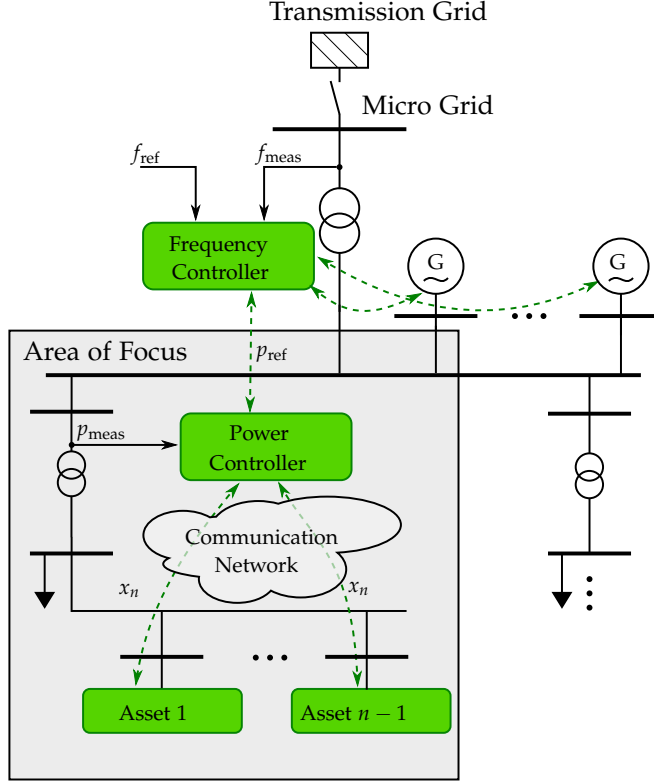
Fig. B.2: Overview of the control system architecture. The Power Controller manages flexible assets to make the distribution grid under its substation follow the reference, p_{ref}, received from the upper layer controller.

and $T = \{\tau_1, \tau_2, \ldots, \tau_{N-1}\}$ can be parametrized using ROC graphs [14], as it is exemplified later on in Section 6.1.

5 Adaptive Controller Design

The purpose of this section is to describe the adaptive power balancing control algorithm. The controller sends setpoints to the flexible assets via a communication network with time-varying characteristics. First, we provide a simple dynamic model of the flexible assets. Then, a controller is designed under the assumption of ideal communication. This is followed by the design of an adaptive algorithm, that takes into account the change in communication network state. The control system architecture is illustrated in Fig. B.3.
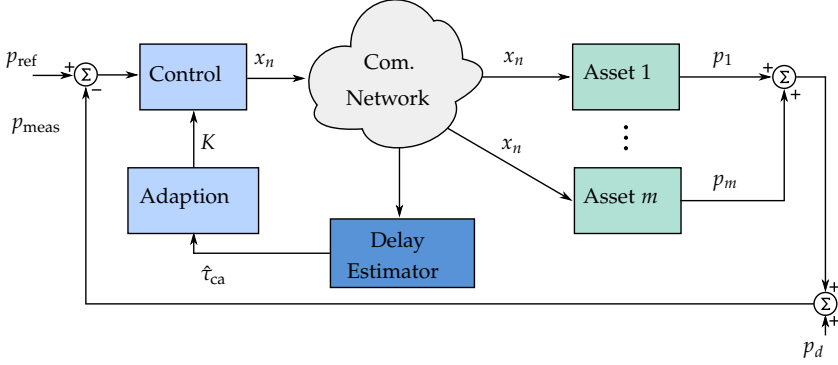
Fig. B.3: Control system architecture. Controller gains, $(K_{P,i}, T_{I,1})$, are adapted based on estimates of the communication network state, $\widehat{S}_i$.

5.1 Flexible Asset Model

We model the transient behavior of assets by constrained first order dynamic systems, in order to capture effects such as rate limitations. The model is given by

$$\dot{x}_i = a_i x_i + b_i u_i, \tag{B.6}$$

$$p_i = c_i x_i \tag{B.7}$$

$$\underline{p}_i \le p_i \le \overline{p}_i, \tag{B.8}$$

where $x_i \in \mathbb{R}$ is the agent state, $u_i \in \mathbb{R}$ is the input, $a_i, b_i, c_i \in \mathbb{R}$ are system parameters, $\underline{p}_i$ and $\overline{p}_i$ are lower and upper bound on asset power output, respectively.

5.2 Control under Ideal Communication

To design the power balancing controller we employ a consensus-based approach, which is a natural way of formulating networked control systems that may experience time-varying delays and changing network topologies [12, 15]. Power balancing is a tracking problem, which in a consensus setting is solved by a leader-follower approach, where the leader agent (in our case the power controller) determines the reference which all follower agents (the flexible assets) need to follow.

From leader-follower consensus we use the following result. Consider a dynamic network of agents connected through a communication graph $G = (V, E)$. Let each follower agents dynamics be given by the first order system in (B.6), and let the number of agents, including the leader be denoted by $n = |V|$. Without the loss of generality let agent n be the leader and let the

remaining $n-1$ agents apply the protocol

$$u_i = \gamma_i x_i - \sum_{j \in N_i} a_{ij}(x_i - x_j), \tag{B.9}$$

where $\gamma_i \in \mathbb{R}$ is a local control gain and $A = [a_{ij}] \in \mathbb{R}^{n \times n}$ is the graph adjacency matrix. Let $u_n = 0$ and $\gamma_i = \frac{a_i}{b_i}$, then the closed loop system can be written as

$$\dot{x} = -Lx, \tag{B.10}$$

where $L \in \mathbb{R}^{n \times n}$ is the graph Laplacian, with all entries of the last row equal to zero. The system in (B.10) reaches leader-follower consensus, i.e.,

$$x_i(t) \to x_n(t), \ \forall i \in V \backslash \{n\}, \text{ for } t \to \infty, \tag{B.11}$$

if and only if the graph G has a directed spanning tree, with agent n as root, see Theorem 3.2 in [16, p. 57]. In other words, if the leader agent has a constant output and there is a directed path from it to all other agents, then all agents will approach the leader agent's state value asymptotically. However, this result cannot directly be used when the leader updates it state dynamically e.g., by a control law. We illustrate this in the following sections. Further, we assume that the communication graph connecting the flexible assets (follower agents) with the power controller (leader), satisfies the above requirement of having a directed spanning tree, rooted at the leader.

Leader Agent Dynamics

We let the leader agent (agent n) update its state value according to a proportional integral (PI) control law. As already stated we can no longer rely solely on the above result from leader-follower consensus, as it assumes a constant leader state.

The leader dynamics is given as

$$\dot{x}_n(t) = u_n = K_P e(t) + \frac{K_P}{T_I} x_I(t), \tag{B.12}$$

$$\dot{x}_I(t) = e(t),$$

where $e(t) = p_{\text{meas}}(t) - p_{\text{ref}}(t)$ is the tracking error, $x_I \in \mathbb{R}$ is the integral state, $K_P \in \mathbb{R}$ is the proportional gain, and $T_I \in \mathbb{R}$ is the integral time. The system dynamics can then be written as

$$\dot{x} = -Lx + B u_n, \tag{B.13}$$

$$p_{\text{meas}} = Cx + p_d,$$

where $p_d \in \mathbb{R}$ is a disturbance originating from the uncontrollable part of the grid and the matrices $B \in \mathbb{R}^{n \times 1}$ and $C \in \mathbb{R}^{1 \times n}$ are as follows

$$B = \begin{bmatrix} \mathbf{0}_{n-1}^T & 1 \end{bmatrix}^T, \tag{B.14}$$

$$C = \begin{bmatrix} c_1 & \cdots & c_{n-1} & 0 \end{bmatrix}. \tag{B.15}$$

Connecting the system of agents with the controller equations yields the closed loop system given by

$$\begin{bmatrix} \dot{x} \\ \dot{x}_\mathrm{I} \end{bmatrix} = A_{cl} \begin{bmatrix} x \\ x_\mathrm{I} \end{bmatrix} + B_r p_{\mathrm{ref}} + B_w p_d \tag{B.16}$$

$$p_{\mathrm{meas}} = \begin{bmatrix} C & 0 \end{bmatrix} \begin{bmatrix} x \\ x_\mathrm{I} \end{bmatrix} + p_d,$$

with

$$A_{cl} = \begin{bmatrix} -L + K_\mathrm{P} BC & \frac{K_\mathrm{P}}{T_\mathrm{I}} B \\ C & 0 \end{bmatrix}, \tag{B.17}$$

$$B_r = \begin{bmatrix} -K_\mathrm{P} B^T & -1 \end{bmatrix}^T, \tag{B.18}$$

$$B_w = \begin{bmatrix} K_\mathrm{P} B^T & 1 \end{bmatrix}^T. \tag{B.19}$$

The value of the leader agent state x_n, is constrained as follows

$$-1 \leq x_n \leq 1, \tag{B.20}$$

where $x_n = -1$ represents full consumption actuation and $x_n = 1$ full production actuation, i.e., if $x_n = -1$ then all follower agents should consume as much as possible ($p_i = \underline{p}_i$) and vice versa ($p_i = \overline{p}_i$). This allows for no explicit anti-windup strategy based on e.g., flexibility information from each follower agent. Also, fairness is achieved, as all follower state values converge to the leader state value. We do however require symmetry in the output of follower agents in the control formulation, i.e., $\underline{p}_i = \overline{p}_i$. This requirement can easily be omitted, by introducing additional notation. Notice that the system can be viewed as a single input single output (SISO) system, allowing the use of classical frequency based control design methods, such as root locus.

In the following we extend the proposed design procedure to a system with communication delays, and establish a gain scheduling procedure that ensures stability for different magnitudes of delays.

5.3 Control under Non-Ideal Communication

To handle the problem of introducing delays between the leader and the followers, we augment the system with a delay system, see Fig. B.4, and assume that all communication links experience the same delay.
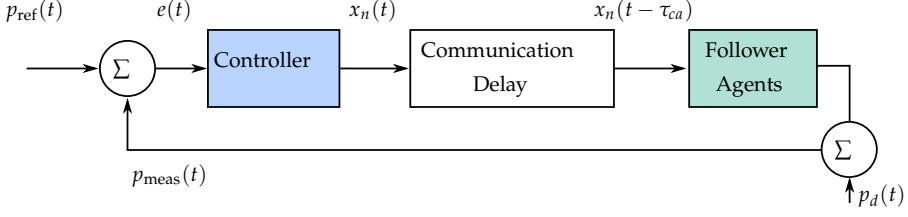
Fig. B.4: Closed loop system, augmented with a dynamic system modeling the delay. A second order Padé approximation is used.

To model the delay we use a second order Padé approximation, which is given by

$$\dot{x}_d = A_d x_d + B_d u_d, \tag{B.21}$$

$$y_d = C_d x_d + D_d u_d, \tag{B.22}$$

where $x_d \in \mathbb{R}^2$ is the delay system state, $u_d \in \mathbb{R}$ is the delay system input, $y_d \in \mathbb{R}$ is the delay system output, and the system matrices are as follows

$$A_d = \begin{bmatrix} -\frac{6}{\hat{\tau}_{ca}} & -\frac{12}{\hat{\tau}_{ca}^2} \\ 1 & 0 \end{bmatrix}, \qquad B_d = \begin{bmatrix} 1 & 0 \end{bmatrix}^T, \tag{B.23}$$

$$C_d = \begin{bmatrix} -\frac{12}{\hat{\tau}_{ca}} & 0 \end{bmatrix}, \qquad D_d = 1, \tag{B.24}$$

where $\hat{\tau}_{ca} \in \mathbb{R}_+$ is an estimate of the current maximum delay between the leader and the followers, i.e., we consider the worst case scenario for all communication links. With the delay system included, the closed loop system is given by

$$\begin{bmatrix} \dot{x} \\ \dot{x}_d \\ \dot{x}_I \end{bmatrix} = A_{cl} \begin{bmatrix} x \\ x_d \\ x_I \end{bmatrix} + B_r p_{\text{ref}} + B_w p_d, \tag{B.25}$$

$$p_{\text{meas}} = \begin{bmatrix} C & 0 & 0 \end{bmatrix} \begin{bmatrix} x \\ x_d \\ x_I \end{bmatrix} + p_d,$$

with

$$A_{cl} = \begin{bmatrix} -L + K_P BC & BC_d & \frac{K_P}{T_I} B \\ K_P B_d C & A_d & \frac{K_P}{T_I} B \\ C & 0 & 0 \end{bmatrix}, \tag{B.26}$$

$$B_r = \begin{bmatrix} -K_P B^T & -K_P B_d^T & -1 \end{bmatrix}^T, \tag{B.27}$$

$$B_w = \begin{bmatrix} K_P B^T & K_P B_d^T & 1 \end{bmatrix}^T. \tag{B.28}$$

Next, we provide a gain scheduling method for adapting the control according to communication network state.
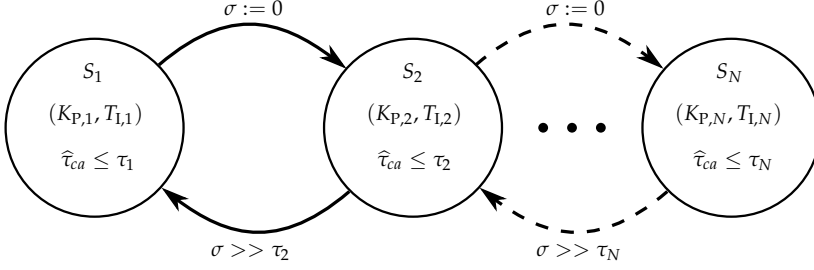
Fig. B.5: Conceptual diagram of how the switching between communication network states affects the control parameters. The clock σ has been added to implement a minimum dwell time before switching to a controller designed for smaller delays, i.e., a more aggressive controller.

5.4 Adaptive Gain Scheduling

It is possible to design a collection of controllers, which are resilient to different delays and then switch between the controllers according to estimates on communication network state. This setup is conceptually illustrated in Fig. B.5.

Let the current estimate of network delay from the controller to the assets be denoted $\widehat{\tau}_{ca}$. Controller i is resilient for delays up to τ_i. If the communication state estimator switches to a state with larger delays, the controller gains are switched to handle the delays associated to the network state. To ensure stability, the controller gains cannot be switched arbitrarily fast to a more aggressive mode (increase of gains). Therefore, a minimum dwell time constraint is added to the system. This is implemented by the clock σ, which is reset ($\sigma := 0$) each time the controller gains are switched to handle a communication network state with higher delays. A guard condition, requiring that the value of the clock σ, should be much larger than the delay associated to the current estimate of network state, for which the new controller gains should be resilient towards. This ensures that we do not switch to a more aggressive controller unless we are confident that the delay estimate is valid. Thereby, the control gains for each communication network state can be designed separately.

In the following section we illustrate the design of a communication network state estimator, for a two state PLC network, and design controllers for the two network states.

6 Communication Network State Estimation and Control Design Example

This section provides a communication network state estimation example along with associated control design. First, the control information exchange is presented, followed by a calibration example of a two state network esti-

mator based on RTT measurements collected from a PLC network. Lastly, the control design procedure is exemplified.

6.1 Control Information Exchange over a PLC network

Networked based closed loop systems typically perform the following three main operations: sampling, computation and actuation. The power controller is situated at the secondary substation, where a power meter samples p_{meas} values in equidistant time steps T_s. Based on these measurements the controller computes a setpoint x_n, and distributes it to the assets in each sample. After a certain delay time τ_{ca}, a setpoint is received by an asset and actuation takes place. Fig. B.6 shows a messaging diagram between the power meter, the power controller, and the flexible assets.
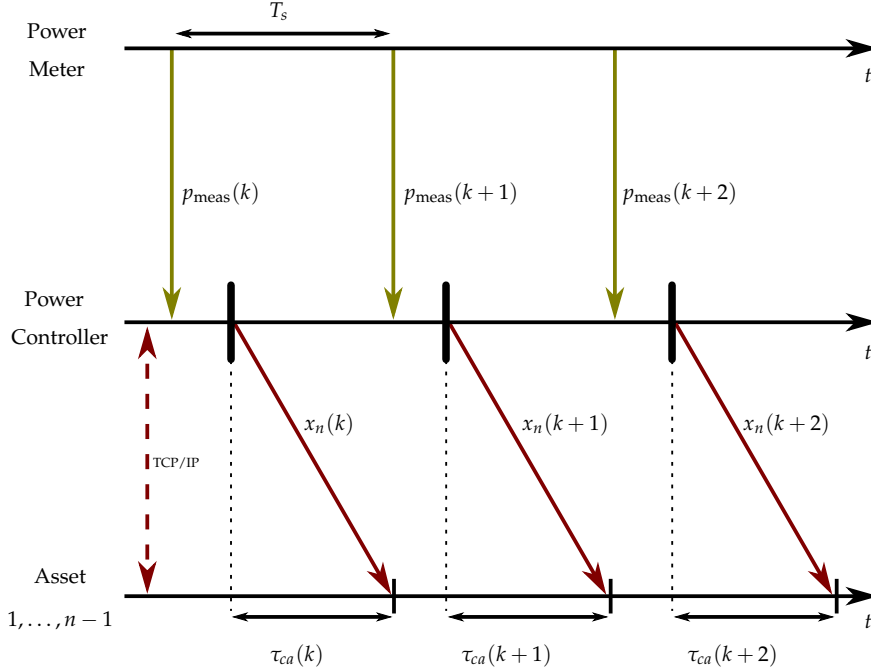

Fig. B.6: Information flow and time measurements between the flexible assets and the Power controller.

All application level messages are transfered using the TCP protocol, as it is practice by electrical utility automation protocols e.g., Modbus/TCP and 61850-7-420, which are running over IP based networks [17]. For the study in this paper, we consider a sampling time of, $T_s = 1$s, in order to support power balancing on a fast time scale required by a *frequency controller*. The actuation messages sent from the power controller, x_n, are subject to time

varying delays caused by additional noises present on a PLC channel [18] and also influenced by additional network cross traffic. The influence of network cross-traffic is illustrated in Fig. B.7, where beside the control, additional ICMP cross traffic (10 kbps per asset) is exchanged between the controller and three flexible assets. RTT values, collected from TCP_{ack} messages, when sending 200B control packets every 1s, are shown for all three assets in the upper part of the figure, together with cumulative cross traffic in the PLC network, shown in the lower part of the figure. All network measurements shown in this paper are obtained from a small PLC network composed of four narrowband G3-PLC modems interconnected with a short low-voltage powerline cable and deployed in our testbed environment, details can be in [19]. One modem is connected to the controller, while the remaining three modems are connected to asset.
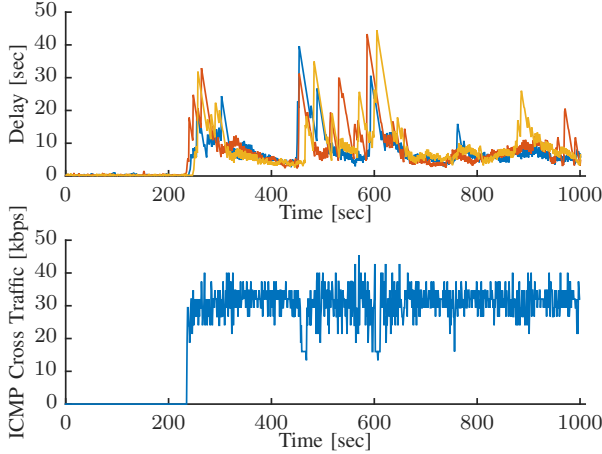

Fig. B.7: Top: RTT delays between the power controller and the three assets plotted over time. Bottom: Total transport layer cross-traffic throughput on the PLC network created by ICMP pings.

The TCP protocol provides ordered and reliable data transfer, for example, a lost controller actuation packet x_n, will be retransmitted and delivered either before the time $x_n(k+1)$ is computed or afterwards, e.g., in case of large delays or burst delivery of multiple actuation messages. When multiple actuations are delivered, only the latest actuation takes place, while the others are discarded. Hence, discarded actuations are referred as *packet losses*, which are observable from processed network traces where τ_{ca} is extracted as shown in Fig. B.20. During non-congested network conditions (time period between 0 s and 230 s in Fig. B.7), no retransmissions are experienced and mean RTT equals 230 ms. During this network state all actuation messages $x_n(k)$ are delivered before subsequent control execution takes place.

However, during a congested network state (from 230 s to 1000 s in Fig. B.7), TCP retransmissions and longer medium access times are causing high RTT delays.

To detect changes in the network to which controller needs to adapt, we utilize the communication state estimation procedure from Section 4 based on *passive* RTT monitoring measurements as shown above. This approach is used in combination with the adaptive control design in Section 5.

6.2 Calibration of the Network Estimator

We consider the two-state network estimation model, where the two states represent congested (when cross traffic is present on the network) and non-congested states (only control traffic is present). To show the difference in observations during these two states, a histogram of RTT delays is shown in Fig. B.8 (constructed from blue data sample in Fig. B.7). It can be seen that samples of the two empiric distributions are overlapping in the delay value regime of 0 s to 1.1 s. Accuracy of an estimation algorithm depends on the capability to detect the true network state when observations from overlapping delay ranges are occurring. For the two cases, non-congested
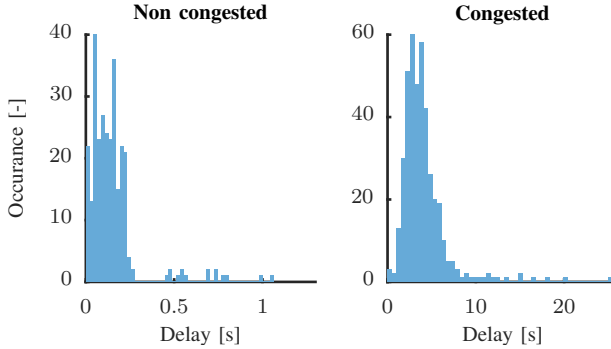

Fig. B.8: Histogram of RTT delays with and without cross-traffic. Notice the difference in maximum delay values.

and congested, we can deduct the following result from the data in Fig. B.8:

- **Non-congested:** 95 % of the RTT delays are below 0.46 s.

- **Congested:** 95 % of the RTT delays are below 5.7 s.

To parameterize the system in (B.4) and (B.5), in the two-state case, the ROC curve in Fig. B.9 is used on this RTT training set. A good threshold is defined as having the highest true positive ratio, and with the lowest false positive ratio. The point $(0, 1)$, with zero false positives and only true positive observations represents the best possible state estimator. We have chosen the

threshold value, by choosing the point closest to the $(0,1)$ point. For points on all curves in Fig. B.9, the Euclidean distance between the point $(0,1)$ and any point on the ROC curve is calculated. The optimal threshold and length l of the moving average filter is then obtained from the minimum distance point. In particular we have chosen, $l = 2$ and $\tau_1 = 0.9$ s.
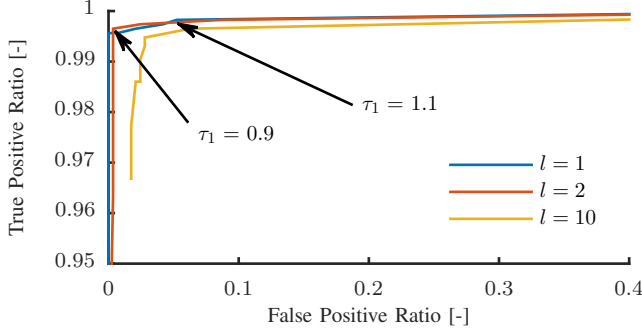

Fig. B.9: The ROC curves for different moving average filter lengths, l.

In the following section we show how the communication state estimator can be used in the control design procedure.

6.3 Design of Controllers for the Two State Communication Network

The design procedure is to choose the parameters for the two controllers, that ensure stability of the system under the delay values for the non-congested and congested communication network state, respectively. This can be achieved in different ways, where we in this work rely on the root-locus technique. Consider the system of agents illustrated in Fig. B.10, with agent 4 as the leader. We assume that each agents dynamics are given by (B.6), and that they implement the protocol in (B.9), with $\gamma_i = \frac{a_i}{b_i}$. For simplicity we let $c_{i,1} = c_{i,2} = 1$ for $i = 1, \ldots, n-1$.

Non-congested Communication State

We consider a RTT delay of 0.46 s, which was established in Section 4. We assume that the delay from controller to assets is half of the RTT delay, $\tau_{ca} = 0.23$ s. In Fig. B.11 we have plotted the root-locus for different values of the integral time, T_I, and the step response of the closed-loop system is shown in Fig. B.12. Particularly we have chosen the following parameters: $K_{P,1} = -0.15$, $T_{I,1} = 5$.
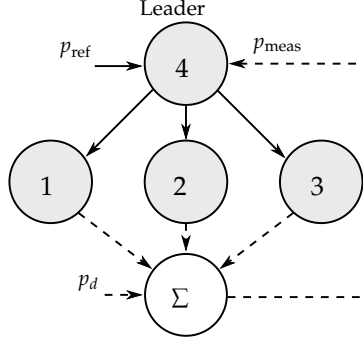
Fig. B.10: Example of a system of agents connected through a communication network (solid arrows), and also through the power grid (dashed arrows). Agent 4 is assigned as leader.

Congested Communication State

We consider a RTT delay of 5.7 s, which was established in Section 4. We assume that the delay from controller to assets is half of the RTT delay, $\tau_{ca} = 2.85$ s. In Fig. B.13 we have plotted the root-locus for different values of integral time, T_I, and the step response of the closed-loop system is shown in Fig. B.14. Particularly we have chosen the following parameters: $K_{P,2} = -0.04$, $T_{I,2} = 20$.

Next, we set up the models and data used for the simulation studies.

7 Simulation Data and Models

This section presents models and data traces used for the simulation studies. We start by describing the electrical LV distribution grid. Then we provide examples of the disturbances entering the system, followed by details on what constitutes a flexible asset. Finally, we describe the different simulation scenarios.

All simulation results haven been obtained through the simulation framework DiSC [20], available here [21].

7.1 Distribution Grid

The electrical distribution grid used for controller and delay estimator evaluation is based on a real rural low voltage (LV) grid, located in the northern part of Denmark. The LV grid is illustrated in Fig. B.15, and consists of a MV/LV (20kV/400V) substation (where the Power Controller is located), 42 busses, three flexible assets (energy storage in combination with PV system, located at busses 3, 20, and 34), and disturbances in form of household loads with additional refrigeration and heat-pump consumption, along with uncontrollable PV systems.
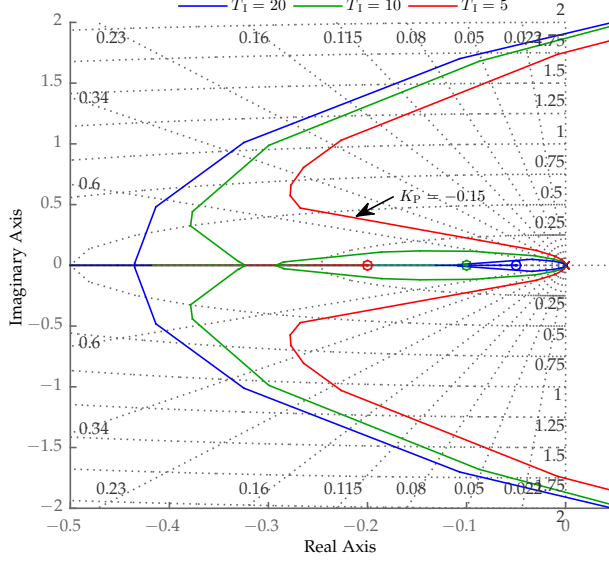
Fig. B.11: Root-locus plot of the controlled system, with a non-congested communication network. The root-locus is plotted for three different integral time values and the arrow indicates the choice of gain value. The graph has been zoomed in to show the critical part of the locus.

7.2 Disturbances

With the focus on residential low voltage grids, disturbances are mainly in form of inflexible household consumption patterns. The inflexible consumption is given by three components

1. Data from real houses located in Denmark, see Fig. B.16.

2. Data from heat pumps located in Denmark, see Fig. B.17.

3. Data from refrigerators located in Denmark, see Fig. B.18.

Notice that the inflexible consumption patterns are not a priori known by the controller; hence it needs to be robust towards these types of disturbances.

7.3 Flexible Assets

We consider assets composed of an energy storage and a solar PV system, both based on the models implemented in DiSC [20]. The assets are capable of following a power reference by utilizing the flexibility of the energy storage and derating the PV system. The asset is designed to maximize renewable production, meaning that as long as the energy storage has flexibility, this
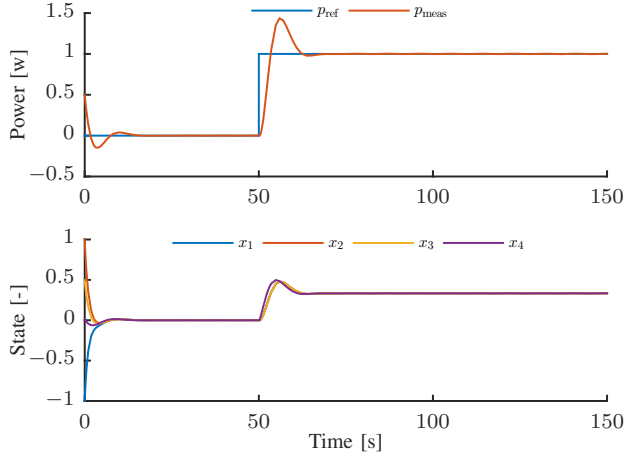
Fig. B.12: Step response of system with a non-congested communication network and $\tau_{ca} = 0.23$ s. The control parameters are, $K_P = -0.15$, $T_I = 5$ Top: reference tracking. Bottom: agent state values. Notice that leader-follower consensus is achieved when the reference value is reached.

is used before derating the PV system. Also, flexible assets might have constraint behavior which is not captured by the simple model in Section 5.1, e.g., an energy storage cannot inject power if it is empty, and available PV power change over time. Such information is not available to the power controller. To illustrate the stochastic nature of the PV system model, one day of production is plotted in Fig. B.19 for changing values of cloud cover. The PV and energy storage models are those implemented in DiSC [20].

7.4 Simulation Scenarios

To evaluate the adaptive control algorithm along with the communication network state estimator, three simulation scenarios are carried out:

1. Constant controller designed for the non-congested communication network state, S_1.

2. Constant controller designed for the congested communication network state, S_2.

3. Adaptive controller with the proposed moving average network state estimator.

Each simulation run has a duration of three hours, from 10:00 AM to 1:00 PM to capture fluctuations in PV production. The scenarios are executed 10 times to allow for statistical evaluation. A new batch of network
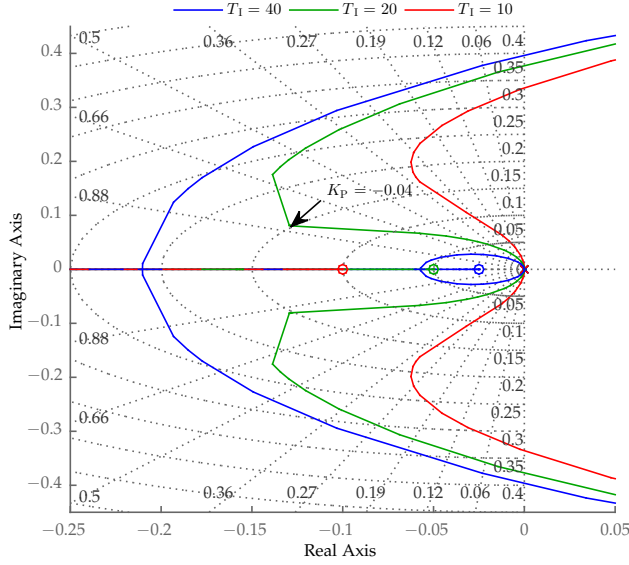
Fig. B.13: Root-locus plot of the controlled system, with a congested communication network. The root-locus is plotted for three different integral time values and the arrow indicates the choice of gain value. The graph has been zoomed in to show the critical part of the locus.

measurements is collected from the PLC network where same amount of the ICMP cross traffic as in Fig. B.7 is generated over the network every 5min., thus creating an ON/OFF pattern. For all simulation runs the communication network RTT delays are kept the same. Thereby, the stochasticity of the simulation originates from the uncontrollable disturbances.

In the following section we evaluate the simulation results.

8 Evaluation of Simulation Studies

This section evaluates the results obtained through the simulation studies. The reference tracking capabilities for the three simulation scenarios are illustrated in Figure B.20, and a closeup, for a small duration of the simulations, are shown in Fig. B.21. Further, the power output and state of charge of one energy storage is shown in Fig. B.22 for all three scenarios. The results are collected and summarized in TABLE B.1.

A number of interesting results are observed. From the data in TABLE B.1 it is clearly seen that the adaptive controller exhibits the best tracking performance in term of the root mean square error (RMSE). Keeping a constant controller designed for the non-congested communication network state, S_1,
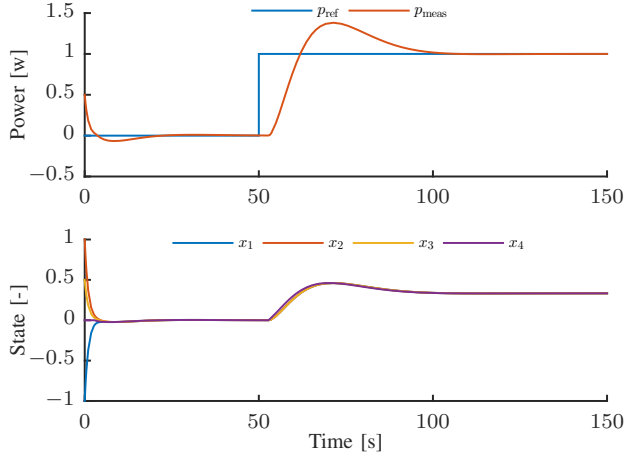
Fig. B.14: Step response of system with a congested communication network and $\tau_{ca} = 2.85$ s. The control parameters are, $K_P = -0.04$, $T_I = 20$ Top: reference tracking. Bottom: agent state values. Notice that leader-follower consensus is achieved when the reference value is reached.

creates large oscillations around the reference point when the communication network is congested, whereas keeping a constant controller designed for the non-congested communication network state, S_2, results in long time periods with poor reference tracking, when the communication network is non-congested.

Table B.1: Results from the three simulation scenarios. All scenarios have been conducted 10 times to allow for statistical evaluation.

Scenario	Mean RMSE [kW]	95% Confidence Interval [kW]
Const. Ctrl., S_1	2.422	[2.185 2.659]
Const. Ctrl., S_2	2.197	[2.117 2.277]
Adaptive Control	1.303	[1.257 1.349]

9 Conclusion and Perspectives

Here we present the concluding remarks and give an outlook on future directions.

9.1 Conclusion

In this work we presented a control scheme for managing the power flexibility in a residential electrical distribution grid towards a power reference. To han-
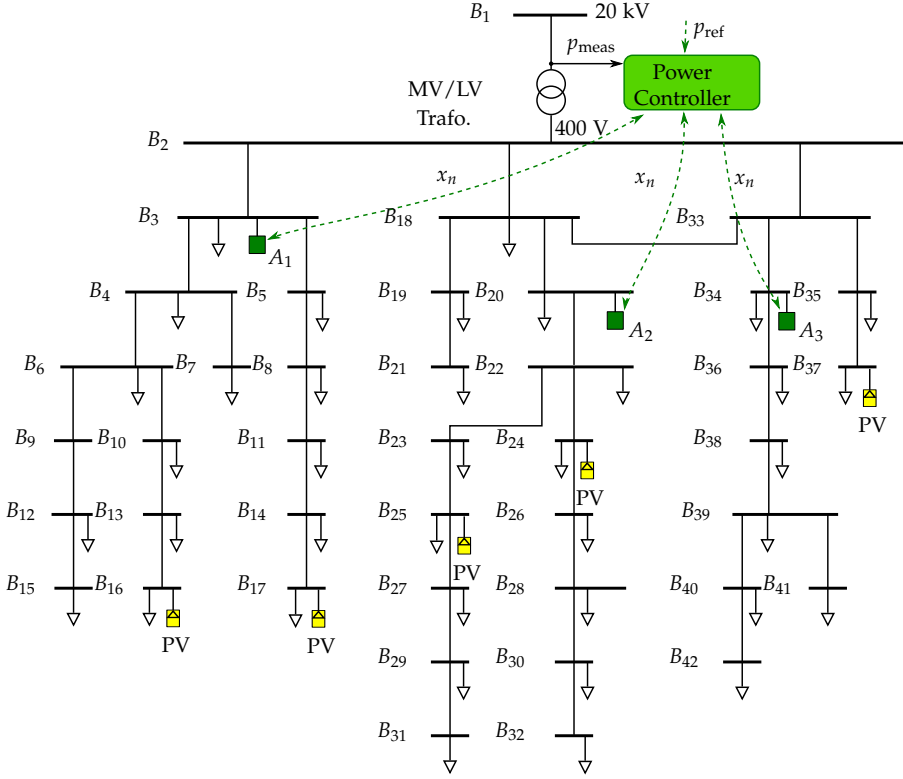
Fig. B.15: Low voltage distribution grid used for the simulation studies. It contains three flexible assets (green), five inflexible photovoltaic systems (yellow) and loads (arrows) are based on real data from danish households.

dle time-varying communication network properties a network state estimation procedure was proposed; which in combination with a gain scheduling technique enabled the controller to adapt to the changes in communication network state.

To estimate the communication network states we relied on a moving average threshold estimator and provided numbers for both buffer length and threshold value, in the case of a two-state (congested/non-congested) PLC communication network. Furthermore, we developed a consensus based multi-agent control system design procedure, which ensured fairness in asset participation, by having all assets states converge to the leader state value. For handling changes in communication network state, we used a gain scheduling approach, where switches between controllers where based on the aforementioned communication network state estimator.

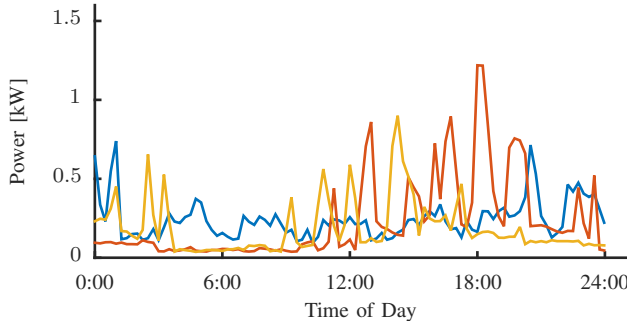The adaptive control setup was validated through numerical simulation

Fig. B.16: Consumption profiles of four households used in the simulation studies.
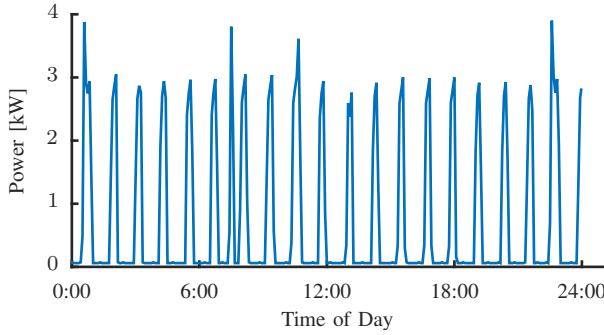

Fig. B.17: Heat pump consumption profile during a weekday.

examples on a large scale, 42 bus, low voltage distribution grid, using a PLC communication network based on real data, consumption patterns based on real household data from Denmark, and realistic asset and PV models. It was shown that the adaptive control scheme outperformed a conservative control approach with approximately 40 %, measured by the root mean square error of the reference tracking.

9.2 Perspectives

Adaptive networked controllers are relying on an estimation of the network state to avoid potential instabilities/oscillations and increase the system's performance. In this paper we have used a *passive* network monitoring technique, based on RTT measurements collected by a TCP protocol, to switch between the gains adjusted to a particular network state described by delay bounds. However, different *active* or *passive* network monitoring techniques and estimation algorithms [22] could be deployed for this purpose. A comprehensive evaluation of different monitoring techniques in combination with
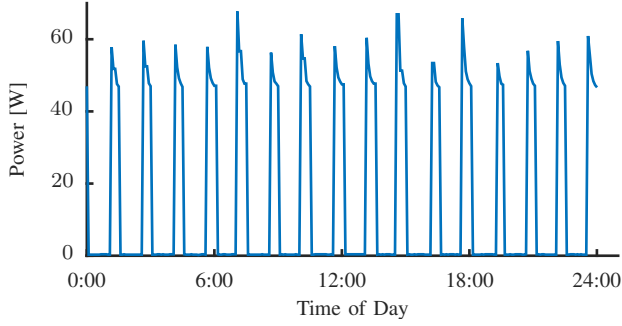
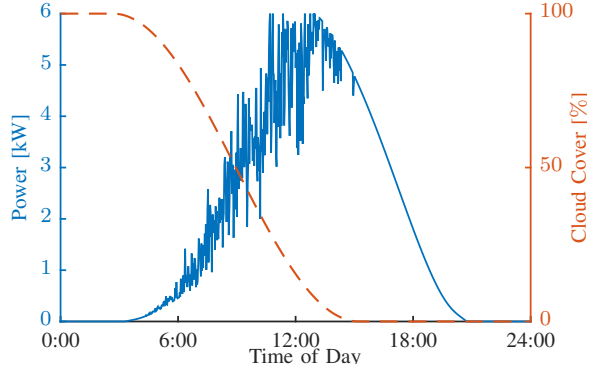**Fig. B.18:** Consumption profile of a household refrigerator.

Fig. B.19: Power production of the implemented PV system model. Observe that when the cloud cover goes to zero the fluctuations in power production decreases.

the estimation algorithms [23] is a topic that requires further investigation for developing an understanding of how existing monitoring techniques which are in practical use by e.g., telecom operators can be applied to support adaptive control in realistic Smart Grid settings.

The control design procedure given in this paper relies on classical frequency based design methods. It would be interesting to pursue a more rigid design procedure based on e.g., Lyapunov-Krasovskii stability analysis [24, 25]. Thereby, if we are provided a maximum delay, it would be possible to directly state the maximum allowable gain values, which ensures stability. Further, we only considered star-like communication topologies in our examples, with the control unit as the central coordinator. The distributed approach however allows for arbitrary communication graphs as long as they have a directed spanning tree, rooted at the leader. It would be natural to extend the analysis and simulation examples to such communication graphs,
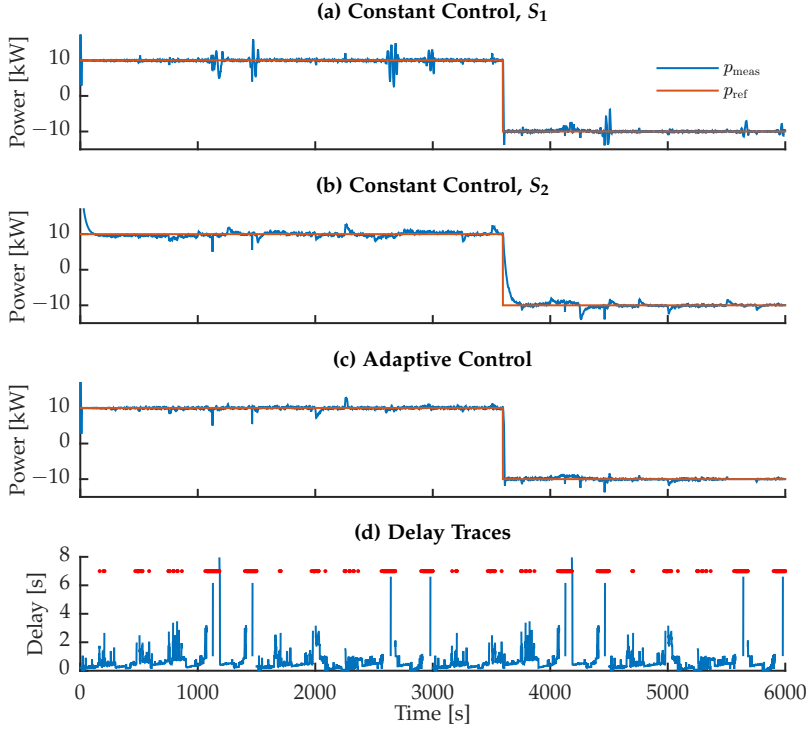
Fig. B.20: Reference tracking for each of the three simulation scenarios (a), (b), and (c). τ_{ca} delay and packet loss (d), missing data indicates packet loss and is marked with a red dot.

considering different delays for each communication link.

Acknowledgments

Fig. B.21: Reference tracking in the time window 2300 - 3300 seconds of Fig. B.20, along with delay and loss of packets and is marked with a red dot.

References

[1] "The energy- and climate goals of the danish government and results of the energy agreement 2020 (regeringens energi- og klimapolitiske mål og resultaterne af energiaftalen i 2020)," Danish Ministry for Climate, Energy and Buildings (Klima, energi og bygningsministeriet), Tech. Rep., 2012.

[2] P.-C. Chen, R. Salcedo, Q. Zhu, F. de León, D. Czarkowski, Z.-P. Jiang, V. Spitsa, Z. Zabar, and R. E. Uosef, "Analysis of voltage profile problems due to the penetration of distributed generation in low-voltage secondary distribution networks," *IEEE Transactions on Power Delivery*, no. 4, pp. 2020 – 2028, Sep. 2012.

[3] EDSO, "Flexibility: The role of DSOs in tomorrow's electricity market," European Distribution System Operators for Smart Grids, Tech. Rep.,
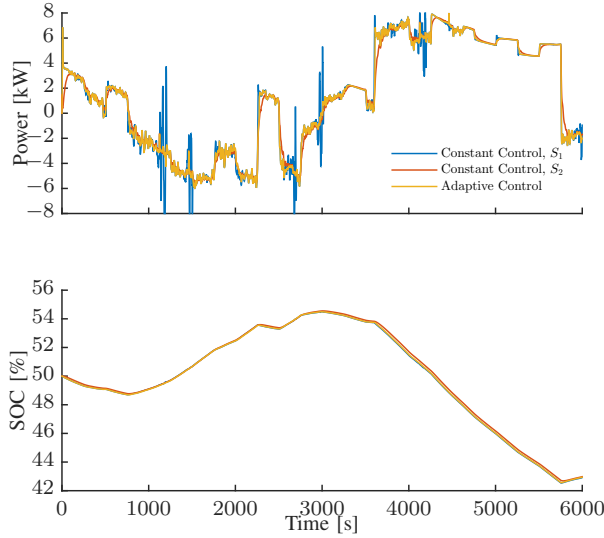
Fig. B.22: Top: Power output of one assets for the three different scenarios. Bottom: Energy storage state of charge.

2014.

[4] "Cell controller pilot project," Energinet.dk, Tech. Rep. Doc. 8577/12, 2011.

[5] N. Hatziargyriou, H. Asano, R. Iravani, and C. Marnay, "Microgrids," *IEEE Power and Energy Magazine*, vol. 5, no. 4, pp. 78–94, July 2007.

[6] European Commission, "Study on broadband coverage in europe," 2014. [Online]. Available: https://ec.europa.eu/digital-single-market/en/news/study-broadband-coverage-europe-2014/

[7] M. Kuzlu, M. Pipattanasomporn, and S. Rahman, "Communication network requirements for major smart grid applications in HAN, NAN and WAN," *Computer Networks*, vol. 67, pp. 74 – 88, 2014.

[8] K. Tomsovic, D. E. Bakken, V. Venkatasubramanian, and A. Bose, "Designing the next generation of real-time control, communication, and computations for large power systems," *Proceedings of the IEEE*, vol. 93, no. 5, pp. 965–979, may 2005.

[9] S. Wang, X. Meng, and T. Chen, "Wide-area control of power systems through delayed network communication," *IEEE Transactions on Control Systems Technology*, vol. 20, no. 2, pp. 495–503, mar 2012.

[10] A. Papachristodoulou and A. Jadbabaie, "Synchronization in oscillator networks: Switching topologies and non-homogeneous delays," in *44th IEEE Conference on Decision and Control, and The European Control Conference*, Seville, Spain, 2005, pp. 5692–5697.

[11] C. D. Persis, T. N. Jensen, R. Ortega, and R. Wisniewski, "Output regulation of large-scale hydraulic networks," *IEEE Transactions on Control Systems Technology*, vol. 22, no. 1, pp. 238–245, jan 2014.

[12] W. Ren, "Consensus based formation control strategies for multi-vehicle systems," in *Proceedings of the American Control Conference*, Minneapolis, MN, USA, 2006, pp. 4237–4242.

[13] J. W. Simpson-Porco, F. Dörfler, F. Bullo, Q. Shafiee, and J. M. Guerrero, "Stability, power sharing, & distributed secondary control in droop-controlled microgrids," in *IEEE SmartGridComm Symposium*, Vancouver, BC, Canada, Oct. 2013, pp. 672 – 677.

[14] A. Nickelsen, J. Grønbæk, T. Renier, and H. P. Schwefel, "Probabilistic network fault-diagnosis using cross-layer observations," in *2009 International Conference on Advanced Information Networking and Applications*, May 2009, pp. 225–232.

[15] R. Olfati-Saber and R. M. Murray, "Consensus problems in networks of agents with switching topology and time-daleys," *IEEE Transactions on Automatic Control*, vol. 49, no. 9, pp. 1520–1533, sep 2004.

[16] W. Ren and R. W. Beard, *Distributed Consensus in Multi-Vehicle Cooperative Control*, 1st ed. Springer, 2008.

[17] F. Andrén, R. Bründlinger, and T. Strasser, "IEC 61850/61499 control of distributed energy resources: Concept, guidelines, and implementation," *IEEE Transactions on Energy Conversion*, vol. 29, no. 4, pp. 1008–1017, Dec 2014.

[18] M. Wolkerstorfer, B. Schweighofer, H. Wegleiter, D. Statovci, H. Schwaiger, and W. Lackner, "Measurement and simulation framework for throughput evaluation of narrowband power line communication links in low-voltage grids," *Journal on Network and Computer Applications*, vol. 59, no. C, pp. 285–300, jan 2016.

[19] M. Findrik, R. Pedersen, E. Hasenleithner, C. Sloth, and H. P. Schwefel, "Test-bed assessment of communication technologies for a power-balancing controller," in *2016 IEEE International Energy Conference (ENERGYCON)*, April 2016, pp. 1–6.

[20] R. Pedersen, C. Sloth, G. B. Andresen, and R. Wisniewski, "DiSC: A simulation framework for distribution system voltage control," in *European Control Conference*, Linz, Austria, Jul. 2015.

[21] R. Pedersen, C. Sloth, G. B. Andresen, R. Wisniewski, J. R. Pillai, and F. Iov, "DiSC - A Simulation Framework for Distribution System Voltage Control," 2014. [Online]. Available: http://kom.aau.dk/project/SmartGridControl/DiSC/

[22] Z. Li, R. Vanijjirattikhan, M. Y. Chow, and Y. Viniotis, "Comparison of real-time network traffic estimator models in gain scheduler middleware by unmanned ground vehicle network-based controller," in *31st Annual Conference of IEEE Industrial Electronics Society, 2005. IECON 2005.*, Nov 2005, pp. 2439–2444.

[23] M. Findrik, R. Pedersen, C. Sloth, and H.-P. Schwefel, "Evaluation of communication network state estimators for adaptive power-balancing," *Computer Science - Research and Development*, pp. 1–8, 2016.

[24] A. Papachristodoulou, M. Peet, and S. Lall, "Constructing lyapunov-krasovskii functionals for linear time delay systems," in *American Control Conference*, Portland, OR, USA, 2005, pp. 2845 – 2850.

[25] A. Seuret and F. Gouaisbaut, "Integral inequality for time-varying delay systems," in *European Control Conference*, Zü rich, Switzerland, 2013, pp. 3360 – 3365.

Paper C

Coordination of Electrical Distribution Grid Voltage
Control - A Fairness Approach

Rasmus Pedersen, Christoffer Sloth, and Rafael Wisniewski

Abstract

In this paper, we present a method for distributing controller gains to assets offering local volt/var control. Gains are distributed based on a fairness principle, where all assets contribute equally to the voltage control, eliminating effects such as physical location. The method relays on a limited need for communication, and is inherently robust against connection loss, since only gains are updated. Through simulation examples it is shown that applying local volt/var control can reduce the amount of tap-changes with up to 84%, and updating local controller gains with the proposed algorithm can decrease the difference in reactive output between assets with 60%, while maintaining the same voltage levels. Thus the proposed control, provides significant economic benefit for distribution system operators.

1   Introduction

The increasing penetration of distributed energy resources (DERs) into electrical distribution grids are raising new concerns for the distribution system operators (DSOs) [1]. One of the main challenges is ensuring that voltage magnitudes throughout the grid are within specified limits. Many DERs are connected to the grid through inverter based technologies, enabling new control functionalities such as variable reactive power output. Therefore, DSOs around the world are formulating new rules and regulations to take advantage of the control opportunities. In Germany, PV systems connected to the distribution grid must provide local reactive power support [2], and similar changes have been proposed for the California Rule 21, which regulates grid connected distributed generation [3]. However, the question still stands on how to effectuate these new rules, accommodating interests of both the DSOs and the DER system owner.

The use of inverters for local voltage control has been investigated in several works, see e.g., [4, 5], where each inverter implements a specified relation between locally measured voltage and reactive power output, also known as a droop curve. By following this strategy each system participates in the voltage control solution; however, it is observed that the control effort required by the inverters varies significantly. This is caused by the voltage magnitudes at the far end of a distribution feeder varying more than close to the substation because of the voltage drops across lines, thus the wear and tear on individual systems is unfairly distributed. In [6–8] both centralized and distributed control of PV inverters are used to ensure voltage stability while at the same time reduce power losses in electrical distribution grids. Stability and loss minimization is of cause of great importance and should be part of the total voltage control solution. However, the referenced work do not consider any notion of fairness in the voltage control formulation. In [9, 10] active power curtailment is used to limit voltage variations, based on the tra-
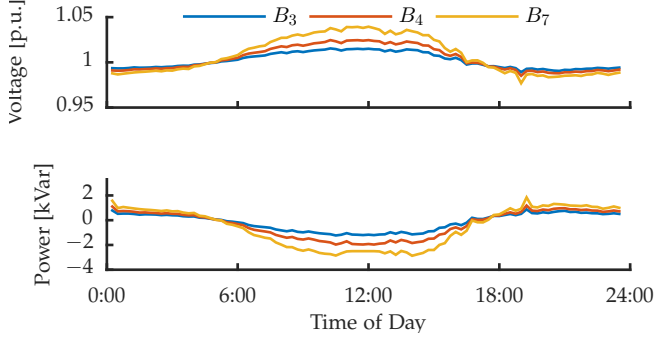
Fig. C.1: Voltage magnitude at busses with PV systems and the reactive power output of the PV systems.

ditional droop curves. It is shown how droop coefficients can be determined offline based on electrical grid parameters, to achieve equal curtailment of all systems. However, this method shows an increase in overall active power loss due to curtailment, compared to a method of all systems having equal droop coefficients. Moreover, the droop coefficients are only set ones, utilizing no feedback of the actual system state. The approach taken in [11], and extended in [12], is based on a central unit scheduling the active and reactive power output of all flexible units throughout a day. Here the goals are to keep voltages within constraints and reduce power loss. This method relies on estimation of future system behavior and environmental data, and does not consider fairness in participation. The above illustrates both the complexity in voltage control and the conflict of interest between the DSO and the inverter owner. The DSO is interested in reducing losses and voltage variations where they happen, but the DER owner is interested in overall system lifetime and profit maximization. This indicates that fairness can not be ignored, when the DSO deploys new distributed voltage control functionalities.

We illustrate, through an example, what we mean by fairness. Consider a radial distribution grid with seven busses, similar to the one shown in Fig. C.2, with solar photovoltaic (PV) systems at bus B_3, B_4 and B_7. The PV systems have the same rated power and are connected through inverters offering local volt/var control, with a predefined droop gain. The voltage magnitudes at B_3, B_4 and B_7 are shown in Fig. C.1, along with reactive power output of the PV systems. It is clearly seen that the amount of reactive power support offered depends on physical location. For a PV system owner, this might be seen as unfair. A more fair approach would be to increase the reactive power output at B_3, thereby lowering the amount needed at B_7.

In this work we focus on designing a more fairly distributed volt/var control strategy. We define fairness as all systems contributing equally to

the volt/var control, i.e., their reactive power output should be equal over time. This definition of fairness is different from e.g., all systems contribution according to size. However, this notion of fairness can easily be incorporated by adding weights to the output of each system, where the weight is size based. We formulate a strategy, where a DSO distributes droop gains to all assets, based on historical data and knowledge of electrical grid structure and parameters. This method relies on a communication infrastructure where all busses and assets are equipped with smart meters, capable of communicating directly with the DSO.

The remainder of the paper is structured as follows. First, in Sec. 2 the system architecture and modeling approach is presented. Following, in Sec. 3 the local volt/var coordination strategy is described. In Sec. 4 the approach is illustrated by simulation examples, and finally in Sec. 5 we conclude the work.

2   Architecture & Modeling

In this section we present notation, followed by an overview of the system architecture. We then briefly outline the classical AC power flow theory along with the local volt/var controllers.

2.1   Notation

Given a matrix A, let A_{ij} denote the i, j element of A. Given a complex valued matrix $A_{ij} \in \mathbb{C}$, let $|A_{ij}|$ be the magnitude and $\angle A_{ij}$ the argument of A_{ij}, respectively. The imaginary unit is dentoed $\mathrm{j} = \sqrt{-1}$. We let $\mathbb{R}$ denote the set of real numbers, where $\mathbb{R}_-$ and $\mathbb{R}_+$ is the negative and positive orthants of $\mathbb{R}$. The absolute value of any real number $a \in \mathbb{R}$ is denoted $|a|$.

2.2   System Architecture

A distribution system operator (DSO) is capable of communicating with assets (systems offering volt/var support) and busses through smart meters. Based on the received data and knowledge of electrical grid structure, the DSO calculates and dispatches droop gains for the local volt/var controllers implemented by assets. To maintain the simple and reliable nature of the local droop controllers, gains are not updated continuously, but at certain sample times e.g., once a day. The architecture of the control system is depicted in Fig. C.2.

2.3   Electrical Grid

We adopt the standard model of an electrical grid defined by its admittance matrix $Y \in \mathbb{C}^{n \times n}$, with the set of busses $\mathcal{V} = \{1, \ldots, n\}$, and the set of lines
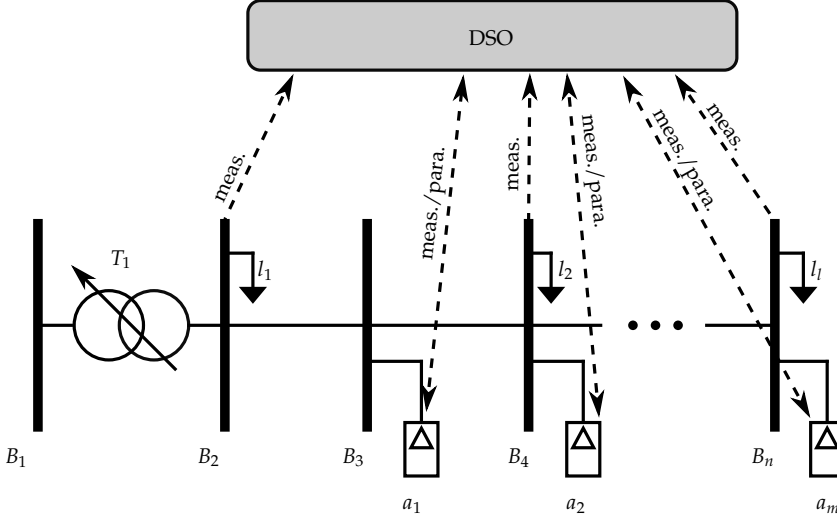
Fig. C.2: Overview of the system architecture, consisting of a radial distribution grid with n busses, l inflexible loads, m flexible assets, and a DSO as the central coordinator. The dashed arrows represent communication channels. The parameters sent from the DSO to the assets, is in this case droop gain values.

$\mathcal{E} \subset \mathcal{V} \times \mathcal{V}$, where each line is represented by an admittance $y_j \in \mathbb{C}$, for all $j \in \mathcal{E}$. For each bus $i \in \mathcal{V}$ we associate a complex power injection $s_i = p_i + jq_i \in \mathbb{C}$ and a phasor voltage $v_i = V_i e^{j\delta_i}$, with magnitude V_i and phase angle δ_i. The active and reactive power flow equations for the i-th bus are given by

$$p_i = \sum_{j \in \mathcal{V}} V_i V_j |Y_{ij}| \cos(\angle Y_{ij} - \delta_i + \delta_j), \tag{C.1}$$

$$q_i = - \sum_{j \in \mathcal{V}} V_i V_j |Y_{ij}| \sin(\angle Y_{ij} - \delta_i + \delta_j). \tag{C.2}$$

In the following we assume that the voltages evolve closely around a specified operating point and use the linearized power flow equations, with the slack bus removed.

$$\begin{bmatrix} \Delta p \\ \Delta q \end{bmatrix} = J \begin{bmatrix} \Delta \delta \\ \Delta V \end{bmatrix}, \tag{C.3}$$

where $\Delta p \in \mathbb{R}^{n-1}$ is a column vector of active power changes, $\Delta q \in \mathbb{R}^{n-1}$ is a column vector of reactive power changes, $\Delta \delta \in \mathbb{R}^{n-1}$ is a column vector of phase angle changes, $\Delta V \in \mathbb{R}^{n-1}$ a column vector of voltage magnitude changes, and $J \in \mathbb{R}^{2n-1 \times 2n-1}$ being the Jacobian of the power flow equations [13, p. 233].

2.4 Local Volt/Var Control

Each asset implements the volt/var controller seen in Fig. C.3, and given by

$$\Delta q_i = K_i(V_i^{\text{ref}} - V_i^{\text{meas}}), \tag{C.4}$$

$$\underline{q}_i \leq \Delta q_i \leq \overline{q}_i, \tag{C.5}$$

where $i \in \mathcal{A} = \{1, \ldots, m\}$ is the set of assets, $\Delta q_i \in \mathbb{R}$ is the change in reactive power output, $d_i \in \mathbb{R}_-$ is the droop gain, $V_i^{\text{ref}} \in \mathbb{R}_+$ is the voltage reference, $V_i \in \mathbb{R}_+$ is the measured voltage magnitude, $\underline{q}_i \in \mathbb{R}_-$ is the lower bound on reactive power output, and finally $\overline{q}_i \in \mathbb{R}_+$ is the upper bound on reactive power output. Note that by changing the gain, K_i, the slope of the curve in Fig. C.3 is altered, thus changing at which voltage deviation the limits on reactive power are reached. In the following we formulate the coordination strategy for achieving fairness.
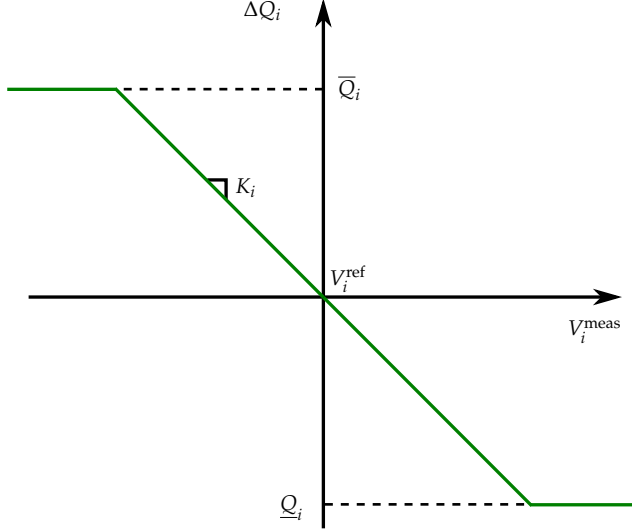
Fig. C.3: Illustration of the linear volt/var droop curve. The gain K_i corresponds to the slope of the curve.

3 Coordination Strategy

In this section we present the algorithm for dispatching controller gains to the assets. The algorithm is formulated as an optimization problem, with the objective of reaching fairness in the reactive power output of assets. Fairness is seen as all assets having equal reactive power output over time, which is in contrast to e.g., all assets contributing according to size. However, this is

easily added by weighting the reactive power output of the assets based on size. What should be noted from the presented algorithm is its robustness against communication failures and limited need for communication; if e.g., the DSO looses connection to an asset, the asset can just continue with the previous dispatched controller gain. The frequency of updating controller gains can freely be chosen by the DSO, i.e., it could be daily, weekly, or even seasonally. This results in a functionality which is easy to implement and serves the needs of both the DSO and the DER owner.

3.1 Preliminaries

Each bus and asset is assumed to sample and store data with sampling time $T_s \in \mathbb{R}_+$. We define $H \in \mathbb{N}$ as the number of samples we look back in time, e.g., if $T_s = 15$ min. and we want to look 24 hours back, $H = 96$. Note that T_s does not represent the local control loop sampling time, which is typically much faster. At a given sample instance, κ, the DSO receives from each bus, $B_2, \ldots, B_n$, (except the slack bus, assumed to be B_1) the following data, which is stacked on vector form

$$V_k^{\text{meas}} = \begin{bmatrix} V_{2,k}^{\text{meas}} & \cdots & V_{n,k}^{\text{meas}} \end{bmatrix}^T, \tag{C.6}$$

$$q_k^{\text{meas}} = \begin{bmatrix} q_{2,k}^{\text{meas}} & \cdots & q_{n,k}^{\text{meas}} \end{bmatrix}^T, \tag{C.7}$$

$$p_k^{\text{meas}} = \begin{bmatrix} p_{2,k}^{\text{meas}} & \cdots & p_{n,k}^{\text{meas}} \end{bmatrix}^T, \tag{C.8}$$

and from each asset

$$\Delta q_k^{\text{meas}} = \begin{bmatrix} \Delta q_{1,k}^{\text{meas}} & \cdots & \Delta q_{m,k}^{\text{meas}} \end{bmatrix}^T, \tag{C.9}$$

where $q_k^{\text{meas}} \in \mathbb{R}^{n-1}$ is measured reactive power at all busses, $\Delta q_k^{\text{meas}} \in \mathbb{R}^m$ is measured reactive power output from all assets, $p_k^{\text{meas}} \in \mathbb{R}^{n-1}$ is measured active power, and $k \in \mathcal{K} = \{\kappa - H, \ldots, \kappa - 1\}$ is the sample index set. Further, the DSO is assumed to know the grid admittance matrix, Y, along with physical placement of assets (asset a_1 might be connected to bus B_4, and so on). Notice, that if the grid admittance matrix is not know there are methods for estimating topology and parameters [14, 15]. In the following we set up the optimization problem to be solved at sample instance κ.

3.2 Objective Function

The objective is based on a fairness principle where all assets should contribute equally to the voltage control. We define fairness as all assets having the same reactive output in the window $\mathcal{K}$. Thereby, the objective function

can be written as

$$F = \sum_{k \in \mathcal{K}} ||D\Delta q_k||_1, \tag{C.10}$$

where $F \in \mathbb{R}$ is the objective function, $|| \cdot ||_1$ denotes the 1-norm, $\Delta q_k \in \mathbb{R}^m$ is a column vector representing reactive output of assets, given by

$$\Delta q_k = \begin{bmatrix} \Delta q_{1,k} & \cdots & \Delta q_{m,k} \end{bmatrix}^T, \tag{C.11}$$

and $D \in \mathbb{R}^{m-1 \times m}$ is an upper triangular difference matrix defined as

$$D_{ij} = \begin{cases} m - i, & j = i \\ -1, & j > i \\ 0, & \text{otherwise} \end{cases}. \tag{C.12}$$

The structure of D ensures that each entry in Δq_k is only subtracted once from any other entry, e.g, if $\mathcal{A} = \{1, 2, 3\}$, then

$$D\Delta q_k = \begin{bmatrix} 2 & -1 & -1 \\ 0 & 1 & -1 \end{bmatrix} \begin{bmatrix} \Delta q_{1,k} \\ \Delta q_{2,k} \\ \Delta q_{3,k} \end{bmatrix}$$
$$= \begin{bmatrix} 2\Delta q_{1,k} - \Delta q_{2,k} - \Delta q_{3,k} \\ \Delta q_{2,k} - \Delta q_{3,k} \end{bmatrix}.$$

3.3 Constraints

We apply knowledge of the electrical grid structure to ensure that voltage magnitudes are kept within constraints. Under the assumption that voltages evolve closely around the operating point we use the linearized power flow equations in (C.3) and set constraints on voltage magnitudes as follows

$$\begin{bmatrix} \Delta \delta_k \\ \Delta V_k \end{bmatrix} = J^{-1} \begin{bmatrix} p_k^{\text{meas}} \\ q_k^{\text{meas}} - B\Delta q_k^{\text{meas}} + B\Delta q_k \end{bmatrix}, \tag{C.13}$$

$$\underline{\Delta V} \leq \Delta V_k \leq \overline{\Delta V}, \tag{C.14}$$

where $\underline{\Delta V}, \overline{\Delta V} \in \mathbb{R}^{n-1}$ are lower and upper bounds on voltage magnitudes, respectively, and $B \in \mathbb{R}^{(n-1) \times m}$ maps assets to busses and is defined by

$$B_{ij} = \begin{cases} 1, & \text{if asset } j \text{ is connected to bus } i \\ 0, & \text{otherwise} \end{cases}.$$

We to not consider constraints on the voltage angles $\Delta \delta_k$ as focus is on volt/var control and not on e.g., maintaining frequency within bounds.

Each entry in the vector Δq_k is given by the volt/var control strategy in (C.4). This can be compactly written as

$$\Delta q_k = \tilde{K} \Delta V_k^{\text{meas}}, \tag{C.15}$$
$$\Delta V_{i,k}^{\text{meas}} = V_i^{\text{ref}} - V_{i,k}^{\text{meas}},$$

where $\tilde{K} \in \mathbb{R}^{m \times m}$ is a diagonal matrix given by

$$\tilde{K}_{ij} = \begin{cases} K_i, & \text{if } i = j \\ 0, & \text{otherwise} \end{cases}. \tag{C.16}$$

Additional constraints are added on the controller gains as follows

$$\underline{K}_i \leq K_i \leq \overline{K}_i, \tag{C.17}$$

where $\underline{K}_i, \overline{K}_i \in \mathbb{R}_-$ are lower and upper bounds on controller gains, respectively. These constraints ensure that if e.g., connection is lost an assets will at least provide reactive support corresponding to the minimum gain. Moreover, effects such as oscillations from introducing too high gains, can be avoided. The constraint values on gains are system dependent, and a method for selecting these are left for future work.

3.4 Optimization Problem

The optimization problem which must be solved at sample κ, is given by

$$\begin{aligned} \min_{K_1,\ldots,K_m \in \mathbb{R}} \quad & \sum_{k=\kappa-H}^{\kappa-1} ||D\Delta q_k|| \\ \text{s.t.} \quad & \text{(C.5), (C.13), (C.14)} \\ & \text{(C.15), (C.17)} \\ & \forall i \in \mathcal{A}, \end{aligned} \tag{C.18}$$

with variables $K_1, \ldots, K_m$, $\Delta q_{\kappa-H}, \ldots, \Delta q_{\kappa-1}$, and $\Delta V_{\kappa-H}, \ldots, \Delta V_{\kappa-1}$, and data $\underline{q}_1, \ldots, \underline{q}_m$, $\overline{q}_1, \ldots, \overline{q}_m$, $p_{\kappa-H}^{\text{meas}}, \ldots, p_{\kappa-1}^{\text{meas}}$, $q_{\kappa-H}^{\text{meas}}, \ldots, q_{\kappa-1}^{\text{meas}}$, $V_{\kappa-H}^{\text{meas}}, \ldots, V_{\kappa-1}^{\text{meas}}$, J, D, B, T_s, H, $\mathcal{A}$, and $\mathcal{K}$. Notice that the problem is convex and scales well with both number of variables and horizon. What is left to decide is the value of H and how often the gains should be updated, i.e., the time between κ's. An example would be to set H so it covers one day, and then solve (C.18) at midnight each day. This is exemplified in the following section.

4 Simulation Results

In this section we illustrate the proposed solution through numerical simulations. First we show how the example given in the introduction, can be
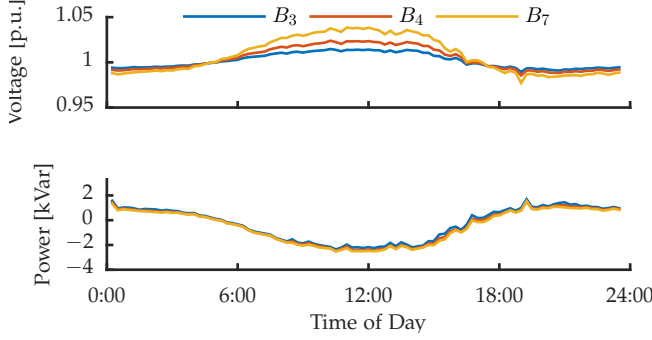
Fig. C.4: Voltage magnitude at busses with PV systems and the reactive power output of the PV systems, with updated droop gains.

solved using the proposed coordination strategy. Then, we apply the method to a larger radial distribution feeder equipped with an on-load tap-changer (OLTC) at the transformer station, see Fig. C.5. All simulation results have been obtained through the simulation framework DiSC [16].

4.1 Small Scale Example

We consider an $n = 7$ bus radial system similar to the one shown in Fig. C.2, with three PV systems capable of offering volt/var control. The PV systems are identical and placed at B_3, B_4 and B_7, with equal initial gains $K_i = -200$, and rated apparent power of 6.5 kVA. Loads based on real data are placed at $B_2, \ldots, B_7$, and all lines between busses are assumed identical. Parameters for the optimization problem are as follows: $T_s = 15$ minutes, $H = 96$ samples corresponding to 24 hours, $\underline{\Delta V} = -0.05$ p.u., $\overline{\Delta V} = 0.05$ p.u., $\underline{K_i} = -400$, and $\overline{K}_i = -100$. The results are shown in Fig. C.4, where it is seen that we accomplish the same reduction in voltage variations, as in the case with identical static gains, but with a much more fair distribution of the reactive power output.

4.2 Large Scale Example

For the large scale example we use the low voltage distribution feeder shown in Fig. C.5. All asset, $a_1, \ldots, a_6$, are PV systems identical to the ones from the previous example, and the loads, $l_1, \ldots, l_{14}$, are based on real consumption data from danish households. The OLTC is present for a number of reasons; first, to illustrate how traditional voltage control would be carried out if no asset volt/var control is active. Secondly, it demonstrates that when implementing new voltage control features, those already in place, can not be ignored. We run three simulations over a one year period starting at January

133

1st; one with only the OLTC responsible for voltage control, one where all assets are applying local voltage control with equal gains $K_i = -200$, and one demonstrating the method outlined in this paper. The optimization parameters are as follows: $T_s = 15$ minutes, $H = 96$ samples, $\underline{\Delta V} = -0.04$ p.u., $\overline{\Delta V} = 0.04$ p.u., $\underline{K_i} = -400$, and $\overline{K_i} = -170$. Remark: the constraints on voltage magnitude are used to calculate new droop gains, hence these constraints might be violated at run time. The three simulation scenarios are compared in TABLE C.1 and C.2, and the evolution of volt/var control gains from the third simulation are shown in Fig. C.6.
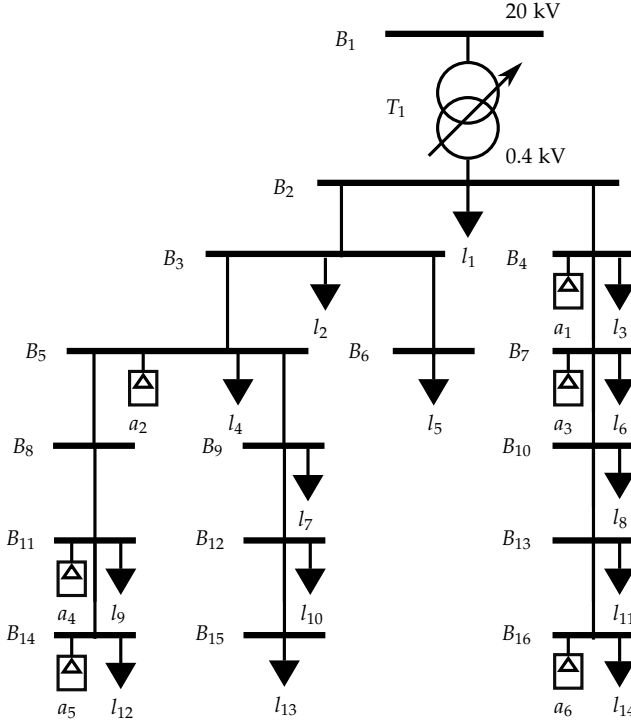
Fig. C.5: Distribution feeder used for the large scale example.

A number of interesting results are observed. First, a significant reduction in tap changes is achieved with distributed volt/var control, along with a reduction in voltage variation when measured using standard deviation (STD). Secondly, there is a slight increase in total reactive power injection from assets, when updating gains once a day. However, the number of tap-changes needed is further decreased. From Tab. C.2 it is seen that the maximum difference between assets reactive power output, has been decreased significantly, when gains are regularly updated. Also, Fig. C.6 shows how tap-changes affect the calculation of droop gains during the winter period with little solar

Method	Taps		Voltage (STD)		Total Δq	
	[-]	%	[p.u.]	%	[MVArh]	%
Only OLTC	425	100	0.0131	100	-	-
Identical K_i	91	21	0.0124	94	29.2	100
Updated K_i	67	16	0.0125	95	30.1	103

Table C.1: Comparison between different methods of applying voltage control for a one year period. The voltage standard deviations are the maximum throughout the entire grid.

Asset	Ident. K_i $\sum |\Delta q_i|$ [MVArh]	Updated K_i $\sum |\Delta q_i|$ [MVArh]	Diff. %
a_1	3.1	4.6	33
a_2	4.4	5.0	11
a_3	3.7	4.9	24
a_4	6.1	5.2	-18
a_5	6.6	5.6	-19
a_6	5.3	4.9	-9
Max Diff.	3.5	1.0	60

Table C.2: Difference in total reactive power delivered by the assets for a one year period. Maximum difference can be seen as an evaluation of (C.10).
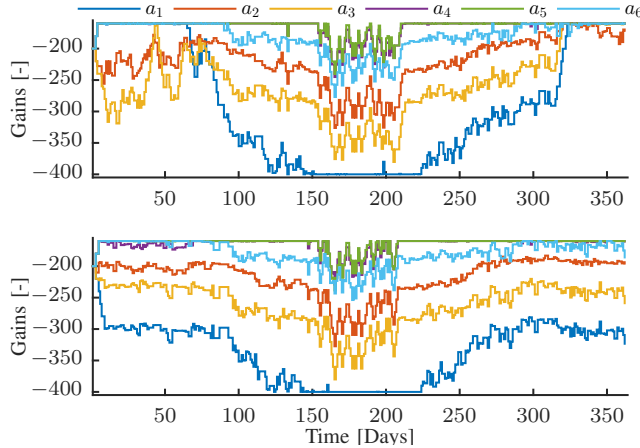

Fig. C.6: Evolution of volt/var control gains over time. Top: with the OLTC active, 67 tap-changes performed. Bottom: With the OLTC inactive.

irradiance. This results in gain values changing more rapidly or all are set to the minimum value. It is expected that this effect could be mitigated by either adding additional constraints on the how fast the gains can change or if the DSO had knowledge of when tap-changes occur. Another interesting observation is that when controller gains are updated, the system adapts to seasonal changes, which further motivates the developed approach.

5 Conclusion & Discussion

In this paper we demonstrated how a distribution system operator was capable of computing and dispatching droop gains for local asset volt/var control, based on a fairness principle where all assets contribute equally. This eliminated the challenge associated with the physical placement of assets in the electrical grid. From historical measurements it was shown how an optimal solution could be formulated and computed which minimized the difference between reactive power output from assets, while still respecting local voltage and asset constraints. The developed method was reliable, simple by nature, and with a limited need for communication; making it a functionality witch could easily be implementable by distribution system operators.

Through simulations it was shown how utilizing local volt/var control could reduce the need for tap-changes, with up to 84 %, when applying the proposed algorithm. Further, the maximum difference in reactive power output between any two assets was reduced with 60 %, compared to a strategy where all assets had a fixed gain.

In future work it would be interesting to loosen the assumption of voltages evolving closely around the nominal operating point and use the full non-linear power flow equations. Doing so, would turn the problem more realistic but at the same time eliminate the convexity of the optimization problem making it much harder to solve. Further, adding curtailment in active power to the voltage control problem should be considered, as some systems can not rely solely on reactive power support. Finally, distributing the control among the assets, without the need for a central coordinating unit is seen as an interesting extension.

Acknowledgments

References

[1] EDSO, "Flexibility: The role of DSOs in tomorrow's electricity market," European Distribution System Operators for Smart Grids, Tech. Rep., 2014.

[2] J. v. Appen, M. Braun, T. Stetz, K. Diwold, and D. Geibel, "Time in the sun - the challenges of high PV penetration in the German electric grid," *IEEE - Power and Energy Magazine*, pp. 55 – 64, Mar. 2013.

[3] "Interim decision adopting revisions to electric tariff Rule 21 for Pacific Gas and Electric Company, Southern California Edison Company, and San Diego Gas & Electric Company to require "smart" inverters," California Public Utilities Commission, Tech. Rep. R.11-09-011 COM/MP6/lil, 2014.

[4] P. Aristidou, F. Olivier, M. E. Hervas, D. Ernst, and T. V. Cutsem, "Distributed model-free control of photovoltaic units for mitigating overvoltages in low-voltage networks," in *CIRED Workshop*, Rome, Jun. 2014.

[5] J. W. Smith, W. Sunderman, R. Dugan, and B. Seal, "Smart inverter volt/var control functions for high penetration of PV on distribution systems," in *IEEE Power Systems Conference and Exposition (PSCE)*, Pnoenix, AZ, USA, Mar. 2011, pp. 1 – 6.

[6] S. Bolognani, R. Carli, G. Cavraro, and S. Zampieri, "Distributed reactive power feedback control for voltage regulation and loss minimization," *arXiv: 1303.7173v2*, vol. math.OC, Nov. 2014.

[7] N. Li, G. Qu, and M. Dahleh, "Real-time decentralized voltage control in distribution networks," in *52nd Annual Allerton Conference*, Allerton House, UIUC, Illinois, USA, 2014, pp. 582–588.

[8] S. Kundu, S. Backhaus, and I. A. Hiskens, "Distributed control of reactive power from photovoltaic inverters," in *IEEE International Symposium on Circuits and Systems*, Beijing, China, 2013, pp. 249–252.

[9] R. Tonkoski, L. A. C. Lopes, and T. H. M. El-Fouly, "Droop-based active power curtailment for overvoltage prevention in grid connected PV inverters," in *IEEE International Symposium on Industrial Electronics (ISIE)*, Bari, Italy, Jul. 2010, pp. 2388 – 2393.

[10] R. Tonkoski and L. A. Lopes, "Impact of active power curtailment on overvoltage prevention and energy production of PV inverters connected to low voltage residential feeders," *Renewable Energy*, vol. 36, no. 12, pp. 3566 – 3574, 2011.

[11] M. Juelsgaard, C. Sloth, R. Wisniewski, and J. Pillai, "Loss minimization and voltage control in smart distribution grid," in *Proceedings of the 19th IFAC World Congress*, Cape Town, South Africa, Aug. 2014.

[12] M. Juelsgaard, P. Andersen, and R. Wisniewski, "Distribution loss reduction by household consumption coordination in smart grids," *IEEE Transactions on Smart Grid*, vol. 5, no. 4, pp. 2133 – 2144, 2014.

[13] H. Saadat, *Power System Analysis*, 2nd ed. McGraw-Hill, 2002.

[14] S. Bolognani, N. Bof, D. Michelotti, R. Muraro, and L. Schenato, "Identification of power distribution network topology via voltage correlation analysis," in *52nd IEEE Conference on Decision and Control*, Florence, Italy, Dec. 2013.

[15] J. Songsiri, J. Dahl, and L. Vandenberghe, "Graphical models of autoregressive processes," *Convex Optimization in Signal Processing and Communications*, no. 1, 2009.

[16] R. Pedersen, C. Sloth, G. B. Andresen, and R. Wisniewski, "DiSC: A simulation framework for distribution system voltage control," in *European Control Conference*, Linz, Austria, Jul. 2015.

Paper D

Verification of Power Grid Voltage Constraint
Satisfaction - A Barrier Certificate Approach

Rasmus Pedersen, Christoffer Sloth, and Rafael Wisniewski

Abstract

This paper addresses verification of voltage constraint satisfaction in power systems with distributed production and time-varying consumption. Due to increasing penetration of renewable generation units and additional demand from e.g., electrical vehicles, voltage constraint satisfaction is seen as one of the major future challenges of power system operators. We show that ensuring voltage constraints in power systems is equivalent to finding a barrier function for a differential algebraic system. In order to compute the barrier function we reformulate the original problem to polynomial form and cast it as a sum of squares (SOS) feasibility problem, solvable using available tools.

1   Introduction

For any electrical power system to function properly the voltage levels at all busses must be kept within constraints. Increased voltage variations may lead to system instability [1, 2] and life-time degradation or even destruction of grid connected equipment [3]. Therefore, the system operators are imposed by legislation to ensure that voltages are within ± 10 % of the nominal value [4]. However, with the increasing penetration of renewable production units on all levels of the power grid, along with additional demand from e.g., electrical vehicles, the system is transitioning towards a more dynamic and stochastic behavior, challenging the system operators [5].

To cope with the increasing challenges, system operators around the world are formulating new rules and regulations known as grid codes. In Germany solar photovoltaic systems (PVs) above a certain rated power are limited to 70 % of their capacity, and must be capable of providing local reactive power support [6, 7]. Similar changes to the grid code, have been proposed for the California rule 21, regulating grid connected generation [8]. These rules are general and typically address individually connected systems, without any guarantee of ensuring grid-wide constraint satisfaction. This indicates that the system operators need new tools for verifying system behavior under high penetration of renewable production, additional demand, and when deploying new control functionalities.

The issue of maintaining voltages within constraints has been investigated in several works. In [9] and [10] PV inverters implement a relation between locally measured voltage and reactive power injection, known as a droop curve. The approach taken in [11] shows how local quadratic droop controllers on reactive power can be designed and coordinated for a microgrid to reach a stable voltage equilibrium, under the assumptions of lines being purely inductive and voltage angle shift being negligible. However, relaying on reactive power as the only remedy to alleviate voltage problems, might not be possible in all systems. In [12, 13] active power injection of PV sys-
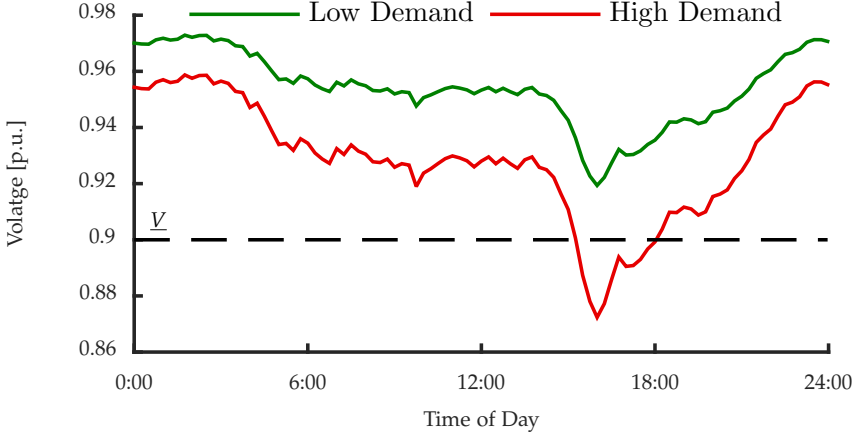
Fig. D.1: Voltage magnitude at bus B_2 in Fig. D.3, under low and high demand.

tems is curtailed to limit voltage variations, using traditional droop curves. While this approach alleviates over-voltage issues, it comes with no guarantees of voltage constraints being satisfied, and conservative tuning might lead to a reduction in the utilization of renewable energy resources. In [14] a model predictive controller for demand shedding was proposed for mitigating voltage collapse after a large disturbance has occurred. The solution shows promising results, but it is dependent on the amount of sheddable demand and thus comes with no guarantee of ensuring voltage constraints for a generic power system. The above illustrates the need for a method to verify that for a given power system, voltage constraints will be satisfied under different demand/generation, as well as under both local and global voltage control approaches.

In this work we provide a method for verifying power grid voltage constraint satisfaction. The approach relies on turning the static power flow equations into a system of differential algebraic equations, and applying a safety verification technique known as the barrier certificate method [15], to prove that constraints are always satisfied. In order to solve the problem of computing a barrier certificate, we show how the differential algebraic equations describing a power grid, can be put on polynomial form, and cast as a sum of squares (SOS) program. While our outset is to verify voltage constraint satisfaction in power systems, we aim at keeping the definitions and problem formulations throughout the paper as general as possible, making the approach applicable to other systems. Thererfore, we alternate between mathematical formulation and physical interpretation throughout the paper. Also, it should be noted that no assumptions of electrical grid structure, parameters, or system behavior are applied. The following example illustrates

the core idea of the paper.

Consider the power system illustrated in Fig. D.3, with the demand of load L_1 on bus B_2 being either low or high. In Fig. D.1 it is illustrated that if load L_1 has a low demand the system will not violate voltage constraints. However, if L_1 has high demand the voltage magnitude at B_2 will violate the lower bound during the evening peak. It is desirable to provide a methodology making it possible to state if a system will always satisfy constraints, without the need for simulation studies. This work provides such a method.

The remainder of the paper is structured as follows. The voltage constraint satisfaction problem is formulated in Section 2. In Section 3, the problem is put on polynomial form and safety of the system is defined. Following in Section 4, we state the sum of squares programming problem to be solved. Section 5 provides examples. Finally, the work is concluded in Section 6, along with future directions.

2 Problem Formulation

In this section we formulate the problem of verifying that voltage constraints will never be violated, for a given power system. We name this problem *the voltage constraint satisfaction problem*. Notice that we are not studying power balancing or solving an optimal power flow problem. Throughout, it is assumed that the electrical grid is connected to an entity capable of ensuring power balance, i.e., the grid is connected to a slack bus [16, pp. 255].

2.1 Preliminaries and Notation

$\mathbb{R}$, $\mathbb{R}_+$, $\mathbb{R}_-$ denote the set of real numbers, non-negative real numbers, and non-positive real numbers. By $\mathbb{R}_{>0}$ ($\mathbb{R}_{<0}$) we denote the positive (negative) orthants of $\mathbb{R}$. Similarly, $\mathbb{C}$ is the set of complex numbers, $\mathbb{C}_+$ ($\mathbb{C}_-$, $\mathbb{C}_{>0}$, $\mathbb{C}_{<0}$) denotes the right (left, open right, open left) half complex plane. The imaginary unit is denoted j, and for a complex number $x \in \mathbb{C}$ the complex conjugate is denoted x^*. For a vector $x \in \mathbb{C}^n$, x^* denotes the entry wise complex conjugate and x^{*T} denotes the conjugate transpose. Let $|\mathcal{V}|$ denote the cardinality of the set $\mathcal{V}$. For a given index set I we write $x_I = \{x_i \mid i \in I\}$. For a vector x the associated diagonal matrix with entries of x in its diagonal is denoted $\mathrm{diag}(x)$.

Given a complex weighted, connected, and undirected graph $G(\mathcal{V}, \mathcal{E}, A)$, with $\mathcal{V} = \{1, \ldots, m\}$ being the set of vertices (busses), $\mathcal{E} \subseteq \mathcal{V} \times \mathcal{V}$ the set of edges (lines), and $A \in \mathbb{C}^{|\mathcal{V}| \times |\mathcal{V}|}$ the weighted adjacency matrix. We define the set of neighbors of node $i \in \mathcal{V}$ as $N_i = \{j \in \mathcal{V} | (j, i) \in \mathcal{E}\}$.

Let $\mathbb{R}[x]$ denote the ring of real polynomials in the variables $(x_1, \ldots, x_n) \in \mathbb{R}^n$. We say that a polynomial $p(x) \in \mathbb{R}[x]$ is sum of squares (SOS), if $p(x) =$

$\sum_{i=1}^{k} p_i(x)^2$, for some polynomials $p_i(x) \in \mathbb{R}[x]$. Given a polynomial p we denote that the polynomial is SOS by $p \in \Sigma[x]$.

2.2 System Model

We consider an electrical grid, modeled by an admittance matrix $Y \in \mathbb{C}^{m \times m}$. The electrical grid is given as a complex weighted, connected, and undirected graph $G(\mathcal{V}, \mathcal{E}, A)$, with busses $\mathcal{V} = \{1, \ldots, m\}$, lines $\mathcal{E} \subset \mathcal{V} \times \mathcal{V}$, and symmetric line admittances $a_{ij} = -Y_{ij} \in \mathbb{C}$, for each line $(i,j) \in \mathcal{E}$. To each bus $i \in \mathcal{V}$ we associate a complex power injection $s_i = p_i + jq_i$ and a phasor voltage $v_i = V_i e^{j\delta_i}$, where $p_i \in \mathbb{R}$ is the active power component and $q_i \in \mathbb{R}$ is the reactive power component, $V_i \in \mathbb{R}$ is the voltage magnitude, and $\delta_i \in [-\pi/2, \pi/2]$ the voltage phase angle. The vector of bus voltages is denoted $v \in \mathbb{C}^m$ and the vector of complex power injections can be expressed as

$$s = \text{diag}(v)(Yv)^* \in \mathbb{C}^m. \tag{D.1}$$

By defining the index sets $I_i = N_i \cup \{i\}$, Eq. (D.1) can be divided into the active and reactive power component resulting in the well-known power flow equations [17, pp. 115]

$$p_i = \sum_{j \in I_i} V_i V_j \left[\text{Im}(Y_{ij}) \sin(\delta_i - \delta_j) \right. \tag{D.2a}$$
$$\left. + \text{Re}(Y_{ij}) \cos(\delta_i - \delta_j) \right], \qquad i \in \mathcal{V},$$
$$q_i = \sum_{j \in I_i} V_i V_j \left[\text{Re}(Y_{ij}) \sin(\delta_i - \delta_j) \right. \tag{D.2b}$$
$$\left. - \text{Im}(Y_{ij}) \cos(\delta_i - \delta_j) \right], \qquad i \in \mathcal{V}.$$

The active and reactive power injections in (D.2) are governed by dynamic systems describing generation and demand behavior at each bus

$$\dot{x}_i = f_i(x_i, d_i), \qquad i \in \mathcal{V}, \tag{D.3a}$$
$$\begin{bmatrix} p_i \\ q_i \end{bmatrix} = \varphi_i(x_i), \qquad i \in \mathcal{V}, \tag{D.3b}$$

where $x_i \in X_i \subseteq \mathbb{R}^n$ is the state, $d_i \in D_i \subseteq \mathbb{R}^l$ is the unknown but bounded disturbance input, $f_i : X_i \times D_i \to X_i$ is the vector field, and $\varphi_i : X_i \to \mathbb{R}^2$ the output.

2.3 The Voltage Constraint Satisfaction Problem

We aim at solving the voltage constraint satisfaction problem described in Problem 3.

Problem 3 (Voltage Constraint Satisfaction). *Given an undirected, connected, and weighted graph $G(\mathcal{V}, \mathcal{E}, A)$, vector fields $f_i : X_i \times D_i \to X_i$, output maps $\varphi_i : X_i \to \mathbb{R}^2$, disturbance sets D_i, upper and lower bounds on voltage magnitude $\overline{V}, \underline{V} \in \mathbb{R}_+$, and bound on difference in bus voltage phase angle $\overline{\Delta}_{ij} \in \mathbb{R}_+$, for $i = 1, \ldots, m$, show that voltage constraints*

$$\underline{V} \leq V_i \leq \overline{V}, \qquad\qquad i \in \mathcal{V},$$
$$\overline{\Delta}_{ij} \geq |\delta_i - \delta_j|, \qquad\qquad (i, j) \in \mathcal{E},$$

are always satisfied, for the system given by (D.2) and (D.3).

3   Safety Verification

To solve Problem 3 we rely on a safety verification technique known as barrier certificate. In order to compute a barrier certificate using polynomial programming, the original problem is reformulated to polynomial form and safety for this system is defined. Throughout the remainder we use that on a compact set, the vector fields in (D.3a) can be approximated arbitrarily close by polynomials, according to Weierstrass Approximation Theorem.

3.1   Problem Reformulation

We show that $(V_i, \delta_i, x_i, d_i)$ is a solution to Problem 3 if and only if (z_{I_i}, x_i, d_i) is a solution to the polynomial reformulation given by

$$\dot{x}_i = f_i(x_i, d_i) \qquad\qquad i \in \mathcal{V}, \qquad \text{(D.4a)}$$
$$0 = \varphi_i(x_i) - \psi_i(z_{I_i}), \qquad\qquad i \in \mathcal{V}, \qquad \text{(D.4b)}$$
$$0 = z_{m+i}^2 + z_{2m+i}^2 - 1, \qquad\qquad i \in \mathcal{V}, \qquad \text{(D.4c)}$$

$$0 \leq \begin{bmatrix} \overline{V} - z_i \\ z_i - \underline{V} \\ \widehat{\Delta}_{ij} - z_{m+i} z_{2m+j} + z_{2m+i} z_{m+j} \\ \widehat{\Delta}_{ij} + z_{m+i} z_{2m+j} - z_{2m+i} z_{m+j} \end{bmatrix}, \qquad i \in \mathcal{V}, \qquad \text{(D.4d)}$$

for all $i = 1, \ldots, m$.

The power flow equations (D.2) have been put on polynomial form by using the trigonometric identities

$$\sin(\delta_i - \delta_j) = \sin(\delta_i) \cos(\delta_j) - \cos(\delta_i) \sin(\delta_j), \qquad\qquad \text{(D.5)}$$
$$\cos(\delta_i - \delta_j) = \cos(\delta_i) \cos(\delta_j) + \sin(\delta_i) \sin(\delta_j), \qquad\qquad \text{(D.6)}$$

resulting in

$$\psi_i(z_{I_i}) = \begin{bmatrix} \sum_{j \in I_i} z_i z_j \left[\alpha_{ij}(z_{m+i}z_{2m+j} - z_{2m+i}z_{m+j}) \right. \\ \left. + \beta_{ij}(z_{2m+i}z_{2m+j} + z_{m+i}z_{m+j}) \right] \\ \sum_{j \in I_i} z_i z_j \left[\beta_{ij}(z_{m+i}z_{2m+j} - z_{2m+i}z_{m+j}) \right. \\ \left. - \alpha_{ij}(z_{2m+i}z_{2m+j} + z_{m+i}z_{m+j}) \right] \end{bmatrix},$$

where $\widehat{\Delta}_{ij} = \sin(\overline{\Delta}_{ij})$, $\alpha_{ij} = \text{Im}(Y_{ij})$, $\beta_{ij} = \text{Re}(Y_{ij})$, $z_i = V_i$, $z_{m+i} = \sin(\delta_i)$, $z_{2m+i} = \cos(\delta_i)$, for $i = 1, \ldots, m$, and equality constraint (D.4c) is added to ensure equivalence between the new variables and the sine and cosine functions. Further, we have used, that for $(\delta_i, \delta_j) \in [-\pi/2, \pi/2]$ it holds that $\sin(|\delta_i - \delta_j|) = |\sin(\delta_i - \delta_j)|$, to rewrite constraints on the voltage phase angle.

3.2 Safety

In order to apply the barrier certificate method we must define safety for a differential algebraic system. This is done similarly to [15].

Definition 8 (Safety of Differential Algebraic System). *Given the differential algebraic system*

$$\dot{x} = f(x, d), \tag{D.7}$$

$$0 = h(x, z), \tag{D.8}$$

the differential state set $X \subseteq \mathbb{R}^n$, the algebraic state set $Z \subseteq \mathbb{R}^k$, the initial differential and algebraic set $(X_0, Z_0) \subseteq X \times Z$, the unsafe differential and algebraic set $(X_u, Z_u) \subseteq X \times Z$, and the disturbance set $D \subseteq \mathbb{R}^l$. The system is safe, if there exist no time instant $T \geq 0$ and an unknown but bounded disturbance $d : [0, T] \to D$ that results in an unsafe system trajectory, i.e., a trajectory $x : [0, T] \to \mathbb{R}^n$ satisfying $x(0) \in X_0 \cap \{x \in \mathbb{R}^n \mid 0 = h(x, z), z \in Z_0\}$, $x(T) \in X_u \cap \{x \in \mathbb{R}^n \mid 0 = h(x, z), z \in Z_u\}$, and $x(t) \in X \cap \{x \in \mathbb{R}^n \mid 0 = h(x, z), z \in Z\}$ for all $t \in [0, T]$.

In the next subsection we show how the classical barrier certificate for dynamic systems in [15], can be extended to differential algebraic systems by defining the state, initial, and unsafe sets according to the algebraic constraints and variables.

3.3 Barrier Certificate for Differential Algebraic System

We rely on the barrier certificate method [15] to verify safety of the system in (D.7) and (D.8). We specialize the method, by defining the sets X', X'_0 and X'_u

as follows

$$X' = \{(x,z) \mid 0 = h(x,z), x \in X, z \in Z\}, \tag{D.9}$$
$$X'_0 = \{(x,z) \mid 0 = h(x,z), x \in X_0, z \in Z_0\}, \tag{D.10}$$
$$X'_u = \{(x,z) \mid 0 = h(x,z), x \in X_u, z \in Z_u\}, \tag{D.11}$$

where X, $X_0 \subseteq X$ and $X_u \subseteq X$ are as stated in Definition 8. Now, consider a continuous system described by ordinary differential equations

$$\dot{x} = f(x,d), \tag{D.12}$$

where $x \in X'$ is the state, and $d \in D$ is the unknown but bounded disturbance input. We assume that the system trajectories are initialized at $x(0) \in X'_0$. The unsafe region is denoted X'_u. Suppose there exists a barrier certificate, $B : X' \to \mathbb{R}$, that satisfies the following conditions:

$$B(x) \leq 0 \ \ \forall x \in X'_0, \tag{D.13}$$
$$B(x) > 0 \ \ \forall x \in X'_u, \tag{D.14}$$
$$\frac{\partial B}{\partial x}(x)f(x,d) \leq 0 \ \ \forall (x,d) \in X' \times D, \tag{D.15}$$

then safety of the system (D.12) is guaranteed. Next, we state the polynomial programming problem.

3.4 Barrier Certificate for Power System

Instead of solving Problem 3 directly, we use the relation established in Section 3.1 and aim at solving the problem of computing a barrier certificate for the differential algebraic equations describing a power system. This problem is stated in Problem 4.

Problem 4 (Find $B(x)$ for Power System). *Given an undirected, connected, and weighted graph $G(\mathcal{V},\mathcal{E},A)$, state sets X'_i, initial state sets $X'_{i,0}$, unsafe state sets $X'_{i,u}$, disturbance sets D_i, vector fields $f_i : X'_i \times D_i \to X'_i$, outputs $\varphi_i : X'_i \to \mathbb{R}^2$, for $i = 1, \ldots, m$, find a barrier certificate, $B(x)$, for the system given by (D.4).*

---

4 Polynomial Programming Problem

The purpose of this section is to cast Problem 4 as a polynomial feasibility problem. The most common method used for reformulating a polynomial

optimization problem to a sum of squares problem is by exploiting Putinar Positivestellensatz, see Theorem 2.14 in [18, pp. 27]. We use the following corollary from Putinar Positivestellensatz.

Corollary 1. *Let*

$$S = \{x \in \mathbb{R}^n \,|\, g_1(x) \geq 0, \ldots, g_m(x) \geq 0\}$$

be a basic semialgebraic set with

$$g_m(x) = N - ||x||_2^2 \tag{D.16}$$

for some $N \in \mathbb{N}$, and let $f \in \mathbb{R}[x]$. If

$$f(x) > 0 \qquad \forall x \in S$$

then

$$f = \sigma_0 + \sum_{i=1}^m \sigma_i g_i$$

for some $\sigma_0, \ldots, \sigma_m \in \Sigma[x]$.

By fixing the degree of the polynomials σ, it is possible to use Putinar Positivestellensatz in a semidefinite programming problem. In the next subsection, we use this fact and formulate the safety problem for a general electrical grid as a sum of squares problem.

4.1 Problem Setup

Following the lines of [11], we use physical interpretation to restrict the algebraic state set Z in (D.9). The electrical grid is modeled using phasor representation, meaning that the voltage magnitudes $V_1, \ldots, V_m$, represented by $z_1, \ldots, z_m$, are intrinsically non-negative. Further, as we aim at verifying that voltage constraints are satisfied, we assume that voltage magnitudes evolve around the nominal high-voltage stable equilibrium point, see [1, pp. 213]. We denote this region $Z_a \subseteq Z$ and call it the attracting region of Z, defined by

$$Z_a = \left\{ (x,z) \in \mathbb{R}^n \times Z \,\middle|\, h(x,z) = 0, \Omega\left(\frac{\partial h}{\partial z}\right) \subset \mathbb{C}_{<0} \right\},$$

where $\Omega\left(\frac{\partial h}{\partial z}\right) \subset \mathbb{C}$ is the set of eigenvalues of the matrix $\frac{\partial h}{\partial z}$, see [11, 19]. Then according to the implicit function theorem [20, pp. 373], a unique solution to the system in (D.7) and (D.8) exists. In the remainder we assume that the algebraic set is given by Z_a. To further motivate this assumption the active power versus voltage magnitude for a two bus system is sketched in
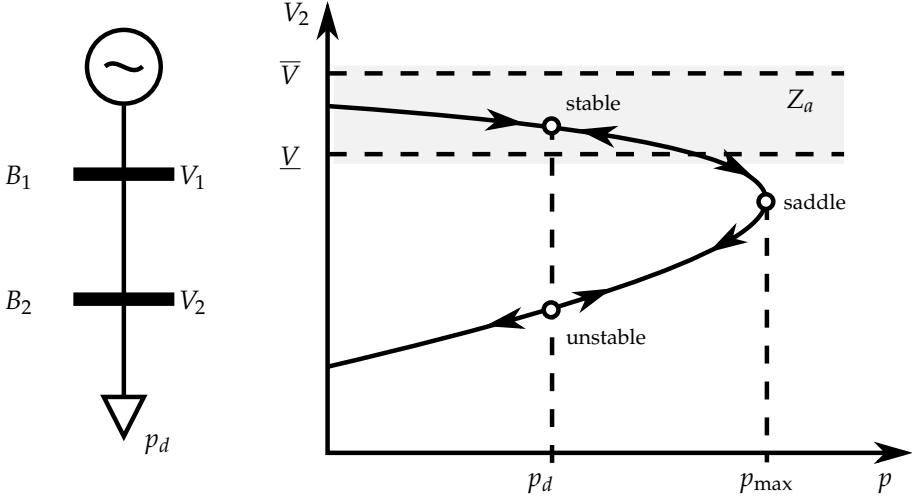
Fig. D.2: Sketch of power versus voltage for a two bus system. The maximum power transfer capability is denoted $p_{\max}$. When power demand p_d is below $p_{\max}$ there is a high-voltage stable equilibrium and a low-voltage unstable equilibrium. Constraints on voltage ensures that the system is operating in the stable region, Z_a.

Fig. D.2. In normal operation, where power demand is below the maximum power transfer capability, the power flow equations have a high-voltage stable equilibrium and a low-voltage unstable equilibrium. To ensure that the system is always operating close to the high-voltage stable equilibrium the voltage constraints $\underline{V}$, $\overline{V}$ are added, i.e., if we can ensure that voltage constraints are always satisfied, the system will be operating in the attracting region Z_a, see [1] for more information on voltage stability.

To get Problem 4 on the same form as in Corollary 1, we replace each equality constraint in (D.4b) and (D.4c) with two inequality constraints, and define

$$h_i(x_i, z_{I_i}) = \begin{bmatrix} \varphi_i(x_i) - \psi_i(z_{I_i}) \\ z_{m+i}^2 + z_{2m+i}^2 - 1 \end{bmatrix}. \tag{D.17}$$

Next we define the sets X_0, X_u, X, and D as follows

$$X_0 \equiv \{x \in \mathbb{R}^n \mid g_{X_0} \geq 0\} \tag{D.18a}$$

$$X_u \equiv \{x \in \mathbb{R}^n \mid g_{X_u} \geq 0\} \tag{D.18b}$$

$$X \equiv \{x \in \mathbb{R}^n \mid g_X \geq 0\} \tag{D.18c}$$

$$D \equiv \{x \in \mathbb{R}^n \mid g_D \geq 0\} \tag{D.18d}$$

where the initial set X_0 is directly given by (D.4d), thus we have

$$g_{X_0}(x, z) = \left[g_1^0(x_1, z_{I_1}), \ldots, g_m^0(x_m, z_{I_m}) \right]^T, \tag{D.19}$$

with

$$g_i^0(x_i, z_{I_i}) = \begin{bmatrix} h_i(x_i, z_{I_i}) \\ -h_i(x_i, z_{I_i}) \\ \left(\frac{\overline{V}_0 - \underline{V}_0}{2}\right)^2 - (z_i - V_{\text{nom}})^2 \\ (\widehat{\Delta}_{ij}^0)^2 - (-z_{m+i}z_{2m+j} + z_{2m+i}z_{m+j})^2 \end{bmatrix}, \qquad \text{(D.20)}$$

where $V_{\text{nom}} \in \mathbb{R}$ is the nominal voltage. The unsafe set X_u is defined as the complement of the set in (D.4d). Thus

$$g_{X_u}(x, z) = \left[g_1^u(x_1, z_{I_1}), \ldots, g_m^u(x_m, z_{I_m}) \right]^T, \qquad \text{(D.21)}$$

with

$$g_i^u(x_i, z_{I_i}) = \begin{bmatrix} h_i(x_i, z_{I_i}) \\ -h_i(x_i, z_{I_i}) \\ (z_i - V_{\text{nom}})^2 - \left(\frac{\overline{V}_u - \underline{V}_u}{2}\right)^2 \\ (-z_{m+i}z_{2m+j} + z_{2m+i}z_{m+j})^2 - (\widehat{\Delta}_{ij}^u)^2 \end{bmatrix}, \qquad \text{(D.22)}$$

where $\underline{V}_0 > \underline{V}_u \geq \underline{V}$, $\overline{V}_0 < \overline{V}_u \leq \overline{V}$, and $\widehat{\Delta}_{ij}^0 < \widehat{\Delta}_{ij}^u \leq \widehat{\Delta}_{ij}$. The state set X is defined using (D.16), as follows

$$g_X(x, z) = \rho(\overline{V} - \underline{V}) - \left\| \begin{bmatrix} x \\ z \end{bmatrix} \right\|^2, \qquad \text{(D.23)}$$

where $\rho \in \mathbb{N} > \sqrt{2}$, insures that $(X_0, X_u) \subset X$. Similarly, we write inequality constraints for the disturbance set D as

$$g_D = \left[g_1^d(d_1), \ldots, g_m^d(d_m) \right]^T. \qquad \text{(D.24)}$$

with

$$g_i^d(d_i) = \left(\frac{\overline{d} - \underline{d}}{2}\right)^2 - d_i^2, \qquad \text{(D.25)}$$

Finally, the vector fields are stacked

$$f(x, d) = [f_1(x_1, d_1), \ldots, f_m(x_m, d_m)]^T. \qquad \text{(D.26)}$$

From the above definitions of g_{X_0}, g_{X_u}, g_X, and g_D it is seen that all generated sets in (D.18) are semialgebraic, and satisfies the conditions of Corollary 1. Thus, the following sum of squares (SOS) program solves Problem 4

$$-B - \lambda_{X_0}^T g_{X_0} \in \Sigma[x, z], \qquad \text{(D.27)}$$

$$B - \epsilon - \lambda_{X_u}^T g_{X_u} \in \Sigma[x, z], \qquad \text{(D.28)}$$

$$-\frac{\partial B}{\partial x} f - \lambda_X^T g_X - \lambda_D^T g_D \in \Sigma[x, z], \qquad \text{(D.29)}$$
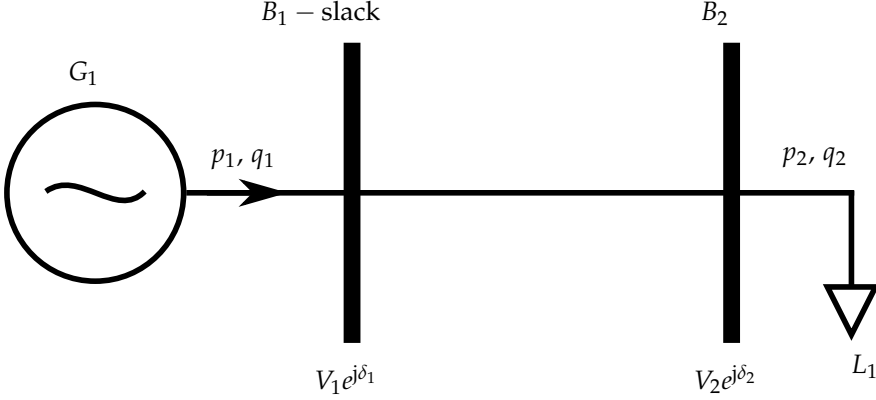
Fig. D.3: Electrical grid used for the illustrative example. The demand of L_1 has been chosen so no constraints are violated, to illustrate that a barrier certificate can be found.

where $\epsilon > 0$, $\lambda_{X_0}^T \in \Sigma[x,z]$, $\lambda_{X_u}^T \in \Sigma[x,z]$, $\lambda_X^T \in \Sigma[x,z]$, and $\lambda_D^T \in \Sigma[x,z]$. The problem is linear in unknown polynomials B, $\lambda_{X_0}^T$, $\lambda_{X_u}^T$, λ_X^T, λ_D^T, and can therefore be solved directly in SOSTOOLS.

5 Illustrative Example

In this section we verify that voltage constraints will be satisfied for the 2 bus electrical grid illustrated in Fig. D.3, when the demand of load L_1 is limited. It is assumed that the generator, G_1, is capable of maintaining a constant voltage at bus B_1, i.e., $V_1 = 1$ and $\delta_1 = 0$ are know constants. The electrical grid admittance matrix is given by

$$Y = \begin{bmatrix} 16 - j8 & -16 + j8 \\ -16 + j8 & 16 - j8 \end{bmatrix}, \tag{D.30}$$

and the constraints are as follows: $\underline{V} = 0.9$, and $\overline{V} = 1.1$. The constraint on voltage angles have been omitted to ease illustration.

5.1 Dynamic System at Bus 2

Bus B_1 in Fig. D.3 is seen as the slack bus, meaning that V_1 and δ_1 are known constants. Therefore, no dynamic system is associated to this bus. The dynamic system governing the active and reactive power demand of L_1, is mod-

eled as a linear deterministic system, given by

$$\dot{x} = Ax, \tag{D.31}$$

$$\begin{bmatrix} p_2 \\ q_2 \end{bmatrix} = Cx + b, \tag{D.32}$$

with

$$A = \begin{bmatrix} 0 & \omega & 0 \\ -\omega & 0 & 0 \\ 0 & 0 & \frac{-1}{\tau} \end{bmatrix}, \tag{D.33}$$

$$C = \begin{bmatrix} c_{11} & 0 & c_{13} \\ c_{21} & 0 & c_{23} \end{bmatrix}, \tag{D.34}$$

$$b = \begin{bmatrix} b_1 \\ b_2 \end{bmatrix}. \tag{D.35}$$

The load model consists of a harmonic oscillator, with frequency ω, to capture periodicity in consumption, and a state that converges to zero with time-constant τ. Parameters for the example are: $\omega = \frac{2\pi}{24 \text{ hours}}$, $\tau = 400$, $c_{11} = 0.045$, $c_{13} = 0.015$, $c_{21} = 0.008$, $c_{23} = 0.015$, $b_1 = -0.83$, and $b_2 = -0.62$.

5.2 Safety Verification

The sets X_0, X_u, and X are given by the stated constraint values and the functions (D.19), (D.21), and (D.23). Notice that we have no disturbance input in this example. Constraint satisfaction of the system was verified using SOS-TOOLS to solve the SOS program, resulting in the following barrier function

$$B(x) = 0.416x_1^2 + 0.416x_2^2 + 0.171x_3^2 - 8.52. \tag{D.36}$$

6 Conclusion and Future Work

We presented a method for verifying that voltage constraints in an electrical power grid will be satisfied. This was achieved by turning the static power flow equations into a differential algebraic system, and putting it on polynomial form. We showed that solving the voltage constraint satisfaction problem in Problem 3 is equivalent to finding a barrier certificate for the polynomial reformulation in Problem 4. Further, it was illustrated how the problem can be stated as a sum of squares (SOS) program using Putinar Positivestellensatz. Finally, the proposed method was illustrated through an example.

Solving a SOS problem is generally computational intense and scales badly with number of variables. It is however expected that the structure of the electrical grid, hinted by the index sets I_i, can be used to decompose

the problem into smaller sub-problems, for which a barrier certificate can be found. It is also desirable to investigate the applicability of the approaches in [21, 22], where under certain assumptions the optimal power flow problem is relaxed, turning the non-convex problem into a semi-definite programming problem. A natural extension would be to introduce both local and global voltage control functionalities and verify constraint satisfaction under these. Further, the stochastic techniques in [23] could be used to determine when voltage control should be applied to e.g., minimize curtailment of renewable resources, while guaranteeing, with some probability, that voltage constraints will be satisfied.

Acknowledgments

References

[1] T. V. Cutsem and C. Vournas, *Voltage Stability of Electric Power Systems*, 6th ed. Springer, 1998.

[2] J. W. Simpson-Porco and F. Bullo, "Distributed monitoring of voltage collapse sensitivity indices," *IEEE Transactions on Smart Grids - Special Issue on Theory of Complex Networks with Application to Smart Grid Operations*, Aug. 2015.

[3] "Overcoming PV grid issues in the urban areas," IEA Internatioal Energy Agency - Photovoltaic Power Systems Programme, Tech. Rep. IEA-PVPS T10-06-2009, 2002.

[4] "Voltage characteristics of electricity supplied by public electricity networks," EN 50160, 2010.

[5] EDSO, "Flexibility: The role of DSOs in tomorrow's electricity market," European Distribution System Operators for Smart Grids, Tech. Rep., 2014.

[6] J. v. Appen, M. Braun, T. Stetz, K. Diwold, and D. Geibel, "Time in the sun - the challenges of high PV penetration in the German electric grid," *IEEE - Power and Energy Magazine*, pp. 55 – 64, Mar. 2013.

[7] "Act on granting priority to renewable energy sources," Renewable Energy Sources Act – EEG, Tech. Rep., 2012.

[8] "Interim decision adopting revisions to electric tariff Rule 21 for Pacific Gas and Electric Company, Southern California Edison Company, and San Diego Gas & Electric Company to require "smart" inverters," California Public Utilities Commission, Tech. Rep. R.11-09-011 COM/MP6/lil, 2014.

[9] P. Aristidou, F. Olivier, M. E. Hervas, D. Ernst, and T. V. Cutsem, "Distributed model-free control of photovoltaic units for mitigating overvoltages in low-voltage networks," in *CIRED Workshop*, Rome, Jun. 2014.

[10] J. W. Smith, W. Sunderman, R. Dugan, and B. Seal, "Smart inverter volt/var control functions for high penetration of PV on distribution systems," in *IEEE Power Systems Conference and Exposition (PSCE)*, Pnoenix, AZ, USA, Mar. 2011, pp. 1 – 6.

[11] J. W. Simpson-Porco, F. Dörfler, and F. Bullo, "Voltage stabilization in microgrids via quadratic droop control," in *IEEE 52nd Annual Conference on Decision and Control*, Firenze, Italy, Dec. 2013.

[12] R. Tonkoski, L. A. C. Lopes, and T. H. M. El-Fouly, "Droop-based active power curtailment for overvoltage prevention in grid connected PV inverters," in *IEEE International Symposium on Industrial Electronics (ISIE)*, Bari, Italy, Jul. 2010, pp. 2388 – 2393.

[13] R. Tonkoski and L. A. Lopes, "Impact of active power curtailment on overvoltage prevention and energy production of PV inverters connected to low voltage residential feeders," *Renewable Energy*, vol. 36, no. 12, pp. 3566 – 3574, 2011.

[14] I. A. Hiskens and B. Gong, "MPC-based load shedding for voltage stability enhancement," in *44th IEEE Conference on Decision and Control, and the European Control Conference*, Seville, Spain, Dec. 2005.

[15] S. Prajna, A. Jadbabaie, and G. J. Pappas, "A framework for worst-case and stochastic safety verification using barrier certificates," *IEEE Transactions on Automatic Control*, vol. 52, no. 8, pp. 1415 – 1428, Aug. 2007.

[16] P. Kundur, *Power System Stability and Control*, ser. The EPRI Power System Engineering Series.   McGraw-Hill, 1993.

[17] J. Machowski, J. W. Bialek, and J. R. Bunby, *Power System Dynamics - Stability and Control*, 2nd ed.   John Wiley & Sons, 2008.

[18] J. B. Lasserre, *Momonets, Positive Polynomials and Their Applications*, 1st ed.   Imperial College Press, 2010.

[19] S. Sastry and C. Desoer, "Jump behavior of circuits and systems," *IEEE Transactions on Circuits and Systems*, no. 12, pp. 1109 – 1124, Dec. 1981.

[20] T. M. Apostol, *Mathematical Analysis*, 2nd ed. Addison-Wesley Publishing Company, 1974.

[21] R. Madani, S. Sojoudi, and J. Lavaei, "Convex relaxation for optimal power flow problem: Mesh networks," *IEEE Transactions on Power Systems*, vol. 30, no. 1, pp. 199–211, jan 2015.

[22] B. Ghaddar, J. Marecek, and M. Mevissen, "Optimal power flow as a polynomial optimization problem," *IEEE Transactions on Power Systems*, vol. 31, no. 1, pp. 539 – 546, jan 2016.

[23] C. Sloth and R. Wisneiweski, "Safety analysis of stochastic dynamical systems," in *IFAC Conference on Analysis and Design of Hybrid Systems*, 2015, pp. 62–67.

References

Paper E

Verification of Power System Voltage Constraint Satisfaction

Rasmus Pedersen, Christoffer Sloth, and Rafael Wisniewski

Abstract

We address the problem of verifying voltage constraint satisfaction for electrical power distribution systems with time-varying consumption and production. Voltage constraint violations are seen as one of the major future challenges for the distribution system operators, mainly caused by the increasing penetration of additional demand units, such as heat pumps and electrical vehicles, and renewable production units in form of wind and solar photovoltaics. In this work, we provide a procedure for verifying that voltages are within bounds, by formulating the problem as a dynamic algebraic system and computing a barrier function for this system. This is achieved by formulating the problem as a sum of squares polynomial program, which can be solved using available software tools. Further, a novel four quadrant voltage control strategy for alleviating potential voltage issues, is proposed. The computation of a barrier certificate is exemplified on a small power system, and simulation studies on a large scale power system further motivate the introduced four quadrant voltage controller.

1   Introduction

There are several reasons for focusing on voltage constraint satisfaction in power systems; first of all increases in voltage variations may lead to instability, which may result in system wide blackouts [1, 2]. Further, grid connected components may experience life-time degradation or even termination caused by overvoltage issues [3]. This has led to legislations, imposing the system operators to guarantee that voltage magnitudes are kept within ± 10 % of the nominal value [4]. However, with the increase of renewable production, down to a household level, along with additional consumption from e.g., electrical vehicles and heat pumps, the traditional power system is experiencing a transition towards a much more volatile behavior, severely challenging the system operators [5].

To handle these increasing challenges, distribution system operators and utility companies around the world are forcing new rules and regulations on distributed production units. In Germany, photovoltaic systems above a certain rated power are limited to a maximum output of 70 % of their rated power, and have to provide reactive power support [6, 7]. Similar changes have been adopted by California in their Rule 21, regulating grid connected generation [8]. The rules are typically formulated to address individual systems, without any guarantee of maintaining the entire system within constraints. Further, predetermining a constant curtailment, as done in Germany, may lead to overly conservative operation conditions, resulting in a significant loss of renewable power. The above indicate the need for new tools to verify system behavior with increased penetration of renewables, additional demand, and when introducing new local control functionalities.

Maintaining voltage magnitudes within bounds is a classical control problem within power systems and has received much attention in recent years. [9, 10] focus on how solar photovoltaic (PV) systems can provide local reactive power support for voltage control. The PV inverters implements a relation between voltage magnitude and reactive power output, known as a droop curve. This approach has been extended in [11], where the aforementioned droop controllers are replaced with quadratic droop controllers, and it is shown how these, with some coordination, can make a micro grid reach a stable voltage equilibrium. However, none of the mentioned work comes with any guarantees of voltage constraints being satisfied. Also, it might not be possible to base the voltage control strategy on reactive power support only. [12, 13] use a similar droop controller on active power to curtail PV systems to decrease overvoltages, during peak production hours. Another approach taken in [14–16] is to combine loss minimization and voltage stability satisfaction in both a centralized and distributed manner using PV inverters. Loss minimization and voltage stability is of cause important, but in the cited work the authors gives no guarantees of voltage constraint being satisfied. Further, [17] proposes a model predictive control scheme for alleviating voltage collapse situation, by load shedding. Nonetheless, it is dependent on the amount of sheddable demand and again comes with no guarantee of voltage constraint satisfaction. A centralized scheduling approach is taken in [18], and extended in [19], where active and reactive power consumption and production of flexible units are scheduled throughout an entire day to ensure voltage constraints and minimize losses. The approach depends on knowledge, or estimates, of future system behavior and environmental data, such as wind speed and solar irradiation, to optimally solve the scheduling problem, and comes with no guarantees on voltages being within bounds during run-time.

In [20] we first introduced *the voltage constraint satisfaction problem*, where a framework was developed for verifying voltage constraint satisfaction for a given power system. This was achieved by turning the classical static power flow equations into a system of dynamic and algebraic equations, and using the barrier certificate method [21], to verify safety for this system. In this context, safety is defined as voltages being within constraints. In this work we extend the analysis by providing more details on the system dynamics and proposing a novel local voltage control law. We show how the problem can be cast as a sum of squares program, using polynomial programming. The main idea of this paper is illustrated through the following example.

Consider the system depicted in Fig. E.6, with high demand from loads L_1 and L_2. Two scenarios are considered; one where the local voltage controller k_1 is inactive and one where it is active. The result is shown in Fig. E.1, where we see that when the local voltage controller is inactive, voltage constraint at bus B_3 is violated, whereas if the local controller is active the constraint is not
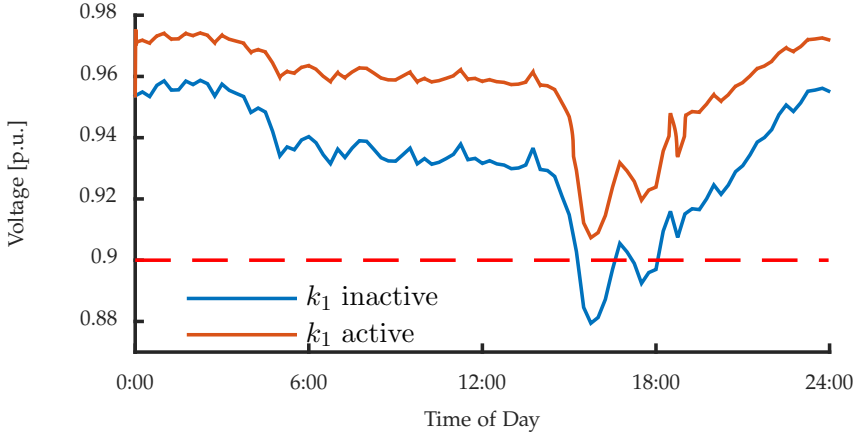
Fig. E.1: Voltage magnitude at bus B_3 in Figure E.6, with and without the local voltage controller k_1 active. Lower voltage bound is given by the red dashed line.

violated. The behavior can be verified through simulations (as done in this example), however with large power systems consisting of a large number of busses and connected systems, conducting simulations to check all possible configurations is time consuming. This paper provides models of dynamic load behavior and local voltage control, along with a methodology making it possible to state if the system will never violate constraints, leaving out the need for simulation studies. This constitutes the main contribution of the paper.

The remainder of the paper is structured as follows. We start by providing a recap of the voltage constraint satisfaction problem in Section 2. Next, in Section 3, we provide a dynamic model of demand behavior, followed in Section 4, by the Four Quadrant Voltage Controller. In Section 5, the problem is stated in polynomial form and safety of the system is defined. Then in Section 6, we arrive at the sum of squares programming problem of finding a barrier function for the polynomial equations. Section 7 provides two examples; one of computing a barrier certificate for a three bus distribution system, and secondly, a large scale simulation example illustrates the proposed voltage control strategy. Finally, the work is concluded in Section 8, along with discussions and future directions.

2 Problem Formulation

In this section, we state *the voltage constraint satisfaction problem*, which was first introduced in [20]. In this work we focus on purely deterministic systems and provide more details on the dynamic parts of the system. Further, we

161

introduce a local voltage controller, which we have named the Four Quadrant Voltage Controller or 4Q-VC for short.

Throughout the paper, we assume that the frequency is kept constant, i.e., the electrical grid is connected to a slack bus [22, p. 255]. This is common practice when studying voltage problems in electrical power networks.

2.1 Preliminaries and Notation

We denote the set of real numbers $\mathbb{R}$ and the set of complex numbers $\mathbb{C}$. By $\mathbb{R}_+$ ($\mathbb{R}_-$) we denote the set of non-negative (non-positive) real numbers, and $\mathbb{R}_{>0}$ denotes the positive real numbers. The imaginary unit is denoted $j^2 = -1$, and for a complex number $x \in \mathbb{C}$ the complex conjugate is denoted x^*. For a vector $x \in \mathbb{C}^n$, x^* denotes the entry wise complex conjugate. Let $|\mathcal{B}|$ denote the cardinality of the set $\mathcal{B}$. For a given index set I, we write $x_I = \{x_i \mid i \in I\}$. Given a set of vertices (busses) $\mathcal{B} = \{1, \ldots, m\}$, let $\mathcal{L} \subseteq \mathcal{B} \times \mathcal{B}$ be the set of edges (lines) connecting the busses. Further, we define the set of neighbors of bus $i \in \mathcal{B}$ (including bus i) as $I_i = \{j \in \mathcal{B} | (j, i) \in \mathcal{L}\} \cup \{i\}$.

2.2 System Model

The electrical grid is modeled by an admittance matrix $Y \in \mathbb{C}^{m \times m}$ [22, p. 199], with the set of busses $\mathcal{B} = \{1, \ldots, m\}$ and lines $\mathcal{L} \subset \mathcal{B} \times \mathcal{B}$. To each bus $i \in \mathcal{B}$ we associate a complex power injection $s_i = p_i + jq_i$, where $p_i \in \mathbb{R}$ is the active power injection and $q_i \in \mathbb{R}$ is the reactive power injection. The bus phasor voltage is given by $v_i = V_i e^{j\delta_i}$ $V_i \in \mathbb{R}$ denotes voltage magnitude, and $\delta_i \in [-\pi/2, \pi/2]$ the voltage phase angle. The vector of bus voltages is defined $v \in \mathbb{C}^m$ and the vector of complex power injections is expressed as

$$s = \text{diag}(v)(Yv)^* \in \mathbb{C}^m, \tag{E.1}$$

where $\text{diag}(x)$ denotes a diagonal matrix with the entries of x in its diagonal and all other entries are zero.

Equation (E.1) can be divided into the active and reactive power component, resulting in the classical power flow equations [23, p. 115]

$$p_i = \sum_{j \in I_i} V_i V_j \left[\alpha_{ij} \sin(\delta_i - \delta_j) + \beta_{ij} \cos(\delta_i - \delta_j) \right], \tag{E.2a}$$

$$q_i = \sum_{j \in I_i} V_i V_j \left[\beta_{ij} \sin(\delta_i - \delta_j) - \alpha_{ij} \cos(\delta_i - \delta_j) \right], \tag{E.2b}$$

where $\alpha_{ij} = \text{Im}(Y_{ij})$ is the susceptance of line (i, j), and $\beta_{ij} = \text{Re}(Y_{ij})$ is the conductance of line (i, j).

We let the active and reactive power injections in (E.2) be governed by dynamic systems representing generation and demand behavior at their bus

3. Dynamic System Model

connection

$$\dot{x}_i = f_i(x_i, V_i), \tag{E.3a}$$

$$\begin{bmatrix} p_i \\ q_i \end{bmatrix} = \varphi_i(x_i, V_i) + k_i(V_i), \tag{E.3b}$$

where $x_i \in X_i \subseteq \mathbb{R}^n$ is the state, $f_i : X_i \times \mathbb{R} \to X_i$ is the vector field, $\varphi_i : X_i \times \mathbb{R} \to \mathbb{R}^2$ is the output, and $k_i : \mathbb{R} \to \mathbb{R}^2$ is a local voltage controller. Notice, that focus is on verifying voltage constraint satisfaction, therefore the dynamic systems and voltage controllers in (E.3) are assumed given. Examples of both are provided in Section 3 and Section 4.

2.3 The Voltage Constraint Satisfaction Problem

In the following sections we aim at solving *the voltage constraint satisfaction problem*, Problem 1 in [20], where we are focusing on voltage magnitudes. Hence, the problem can be written as follows:

Problem 5 (Voltage Constraint Satisfaction). *Given an electrical grid admittance matrix $Y \in \mathbb{C}^{m \times m}$, vector fields $f_i : X_i \times \mathbb{R} \to X_i$, output maps $\varphi_i : X_i \times \mathbb{R} \to \mathbb{R}^2$, local voltage controllers $k_i : \mathbb{R} \to \mathbb{R}^2$, upper and lower bounds on voltage magnitude $(\overline{V}, \underline{V}) \in \mathbb{R}_+$, for $i = 1, \ldots, m$, show if voltage constraints*

$$\underline{V} \le V_i \le \overline{V},$$

are always satisfied, for the system given by (E.2) *and* (E.3), *for proper initial conditions.*

In the following two sections we provide specific models of the dynamic system and control in (E.3).

3 Dynamic System Model

In this section, we provide a model for representing dynamic consumption behavior in (E.3). The i indexes representing each bus, is omitted to ease readability. To model the inflexible demand we adopt the voltage dependent multiplicative generic load model from [1, p. 128] and extend it with linear

dynamics describing the nominal demand behavior. The model is given as

$$
\begin{bmatrix} \dot{x}_1 \\ \dot{x}_2 \\ \dot{x}_3 \end{bmatrix} = \begin{bmatrix} \frac{1}{\tau_p} \left(\frac{1}{V_0} \right)^{a_t} V^{a_t} x_1 + \frac{1}{\tau_p} \left(\frac{1}{V_0} \right)^{a_s} V^{a_s} \\ \frac{1}{\tau_q} \left(\frac{1}{V_0} \right)^{b_t} V^{b_t} x_2 + \frac{1}{\tau_q} \left(\frac{1}{V_0} \right)^{b_s} V^{b_s} \\ A x_3 \end{bmatrix} \tag{E.4a}
$$

$$
\varphi_i(x, V) = \begin{bmatrix} p_d \\ q_d \end{bmatrix} = \begin{bmatrix} x_1 \, C_1 x_3 \left(\frac{1}{V_0} \right)^{a_t} V^{a_t} + b_1 \\ x_2 \, C_2 x_3 \left(\frac{1}{V_0} \right)^{b_t} V^{b_t} + b_2 \end{bmatrix} \tag{E.4b}
$$

where the state $x_1 \in \mathbb{R}$ represents the transient voltage dependency of active power, the state $x_2 \in \mathbb{R}$ represents the transient voltage dependency of reactive power, with $\tau_p \in \mathbb{R}_{>0}$ (resp. $\tau_q \in \mathbb{R}_{>0}$) as the time constant of active power (resp. reactive power), $a_s, a_t, b_s, b_t \in \mathbb{R}_+$ are load exponents describing voltage sensitivity, and $V_0 \in \mathbb{R}_+$ represent the nominal voltage magnitude. The state $x_3 \in \mathbb{R}^n$ represents the nominal demand behavior, with $A \in \mathbb{R}^{n \times n}$ being the system matrix, $C_1, C_2 \in \mathbb{R}^n$ the output matrices, and $b_1, b_2 \in \mathbb{R}$ are constant bias terms.

According to [1, p. 128] the transient load exponents a_t, b_t, usually have larger values than the steady-state exponents a_s, b_s, indicating that the transient characteristic is more voltage sensitive. Further, we restrict the values of the exponents to be non-negative integers, i.e. $a_t, b_t, a_s, b_s \in \mathbb{N}_+$. This restriction allows us to see the equations as polynomials, which is used later on.

3.1 Nominal Demand Behavior

We use the results established in [24] and model the nominal demand behavior with a system of $r \in \mathbb{N}$ oscillators. From [24] it is known that this particular model structure captures the periodic active power demand well, even with a limited number of states, see Fig. E.2. Therefore, we directly adopt this model, which is given by

$$
\dot{x}_3 = A x_3, \tag{E.5}
$$

$$
p_{\text{nom}} = C_1 x_3 + b_1, \tag{E.6}
$$

$$
q_{\text{nom}} = C_2 x_3 + b_2, \tag{E.7}
$$

where A is a block diagonal matrix, where each block is on the skew symmetric form

$$
A = \text{diag} \left(\begin{bmatrix} 0 & \omega_1 \\ -\omega_1 & 0 \end{bmatrix}, \dots, \begin{bmatrix} 0 & \omega_r \\ -\omega_r & 0 \end{bmatrix}, 0 \right), \tag{E.8}
$$

with $\omega_j \in \mathbb{R}$ describing the frequency of a single oscillator, $j = 1, \dots, r$, and $\text{diag}(X, Y, \dots)$ is a block diagonal matrix with $X, Y, \dots$ as diagonal blocks. It
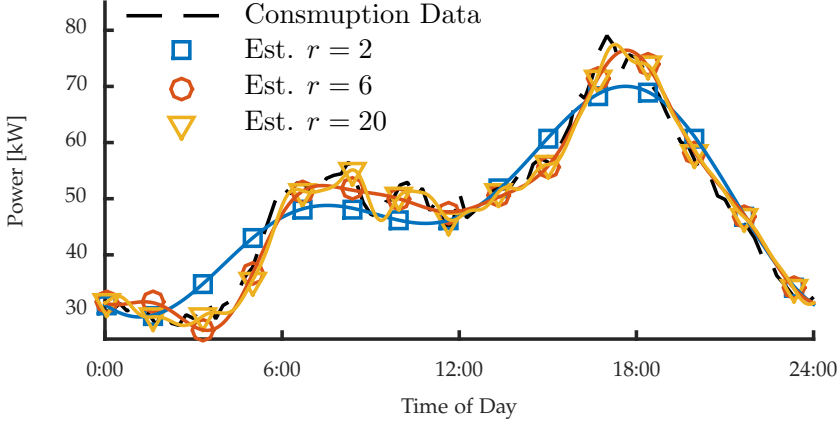
Fig. E.2: Comparison between modeling approach for the nominal demand behavior and real data; for different model orders.

should be noted that the values of ω_j represent the harmonics that the model should capture. The output matrix $C_1 \in \mathbb{R}^n$ is given by

$$C_1 = \begin{bmatrix} \varrho_{11} & \varrho_{12} & \cdots & \varrho_{r1} & \varrho_r & 1 \end{bmatrix}, \tag{E.9}$$

with $\varrho_{11}, \varrho_{12}, \ldots, \varrho_{r1}, \varrho_{r2} \in \mathbb{R}$ being the amplitudes associated to the r oscillators. To model the reactive power demand, we assume a constant power factor $\theta \in \mathbb{R}$, where a list of power factors for different loads can be found in [22, p. 632]. Hence, the output matrix C_2 and bias term b_2 for nominal reactive power consumption is given as

$$C_2 = C_1 \tan\left(\cos^{-1}(\theta)\right), \tag{E.10}$$

$$b_2 = b_1 \tan\left(\cos^{-1}(\theta)\right). \tag{E.11}$$

To illustrate the validity of the modeling approach, it is compared with real data in Fig. E.2, for different number of oscillators. The frequency of the oscillators are given as follows $\omega_i = \frac{i2\pi}{24 \text{ hours}}$, for $i = 1, \ldots, r$. Notice that the demand behavior can be constantly estimated using e.g., a Kalman filter, see [24].

3.2 Demand Model Example

An example of the voltage dependent demand model is plotted in Fig. E.3, for a one day period, where the following parameters have been used: $\tau_p = 120$ [sec], $\tau_q = 60$ [sec], $a_t = 2$ [-], $a_s = 1$ [-], $b_t = 2$ [-], $b_s = 1$ [-], $V_0 = 1$ [p.u.], $r = 2$ [-], $\omega_1 = \frac{2\pi}{24\text{hours}}$ [rad/sec], $\omega_2 = \frac{4\pi}{24\text{hours}}$ [rad/sec], $\theta = 0.95$ [-], $b_1 = 50$ [kW], $\varrho_{11} = 2$ [kW], $\varrho_{12} = -9$ [kW], $\varrho_{21} = -5$ [kW], $\varrho_{22} = -3.5$ [kW].
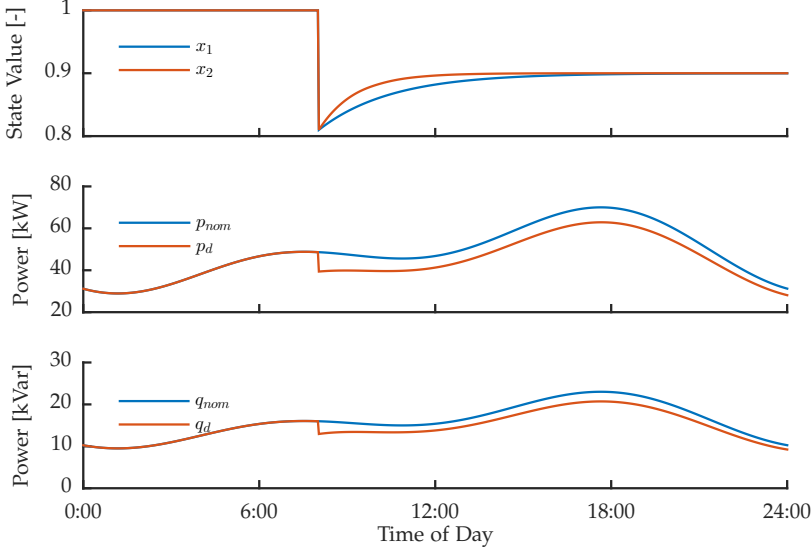
Fig. E.3: Example of the demand model trajectory during one day. At $12:00$ a sudden voltage drop from 1 p.u. to 0.9 p.u. occurs.

4 Four Quadrant Voltage Control (4Q-VC)

This section introduces the four quadrant voltage control (4Q-VC) strategy for ensuring voltage constraint satisfaction. The control strategy is described for all four quadrants of the pq-plane, but can easily be specialized to systems only capable of operating in a subset of the pq-plane, e.g., a PV system can only operate with non-negative active power. The 4Q-VC is illustrated in Fig. E.4. Again we omit the i indexes to ease notation. The active and reactive power output of the controller is given by

$$\begin{bmatrix} p_c \\ q_c \end{bmatrix} = k(V), \tag{E.12}$$

with $p_c, q_c \in \mathbb{R}$ being the active and reactive power output of the control and $k : \mathbb{R} \to \mathbb{R}^2$ is the control law detailed in the following.

The relation between locally measured voltage magnitude, V, and active power output is

$$p_c = \begin{cases} \overline{p}_c, & \text{if } V < \underline{V} \\ K_p(V - \underline{\overline{V}}_c), & \text{if } \underline{V} \le V \le \underline{\overline{V}}_c \\ K_p(V - \overline{V}_c), & \text{if } \overline{V}_c \le V \le \overline{V} , \\ \underline{p}_c, & \text{if } V > \overline{V} \\ 0, & \text{otherwise} \end{cases} \tag{E.13}$$
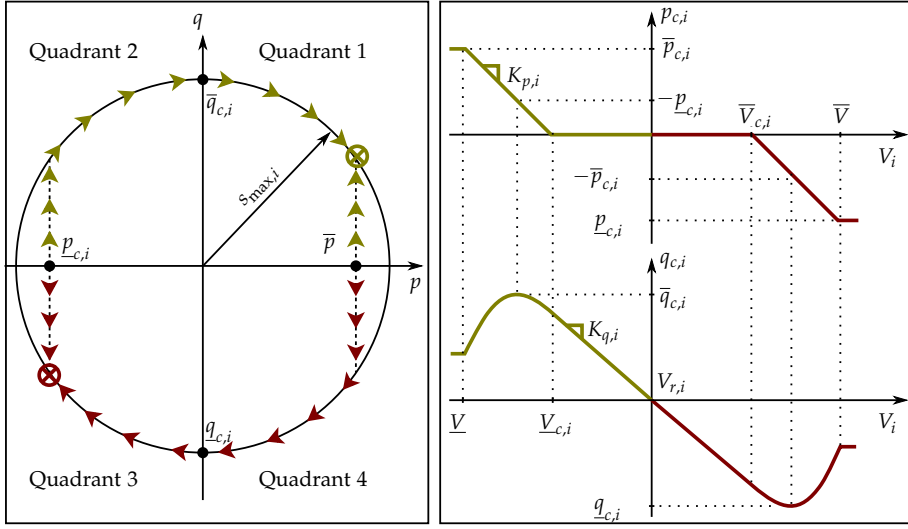
Fig. E.4: Four quadrant voltage control strategy. Left: illustrates trajectories in the pq-plane. Right: is the associated active and reactive power control strategies.

and the relation between measured voltage magnitude and reactive power is

$$
q_c = \begin{cases} \sqrt{s_{\max}^2 - (\underline{p}_c + p_c)^2} & \text{if } V < \underline{V}_c \\ -\sqrt{s_{\max}^2 - (\overline{p}_c + p_c)^2} & \text{if } V > \overline{V}_c \\ K_q(V - V_0), & \text{otherwise} \end{cases} \tag{E.14}
$$

where $\overline{p}_c, \underline{p}_c, \overline{q}_c, \underline{q}_c \in \mathbb{R}$ are the upper and lower bounds on active and reactive power, $\overline{V}_c, \underline{V}_c \in \mathbb{R}$ are the upper and lower bounds on when active power voltage control should be started, $V_0 \in \mathbb{R}$ is the nominal voltage, $K_p \in \mathbb{R}_-$ are the droop gain on active power, $K_q \in \mathbb{R}_-$ is the droop gain on reactive power, and $s_{\max} \in \mathbb{R}_+$ is the maximum apparent power of the control. The gains K_p and K_q are calculated as follows

$$
K_p = \frac{\overline{p}_c}{\underline{V} - \underline{V}_c} = \frac{-\underline{p}_c}{\overline{V}_c - \overline{V}}, \tag{E.15}
$$

$$
K_q = \frac{\overline{q}_c}{\underline{V}_c} = \frac{-\underline{q}_c}{-\overline{V}_c}. \tag{E.16}
$$

The design parameters are $\overline{V}_c$, and $\underline{V}_c$ defining at what voltage magnitudes active power curtailment/injection should initiate. The 4Q-VC strategy is illustrated in Fig. E.4.

5 Safety Verification

To solve the verification problem in Problem 5, we apply the safety verification technique known as a barrier certificate [21]. In order to find a barrier certificate, we reformulate the problem to polynomial form and define safety for the new system.

5.1 Problem Reformulation

For convenience, we write $\tilde{z}_i = (z_i, z_{m+i}, z_{2m+i})$ and let $z_i = V_i$, $z_{m+i} = \sin(\delta_i)$, and $z_{2m+i} = \cos(\delta_i)$. Next, we show that if and only if (V_i, δ_i, x_i) is a solution to Problem 5, then $(\tilde{z}_i, x_i)$ is a solution to the polynomial reformulation given by

$$\dot{x}_i = f_i(x_i, z_i), \tag{E.17a}$$

$$0 = \varphi_i(x_i, z_i) + k_i(z_i) - \psi_i(\tilde{z}_{I_i}), \tag{E.17b}$$

$$0 = z_{m+i}^2 + z_{2m+i}^2 - 1, \tag{E.17c}$$

$$0 \leq \begin{bmatrix} \overline{V} - z_i \\ z_i - \underline{V} \end{bmatrix}, \tag{E.17d}$$

for all $i = 1, \ldots, m$.

To put the power flow equations in (E.2), on polynomial form we have used the following trigonometric identities

$$\sin(\delta_i - \delta_j) = \sin(\delta_i)\cos(\delta_j) - \cos(\delta_i)\sin(\delta_j), \tag{E.18}$$

$$\cos(\delta_i - \delta_j) = \cos(\delta_i)\cos(\delta_j) + \sin(\delta_i)\sin(\delta_j), \tag{E.19}$$

resulting in

$$\psi_i(\tilde{z}_{I_i}) = \begin{bmatrix} \sum_{j \in I_i} z_i z_j \left[\alpha_{ij}(z_{m+i}z_{2m+j} - z_{2m+i}z_{m+j}) \right. \\ \left. + \beta_{ij}(z_{2m+i}z_{2m+j} + z_{m+i}z_{m+j}) \right] \\ \sum_{j \in I_i} z_i z_j \left[\beta_{ij}(z_{m+i}z_{2m+j} - z_{2m+i}z_{m+j}) \right. \\ \left. - \alpha_{ij}(z_{2m+i}z_{2m+j} + z_{m+i}z_{m+j}) \right] \end{bmatrix},$$

where the equality constraint in (E.17c) has been added to ensure equivalence between the new variables and the sine and cosine functions in (E.2a) and (E.2b). Note, in this work the dynamic systems and controllers in (E.3) are only dependent on the voltage magnitudes V_i, i.e., there is no explicit modeling or control of the voltage angles δ_i. This easily be included, by letting the system in (E.3) be dependent on $\tilde{z}_i$ instead of z_i. However, for simplicity and readability we leave it out for now. Next, we define safety for the reformulated problem.

5.2 Safety

To apply the barrier certificate method, safety for the new system dynamic algebraic system need to be defined. We do this following the lines of [21].

Definition 9 (Safety of Differential Algebraic System). *Given the differential state set $X \subseteq \mathbb{R}^n$, the algebraic state set $Z \subseteq \mathbb{R}^k$, the initial set $(X_0, Z_0) \subseteq X \times Z$, the unsafe set $(X_u, Z_u) \subseteq X \times Z$, and the differential algebraic system*

$$\dot{x} = f(x, z), \tag{E.20}$$
$$0 = h(x, z), \tag{E.21}$$

The system is safe, if there exist no time instant $T \geq 0$ that results in an unsafe system trajectory, i.e., a trajectory $x : [0, T] \rightarrow X$ satisfying $x(0) \in X_0 \cap \{x \in X \mid 0 = h(x, z), z \in Z_0\}$, $x(T) \in X \cap (\{x \in X \mid 0 = h(x, z), z \in Z_u\} \cup \{x \in X_u \mid 0 = h(x, z), z \in Z\})$, for all $t \in [0, T]$.

Next it is shown how the classical barrier certificate for dynamic systems in [21], can be extended to dynamic algebraic systems by defining the state, initial, and unsafe sets according to the additional algebraic constraints and variables.

5.3 Barrier Certificate for Differential Algebraic System

The barrier certificate method is applied to verify safety of the differential algebraic system in (E.20) and (E.21). Consider a system described by ordinary differential equations

$$\dot{x} = f(x, z), \tag{E.22}$$

with the sets X', X_0', and X_u' defined as follows

$$X' = \{(x, z) \mid 0 = h(x, z), x \in X, z \in Z\}, \tag{E.23}$$
$$X_0' = \{(x, z) \mid 0 = h(x, z), x \in X_0, z \in Z_0\}, \tag{E.24}$$
$$X_u' = \{(x, z) \mid 0 = h(x, z), x \in X, z \in Z_u\} \cup \tag{E.25}$$
$$\{(x, z) \mid 0 = h(x, z), x \in X_u, z \in Z\},$$

where X, $X_0 \subseteq X$, and $X_u \subseteq X$ are given in Definition 9.

Let the system trajectories be initialized at $x(0) \in X_0'$ and let the unsafe region be given by X_u'. Suppose there exists a barrier certificate, $B : X \rightarrow \mathbb{R}$, that satisfies the following conditions:

$$B(x) \leq 0 \quad \forall x, \in X_0', \tag{E.26}$$
$$B(x) > 0 \quad \forall x, \in X_u', \tag{E.27}$$
$$\frac{\partial B}{\partial x}(x) f(x, z) \leq 0 \quad \forall (x, z) \in X', \tag{E.28}$$

then safety of the system (E.22) is guaranteed. The classical barrier certificate method has now been specialized to the differential algebraic system in (E.20) and (E.21). Next, we use the above definition to state the polynomial programming problem of finding a barrier certificate.

5.4 Barrier Certificate for Power System

Instead of solving Problem 5 directly, we use the established relation in Section 5.1 to solve the problem of computing a barrier certificate for the differential algebraic system of equations representing a power system. This problem is stated in Problem 6.

Problem 6 (Computation of Barrier Function). *Given an electrical grid admittance matrix $Y \in \mathbb{C}^{m \times m}$, state sets X_i', initial state sets $X_{i,0}'$, unsafe state sets $X_{i,u}'$, vector fields $f_i : X_i \times \mathbb{R} \to X_i$, outputs $\varphi_i : X_i \times \mathbb{R} \to \mathbb{R}^2$, voltage controllers $k_i : \mathbb{R} \to \mathbb{R}^2$, for $i = 1, \ldots, m$, find a barrier certificate, B, for the system given by* (E.17).

In the following section we provide details on how Problem 6 can be solved usin polynomial programming.

6 Polynomial Programming Problem

The purpose of this section is to cast Problem 6 as a polynomial feasibility problem. We use the following notation. Let $\mathbb{R}[x]$ denote the ring of real polynomials in the variables $(x_1, \ldots, x_n) \in \mathbb{R}^n$. We say that a polynomial $p(x) \in \mathbb{R}[x]$ is sum of squares (SOS), if $p(x) = \sum_{i=1}^{k} p_i(x)^2$, for some polynomials $p_i(x) \in \mathbb{R}[x]$. Given a polynomial p we denote that the polynomial is SOS by $p \in \Sigma[x]$.

The most common method used for reformulating a polynomial optimization problem to a sum of squares problem is by exploiting Putinar Positivestellensatz, see Theorem 2.14 in [25, p. 27]. We use the following corollary from Putinar Positivestellensatz.

Corollary 2. *Let*

$$S = \{x \in \mathbb{R}^n \mid g_1(x) \geq 0, \ldots, g_m(x) \geq 0\}$$

be a basic semialgebraic set with

$$g_m(x) = N - ||x||^2 \tag{E.29}$$

for some $N \in \mathbb{N}$, and let $f \in \mathbb{R}[x]$. If

$$f(x) > 0 \qquad \forall x \in S$$

then

$$f = \sigma_0 + \sum_{i=1}^{m} \sigma_i g_i$$

for some $\sigma_0, \ldots, \sigma_m \in \Sigma[x]$.

By fixing the degree of the polynomials σ, it is possible to use Putinar Positivestellensatz in a semidefinite programming problem. In the next subsection, we use this fact and formulate the safety problem for a general electrical grid as a sum of squares problem.

6.1 Problem Setup

As already mentioned in [20] the algebraic state set Z in (E.23) needs to be restricted for the problem to make sense, i.e., the equations may have several solutions. We use physical interpretation to restrict the algebraic state set, similar to what was done in [11]. The voltage magnitude are intrinsically non-negative meaning that $z_1, \ldots, z_m$ are positive. and we assume that they evolve close to the nominal voltage, see [1, p. 213]. We define this region, similarly to [11, 26], as follows; let $Z_a \subseteq Z$ be the attracting region of Z, given by

$$Z_a = \left\{ (x, z) \in \mathbb{R}^n \times Z \,\middle|\, h(x, z) = 0, \Omega\left(\frac{\partial h}{\partial z}\right) \subset \mathbb{C}_{<0} \right\},$$

where $\Omega\left(\frac{\partial h}{\partial z}\right) \subset \mathbb{C}$ is the set of eigenvalues of the matrix $\frac{\partial h}{\partial z}(x, z)$. Then according to the implicit function theorem [27, p. 373], a unique solution to the system in (E.20) and (E.21) exists.

In the remainder, we restrict the algebraic set to Z_a. To further motivate this assumption the active power versus voltage magnitude for a two bus system is sketched in Fig. E.5. When power demand is below the systems maximum transfer capability, the power flow equations will have a high-voltage stable equilibrium and a low-voltage unstable equilibrium. If voltages evolve close to the high-voltage equilibrium, i.e., within voltage constraints, then the system will be operating within the domain of attraction Z_a, see [1] for more information on voltage stability.

To get Problem 6 on the same form as in Corollary 2, we replace each equality constraint in (E.17b) and (E.17c) with two inequality constraints, and define

$$h_i(x_i, \tilde{z}_{I_i}) = \begin{bmatrix} \varphi_i(x_i, \tilde{z}_i) + k_i(z_i) - \psi_i(\tilde{z}_{I_i}) \\ z_{m+i}^2 + z_{2m+i}^2 - 1 \end{bmatrix}. \tag{E.30}$$
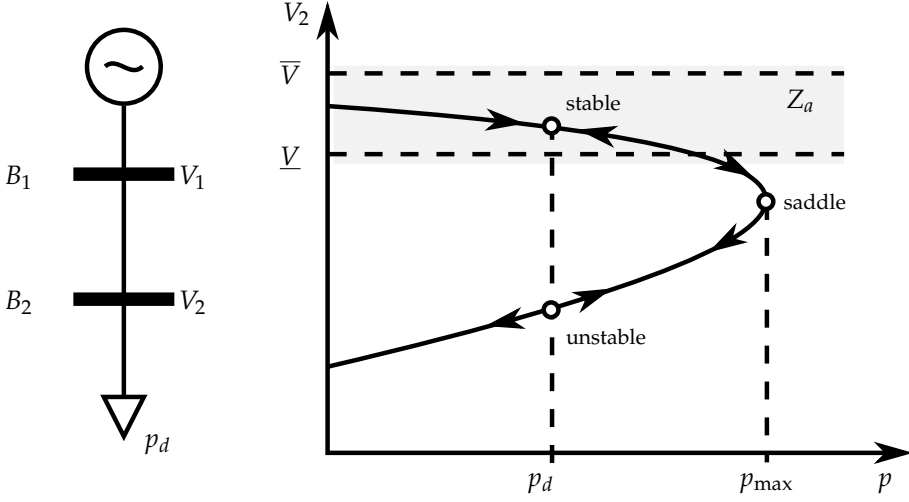
Fig. E.5: Sketch of power versus voltage for a two bus system. The maximum power transfer capability is denoted $p_{\max}$. When power demand p_d is below $p_{\max}$ there is a high-voltage stable equilibrium and a low-voltage unstable equilibrium. Constraints on voltage ensures that the system is operating in the stable region, Z_a.

Next we define the sets X_0, X_u, and X as follows

$$X_0 \equiv \{x \in \mathbb{R}^n \mid g_{X_0} \geq 0\} \tag{E.31a}$$

$$X_u \equiv \{x \in \mathbb{R}^n \mid g_{X_u} \geq 0\} \tag{E.31b}$$

$$X \equiv \{x \in \mathbb{R}^n \mid g_X \geq 0\} \tag{E.31c}$$

where the initial set X_0 is directly given by (E.17d), thus we have

$$g_{X_0}(x,z) = \left[g_1^0(x_1, \tilde{z}_{I_1}), \ldots, g_m^0(x_m, \tilde{z}_{I_m}) \right]^T, \tag{E.32}$$

with

$$g_i^0(x_i, \tilde{z}_{I_i}) = \begin{bmatrix} h_i(x_i, \tilde{z}_{I_i}) \\ -h_i(x_i, \tilde{z}_{I_i}) \\ \left(\frac{\overline{V}_0 - \underline{V}_0}{2} \right)^2 - (z_i - V_0)^2 \end{bmatrix}, \tag{E.33}$$

where $V_0 \in \mathbb{R}$ is the nominal voltage. The unsafe set X_u is defined as the complement of the set in (E.17d). Thus

$$g_{X_u}(x,z) = \left[g_1^u(x_1, \tilde{z}_{I_1}), \ldots, g_m^u(x_m, \tilde{z}_{I_m}) \right]^T, \tag{E.34}$$

with

$$g_i^u(x_i, \tilde{z}_{I_i}) = \begin{bmatrix} h_i(x_i, \tilde{z}_{I_i}) \\ -h_i(x_i, \tilde{z}_{I_i}) \\ (z_i - V_0)^2 - \left(\frac{\overline{V}_u - \underline{V}_u}{2} \right)^2 \end{bmatrix}, \tag{E.35}$$

where $\underline{V}_0 > \underline{V}_u$ and $\overline{V}_0 < \overline{V}_u$. The state set X is defined using (E.29), as follows

$$g_X(x,z) = \rho(\overline{V} - \underline{V}) - \left\| \begin{bmatrix} x \\ z \end{bmatrix} \right\|^2, \tag{E.36}$$

where $\rho \in \mathbb{N} > \sqrt{2}$, insures that $(X_0, X_u) \subset X$. Finally, the vector fields are stacked

$$f(x,z) = [f_1(x_1, \tilde{z}_1), \ldots, f_m(x_m, \tilde{z}_m)]^T. \tag{E.37}$$

6.2 Sum of Squares Program

From the above definitions of g_{X_0}, g_{X_u}, and g_X it is seen that all generated sets in (E.31) are semialgebraic, and satisfies the conditions of Corollary 2. Thus, the following sum of squares (SOS) program solves Problem 6

$$-B - \lambda_{X_0}^T g_{X_0} \in \Sigma[x,z], \tag{E.38}$$

$$B - \epsilon - \lambda_{X_u}^T g_{X_u} \in \Sigma[x,z], \tag{E.39}$$

$$-\frac{\partial B}{\partial x} f - \lambda_X^T g_X \in \Sigma[x,z], \tag{E.40}$$

where $\epsilon > 0$, $\lambda_{X_0}^T \in \Sigma[x,z]$, $\lambda_{X_u}^T \in \Sigma[x,z]$, and $\lambda_X^T \in \Sigma[x,z]$. The problem is linear in unknown polynomials B, $\lambda_{X_0}^T$, $\lambda_{X_u}^T$, λ_X^T, and can therefore be solved directly using sum of squares programming.

In the following we provide examples illustrating the presented work.

7 Examples

The example section is divided into two parts: first we investigate solution to Problem 6, for a small scale power grid consisting of three busses, with and without the proposed local voltage control strategy. Next, we show a large scale simulation example of a power system with high penetration of solar PV, where each PV inverter implements different local voltage control strategies, including the one introduced in Section 4. For the large scale example, it is simply not computationally possible to solve Problem 6, in its current form. However, we have included this example to further motivate the proposed 4Q-VC. The large scale simulation example is carried out in the power distribution system simulation tool GridLab-D [28].

7.1 Barrier Certificate for Small Scale Power Grid

In this illustrative example we consider the power grid depicted in Fig. E.6, which consists of three busses, two loads and one 4Q-VC. Bus B_1 is seen
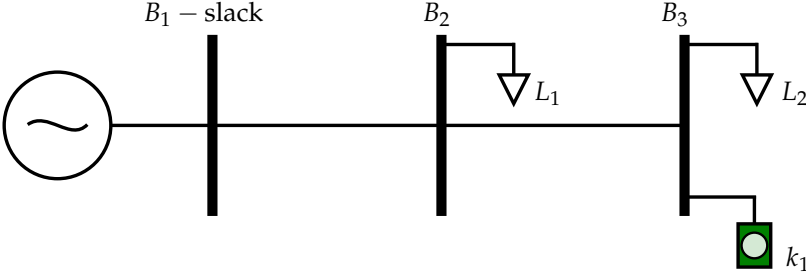
Fig. E.6: Three bus power grid system used for the small scale example. Arrows indicate loads, and the green box is a four quadrant voltage controller.

as the slack bus, meaning that V_1 and δ_1 are known constants. The grid admittance matrix is given by

$$
Y = \begin{bmatrix} y_1 & -y_1 & 0 \\ -y_1 & 2y_1 & -y_1 \\ 0 & -y_1 & y_1 \end{bmatrix}, \tag{E.41}
$$

where $y_1 = 8 - j4$ represent the lines admittance, i.e. all lines are identical. We let each load be represented by two oscillators with parameters: $\omega_1 = \frac{2\pi}{24 \text{ hours}}$, $\omega_2 = \frac{4\pi}{24 \text{ hours}}$, $\varrho_{1,11} = -0.15$, $\varrho_{1,12} = 0$, $\varrho_{1,21} = -0.1$, $\varrho_{1,22} = 0$, $\varrho_{2,11} = -0.08$, $\varrho_{2,12} = 0$, $\varrho_{2,21} = -0.05$, $\varrho_{2,22} = 0$ $b_1 = b_2 = 0$. We only consider constraints on voltage magnitude $\underline{V} = 0.9$ and $\overline{V} = 1.1$, meaning that there are no constraints on the differential states, i.e., the unsafe set is associated to the algebraic states only. Furthermore, we have omitted the voltage dependence of the load models to ease computation. This results in a model with 8 differential states, 6 algebraic states, 18 algebraic equality constraints and 4 algebraic inequality constraints. The controller k_1 has the following parameters: $\overline{p}_c = \overline{q}_c = 0.2$, $\underline{V}_c = 0.95$ $\overline{V}_c = 1.05$ $K_p =$, $K_q =$.

Notice that the system parameters have been chosen such that voltage constraints will be violated when the controller k_1 is inactive. To solve the SOS program stated in Sec. 6.2, with the parameters given here, we have implemented it in MATLAB using the YALMIP toolbox along with the MOSEK solver. As expected, when the controller k_1 is inactive the problem of finding a barrier certificate is infeasible, whereas when the controller is active it is possible to compute a barrier certificate. Consequently, the system will not violate constraints as long as the 4Q-VC is active.

For brevity we will not state the barrier function here, but we will make the script used for computing it available online at [29].

Table E.1: Total amount of active and reactive power produced by PV systems.

Scenario	Active Power		Reactive Power	
	[MWh]	%	[MVArh]	%
1	29.4	100.0	0	-
2	29.3	99.4	29.4	100.0
3	27.2	92.4	29.0	98.8
4	28.9	98.1	29.6	100.9

7.2 Large Scale Simulation Example: 4Q-VC

In this simulation example we illustrate the local voltage controller, 4Q-VC from Section 4, through simulation studies on a large scale low voltage distribution grid. The distribution grid was originally used as a benchmark grid, in the SmartC2Net project [30]. Parameters for this grid can be found at [29], and we use a three phase GridLab-D implementation, to further strengthen the reliability of the results. Four simulations are conducted, where all PV systems implements the following voltage control strategy:

1. No curtailment of active power and no reactive power is injected.

2. No curtailment of active power and reactive power is used for voltage control.

3. 30 % curtailment of active power and reactive power is used for voltage control.

4. Curtailment of active power and injection of reactive power according to the 4Q-VC.

All PV systems have a rated apparent power of 6 kVA and each PV block in Fig. E.7 represents two PV systems. The loads, indicated by the arrows in Fig. E.7, represent from 1-8 houses (total of 116 houses), where consumption profiles are based on real data from danish households [31]; data which is freely available at [29]. The four simulation scenarios all have a duration of 20 days, where results for a sunny day with low cloud coverage and thus large PV production, are shown in Figures E.8-E.11. Further, the simulation results for the 20 days are summarized in Table E.1 and E.2.

We observe a number of interesting results, for both PV power production and bus voltage variations, are observed. In Scenario 1 we see that when the PV systems are allowed to produce the available power, voltage constraints are violated, see Fig. E.8. Further, in Scenario 2, when relying only on reactive power for voltage control, voltage constraints are still violated during peak production hours, see Fig. E.9. This is caused by the PV systems constraint
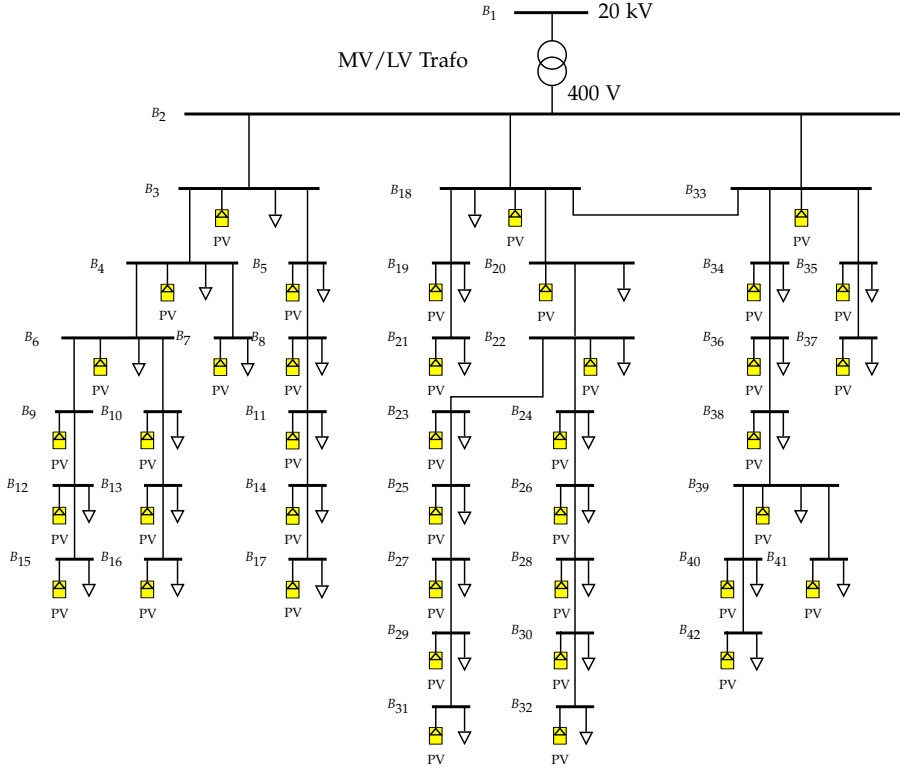
Fig. E.7: Low voltage distribution grid used for the large scale simulation examples. The loads consist of several houses and the PV boxes each represent two 6 kW solar PV systems.

Table E.2: Voltage variations over all busses.

Scenario	Voltage Mean [p.u.]	Voltage STD [p.u.]	%	Voltage Max [p.u.]	%
1	0.989	0.034	100.0	1.100	100.0
2	0.994	0.018	51.4	1.073	73.3
3	0.993	0.013	39.1	1.028	28.7
4	0.994	0.013	39.1	1.043	43.4

on apparent power output, i.e., when active power injection is equal to rated power, reactive power injection has to be zero. When the PVs active power injections are curtailed by 30 % in Scenario 3, no voltage constraints are violated, see Fig. E.10. This is because of the decrease in active power injection, but also because of the extra reactive power available during peak production hours. Finally in Scenario 4, we observe that by deploying the 4Q-VC we let
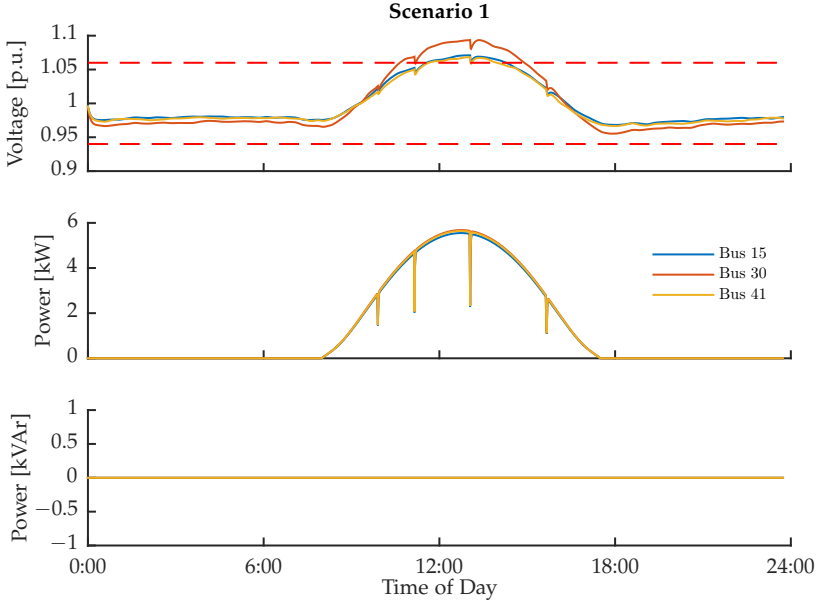
Fig. E.8: Scenario 1, No curtailment of active power and no reactive power is injected. Top: Shows the voltage magnitude, where the red dashed lines are the constraints. Middle: Shows the active power injection. Buttom: Shows the reactive power injection.

the voltages increase a little, which in turn allows for an approximately 6 % increase in active power production compared to the 30 % curtailment case in Scenario 3. These results further motivate the 4Q-VC strategy introduced in this work.

8 Conclusion and Perspectives

In this work, we attacked the problem of verifying power grid voltage constraint satisfaction, introduced in [20]. We limited our analysis to deterministic systems, but added explicit models for both consumers and local voltage controllers, and illustrated how the problem could be reformulated to polynomial form. We showed that finding a barrier certificate for the polynomial reformulation was equivalent to solving the original voltage constraint satisfaction problem. Using Putinar Positivestellensatz, the polynomial problem was cast as a sum of squares program, where solvers are available. The method for verifying voltage constraint satisfaction was illustrated through an example on a four bus system. Further, a large scale simulation study was conducted to illustrate the effectiveness of the Four Quadrant Voltage Controller (4Q-VC), introduced in this work.
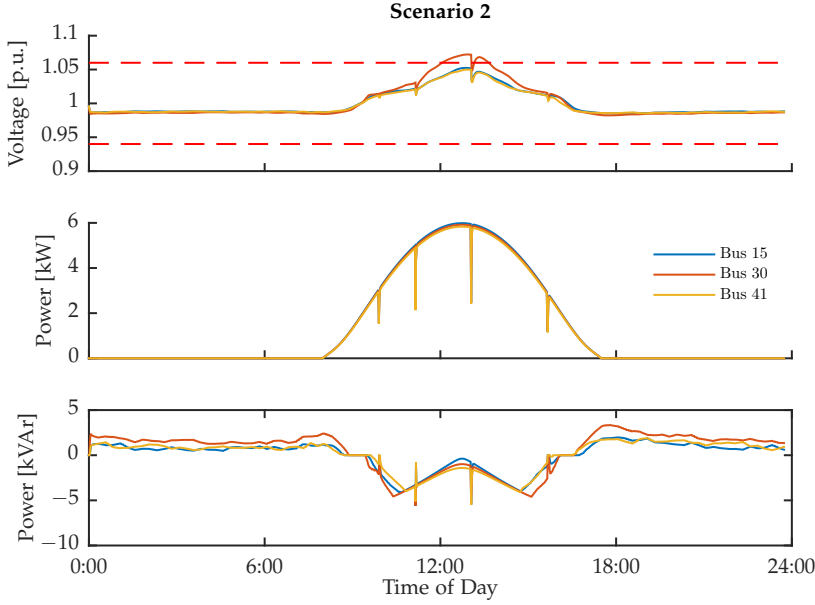
Fig. E.9: Scenario 2, No curtailment of active power and reactive power is used for voltage control. Top: Shows the voltage magnitude, where the red dashed lines are the constraints. Middle: Shows the active power injection. Buttom: Shows the reactive power injection.

Generally, solving sum of squares problems are computationally hard, and scales badly with the number of variables. This makes the method, in its current form, applicable to only small power systems, with a few busses. However, there is structure in the problem which has not yet been utilized. Each bus in the grid is only connected to a subset of the other busses, indicated by the index sets I_i. Therefore, it is believed that this structure can be used to decompose the problem into smaller sub-problems, for which it would be computational feasible to solve the sum of squares problem. Another approach would be to relax the non-convex problem using techniques similar to [32], where the optimal power flow problem is turned into a semi-definite problem, using assumptions on grid structure.

With the introduction of the 4Q-VC, a question still stands on how to tune the controllers to maximize renewable power production, while at the same time ensuring voltage constraint satisfaction. Solving this problem is equivalent to finding the largest initial set Z_0 in (E.24), that would still guarantee no voltage constraint violations. To also solve this problem in a stochastic setting, the techniques introduced in [33] could be used to determine a initial set, that guarantees, with some probability, that voltage constraints will be satisfied.
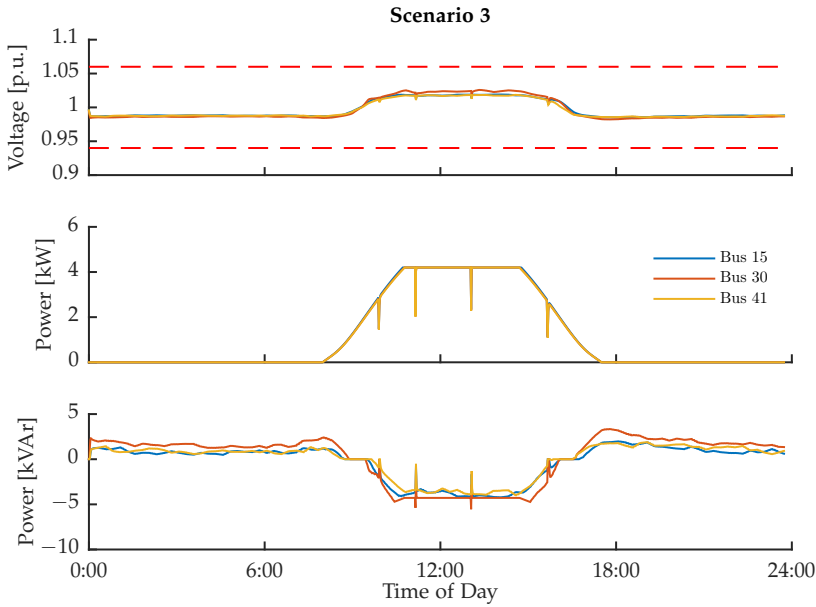
Fig. E.10: Scenario 3, 30 % curtailment of active power and reactive power is used for voltage control. Top: Shows the voltage magnitude, where the red dashed lines are the constraints. Middle: Shows the active power injection. Buttom: Shows the reactive power injection.

Acknowledgments

References

[1] T. V. Cutsem and C. Vournas, *Voltage Stability of Electric Power Systems*, 6th ed. Springer, 1998.

[2] J. W. Simpson-Porco and F. Bullo, "Distributed monitoring of voltage collapse sensitivity indices," *IEEE Transactions on Smart Grids - Special Issue on Theory of Complex Networks with Application to Smart Grid Operations*, Aug. 2015.

[3] "Overcoming PV grid issues in the urban areas," IEA Internatioal Energy Agency - Photovoltaic Power Systems Programme, Tech. Rep. IEA-PVPS T10-06-2009, 2002.
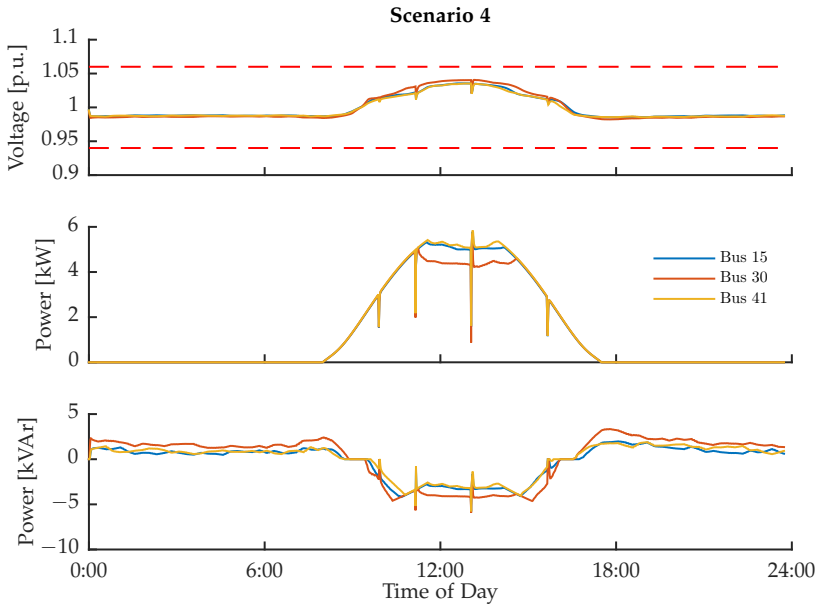
Fig. E.11: Scenario 4, Curtailment of active power and injection of reactive power according to the 4Q-VC. Top: Shows the voltage magnitude, where the red dashed lines are the constraints. Middle: Shows the active power injection. Buttom: Shows the reactive power injection.

[4] "Voltage characteristics of electricity supplied by public electricity networks," EN 50160, 2010.

[5] EDSO, "Flexibility: The role of DSOs in tomorrow's electricity market," European Distribution System Operators for Smart Grids, Tech. Rep., 2014.

[6] J. v. Appen, M. Braun, T. Stetz, K. Diwold, and D. Geibel, "Time in the sun - the challenges of high PV penetration in the German electric grid," *IEEE - Power and Energy Magazine*, pp. 55 – 64, Mar. 2013.

[7] "Act on granting priority to renewable energy sources," Renewable Energy Sources Act – EEG, Tech. Rep., 2012.

[8] "Interim decision adopting revisions to electric tariff Rule 21 for Pacific Gas and Electric Company, Southern California Edison Company, and San Diego Gas & Electric Company to require "smart" inverters," California Public Utilities Commission, Tech. Rep. R.11-09-011 COM/MP6/lil, 2014.

[9] P. Aristidou, F. Olivier, M. E. Hervas, D. Ernst, and T. V. Cutsem, "Distributed model-free control of photovoltaic units for mitigating overvoltages in low-voltage networks," in *CIRED Workshop*, Rome, Jun. 2014.

[10] J. W. Smith, W. Sunderman, R. Dugan, and B. Seal, "Smart inverter volt/var control functions for high penetration of PV on distribution systems," in *IEEE Power Systems Conference and Exposition (PSCE)*, Pnoenix, AZ, USA, Mar. 2011, pp. 1 – 6.

[11] J. W. Simpson-Porco, F. Dörfler, and F. Bullo, "Voltage stabilization in microgrids via quadratic droop control," in *IEEE 52nd Annual Conference on Decision and Control*, Firenze, Italy, Dec. 2013.

[12] R. Tonkoski, L. A. C. Lopes, and T. H. M. El-Fouly, "Droop-based active power curtailment for overvoltage prevention in grid connected PV inverters," in *IEEE International Symposium on Industrial Electronics (ISIE)*, Bari, Italy, Jul. 2010, pp. 2388 – 2393.

[13] R. Tonkoski and L. A. Lopes, "Impact of active power curtailment on overvoltage prevention and energy production of PV inverters connected to low voltage residential feeders," *Renewable Energy*, vol. 36, no. 12, pp. 3566 – 3574, 2011.

[14] S. Bolognani, R. Carli, G. Cavraro, and S. Zampieri, "Distributed reactive power feedback control for voltage regulation and loss minimization," *arXiv: 1303.7173v2*, vol. math.OC, Nov. 2014.

[15] N. Li, G. Qu, and M. Dahleh, "Real-time decentralized voltage control in distribution networks," in *52nd Annual Allerton Conference*, Allerton House, UIUC, Illinois, USA, 2014, pp. 582–588.

[16] S. Kundu, S. Backhaus, and I. A. Hiskens, "Distributed control of reactive power from photovoltaic inverters," in *IEEE International Symposium on Circuits and Systems*, Beijing, China, 2013, pp. 249–252.

[17] I. A. Hiskens and B. Gong, "MPC-based load shedding for voltage stability enhancement," in *44th IEEE Conference on Decision and Control, and the European Control Conference*, Seville, Spain, Dec. 2005.

[18] M. Juelsgaard, C. Sloth, R. Wisniewski, and J. Pillai, "Loss minimization and voltage control in smart distribution grid," in *Proceedings of the 19th IFAC World Congress*, Cape Town, South Africa, Aug. 2014.

[19] M. Juelsgaard, P. Andersen, and R. Wisniewski, "Distribution loss reduction by household consumption coordination in smart grids," *IEEE Transactions on Smart Grid*, vol. 5, no. 4, pp. 2133 – 2144, 2014.

[20] R. Pedersen, C. Sloth, and R. Wisniewski, "Verification of power grid voltage constraint satisfaction - a barrier certificate approach," in *European Control Conference*, Aalborg, Denmark, Jul. 2016.

[21] S. Prajna, A. Jadbabaie, and G. J. Pappas, "A framework for worst-case and stochastic safety verification using barrier certificates," *IEEE Transactions on Automatic Control*, vol. 52, no. 8, pp. 1415 – 1428, Aug. 2007.

[22] P. Kundur, *Power System Stability and Control*, ser. The EPRI Power System Engineering Series.   McGraw-Hill, 1993.

[23] J. Machowski, J. W. Bialek, and J. R. Bunby, *Power System Dynamics - Stability and Control*, 2nd ed.   John Wiley & Sons, 2008.

[24] R. Pedersen, C. Sloth, and R. Wisniewski, "Active power management in power distribution grids: Disturbance modeling and rejection," in *European Control Conference*, Aalborg, Denmark, Jul. 2016.

[25] J. B. Lasserre, *Momonets, Positive Polynomials and Their Applications*, 1st ed.   Imperial College Press, 2010.

[26] S. Sastry and C. Desoer, "Jump behavior of circuits and systems," *IEEE Transactions on Circuits and Systems*, no. 12, pp. 1109 – 1124, Dec. 1981.

[27] T. M. Apostol, *Mathematical Analysis*, 2nd ed.   Addison-Wesley Publishing Company, 1974.

[28] Pacific Northwest National Laboratory, "GridLAB-D - Power Distribution System, Simulation and Analysis Tool," 2009. [Online]. Available: http://www.gridlabd.org

[29] R. Pedersen, C. Sloth, G. B. Andresen, R. Wisniewski, J. R. Pillai, and F. Iov, "DiSC - A Simulation Framework for Distribution System Voltage Control," 2014. [Online]. Available: http://kom.aau.dk/project/SmartGridControl/DiSC/

[30] FP7 - SmartC2Net Project, "Smart control of energy distribution grids over heterogeneous communication networks," 2015. [Online]. Available: www.smartc2net.eu

[31] R. Pedersen, C. Sloth, G. B. Andresen, and R. Wisniewski, "DiSC: A simulation framework for distribution system voltage control," in *European Control Conference*, Linz, Austria, Jul. 2015.

[32] R. Madani, S. Sojoudi, and J. Lavaei, "Convex relaxation for optimal power flow problem: Mesh networks," *IEEE Transactions on Power Systems*, vol. 30, no. 1, pp. 199–211, jan 2015.

[33] C. Sloth and R. Wisneiweski, "Safety analysis of stochastic dynamical systems," in *IFAC Conference on Analysis and Design of Hybrid Systems*, 2015, pp. 62–67.

References

Paper F

DiSC: A Simulation Framework for Distribution System Voltage Control

Rasmus Pedersen, Christoffer Sloth, Gorm Bruun Andresen, and Rafael Wisniewski

Abstract

This paper presents the MATLAB simulation framework, DiSC, for verifying voltage control approaches in power distribution systems. It consists of real consumption data, stochastic models of renewable resources, flexible assets, electrical grid, and models of the underlying communication channels. The simulation framework makes it possible to validate control approaches, and thus advance realistic and robust control algorithms for distribution system voltage control. Two examples demonstrate the potential voltage issues from penetration of renewables in the distribution grid, along with simple control solutions to alleviate them.

1   Introduction

High penetration of renewable energy resources in the distribution grid introduces new challenges to voltage control, as the assumption of a unidirectional power flow from the high voltage (HV) transmission grid down to the end consumer is no longer valid [1]. Production units on the medium voltage (MV) and low voltage (LV) distribution grids cause over-voltage issues in places where the distribution system operators (DSOs) have no means of affecting the voltage level [2]. Thus, there is a need to redesign the voltage control on the distribution grid, and to exploit flexible assets in the LV and MV grids for control.

The analysis of voltage issues is complicated by lack of time resolved measurements from the LV grid, although the ongoing deployment of smart meters offers new opportunities for new data-driven models and studies, see [3] for an example. Here, we present a novel simulation framework that includes models of flexible assets, communication, renewable power generation and real consumption data. It follows the mission of IEEE task force on open source software for power systems [4]. Other tools address related issues, where some examples are; MATPOWER [5] for solving power flow and optimal power flow and GridLAB-D [6], which is a detailed simulation framework tailored for the American distribution system, which has a significantly different structure than European distribution grids. The existing tools have not been developed with a main focus on electrical grid control validation. They do e.g., not include modern assets such as electrical vehicles (EVs) and solar photovoltaics (PVs), realistic consumption and production patterns, a model of the underlying communication network, the importance of empirical data, or the implementation in a control design environment, such as MATLAB.

To motivate the need for novel voltage control approaches, the impact on the grid voltage of increased penetration of wind and solar power is illustrated by two examples. Fig. F.1 shows the power production of a collection of wind turbines connected to the MV grid, and the resulting control of on-
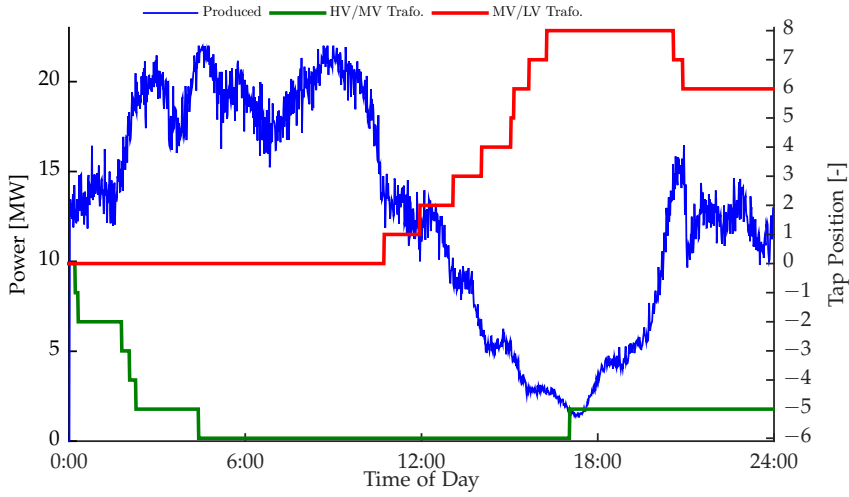
Fig. F.1: Power production of a wind power plant consisting of ten 2.2 MW wind turbines along with the tap position of the HV/MV and MV/LV transformers. To ensure satisfactory voltage levels throughout the distribution grid, a total of 17 tap changes are needed, 7 on the HV/MV transformer and 10 on the MV/LV transformer. The grid setup can be seen in Fig. F.8.

load tap-changers on the HV/MV and MV/LV transformers, responsible for voltage control. It is seen that the fluctuating wind power production causes several tap changes. This is unacceptable, since excessive tap-changing is very expensive due to wear on the equipment [7]. Thus, other actuators (flexible assets) in the grid must do the voltage control.

The solar power production from PV panels is highly correlated, and contributes with a large peak production around noon. This may cause overvoltage issues especially in residential low voltage grids, as illustrated in Fig. F.2. The issue in residential low voltage grids is that the consumption is relatively low around noon, where most people are at work, and assets such as electrical vehicles are not available in the residential grid [8]. Moreover, voltages drop during evening and night, when people return from work and PV production is low. It can also be seen that the voltage issues can not be solved by a tap-changing transformer, as the voltages throughout a residential grid can vary greatly, depending on the placement of PVs. Therefore, flexible assets on a household level must participate in the voltage control [9]. This requires coordination, implying that a communication infrastructure is needed.

Several works have addressed voltage control in the distribution grid [10–12], most of which do not capture the lack of spatial and temporal correlation between available EVs and production from PVs, the stochasticity of distributed energy resources, the underlaying communication network, or the
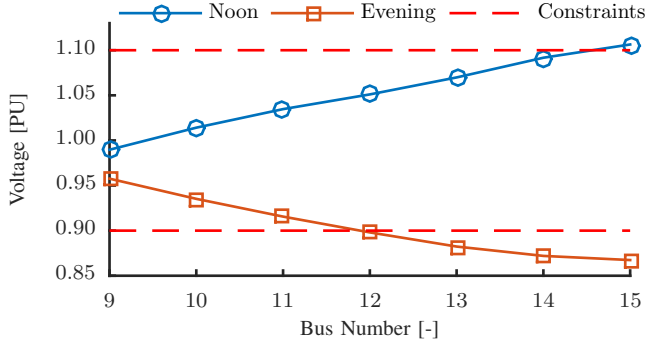
Fig. F.2: Voltage profile throughout the LV grid at two instances in time on a sunny summer day. Bus 9 is at the secondary side of the MV/LV transformer. The grid setup can be seen in Fig. F.8.

physical constraints imposed by the grid. Therefore, these solutions cannot be readily used for the control of distribution grids.

This paper introduces a MATLAB distribution grid simulation framework based on stochastic models of renewables and measurement data from residential households, industry, supermarkets and agriculture. The simulation framework allows the study of voltage issues in European distribution networks, based on realistic asset models and measurement data. The framework also includes a model of communication channels with delays and packet losses, which allow simulation of realistic communication patterns in the control. Thereby, grid control algorithms can be validated on a realistic model, which is an important step towards further penetration of renewable resources in the distribution grid. The DiSC simulation framework can be found at [13], along with a detailed description of models, examples and a user guide.

The paper is structured as follows; Sec. 2 outlines the current and envisioned future control structure. In Sec. 3, real household consumption data is presented and discussed. In Sec. 4, the models spanning from the electrical grid, through communication network to flexible assets are detailed. Sec. 5, explains the two examples presented in the introduction, and an approach to solve the voltage issues. Finally, Sec. 6, concludes the work.

2 Control Structure

An overview of the present and envisioned future distribution system control structure is depicted in Fig. F.3, and illustrates the control setup, along with communication links. The basic idea is to transform the current centrally controlled system into a hierarchical control system.

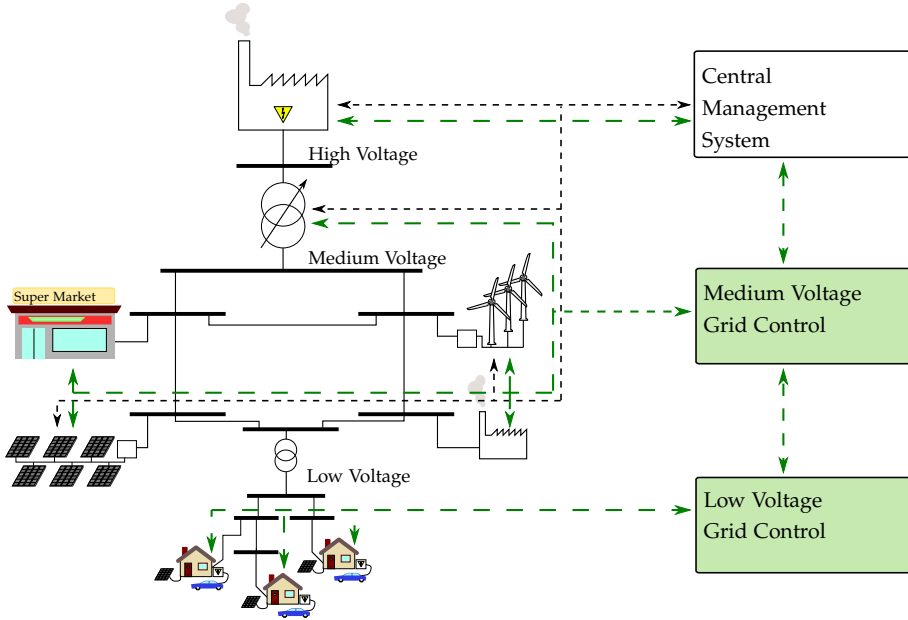In the hierarchical control structure, the controller on each level has two

Fig. F.3: Current and envisioned future control structure of the electrical distribution grid. By adding a controller on each voltage layer a hierarchical control structure is obtained. The black dashed lines indicate the current communication links. Whereas, the green dashed lines indicate the envisioned future communication links.

objectives; first, it must ensure that the voltage on each bus is within constraints. Secondly, it must offer flexibility to the upper layer controller, by managing the flexible assets. To verify the hierarchical control structure; realistic simulation tools are needed that not only focus on the electrical grid, but also on flexible assets and communication networks.

To simulate realistic control scenarios the communication links between assets and controllers must be included. The developed simulation framework makes it possible to implement any delay and loss probability distribution functions to represent the communication technology used. This is done by applying inverse transfer sampling to generate delay and loss values which are distributed according to the specified inverse cumulative density functions. Further, each flexible asset is equipped with local control functionality enabling distributed control scenarios. For further details on the implemented model of communication links, see [13].

3 Consumption Data

Due to the introduction of smart meters, households consumption data with high temporal resolution is now being logged by many DSOs mainly for
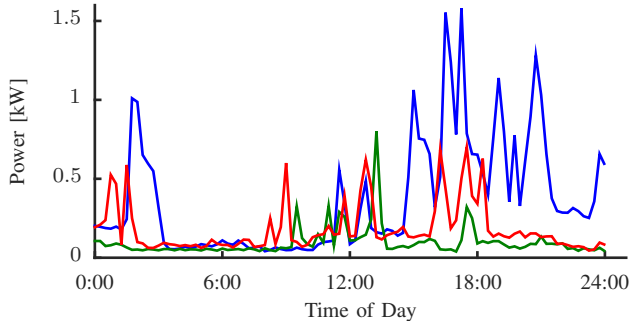
Fig. F.4: Consumption profiles of three different households during a day in November 2011.

billing purposes. But it is not readily available for research, because of privacy issues. The data included in this simulation framework were obtained as anonymized data from the Danish DSO NRGi, and it represents about 1200 individual household consumption profiles from the area around the Danish city Horsens. Each profile has a temporal resolution of 15 minutes, spans more than a year, and have been validated by the DSO for billing purposes. Significant variations between individual profiles reveals that basing household consumption patterns on an average profile is not possible. This is illustrated in Fig. F.4, where consumption profiles from three different households are depicted. Not only do the individual profiles differ in magnitude but also in time. The data provided in the simulation framework will allow for realistic simulation scenarios, and is thus a key feature of DiSC.

4 Models

The purpose of this section is to describe the models of the electrical grid, flexible assets, and grid components implemented in the simulation framework. All models are implemented in MATLAB as classes, which gives a modular model that makes it easy to implement new models, change the simulation scenario and add/remove assets on each bus.

Flexible assets are characterized by being able to offer flexibility in active and/or reactive power consumption/production. The implemented flexible assets are: wind power plant, solar power plant, energy storage, electrical vehicle, and supermarket. The simulation framework also includes the following grid components: on-load tap changing transformer (OLTC), static compensator, capacitor bank and tie-switch. Only a subset of the models are described here, but details on all models can be found at [13]. Further, default parameter values for all models are given in their MATLAB class file. The sampling time for simulations can freely be chosen, however the realistic

dynamic behavior of e.g., a wind power plant is not captured at sampling times below 1 second.

4.1 Electrical Grid

The implemented Newton-Raphson power flow solver [14] assumes a balanced three phase system, similar to other popular MATLAB power flow analysis tools, such as MATPOWER [5]. It is assumed that the high voltage grid is capable of delivering the active and reactive power needed; thus the frequency is kept constant. This allow for focusing on voltage control issues, which differs from frequency problems by being local instead of global, i.e., they must be handled at the bus where they occur. Also, the system can be simulated using phasor representation, which significantly decreases simulation time. The topology and parameters of the underlying electrical grid can freely be chosen to represent any grid of interest. Moreover, it is easy to setup the grid topology and parameters, and automatically generate the grids admittance matrix, required for solving the power flow equations. An example of a grid setup used in the simulation framework can be found in Fig. F.8.

4.2 Wind Power Plant

The wind power plant model is formed by a collection of wind turbine models similar to the model presented in Section 3.7 of [15], and consist of three parts:

1. A wind speed model based on the Van der Hoven spectrum for the mean component and a von Karman spectrum for the turbulence component,

2. A wind power plant model based on a model of variable-speed, variable-pitch wind turbine,

3. A control interface for active and reactive power.

The wind power plant model includes a number of single wind turbines with identical mean wind, but with separate turbulent wind components. Because of the focus on voltage control in this paper, the wind turbines are assumed to have simple dynamics; for further details in wind turbine dynamics and control, see [15, 16].

Wind Speed Model

The wind speed model relies on standard models, which are found in [15, 17].

Wind Turbine Model

We consider a variable-speed, variable-pitch wind turbine [15]. This type of wind turbine is controlled to maximize power capture at low wind speeds and produce a constant power at high wind speeds. The power of the wind in the rotor swept area is given by

$$P_w = \frac{1}{2}\rho A v_w^3, \tag{F.1}$$

where v_w is the point wind speed, P_w is the power of the wind, ρ is the air density, and A is the rotor swept area.

To model the dynamics of the rotor shafts and drive train, a first order model is added to represent the inertia of the system, where typical time-constant values are between 10-30 seconds.

Control Interface

The active and reactive power of the wind power plant can be controlled; thus, (F.1) is modified to describe the normal operation of a wind turbine and to take into account control of active power. We allow the active power to be controlled in two different ways

- Derate active power,

- Increase/decrease active power.

To derate power means that the maximum power of the wind turbine (p_r) is limited to a value $p_r - \Delta p_{\text{lim}}$, where $\Delta p_{\text{lim}} > 0$ is a control variable. If the wind turbine is operated in derated mode, the active power output can be both increased and decreased by the control variable Δp_{ref}.

The wind power plant model in steady state, with the control of active power is

$$p = \begin{cases} 0 & \text{if } \bar{v}_w < v_{\text{ci}} \vee \bar{v}_w > v_{\text{co}} \\ \frac{1}{2}\rho A C_{\text{p,max}} v_w^3 + \Delta p_{\text{ref}} & \text{if } v_{\text{ci}} \leq v_w < v_r \\ p_r - \Delta p_{\text{lim}} + \Delta p_{\text{ref}} & \text{if } v_r \leq v_w < v_{\text{co}} \\ 0 & \text{otherwise} \end{cases},$$

where $C_{\text{p,max}}$ is the maximum power coefficient of the wind turbine [18], v_{ci} and v_{co} are the cut-in and cut-out wind speeds, which determine the operating range of the wind turbine, p_r is the maximum output power, v_r is the minimum speed at which the wind turbine can produce an output power equal to $p_r - \Delta p_{\text{lim}}$ and $\bar{v}_w$ is a ten minute average of the wind speed. Further, physical constraints implies that: $0 \leq p_r - \Delta p_{\text{lim}} + \Delta p_{\text{ref}} \leq \frac{1}{2}\rho A C_{\text{p,max}} v_w^3$, is always obeyed.

We allow the reactive power of the wind power plant to be controlled in three different modes

- Constant power factor (*mode* = 0),

- Reference following on reactive power (*mode* = 1),

- Voltage control (*mode* = 2).

Thus, the reactive power reference can be described as:

$$q_{\text{ref}} = \begin{cases} p \tan(\cos^{-1}(\delta)) & \text{if } mode = 0 \\ \bar{q}_{\text{ref}} & \text{if } mode = 1 \\ \alpha(v_{\text{ref}}, v_{\text{mes}}) & \text{if } mode = 2 \end{cases}, \tag{F.2}$$

where $\bar{q}_{\text{ref}}$ is the external reactive power reference, δ is the desired power factor, v_{ref} is a reference voltage, v_{mes} is the measured voltage at the connection point and $\alpha : \mathbb{R}^2 \to \mathbb{R}$ is a voltage droop control function given by

$$\alpha(v_{\text{mes}}, v_{\text{ref}}) = \frac{-2s_{\text{max}}}{v_{\text{max}} - v_{\text{min}}}(v_{\text{mes}} - v_{\text{ref}}), \tag{F.3}$$

where s_{max} is the maximum apparent power and v_{max} and v_{min} is the maximum and minimum allowable voltage values, respectively. The reactive power output of the wind power plant is limited by the maximum apparent power s_{max} of the converter; hence, the reactive power output is

$$q = \begin{cases} q_{\text{ref}} & \text{if } |q_{\text{ref}}| \leq q_{\text{max}}(p) \\ \text{sign}(q_{\text{ref}})q_{\text{max}}(p) & \text{otherwise} \end{cases}, \tag{F.4}$$

where $q_{\text{max}}(p) = \sqrt{s_{\text{max}}^2 - p^2}$, and the apparent power is defined as $s = \sqrt{p^2 + q^2}$.

4.3 Solar Power Plant

The solar power plant model consists of three parts:

1. A solar irradiance model, based on a stochastic Markov model depending on cloud cover,

2. A model of a photovoltaic system,

3. A control interface for active and reactive power.

The solar power plant model consists of a number of single photovoltaic (PV) systems. As the PV model is intended for studying how these systems affect the underlying electrical grid, their dependence on temperature and tilt angle are neglected; for further details on modeling of PV systems, see [19, 20]. Further, the control interface is identical to the one detailed in the previous section.
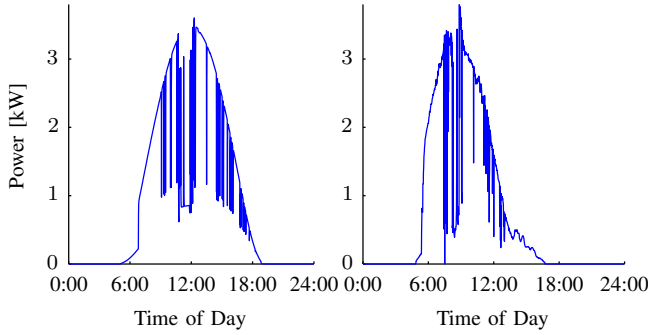
Fig. F.5: Left; power production of the implemented solar PV model during a day in September. Right; power production of a real PV system during the same day.

Solar Irradiance Model

The solar irradiance model relies on the one developed in [21].

Photovoltaic System Model

The PV model is given by the area it covers, efficiency of its cells, and constraints on the inverter. In normal operation the power produced by an ideal photovoltaic system is given by

$$p = \begin{cases} p_{\text{rated}} & \text{if } \eta A I_{\text{solar}} \geq p_{\text{rated}} \\ \eta A I_{\text{solar}} & \text{if } \eta A I_{\text{solar}} < p_{\text{rated}} \\ 0 & \text{otherwise} \end{cases} \tag{F.5}$$

where I_{solar} is the solar irradiance, η is the efficiency of the solar cells, A is the area they cover and p_{rated} is the rated power of the inverter.

To illustrate the performance of the model, power production during one day in September is compared with the power production of a real household PV system located in Denmark. This comparison can be seen in Fig. F.5. The difference during the start and end of the day is caused by difference in tilt angles of the two systems. Moreover, the model is intended to capture the general stochastic nature of real PV systems and not the statistic behavior.

Control Interface

The active and reactive power of the solar power plant can be controlled in the same way as for the wind power plant, detailed in the previous section. For further details on the PV system control, see [13].

4.4 Energy Storage

The energy storage model is similar to the model presented in [22]. The model consists of two parts

1. Model of energy storage,

2. Control interface for active and reactive power.

The energy storage is modeled as a first-order system, and is intended to simulate different kinds of energy storages, such as batteries and thermal systems [23].

Energy Storage Model

We consider an energy storage system capable of increasing consumption, and consequently filling its storage, and to inject active power into the system when energy is available in the storage. The energy storage level is described by

$$
e_{k+1} = \begin{cases} ae_k + T_s\eta_1 p_k & \text{if } p_k \geq 0 \\ ae_k + T_s\eta_2 p_k & \text{if } p_k < 0 \end{cases} \tag{F.6}
$$

where e is the stored energy, p is the power consumption/injection, T_s is the sampling time, k is the sample number, a is the drain rate, and η_1, η_2 are the system's efficiency when charging or discharging, respectively. For an efficient energy storage the drain rate a is close to one, where $a = 1$ is an ideal storage, and $a \leq 1$ is a prerequisite for the system to be stable.

Both the energy level and power consumption/injection are bounded by constraints

$$
e_{\min} \leq e_k \leq e_{\max}, \tag{F.7}
$$
$$
p_{\min} \leq p_k \leq p_{\max}, \tag{F.8}
$$
$$
|p_k - p_{k-1}| \leq p_{\text{rate}}, \tag{F.9}
$$

where p_{rate} is the limit on power (dis)charge rate, $e_{\min}$ and $e_{\max}$ are the minimum and maximum energy level, and $p_{\min}$ and $p_{\max}$ are the minimum and maximum bounds on power consumption/injection.

Control Interface

The active power of the energy storage can be controlled, as long as the bounds on energy level and power consumption/injection are not violated. We allow the active power to be controlled in two different ways

- Reference following on active power (*mode* = 0),

- Voltage control (*mode* = 1).

Thus, the active power reference can be described as:

$$p_{\text{ref}} = \begin{cases} \bar{p}_{\text{ref}} & \text{if } mode = 0 \\ \alpha(v_{\text{ref}}, v_{\text{mes}}) & \text{if } mode = 1, \end{cases} \tag{F.10}$$

where $\bar{p}_{\text{ref}}$ is the external active power reference, v_{ref} is a reference voltage, v_{mes} is the measured voltage at the connection point and $\alpha(v_{\text{ref}}, v_{\text{mes}})$ is given in (F.3). The limits on energy and power are handled as follows

$$p_k = \begin{cases} p_{\text{min}} & \text{if } 0 < e < e_{\text{max}} \wedge p_{\text{ref}} < p_{\text{min}} \\ p_{\text{max}} & \text{if } 0 < e < e_{\text{max}} \wedge p_{\text{ref}} > p_{\text{max}} \\ p_{\text{ref}} & \text{if } 0 < e < e_{\text{max}} \wedge p_{\text{min}} \leq p_{\text{ref}} \leq p_{\text{max}} \\ 0 & \text{if } (e = 0 \wedge p_{\text{ref}} \leq 0) \vee (e = e_{\text{max}} \wedge p_{\text{ref}} \geq 0) \end{cases}.$$

When including the rate constraint the power consumption/injection is given by

$$p_k = \begin{cases} p_{k-1} + \text{sign}(\Delta p) p_{\text{rate}} & \text{if } |\Delta p| > p_{\text{rate}} \\ p_k & \text{otherwise} \end{cases}, \tag{F.11}$$

where $\Delta p = p_k - p_{k-1}$.

Reactive power control is identical to that of the wind turbine, described in Sec. 4.2.

4.5 Electrical Vehicle

Electrical vehicles, and their availability at households are modeled by the following three components

1. Electrical vehicle mobility model,

2. Charging of the electrical vehicle,

3. Control interface for active and reactive power.

To model the battery of the electrical vehicle, the same model used for describing an energy storage is used, see the previous section.

Mobility Model

The mobility model is built upon the National Travel Survey from Great Britain [8]. The model is only intended to capture trends in the vehicle usage such that the availability of cars at the household is low during the day, which is seen from Fig. F.6 that shows the number of car trips in progress.
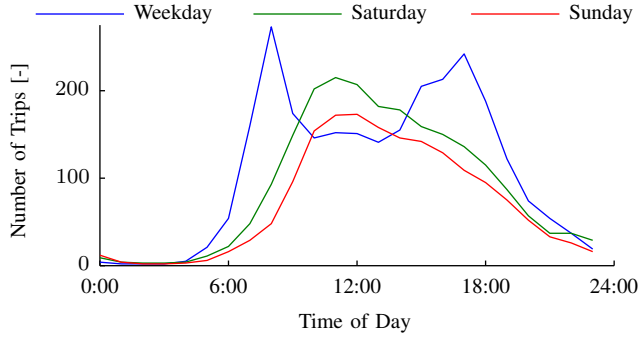
Fig. F.6: Trips in progress during a week.

It is seen that the general driving pattern depends on the day of the week. This dependence is captured by the proposed model, which has the following components:

- Trip rates by day of weak during a year.

- Average trip length.

- Trip purpose by trip start time.

We consider the characteristics of trips with different purposes such as commute and shopping trips.

The available data does not distinguish between driving e.g., to or from work. Therefore, the data are divided into starting a trip and ending a trip, and it is assumed that a driver starts and ends every trip at home. This was necessary to obtain realistic driving patterns from the statistical data.

To obtain the vehicles state of charge each trip is assumed to have a distance equal to the average trip length for a considered purpose of travel and an average mileage.

Electrical Vehicle Charging

To model the charging of the electrical vehicles battery it is seen as an energy storage. The battery can be charged according to the constraints on energy and power. When a vehicle has left the household, it will return after a trip with a change in state of charge according to the mobility model. There is assumed no vehicle to grid power control, i.e., the electrical vehicle battery can not inject power into the grid.

Control Interface

The active power consumption resulting from charging the electrical vehicle battery, can be controlled in two different ways

- Charge with maximum power consumption (*mode* = 0),

- Reference following on active power (*mode* = 1).

The active power reference can be describes as:

$$p_{\text{ref}} = \begin{cases} p_{\max} & \text{if } mode = 0 \text{ and vehicle available} \\ \bar{p}_{\text{ref}} & \text{if } mode = 1 \text{ and vehicle available} \\ 0 & \text{otherwise,} \end{cases} \qquad \text{(F.12)}$$

where $\bar{p}_{\text{ref}}$ is the external active power reference. The active power consumption is limited by the constraints imposed by the battery, which are identical to those described in the previous section.

Reactive power control is identical to that of the wind turbine, described in Sec. 4.2.

4.6 On-Load Tap Changing Transformer

The on-load tap changing transformer (OLTC) consist of two parts:

1. A model of the OLTC,

2. A control interface for changing tap position.

The OLTC is a transformer which is capable of changing its turns ration to either raise or lower the voltage magnitude on its secondary side. On-load means that the transformer is capable of changing taps without de-energizing the transformer and they are typically installed where the ratio needs to be changed frequently; e.g., to handle daily variations in system conditions. Given the assumption of balance between phases and using phasor representation, the OLTC is modeled as a two-winding transformer. For more information in modeling transformers, see [14].

Model of OLTC

The OLTC is modeled as a two-winding transformer with a variable turns ratio, see Fig. F.7 for a standard representation. The transformer is essentially modeled by three admittances, which values dependent on the turns ration

as follows

$$y_1(n) = \frac{1}{n} y_e \tag{F.13}$$

$$y_2(n) = \left(\frac{1}{n^2} - \frac{1}{n} \right) y_e \tag{F.14}$$

$$y_3(n) = \left(1 - \frac{1}{n} \right) y_e \tag{F.15}$$

where $y_e = 1/z_e$, n is the turns ratio, and z_e is the transformers impedance. Here y_1 describes the admittance between the two busses where the transformer is placed, y_2 describes the admittance from the primary side of the transformer to ground and y_3 describes the admittance from the secondary side of the transformer to ground. The values of y_1, y_2 and y_3 then change according to the turns ratio n.
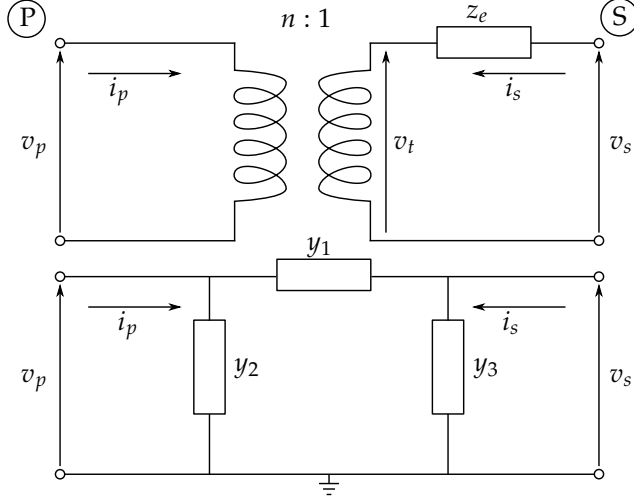
Fig. F.7: Standard equivalent circuit for a transformer (top) and the general π-network representation of it (bottom). P denotes the primary side and S the secondary side.

From Fig. F.7 the current equations are put on matrix form, which results in the following linear system

$$\begin{bmatrix} i_p \\ i_s \end{bmatrix} = \underbrace{\begin{bmatrix} (y_1(n) + y_2(n)) & -y_1(n) \\ -y_1(n) & (y_1(n) + y_3(n)) \end{bmatrix}}_{Y_u(n)} \begin{bmatrix} v_p \\ v_s \end{bmatrix}, \tag{F.16}$$

where Y_u represents a sub-matrix of the grid impedance matrix. This sub-matrix is changed whenever a tap-change has occurred. We represent the tap position by $u \in \mathbb{Z}$, where $u = 0$ indicates that the transformer operates at its

nominal value. This results in a switched algebraic system, where the value of $Y_u(n)$ changes according to n which depend on u, as follows

$$n = n_{\text{nom}} - \beta u, \tag{F.17}$$

where β represents the percentage change in turn ratio and n_{nom} is the nominal turns ratio.

Control Interface

We allow the transformers tap position to be controlled in two different modes

- Follow tap position reference (*mode* = 0),

- Voltage control (*mode* = 1).

Further, we put a constraint on the minimum time between tap changes. The OLTC is characterized by number of taps and the voltage change per tap, in percent from nominal voltage. The tap position reference is then given as:

$$u_{\text{ref}} = \begin{cases} \bar{u}_{\text{ref}} & \text{if } mode = 0 \\ \alpha(v_{\text{ref}}, v_{\text{mes}}) & \text{if } mode = 1, \end{cases} \tag{F.18}$$

where $\bar{u}_{\text{ref}} \in \mathbb{Z}$ is the tap position reference, v_{ref} is a reference voltage, v_{mes} is the measured voltage at the secondary side of the transformer and $\alpha : \mathbb{R}^2 \to \mathbb{Z}$ is a voltage control functionality given by

$$\alpha(v_{\text{ref}}, v_{\text{mes}}) = \begin{cases} u+1 & \text{if } \bar{v}_{\text{mes}} < v_{\text{ref}} - \sigma \\ u-1 & \text{if } \bar{v}_{\text{mes}} > v_{\text{ref}} + \sigma \;, \\ u & \text{otherwise} \end{cases} \tag{F.19}$$

where σ is a hysteresis and $\bar{v}_{\text{mes}}$ is a ten minute average of the measured voltage.

The tap position is limited by constraints on number of taps and a minimum time between tap changes (dwell time). It should be noted that it is only possible to change between consecutive taps, i.e., if $u = 0$ then a change to $u = 2$ is not possible, it has to go through $u = 1$. Thereby, the tap position is

$$u = \arg \min(||u(k) - u_{\text{ref}}(k)||)$$
$$\text{s.t. } \sum_{i=0}^{k_{\text{min}}} |u(k-1-i) - u(k-i)| \leq 1$$
$$u_{\text{min}} \leq u(k) \leq u_{\text{max}},$$

where $u_{\text{min}} \in \mathbb{Z}$ is the minimum allowable tap position, $u_{\text{max}} \in \mathbb{Z}$ is the maximum allowable tap position, k_{min} is the minimum number of samples between tap changes and k is the current sample.
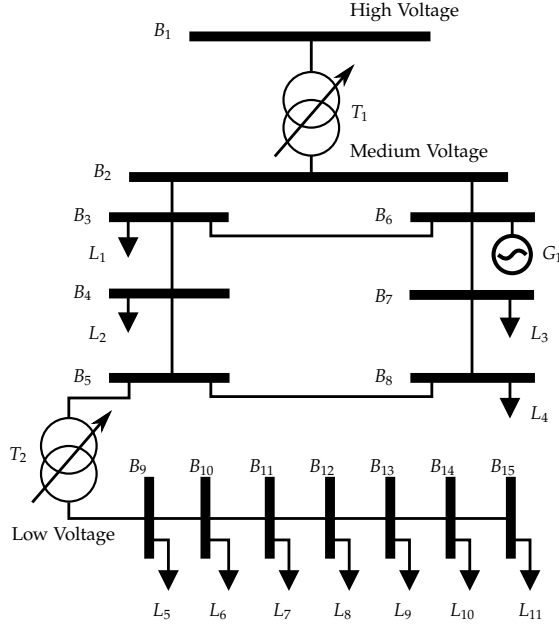
Fig. F.8: Grid used for the simulations. The generator on bus 6 (G_1), can be a wind power plant or a solar power plant. L_1 is an aggregated residential grid, L_2 is a commercial load, L_3 is an industrial load, L_4 is an agricultural load and L_5-L_{11} are aggregated residential loads of approx. 20 households each. All loads are based on real consumption data.

5 Simulation Scenarios

Two simulations are presented to demonstrate the simulation framework: first, an example illustrating voltage issues with large penetration of wind power on the MV grid is shown, followed by an example illustrating the problems of PV production in low voltage residential grids. Further, we provide simple control solutions that rely on the flexible assets. The grid setup used for the simulations, is shown in Fig. F.8, and the voltage requirement on the medium and low voltage level is: *the 10 min. mean value of the supply voltage at each bus must be within ±10 % of the nominal voltage* [24]. Remark: voltage control is not a tracking problem.

It should be noted that the control values for the two scenarios have been chosen a priori based on trial and error. Therefore, it is expected that performance can be improved significantly with more sophisticated control laws. Further, the simulations presented here are available at [13], along with models and control parameters.
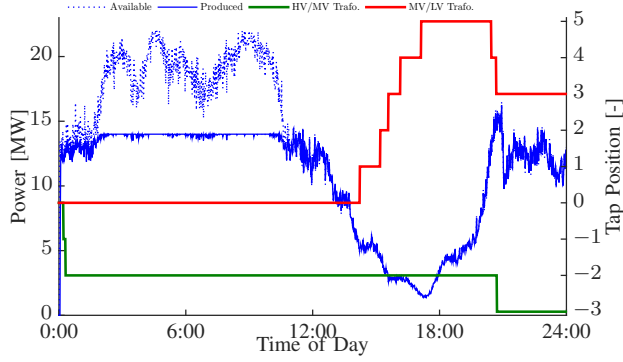
Fig. F.9: Same simulation as seen in Fig. F.1, with control of the wind power plant and EV charging. The number of tap changes needed has been reduced from 17 to 10, 3 on the HV/MV transformer and 7 on the MV/LV transformer.

5.1 MV Grid with High Penetration of Wind Power

We consider the grid setup seen in Fig. F.8, where G_1 is a small wind power plant with 22 MW capacity. Further, tap changing transformers (T_1,T_2) are installed at the HV/MV and MV/LV substations. These are responsible for maintaining the voltage levels throughout the distribution grid. EVs are distributed in the LV grid as follows: one on B_9, three on B_{13}, four on B_{14} and five on B_{15}, and the rated charging power has arbitrarily been chosen to 4 kW.

The high penetration of wind power and no coordination of flexible assets results in a total of 17 tap changes, as depicted in Fig. F.1. However, if the wind power plant and EVs contribute to the voltage control the number of tap changes needed can be lowered to 10, see Fig. F.9. This is achieved by derating the wind power plant with 8 MW, during its peak production hours in the morning. Moreover, instead of the EVs charging with full power capacity when available at the household, they are charging at half capacity, thereby reducing any voltage decreases in the evening and increases during night time.

5.2 LV Grid with High Penetration of PV

The grid setup in Fig. F.8 is used, with G_1 being a 6 MW solar power plant. Moreover, EVs are distributed as in the previous example and PVs are distributed as follows: two on B_{10}, two on B_{11}, three on B_{14} and five on B_{15}. The rated power of all PVs has arbitrarily been chosen to 6 kW.

The PV systems in the residential LV grid causes the voltages to increase during noon where consumption is low as most people are at work. Further, voltage drops during evening and night as consumption increases and PV production decreases, see Fig. F.2. The MV/LV tap-changing transformer is
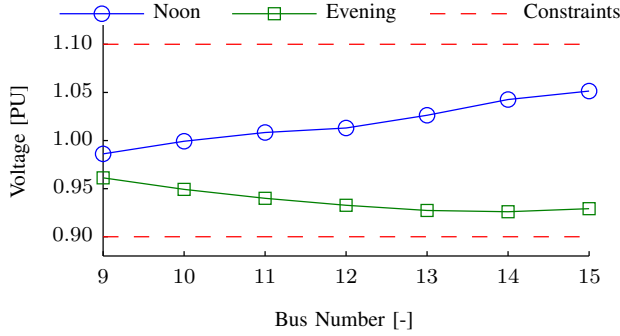
Fig. F.10: Same simulation as seen in Fig. F.2, with control of EV charging and inclusion of two energy storages in the LV grid.

still active but can not control the voltages, as it only measures the voltage at bus 9. To alleviate the voltage issues in the LV grid, two energy storages with a rated power of 10 kW and energy capacity of 100 kWh are added at bus 12 and 15. They are both set to voltage control mode on active power and their initial state of charge is set to zero, see Sec. 4.4. Further, the EV charging rate is decreased to one-third to lower the peak consumption. The resulting voltage levels throughout the LV grid at the same instances in time are depicted in Fig. F.10, and shows a significant improvement compared to the case without control.

6 Conclusion

In this paper we presented a MATLAB simulation framework that enables the verification and design of control algorithms for ensuring voltage profiles in power distribution grids. The framework features real consumption data, tools for setting up grid topology and parameters and for solving the power flow equations, model of communication channels, and multiple controllable flexible assets and grid components. This allows for a wide variety of simulation scenarios representing future distribution grids with high penetration of renewable resources.

The need for distributions system control was illustrated through two examples showing the potential voltage issues, resulting from high penetration of renewable resources in both the medium and low voltage grids. First, it was shown how the stochastic production from a wind power plant can lead to numerous transformer tap-changes. Secondly, it was demonstrated how photovoltaic systems in a low voltage grid can lead to voltage increase during noon when consumption is low, and how the voltage quickly drops during the evening when consumption increases. Finally, it was shown how both problems can be alleviated with simple control, by exploiting the flexible as-

sets implemented in the simulation tool.

The simulation tool is freely available at: `http://kom.aau.dk/project/SmartGridControl/DiSC/`

Acknowledgments

References

[1] G. Harrison and A. R. Wallace, "Optimal power flow evaluation of distribution network capacity for the connection of distributed generation," vol. 152, no. 1, Feb. 2005, pp. 115 – 122.

[2] P.-C. Chen, R. Salcedo, Q. Zhu, F. de León, D. Czarkowski, Z.-P. Jiang, V. Spitsa, Z. Zabar, and R. E. Uosef, "Analysis of voltage profile problems due to the penetration of distributed generation in low-voltage secondary distribution networks," *IEEE Transactions on Power Delivery*, no. 4, pp. 2020 – 2028, Sep. 2012.

[3] Green Tech Center, "Smart grid living lab," 2015. [Online]. Available: www.greentechcenter.dk

[4] "IEEE task force on open source software for power systems," Webpage. [Online]. Available: http://ewh.ieee.org/cmte/psace/CAMS_taskforce/

[5] R. D. Zimmerman, C. E. Murillo-Sánchez, and D. Gan, "MATPOWER - a MATLAB power system simulation package," Webpage, 1997, http://www.pserc.cornell.edu//matpower/.

[6] Pacific Northwest National Laboratory, "GridLAB-D - Power Distribution System, Simulation and Analysis Tool," 2009. [Online]. Available: http://www.gridlabd.org

[7] Y. jun Zhang and Z. Ren, "Optimal reactive power dispatch considering costs of adjusting the control devices," *IEEE Transactions on Power Systems*, vol. 20, no. 3, pp. 1349 – 1356, aug 2005.

[8] "National travel survey: 2012," Department for Transport, Tech. Rep., 2012. [Online]. Available: https://www.gov.uk/government/publications/national-travel-survey-2012

[9] I. Leisse, O. Samuelsson, and J. Svensson, "Coordinated voltage control in distribution systems with DG – control algorithm and case study," in *CIRED Workshop*, Lisbon, Portugal, May 2012.

[10] M. Juelsgaard, C. Sloth, R. Wisniewski, and J. Pillai, "Loss minimization and voltage control in smart distribution grid," in *Proceedings of the 19th IFAC World Congress*, Cape Town, South Africa, Aug. 2014.

[11] J. W. Simpson-Porco, F. Dörfler, and F. Bullo, "Voltage stabilization in microgrids via quadratic droop control," in *IEEE 52nd Annual Conference on Decision and Control*, Firenze, Italy, Dec. 2013.

[12] F. Viawan and A. Sannino, "Voltage control with distributed generation and its impact on losses in LV distribution systems," in *IEEE Russia Power Tech*, St. Petersburg, Russia, Jun. 2005.

[13] R. Pedersen, C. Sloth, G. B. Andresen, R. Wisniewski, J. R. Pillai, and F. Iov, "DiSC - A Simulation Framework for Distribution System Voltage Control," 2014. [Online]. Available: http://kom.aau.dk/project/SmartGridControl/DiSC/

[14] P. Kundur, *Power System Stability and Control*, ser. The EPRI Power System Engineering Series. McGraw-Hill, 1993.

[15] F. D. Bianchi, H. de Battista, and R. J. Mantz, *Wind Turbine Control Systems: Principles, Modelling and Gain Scheduling Design*, ser. Advances in Industrial Control. Springer, 2007.

[16] C. Sloth, T. Esbensen, and J. Stoustrup, "Robust and fault-tolerant linear parameter-varying control of wind turbines," *Mechatronics*, vol. 21, no. 4, pp. 645—-659, June 2011.

[17] I. V. der Hoven, "Power spectrum of horizontal wind speed spectrum in the frequency range from 0.0007 to 900 cycles per hour," *Journal of Meteorology*, vol. 14, pp. 160–164, April 1957.

[18] K. E. Johnson, L. Y. Pao, M. J. Balas, and L. J. Fingersh, "Control of variable-speed wind turbines: Standard and adaptive techniques for maximizing energy capture," *IEEE Control Systems Magazine*, vol. 26, no. 3, pp. 70–81, June 2006.

[19] M. G. Villalva, J. R. Gazoli, and E. R. Filho, "Comprehensive approach to modeling and simulation of photovoltaic arrays," *IEEE Transactions on Power Electronics*, vol. 24, no. 5, pp. 1198–1208, May 2009.

[20] M. K. Deshmukh and S. S. Deshmukh, "Modeling of hybrid renewable energy systems," *Renewable and Sustainable Energy Reviews*, vol. 12, no. 1, pp. 235 – 249, 2008.

[21] H. Morf, "A stochastic solar irradiance model adjusted on the Ångström-Prescott regression," *Solar Energy*, vol. 87, pp. 1–21, 2013.

[22] K. Heussen, S. Koch, A. Ulbig, and G. Andersson, "Unified system-level modeling of intermittent renewable energy sources and energy storage for power system operation," *Systems Journal, IEEE*, vol. PP, no. 99, p. 1, 2011.

[23] R. Pedersen, J. Schwensen, B. Biegel, J. Stoustrup, and T. Green, "Aggregation and control of supermarket refrigeration systems in a smart grid," in *Proceedings of the 19th IFAC World Congress*, Cape Town, South Africa, Aug. 2014.

[24] "Voltage characteristics of electricity supplied by public electricity networks," EN 50160, 2010.